"LOW TEMPERATURE SOLAR COOLING SYSTEM WITH ABSORPTION CHILLER AND DESICCANT WHEEL"

Paolo Corrada

Prof Nunzio Motta, Prof John Bell, Dr Lisa Guan, Prof Cesare Maria Joppolo

Submitted in fulfilment of the requirements for the degree of
Doctor of Philosophy
Science and Engineering Faculty
Queensland University of Technology
2015

Abstract

Absorption chillers and desiccant wheel are today well-proven technologies. Their main application is in the heating, ventilating, and air-conditioning (HVAC) systems where absorption chiller are used to provide chilled water used to remove the heat load from an air-conditioned space and desiccant wheel are used in desiccant evaporative cooling system. Nowadays Solar Cooling systems are becoming popular to reduce the carbon footprint of air conditioning. The use of an absorption chiller connected to solar thermal panels is increasing, but little study has been carried out to assess the advantage of join together an absorption chiller and a desiccant wheel to remove the sensible heat and the latent heat in different ways than the current design adopted in the industry. The amount of heat rejected by an absorption chiller is higher than heat rejected by a vapour compressor chiller, which can be exploited through a heat recovery system. However, limited research has been done to investigate the possibility of recovering part of the heat rejected by an absorption chiller.

In this work I assess the possibility of implement a desiccant wheel in a conventional solar cooling system and the possibility of recovering the heat rejected by the absorption chiller which is then used for the regeneration of the desiccant wheel. The implementation of a desiccant wheel and the recovery of the heat rejected could provide a significant energy saving when compared to traditional solar cooling system.

The results will assist in the practical development of a solar cooling system which simultaneously uses absorption and adsorption technology.

Keywords

Keywords: Solar cooling system, Desiccant Wheel, Silica Gel, Lithium Chloride, Selective water sorbent, Dehumidification, Absorption chiller, Air Conditioning.

List of publications

P. Corrada, Bell, J., Guan, L., Motta N., " *Adsorption and absorption technologies applied to solar air conditioning system,*" Solar energy, to be submitted.

P. Corrada, Bell, J., Guan, L., Motta, N., Piloto, C., "*Determination of the optimum tilt angle for solar collectors in Australia using new correlations,*" Solar energy, under review.

P. Corrada, J. M. Bell, L. Guan, and N. Motta, "*Heat reject recovery in solar air conditioning.*" Conference Solar2011, the 49th AuSES Annual Conference, Sydney, 1-3 December 2011.

P. Corrada, J. Bell, L. Guan, and N. Motta, "*Optimizing solar collector tilt angle to improve energy harvesting in a solar cooling system,*" Energy Procedia, vol. 48, pp. 806-812, 2014.

Conference Presentations

Poster "*Heat Recovery System from Solar Cooling Application*" at the Conference Solar2011, the 49th AuSES Annual Conference, Sydney, 1-3 December 2011.

Poster "*Optimizing solar collector tilt angle to improve energy harvesting in a solar heating & cooling system*" at the International Conference on Solar Heating and Cooling for Building and Industry, SHC 2013 Conference, Freiburg, Germany, 23-25 September 2013.

Table of Contents

List of Figures

List of Tables

List of Abbreviations

Nomenclature

AHU – Air Handling Unit

A_a - area of the solar collector

a_i - Coefficients

ASHRAE – American Society of Heating, Refrigerating and air conditioning Engineers

BTU - British Thermal Unit

c – heat capacity

C - effective thermal capacity of the collector

c_0 - Optical efficiency value

c_1 - Linear heat loss coefficient

c_2 - Quadratic heat loss coefficient

COP - Coefficient of performance

c_p - Specific heat at constant pressure

DEC – Desiccant Evaporative Cooling

EnSolHX- Solar energy for desiccant wheel regeneration

f - Solution circulation ratio

F' – Solar collector efficiency factor

Ft - Corrector factor for heat exchanger

G – hemispherical global solar irradiance on horizontal plane (W/m^2)

h - Enthalpy ($kJ\ kg^{-1}$)

H – Daily sum of the global irradiance on horizontal plane (W/m^2)

H_2O = Water

HVAC - Heating Ventilation and Air Conditioning

h_l - 'h_l' denotes function for enthalpy of the solution ($kJ\ kg^{-1}$)

h_v – 'h_v' denotes function enthalpy of the vapour ($kJ\ kg^{-1}$)

h_n – Enthalpy of solution or vapour at state n ($kJ\ kg^{-1}$)

I - Global solar radiation normal to the collector surface (W/m^2)

kW = Kilo Watt

K(θ) - Incident angle modifier

M - Molar weight ($kg\ mol^{-1}$)

$\dot{m}$ - mass flow rate (kg/h)

m_n - 'm' denotes mass of solution or vapour at state number n

n - Number of data points

NAT – Novel Air Technology

NH_3–H_2O = Ammonia – Water

NTU - Number of Transfer Unit

P – Pressure

Q – Heat transfer

Q_E – Energy exchanged in the evaporator

Q_G – Energy exchanged in the generator

Q_H – Condensation heat in a refrigeration system

Q_L – Evaporation heat

R - Factor used to evaluate Ft

RH – Relative Humidity

ROI – Return Of Investment

S - Factor used to evaluate Ft

t - Temperature (˚C)

t_a - ambient surrounding air temperature (˚C)

t_{in} – collector inlet temperature (˚C)

t_m - average fluid temperature in the collector $(t_{out}+t_{in})/2$ (˚C)

t_n –'t' denotes temperature at state n (˚C)

t_{out} – collector outlet temperature (˚C)

T_m^* – Reduced temperature difference $\frac{t_m - t_a}{G}$ $(m^2K)/W$

$(\tau\alpha)_{en}$ - effective transmittance–absorbance product at normal incidence

UA Overall heat transfer coefficient

W – External work

wx_0 - Overall weight ammonia concentration

wx - Weight ammonia concentration in the liquid phase

wy - Weight ammonia concentration in the vapour phase

x - Ammonia mole fraction in the liquid phase

x_n - 'x' denotes the mole fraction in liquid state at state number n

y- Denotes the function for mole fraction in vapour state

y_n- 'y' denotes the mole fraction in vapour state at state number n

Subscripts

a – related to the aperture area

A - Ammonia

abs - Absorber

amb - Ambient

av - Average

c - collector

con - Condenser

cond - Conduction

conv - Convective

evap - Evaporator

g - Gas phase

gen - Generator

i - Term of fitting polynomial

in - Inlet

k - Experimental data point

1 - Liquid phase
liq - Liquid
loss - Losses
n - Denotes the state number
opt - Optical losses
out - Outlet
p – pump
rad - Radiative
rect - Rectifier
RHE - Refrigerant heat exchanger
SHE - Solution heat exchanger
strong - Strong solution
sys - System
vap - Vapour
w – Water
weak - Weak solution
0 - Reference value

Greek letters

α - quality of vapour
ε - effectiveness
η - efficiency
ρ - density
φ - adsorption isotherm

Statement of Original Authorship

The work contained in this thesis has not been previously submitted to meet requirements for an award at this or any other higher education institution. To the best of my knowledge and belief, the thesis contains no material previously published or written by another person except where due reference is made.

Signature: _____  _____

Date: _____30/09/2015_____

Acknowledgments

I would like to thank all the people that have helped in the presentation of the project. I would like to thank my supervisor Nunzio Motta for his understanding and extreme helpfulness during the last 4 years. Without his help and input this project would not have be able to get off the ground. I would like to thank 1all the fellow students in Nunzio's group who supported me during the regular group meetings and especially in my most difficult moments.

Also I would like to thanks Lino, Damiano, Manuel and Luca for helping me and making me feel "*at home*". A very big thank to Stefano De Antonellis for his "long term helps" and for sharing all his acknowledge with me in the last four years. Thanks also to the students Adrian, Matthew, Mevin and Mohd for helping with their final projects with me. Last I would like to thank QUT and all its staff that has helped me over the last 4 year in my course.

I would like to acknowledge the support of Prof. John Bell and Lisa Guam, my associate supervisors and the scholarship received from the School of Chemistry Physics and Mechanical Engineering.

Finally, I would like to express my gratitude to my parents for the education they gave me. I am sorry that they are not here with me to share this moment. This is it !!

My PhD is finally finished and I can spend some time with my little boy Luca but before to go I want to say "See you soon Graham" hope you are watching my presentation from the heaven !

Chapter 1: Introduction

1.1 BACKGROUND

A growing world population has seen a commensurate increase in the demand for energy [1]. This increase in energy demand is impacting on the cost of fossil fuel and energy in Australia. As predicted over the past years, the increase of the Queensland residential electricity prices has reached 32% between 2009/10 and 2012/13 [2].

Buildings are among the biggest energy users in the world, where the largest share is related to heating, ventilation and air conditioning (HVAC) systems [3]. This highlights the potential for considerable energy, emissions and cost savings by improving the performance of such HVAC systems.

Nowadays, the most common air conditioning systems are based on the vapour compression cycle using electrically driven compressors which are responsible for the highest proportion of the total consumption of HVAC system.

Electricity consumption of an HVAC system is strongly related to the intensity of solar radiation, as the demand for cooling obviously increases in proportion to irradiation. Due to the carbon content of the fuel used to produce the electricity, this electricity consumption in the end increases the CO_2 emission in the air, which is one of the main causes of global warming.

A system that relates the cooling output to the heating input is well suited to be used as an alternative to current cooling technologies. Research is therefore being carried out on solar cooling air conditioning systems that use mostly solar thermal power to drive the cooling cycle instead of electricity.

In a solar cooling system the thermal energy from the sun is transformed into refrigeration power. This can be done in two different ways:

- by using an **adsorption cycle** through a solid adsorber [4], which adsorbs water (refrigerant) at a lower temperature and releases heat by water desorption; or
- by an **absorption cycle** through a liquid absorber [5] which mixes with the refrigerant at a lower temperature and releases heat at a higher temperature.

The absorption and adsorption machines for purposes of refrigeration or air conditioning systems are currently the subjects of renewed interest after a period during which attention was directed mainly to vapour compression machines, characterised by a greater Coefficient Of Performance (COP). This interest is triggered especially by the limited availability of electric power in remote areas [6, 7]. Studies report that absorption systems are more suitable for air conditioning applications, while adsorption systems are more suitable for low temperature purposes, but the application of solar sorption systems is not limited to these areas. There are many other applications which are not considered because they are not fully developed or have not yet matured [8].

1.2 RESEARCH PROBLEM

Even if a solar cooling system could appear as a viable option to reduce the cost of air conditioning in the long term, the number of installations of solar cooling systems is still small.

Solar cooling systems are attractive as they can satisfy the demand for refrigeration, air conditioning and ice making by using only clean energy. The main advantages of solar cooling systems are:

1) availability of cooling during periods of high solar radiation
2) use of thermal energy as driving energy instead of electricity
3) reduction of demand on the network due to low electrical power rating
4) low operating costs
5) energy conservation
6) durability and environmental compatibility
7) reduced greenhouse gas emissions.

By 2008, a total of approximately 450 solar cooling systems were realised worldwide, the vast majority of which is in Europe, where the market has increased over the last five years by 50%–100% annually. Approximately 60% of these systems use absorption chillers, 11% adsorption chillers and 29% open systems (desiccant evaporative cooling and liquid sorption systems). Even so, the total volume of installations reveals that the solar cooling sector is still a niche market [9]. This is mainly

due to the fact that solar cooling systems require additional research and development. This relates mainly to:

1) upfront installation costs [10]:
    - Costly high-grade solar collectors are required to provide a generator temperature around 90°C [11].
    - The cost of an absorption chiller unit is higher than a vapour compression unit with the same cooling capacity due, also, to the additional heat exchangers needed as the rejected heat from an absorption chiller is higher than the rejected heat from a vapour compression chiller [12]. Studies on the possibility of using solar sorption cooling systems applications in residential settings have been undertaken and the high cost of the chiller has been recognised as the cause of their limited application [13].
2) performance:
    - Solar cooling systems cannot always operate at their nominal rating during periods of low solar radiation and high cooling water temperature [11].

Most of the time the installation costs are the deciding factor when implementing new equipment. Reducing the installation costs for a solar cooling system will make them more viable compared to current vapour compression cycle systems.

The costs associated with a solar cooling system are proportional to the amount of solar thermal panels needed and the size of the chiller installed. By reducing the number of panels and the size of the chiller needed, the total costs of a solar cooling system can be reduced proportionally.

The research questions I will answer in this thesis are:

1) Can installation costs be reduced by implementing a desiccant wheel in the design of currently available solar cooling systems using hot water at a temperature below 100°C?
2) Is it possible to recover the heat, which is currently rejected into the environment by the absorption chiller used in the solar cooling system, to

be reused to regenerate a desiccant wheel implemented in the solar cooling system?

1.3 RESEARCH OBJECTIVES

The objective of my research is to answer the research question listed in paragraph 1.2.

To ascertain whether installation costs can be reduced by implementing a desiccant wheel in the design of a solar cooling system and heat can be recover by the absorption chiller, I develop mathematical models for various major components of a solar cooling system. Using the models and the characteristics of commercial equipment I evaluate the thermodynamic performance of the system including a new Air Handling Unit (AHU) capable of decoupling the latent heat load from the sensible heat load.[1] This approach would allow downsized cooling equipment to handle only the sensible load, resulting in better humidity control, reduced energy consumption and reduced system installation costs.

Efficiency of an air conditioning system using a vapour compression cycle is measured by its COP which is the ratio between its rated cooling capacity and the rated electricity input. In a solar cooling system, efficiency can be measured by the thermal COP which is defined as the ratio of the cooling capacity of the evaporator (Q_E) to the energy supplied to the generator (Q_G). The COP is an useful index of performance in solar cooling where collector costs (and thus costs of Q_G) are important [14].

In this thesis, the COP is the reference parameter used to optimise the system; the increase of COP is achieved by reducing the energy input Q_G, and accordingly costs are reduced by the reduction of the size of the solar field needed. Other cost savings are also achieved by downsizing the chiller used as it will only remove the sensible heat. The savings calculated in the thesis are compared to a solar cooling system using a typical design where latent and sensible heats are removed by the same coil in the AHU.

[1] *Sensible heat is related to the change of temperature in an object while latent heat is the heat needed to evaporate water in vapour and it is measured by the humidity ratio in the air. Currently both kinds of heat are removed by one machine.*

1.4 SIGNIFICANCE OF RESEARCH

During the literature review a wide range of articles regarding solar cooling systems [11, 15-24] has been analysed. Solar cooling systems including absorption chillers and solar fields are already available on the market. But a solar cooling system using both adsorption and absorption technologies at the same time has not been developed and documented so far. I propose, for the first time, to join these two environmentally friendly technologies in a solar cooling system, substantially reducing the energy required to provide air conditioning.

The main novelty of this research is the introduction of a desiccant wheel to remove the latent heat from the fresh air introduced in a conditioned space.

After adsorbing the humidity the desiccant wheel needs to be regenerated by a hot air stream; in this project a part of the required heat for the regeneration of the wheel is obtained by recovering the heat rejected by the absorption chiller and the balance is generated using solar thermal panels. In this way both the sensible and the latent heat are removed together.

The outcome of this research can potentially lower the impact of air conditioning on the electric grid, facilitating a reduction in peak loads, with enormous benefits especially for areas in subtropical and tropical regions.

1.5 SCOPE AND FEASIBILITY

As part of this thesis some assumptions have been made in the design of the new solar cooling system.

The first assumption is that the efficiency of the absorption chiller is constant when the temperatures of the generator, the cooling water and the chiller water are kept constant.

The second assumption is that the peak cooling load occurs at the same time as the peak of the solar irradiation. This means that no thermal inertia has been taken into account in the calculation. This assumption has been made to avoid the necessity of designing a storage system that would otherwise be needed when implementing the system in real life.

Also, this thesis is based on the assumption of limited operational ranges of the absorption chiller due to limited availability of data. These limited ranges are:

- hot water temperature from 80 to 100 °C
- cooling water temperature from 27 to 33 °C.

- chilled water temperature from 5 to 12 °C.

During the research phase of the thesis I have gone through several iterations of system designs as I faced many problems from feasibility to availability of equipment.

The feasibility of this research project is guaranteed by the use of existing parts, found readily in the market, which can be adapted to the proposed HVAC unit with minimal changes. My proposed design considers a stand-alone system based on a field of solar thermal panels, providing the heat to an absorption chiller, which is used to remove the sensible heat, converting heat in cooling power with minimal use of electricity. The latent heat is then removed by the installation of a desiccant wheel which is regenerated by recovered heat from the chiller and heat produced by the solar thermal panels. This makes the proposed design system suitable for application in areas, where little or no electric power is available, as it is based on solar energy.

The feasibility of this system is also linked to the costs. In this respect the proposed system, requiring a smaller chiller and, as a consequence, a smaller solar field, could have costs lower than those of a current solar cooling system.

By exploring and substantiating these key ideas through a mathematical model I will prove the feasibility of my proposed solar cooling system that has more environmental and economic benefits than current solar cooling systems.

1.6 THESIS OUTLINE

Following the introduction, a comprehensive literature review is presented in Chapter 2: . The first equipment reviewed is a solar thermal panel with special consideration given to the evacuated tube as it is the solar panel of choice for this thesis. This chapter also describes a desiccant wheel and reviews several desiccant materials used in this work. Absorption technology is assessed from the operating principles to the limitation of the technology. A full solar cooling system and the latest developments in this technology are also presented.

Chapter 3 provides a brief of the adopted methodology and the scenarios of simulation for each equipment.

Chapter 4 describes the full methodology adopted and the mathematical models for each equipment is described. For each model the equations used are presented.

The solar system is modelled using as a reference the testing standard for solar thermal panels. The desiccant wheel is modelled using previous work descriptions and several desiccant materials. The solar system, desiccant wheel and the absorption chiller

are then joined in the final model where the variation of efficiency of the whole system is calculated based on varying input parameters.

In Chapter 5: the results of the modelling are presented and discussed. Several simulations are presented for the solar system, desiccant wheel and the absorption chiller showing the variation of the efficiency of the equipment by varying the inputs.

With the solar panel model the variation of efficiency of the panels is assessed when the values of the following inputs are varied:

- ambient temperature
- inlet water temperature
- outlet water temperature.

The absorption chiller model is used to assess the output variation by varying the following inputs:

- generator temperature
- chilled water temperature
- cooling water temperatures.

The desiccant wheel simulator is used to assess the variation of performance in terms of humidity ratio reduction for each desiccant material used by varying the value of the following inputs:

- humidity of the process air
- temperature of the process air
- temperature of the regeneration air.

The final result is an estimate of the efficiency of the proposed and tested solar cooling system and its benefits compared to a typical solar cooling system.

The final conclusion and implications for energy policy and further research are described in Chapter 6: .

Chapter 2: Literature Review

2.1 INTRODUCTION

The focus of the literature review was on comparing conventional air conditioning with solar air conditioning systems. It looked at the latest developments in solar technologies, in particular, at individual pieces of equipment which are part of conventional and solar air conditioning systems, and which are very similar on the condensation and evaporation sides but very different when it comes to the pressurization side.

Several studies have been undertaken for both systems with the aim to review the current state of the two technologies, while other studies have had the purpose to assess the behaviours of new refrigerants or the use of mixtures of known refrigerants already available. The purpose of this thesis was to assess the possibility of increasing the performance of a solar cooling systems. Few studies have assessed the opportunities of joining existing technologies to reduce energy consumption, but no study has been found during the literature review that investigated the interaction of a desiccant wheel with an absorption system. The thesis aims to fill this identified knowledge gap.

2.2 CONVENTIONAL AIR CONDITIONING SYSTEM

Air conditioning systems have been used for years to improve human wellbeing and comfort in public buildings, offices and residential dwellings, and, in spite of the improvement in their efficiency, they still require a large amount of power. This constitutes a threat for the environment, in particular, where clean energy sources are not (yet) available, and a challenge for some regions where electricity is scarce or too expensive. An air conditioning system provides cooling, ventilation and humidity control for all or part of a house or a building, by removing heat and humidity through a process called the refrigeration cycle.

2.2.1 Introduction

There are different options for air conditioning a confined space. The application of a particular type of system depends on a number of factors like the size of the area to be conditioned and the total heat load of the area. In a HVAC design, air conditioning units can be considered to be stand-alone systems or part of an integrated system. In the

current market there are four common types of air conditioners; each of them with its own benefits and disadvantages:

1) window air conditioner
2) split air conditioner
3) packaged air conditioner
4) centralised air conditioning.

The first two systems are considered stand-alone systems and cannot provide external fresh air to the conditioned area as there is no ducting to carry air. Systems 3 and 4 fall into the HVAC category as they can provide fresh air to the conditioned rooms.

Window air conditioners are commonly used for single rooms or small areas. In these units all the components are enclosed in a single box. These air conditioners consist of a compressor, a condenser, an expansion valve and an evaporator.

Split systems include an outdoor and an indoor unit connected by refrigerant piping. The outdoor unit includes the compressor and the condenser, whereas the indoor unit contains the evaporator and the expansion valve. These units can provide air conditioning from one up to several rooms of a household. Larger split systems commonly use one outdoor unit and several internal units. This design allows the amount of refrigerant going around the pipes to vary, increasing the efficiency of the system. These systems, although most commonly seen in residential settings, are gaining popularity also in small commercial buildings.

Packaged air conditioners are designed for air conditioning of more than two rooms or for large areas. The system consists of a single box that accommodates all the components, namely the blower, compressor, condenser (which can be air cooled or water cooled), expansion valve and evaporator. The air is distributed through ducts to the different rooms using a blower. This system is difficult to be retrofitted (i.e. to be installed in a home that was not designed to use it), because of the bulky ducts required to carry the air.

For larger settings, centralised air conditioning systems are used. These systems are divided into two parts:

1) cooling production, which includes a chiller and the heat reject system
2) distribution, which includes the circulating pump and the AHU.

In a centralised air conditioning system the cooling is carried to the various AHUs by chilled water. The chilled water is produced in the evaporator of the chiller which consists typically of a shell and tube heat exchanger. On the tube side the refrigerant passes at low temperature, while on the shell side water is passed and gets chilled.

In any of the above air conditioning systems, the evaporator (or the chilled water coil in the AHU for the centralised system) provides dehumidification in air conditioning systems through the condensation of the moisture on the coil since the evaporator or the chilled water coil operate at a temperature below the dew point of the air to be conditioned.

2.2.2 Cooling sources

In a centralised air conditioning system various designs are possible. The main difference is how the chilled water is produced. Chilled water can be produced by either mechanical refrigeration or by absorption processes. Other systems, using desiccant wheels which remove the humidity from the air directly [25] and harnessing the principal of evaporative cooling to cool the air, are not widely used at present. However, they are increasingly attracting interest due to their low energy consumption, which is suitable for applications based on renewable energy sources.

2.2.2.1 The refrigeration cycle

The chiller unit transfers heat from a cold environment (lower temperature) to a hot environment (higher temperature), opposite to the natural heat flow, producing the required cooling. The chiller function is based on the use of a thermodynamic cycle transformations (vapour compression cycle) drawing energy from external work.

The cycle is based on the fact that the liquid-vapour phase change can happen with absorption or release of heat at different temperatures depending on the pressures of the system. The chiller uses a refrigerant fluid, which is able to absorb a high amount of heat per unit mass in the transition phase. The operation of the refrigeration machine appears to be the inverse of a direct heat engine. A direct heat engine produces work using the temperature difference between two reservoirs. In an ideal refrigeration unit, the machine uses the same amount of work to extract heat from the cold tank and transfer it to the warmer tank, running the cycle in the reverse direction.

As indicated in Figure 1, in a refrigeration cycle the amount of heat Q_2 is taken from the source at a lower temperature T_2 using external work W and transferred to the

reservoir at a higher temperature T_1. The total heat transferred Q_1 between the two sources is the sum of the heat absorbed from the source at temperature T_2 plus the work on the system W.

$$Q_1 = W + Q_2 \tag{2-1}$$

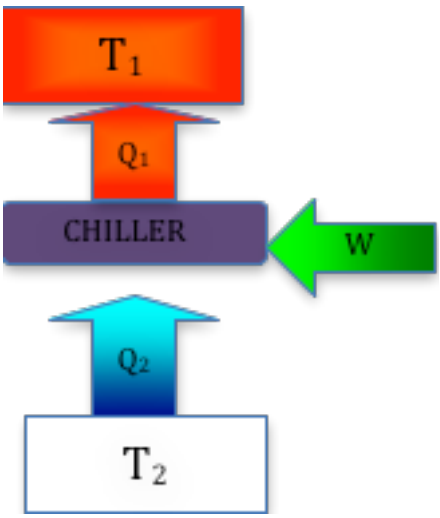

Figure 1 Flow diagram for chiller system

2.2.2.2 Vapour compression refrigeration

The vapour-compression refrigeration system has four components: evaporator, compressor, condenser and expansion valve as indicated in Figure 2. The refrigerant enters the compressor as a slightly superheated vapour at low pressure. It then leaves the compressor as a vapour at higher pressure by the use of external energy W_C and enters the condenser where the refrigerant is condensed and heat Q_H is transferred to a cooling medium. The refrigerant then leaves the condenser as high-pressure liquid. The pressure of the liquid is decreased as it flows through the expansion valve 4, and as a result, some of the liquid flashes into cold vapour.

The remaining liquid, at low pressure and temperature, is vaporised in the evaporator and heat Q_L is transferred from the refrigerated space or chilled water to the refrigerant. This vapour then re-enters the compressor.

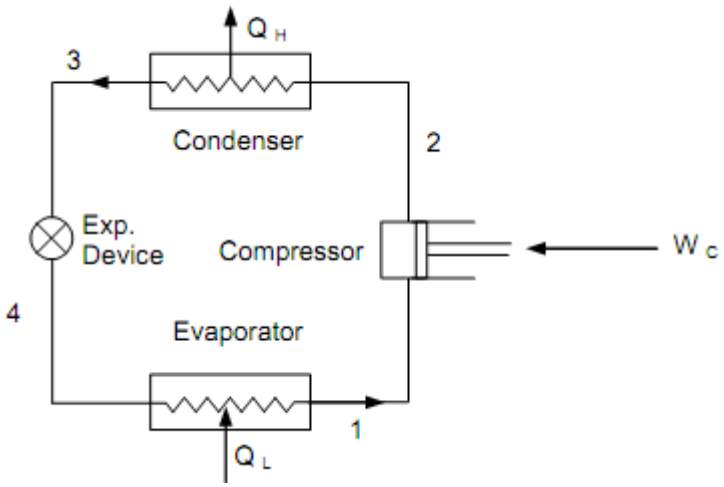

Figure 2 Schematic of electric chiller system (Courtesy of www.expertsmind.com)

The theoretical process is often illustrated in two diagrams. The first diagram shows the relation between the temperature and the entropy of the refrigerant, while the second diagram illustrates the relation between the pressure and the enthalpy variation of the refrigerant during the cycle.

The ideal vapour-compression cycle consists of four processes as shown in Figure 3 and Figure 4:

- 1-2 isentropic compression using W_{in}
- 2-3 constant pressure heat rejection Q_H in the condenser at high temperature
- 3-4 throttling in an expansion valve
- 4-1 constant pressure heat addition Q_L in the evaporator at lower temperature.

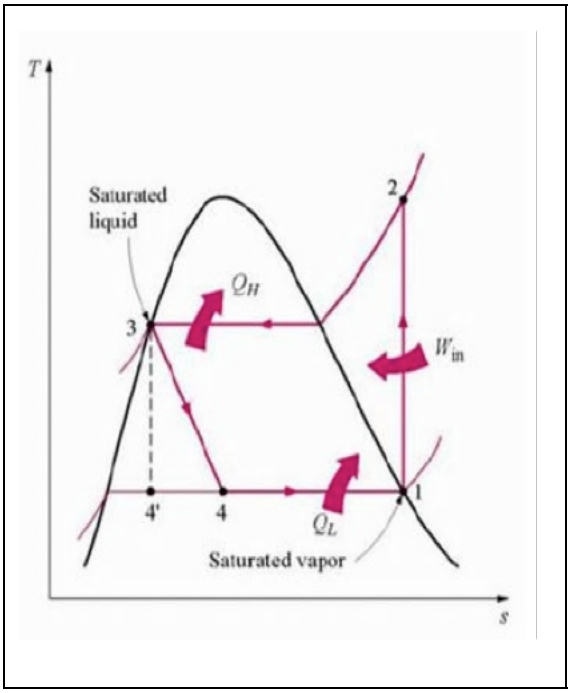

Figure 3 Refrigeration cycle in the T-s diagram (courtesy of http://www.saylor.org)

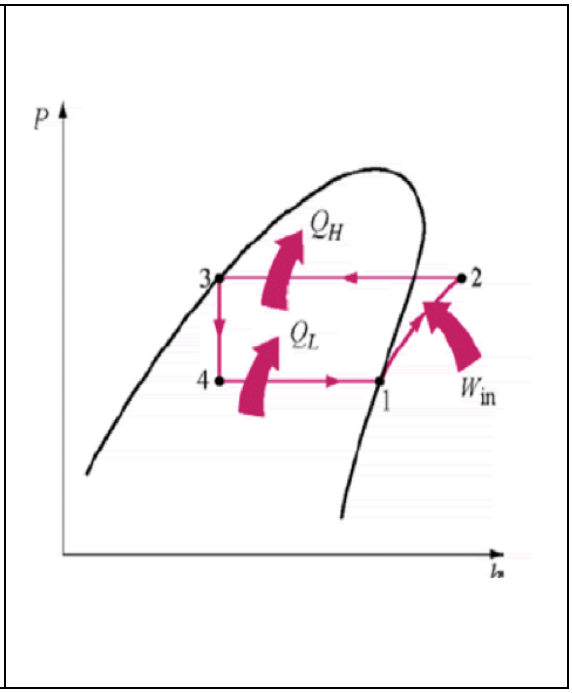

Figure 4 Refrigeration cycle in the p-h diagram (courtesy of http://www.saylor.org)

- 1-2 isentropic adiabatic compression: The pressure of the refrigerant varies from P_1 to P_2. In theory the transformation is adiabatic, but practically is an irreversible adiabatic (and therefore not isentropic). This transformation is made by a dedicated machine (compressor) with non-unitary efficiency. Starts from point 1 (saturated vapour) and ends at point 2 in slightly superheated vapour conditions. The work needed in the compressor can be calculated as:

$$W_{in} = h_2 - h_1 \tag{2-2}$$

- 2-3 isobaric condensation: This phase transition transformation consists of a constant pressure heat rejection in the condenser. In this stage, Q_H is the heat rejected to the ambient or cooling circuit. The heat rejected can be calculated as:

$$Q_H = h_2 - h_3 \tag{2-3}$$

- 3-4 throttling in an expansion valve: Isentropic adiabatic expansion (limit cycle) from $P_3 = P_2$ to $P_4 = P_1$, the transformation starts at Point 3 (saturated liquid) and ends as wet vapour in Point 4. In practice, the expansion is made out of a valve or a capillary, therefore does not produce work and is certainly not isentropic.

- 4-1 constant pressure heat addition: Isobar evaporation, the phase transition transformation in the field of steam, is isothermal. At this stage, the effectiveness consists of the removal of heat Q_L from the cold source. The heat absorbed can be calculated as $Q_L = h_1 - h_4$, the quantity of heat absorbed is called cooling effect.

$$Q_L = h_1 - h_4 \tag{2-4}$$

The performance of the chiller is described by the ratio of the benefit obtained, the cooling effect, divided by the power input.

This value is always greater than 1.0 and it is defined in terms of work as COP. Using the *P-h* diagram the efficiency in term of COP can be calculated as:

$$\eta = COP = \frac{Q_L}{W_{in}} \tag{2-5}$$

The second law of thermodynamic states for the Carnot cycle of Figure 2 that for reversible operation the net entropy production is zero so:

$$\frac{Q_L}{T_0} - \frac{Q_H}{T_1} = 0 \tag{2-6}$$

Where T_0 and T_1 are respectively the temperature of evaporation and condensation in the cycle.

Equation (2-5) can be modified to an expression which includes only temperatures using equation (2-1) and (2-6) by eliminating the *W*.

$$\eta = \frac{T_1}{T_1 - T_0} \tag{2-7}$$

The above expression is typically termed as the Carnot efficiency factor for cooling or refrigeration application. It is also very common for a heat pump application of the above expression that the COP term is used during heating mode and the term EER (Energy Efficiency Ratio) is used during cooling mode. Work in a mechanical refrigeration chiller is usually provided only through electricity to power the compressor.

2.2.3 Air Handling Unit

The first AHU was first marketed in 1860 and was comprised of a simple warm air fan driven system. This is not that much different to today's systems, even though the current systems combine a few more components, but the overall application of the system has not changed significantly. Since 1900 these systems were available for commercial use in homes as well as offices, and in 1908 components for heating, cooling and dehumidifying became available. In the early years the systems were only

installed to simply cool spaces during the summer months [26]. In 1944, Willis Carrier created a design for an air conditioning system that took into consideration numerous parameters, today known as indoor air quality. Overall Carrier's design was a breakthrough in air conditioning as it allowed spaces to be dehumidified, cooled and heated providing clean air due to ventilation [27].

The primary purpose of an AHU is to filter and condition the incoming air from the environment to a specified humidity ratio and temperature set by the user for cooling or heating requirements.

Depending on the specific design, basic components of a normal AHU are as follows: outdoor air intake, mixed-air plenum and outdoor air control, air filter, heating and cooling coils, humidification and/or de-humidification equipment, supply fan, including attenuators, dampers and vanes, return air system and exhaust ducts or extract fans [28]. All the components are divided into two loops:

1) air side consisting of air intake, filters, fan, heat exchanger coils and humidifier
2) water side consisting of pump and piping [29].

Figure 5 shows a typical design of an AHU which is basically a box or a rectangle cross-section. The components are ordered in a manner that lets the air be treated to the designed conditions.

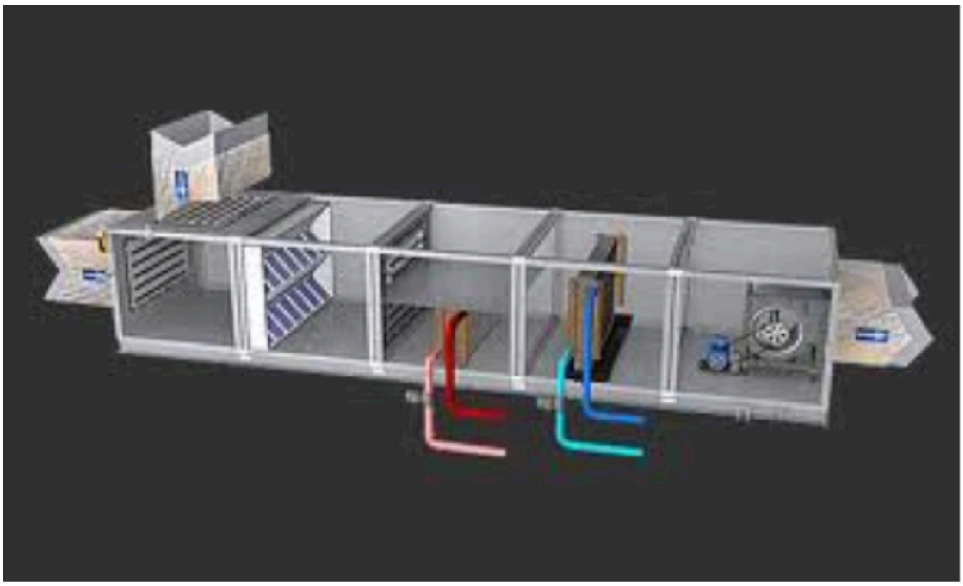

Figure 5 Standard chamber AHU

The fan sucks hot return air from the room via ducts, mixes it with outdoor air and blows it over the cooling coil. The cool air is then cooled through the ducts and

supplied to the space. The water, which has absorbed the room heat, flows back to the evaporator, gets chilled and is pumped back to the coil in the AHU. Fresh air is provided to the system by a grill in the AHU open to the external environment.

Many societies have been created to assist with maintaining a high standard for air conditioning, with the most notable being the American Society of Heating, Refrigeration and Air-Conditioning Engineers (ASHRAE) which releases handbooks for air conditioning systems and refrigeration systems [30].

The design of an AHU is regulated by the ANSI/ASHRAE Standard 62-2001 which specifies a minimum ventilation fresh air provision of 10 l/s per person at all times of operation (ASHRAE 2001). In certain climatic conditions, such as the Tropics and Subtropics, the outdoor air is responsible for the latent heat load that needs to be removed by the cooling coil.

2.2.4 Heat exchanger

Heat exchangers were first introduced in 1930 and have been used in AHUs as a means of transferring heat from one fluid to the next effectively heating or cooling the air [29].

In an AHU rotating heat exchangers are usually used for heat recovery, and finned-tube heat exchangers usually transfer or adsorb the heat to and from the air.

The literature review only considers plate fin heat exchanger and plate heat exchanger as they are the main types of exchangers used in the research.

2.2.4.1 Rotating heat exchangers

One of the most effective air-to-air energy recovery technology used in ventilation and air condition systems is based on the principle of a rotating heat exchanger.

This system installed in a ventilation system recovers heat from one air stream and transfers it to the other reducing energy consumption and associated costs.

The operation of the rotating heat exchanger is based on the principle that one air stream heats (or cools) the exchanger, with the energy then being transferred to the other air stream when the wheel passes through the air stream.

Rotary heat exchangers are an efficient means of heat recovery providing up to 80% energy savings [31, 32].

Depending on the air conditions and using desiccant coated rotors the heat recovery wheel can recover both sensible (heat) and latent (moisture) energy.

Figure 6 shows the diagram of a rotating heat exchanger and a typical rotor.

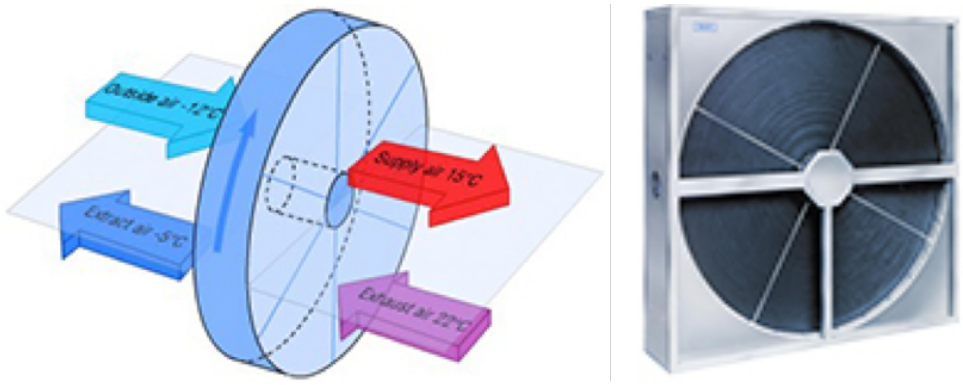

Figure 6 Rotating heat exchanger diagram (left) and typical rotor (right) (courtesy of www.wolf-geisenfeld.de)

2.2.4.2 Finned-tube heat exchanger (air coil)

Finned-tube heat exchangers are a commonly used type of heat exchangers in many air conditioning systems. Finned-tube heat exchangers are designed for maximum heat transfer between two fluids with a minimum pressure drop associated with each fluid.

Finned-tube heat exchangers, or coils, consist of mechanically or hydraulically expanded round tubes in a block of parallel continuous fins.

The sizing of a coil requires solving two energy equations of the air side and water side together with the heat and mass transfer coefficient.

The method used is the Number of Transfer Unit (ε-NTU) method for heat exchangers. The total heat transfer rate used in the calculation is the arithmetic average of the air side and water side heat transfer rates [33]. These are shown in eq. (2-8) to (2-10).

$$\dot{Q}_{air} = \dot{m}_{air} Cp_{air} (\Delta T_{air}) \tag{2-8}$$

$$\dot{Q}_{water} = \dot{m}_{water} Cp_{water} (\Delta T_{water}) \tag{2-9}$$

$$\dot{Q}_{avg} = \frac{\dot{Q}_{air} + \dot{Q}_{water}}{2} \tag{2-10}$$

Where

- $\dot{Q}_{air}$ = Heat transfer rate of air (kW)
- $\dot{Q}_{water}$ = Heat transfer rate of water (kW)
- $\dot{m}_{air}$= Mass flow rate of Air (kg/s)
- $\dot{m}_{water}$ = Mass flow rate of water (kg/s)

- Cp_{air}=Specific heat of air (kJ/kg K)
- Cp_{water}=Specific heat of water (kJ/kg K)
- $\dot{Q}_{avg}$ = Average Heat transfer rate (kW)
- ΔT_{air}= Variation of air temperature across the coil
- ΔT_{water}= Variation of water temperature across the coil

The design of finned-tube heat exchangers for an AHU requires specifications of several parameters, including the following:

- air flow rate
- face velocities which should be between 1.5 m/s and 2.6m/s
- length to height desired ratio 2:1
- coil load
- transverse tube spacing
- longitudinal tube spacing
- tube diameter
- material used which generally consist of copper tubes, with aluminium fins and galvanised steel frames.

2.2.5 Current development of the technology

Over the years some improvements have been made to conventional air conditioning systems. These improvements have been achieved through an increase of COP of the chillers (i.e. by using variable speed drive (VSD) to reduce the speed of the compressor and fans at partial load), or through implementing other equipment in the air side system like a variable air volume (VAV) unit [34]. Other improvements of the conventional air conditioning systems consist of the implementation of heat recovery for electric chiller [35], and heat and enthalpy wheels reducing costs associated with the decrease of thermal load they provide on the chiller [36]. The latter two technologies have been assessed as part of this thesis as there are currently no studies available on the possibility to join them in a solar system.

2.2.5.1 Heat recovery for electric chiller

In conventional chillers heat is rejected through the condenser in the atmosphere. The condenser can be air cooled, where heat is rejected by blowing ambient air on the condenser, or water cooled, where heat is rejected through a water loop implementing a cooling tower.

It is possible to increase the efficiency of the overall system by recovering part of the rejected heat to generate hot water. This can be obtained through a heat exchanger installed in the discharge line of the compressor before the condenser [35] as shown in Figure 7. Hot refrigerant gas from compressor carrying superheat is passed through this heat exchanger before entering the condenser. Superheat of refrigerant is recovered by this heat exchanger which is also called desuperheater [37, 38] whereas the latent heat is then rejected, as usual, to the cooling fluid in the normal condenser.

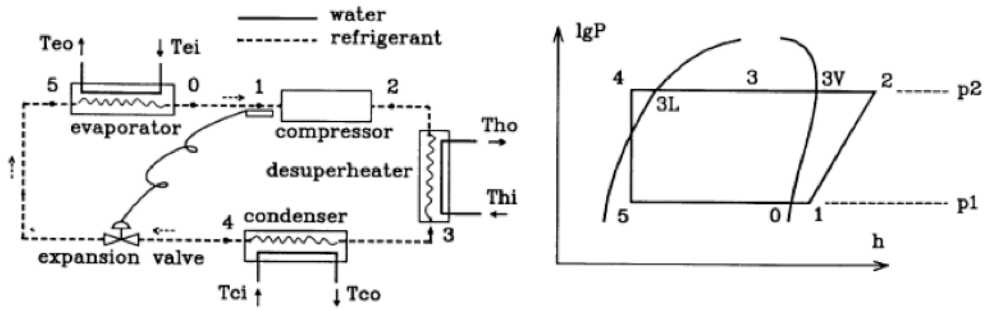

Figure 7 The refrigeration cycle complete with a desuperheater [38]

Other than the heat exchanger, the system includes a three-way valve to direct the refrigerant straight to the condenser when hot water is not needed, and an insulated tank to store and maintain the hot water when refrigeration and hot water are not needed at the same time.

Commonly used heat exchangers for this purpose consist of a shell-and-tube heat exchanger [38] or plate heat exchanger [37], which is a type of heat exchanger that uses metal plates to transfer heat between two fluids. A plate heat exchanger is a unit that transfers heat continuously between fluids without adding energy to the process. The advantage of using this type of heat exchanger is that the fluids are exposed to a large surface area because they spread out over the plates increasing the efficiency of the heat transfer.

Heat recovery systems increase the efficiency of a refrigeration/boiler system [38] in two ways: COP of the chiller is increased as adding the desuperheater increases the condensing area, which in turn leads to a reduced condensing temperature, and energy used in the boiler (or other system) to generate hot water is reduced.

Heat recovery has no operating costs, but the extra exchanger increases the complexity of the machine, requiring higher installation and maintenance costs.

2.2.5.2 Desiccant wheel

Several systems implementing energy recovery devices have been designed in the past [34]. The focus of these systems was on reducing the sensible heat load with little emphasis on latent heat transfer or moisture transfer. Typically fixed plate, sensible heat transfer wheel, heat pipe and coil run around loop heat exchangers have been used. These heat exchangers cannot be used to directly control the indoor humidity. This is usually performed using auxiliary cooling and heating equipment which is costly to install and operate [39].

One way of reducing the humidity is to use the air conditioning system to bring the temperature of the air, which needs to be conditioned, to a temperature below its dew point. In doing so, the humidity in the air condenses. The air is then reheated to the temperature needed [40].

When impregnated with a hygroscopic material, sensible heat transfer wheels are often referred to as enthalpy wheels and are also capable of drying the make-up air supply, thus providing a further thermal load reduction [36]. An enthalpy wheel then exchanges heat and humidity from one air-stream into another.

Hygroscopic materials are also used as desiccant material in the design of HVAC system where non-cyclical types of design are used and the desiccant is contained by surface (or bed) rotary wheel. Rotary wheels are operated within two sections, namely the adsorbing section where dehumidification occurs, and a regeneration section (desorption of water vapour) where the desiccant is reactivated by passing hot air [41]. In this system, regeneration and supply air streams are passing through separate sections of the desiccant wheel which needs to be completely separated. The regeneration and adsorption air streams are in a counter flow arrangement [42]. Leakage of air from one side to the other can cause inefficiencies and reduce the ability of the machine to produce low humidity air.

Another design adopted for the desiccant material consists of desiccant packed into a container and used in a cyclical type of operation. When two containers are used one can be dehumidifying while the other is being regenerated and vice versa. Using this system results in having different levels of dehumidification outputs because of the decreasing adsorber efficiency with the rising moisture content during the dehumidifying stage.

Desiccant materials have hygroscopic properties and high affinity for water vapour. Basically the working principle is the difference of vapour pressure between the desiccant surface and the air that needs to be dried.

Desiccant materials are normally solids (adsorbent) or liquids (absorbent) [43]. Absorbents use consists of a substance to chemically integrate into another. A typical example is salt dissolving in water and becoming salt water. Absorbents generally can attract and hold great quantities of water per each unit of desiccant material, however the issue of handling a liquid becomes a primary consideration.

Adsorbers are mainly solid porous material. Adsorption consists of the physical attraction and adherence of gas or liquid molecules to the surface of a solid. The force of attraction is very small, Van der Waal's forces, and does not change the physical characteristics of the substance. Adsorbent materials hold water molecules in pores at their surface, with no chemical change resulting. Compared with the liquid desiccant system in which the liquid and air directly interact, the solid one is compact and less subject to corrosion [44].

When exposed to low relative humidity, desiccant materials come to equilibrium at low moisture contents, and conversely exposure to high relative humidity results in equilibrium at high moisture contents. When it is cool and dry, desiccants have low surface vapour pressure and they can attract moisture from the air that has a higher vapour pressure when it is moist. After the desiccant adsorbs the moisture, it becomes wet and hot (exothermic reaction) and its surface vapour pressure becomes high.

A system using a desiccant wheel uses hot air to regenerate the rotor and this occurs by desorbing the moisture that is adsorbed by the adsorption material, therefore requiring less energy to cool the air [45].

When the level of humidity in the air stream falls below the saturation point of the desiccant, it will begin to release moisture back into the air stream.

A desiccant evaporative cooling (DEC) system consists of three main parts, namely the process side, regeneration side and the desiccant wheel [46] as shown in Figure 8.

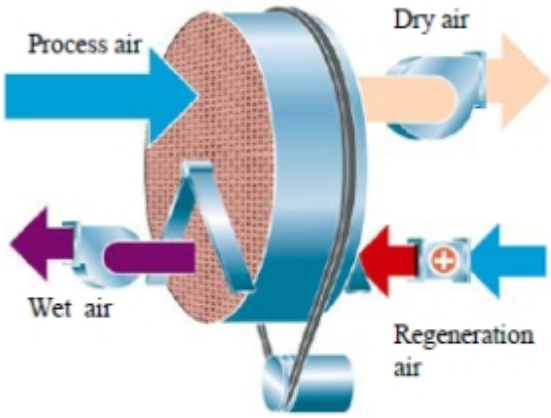

Figure 8 Typical desiccant wheel (courtesy of www.foodprocessing-technology.com)

The desiccant wheel is a revolving cylinder-shaped wheel divided into two sections; the process section and the regeneration section. The wheel rotates slowly; the process air from one side is sent through to the other side of the wheel. As the air passes the desiccant wheel, the desiccant material adsorbs and holds the moisture. Heat of sorption is released as desiccant adsorbs water vapour. The heat generated in the desiccant is transmitted through the material which decreases the sorption capacity. Therefore, the heat and mass transfer within the desiccant are coupled and should be considered simultaneously in developing mathematical models [44]. The condition of the process air, which goes into the desiccant wheel, is hot and humid. However, when the air leaves the desiccant wheel the condition of the air is hotter and dry. Simultaneously, at the regeneration side, the air is heated to raise its temperature and passed through the wheel in the opposite direction of the process air. During the desorption phase the surface vapour pressure of the desiccant material rises, and the moisture from the desiccant material is transferred to the regeneration air stream. The air leaving the desiccant wheel at regeneration side is warm and wet [47].

Desiccant wheels are quickly becoming popular as an environmentally friendly alternative to the typical system due to the fact that they can be powered by low-grade thermal energy sources such as geothermal heat, solar energy and waste/combustion heat from fossil fuels [44, 47-49].

Since this system has been patented, there have been many reports on desiccant cooling system performance so far. Parameters optimisation on DEC was one of the important works. However, to date, COP for DEC has been usually about 0.5-1.0 [42, 50].

The moisture is reduced by the desiccant until it reaches equilibrium [43]. For the regeneration of the desiccant, the moisture can be removed exposing it to a regenerative air stream heated to temperatures around 60–90 °C [42].

The overall performance of rotary wheels is influenced by several design and operating parameters such as [41]:

- the number and area of different regions
- flute geometry
- depth of rotary wheel
- desiccant loading
- adsorption characteristics of the desiccant
- airflow rates (and temperature through different regions)
- wheel speed.

Also, the wheel performance decreases as the outdoor temperature increases and the humidity decreases. To reduce this effect, the regeneration temperature needs to be increased [48]. This is evidenced by the fact that the use of solar desiccant systems presents some technical limitations in hot and humid climates, mainly due to the high latent loads handled by the wheel [51].

Control of the rotation speed of the rotor to the optimum is needed to bring out the best performance in a rotary adsorptive dehumidifier itself and in the desiccant cooling process [52]. The rotational speed of a rotary desiccant dehumidifier is at an optimum when the average outlet humidity ratio of the process air flow is at a minimum [42].

The sorption behaviour of a substance is represented in a graphic called sorption isotherm as shown in Figure 9. It describes the relationship between the water content of the substance and the relative humidity of the ambient air at a constant temperature.

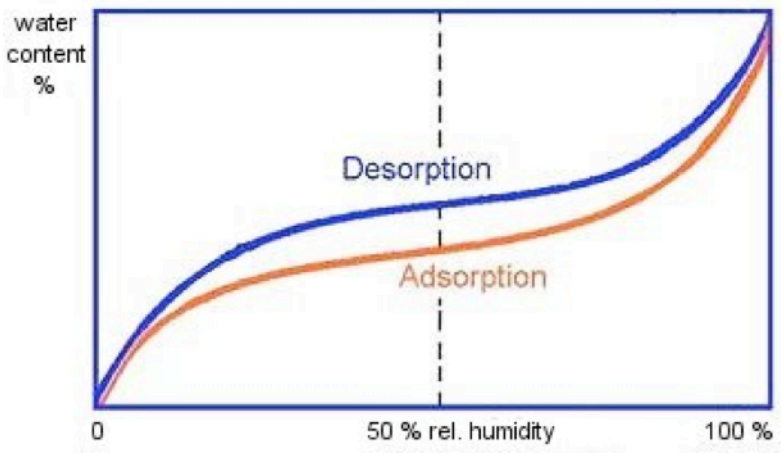

Figure 9 Adsorption and desorption curve (courtesy of Transport Information Service)

Sorption processes are complex to model and calculate. The values during water vapour adsorption and water vapour desorption need to be recorded experimentally for each product. As shown in Figure 9 the values between adsorption and desorption are different. The values for the desorption isotherm are always higher than those for the adsorption isotherm. The differences between adsorption and desorption isotherms are at their greatest at 50% relative humidity. The adsorption isotherm at 20°C, which describes the state of hygroscopic goods after manufacture, is generally used in practice.

The profile of a sorption isotherm is characteristic of the hygroscopicity of a product. Highly hygroscopic substances exhibit a steep sorption isotherm, while sparingly hygroscopic goods exhibit flat sorption isotherms.

Various aspects of desiccant cooling systems and absorption chillers have been investigated and published by many researchers. Most of the studies on desiccant dehumidification relate to feasibility studies [46, 53], performance predictions [45, 54-56], wheel optimisations [53, 57], and the development of new materials [58-60].

As explained before, the critical component of the wheel is the desiccant material which is used to adsorb the moisture. Currently, one of the most common solid desiccant materials used is silica gel [54]. So far, silica gel has been the most popular and the best material to remove moisture in the air. It has been widely used in industrial sectors [59]. Other common desiccant materials used are:

- activated alumina [61]
- natural and synthetic zeolites [50]
- titanium silicate [50, 62]
- lithium chloride [63]

- synthetic polymers [50]
- calcium chloride [46].

Some of these materials can be regenerated (purged of contaminants and reused) and some cannot. It depends on the change in the physical structure of the desiccant and the deleterious effects of regeneration on the material [50].

The adsorption capacity of silica gel decreases quickly with the rise of temperature, especially when the partial pressure of water vapour is low. The adsorption capacity of natural and synthetic zeolites is not very sensitive to the water vapour partial pressure. Compared with silica gel, lithium chloride and calcium chloride have a higher hygroscopic capacity, but the lyolysis phenomenon, which leads to the loss of desiccant materials and may reduce the performance, often takes place after the formation of solid crystalline hydrate [55].

Recent research on the desiccant system is mainly focused on the development of advanced desiccant materials that have improved sorption capacity and better moisture and heat diffusion rates, as well as favourable equilibrium isotherms [55].

New composite desiccant wheels can remove more moisture from the air, about 40-50% higher as compared to the silica gel one [50].

Alternative materials such as zeolite and super adsorbent polymer have been tested at low temperature [59]. It was found that silica gel showed better performance compared to zeolite in low humidity environments; however, it has been observed that both materials show similar performance in high humidity environment. At a lower regeneration temperature, the super adsorbent polymer performs better than the silica gel, but decreases rapidly when the air relative humidity reduces. It was concluded that the silica gel overall has better performance compared to zeolite and polymer.

A two-layered combination of silica gel and lithium chloride, which can operate at low regeneration temperature, has been tested. It was observed that the new composite desiccant material has higher ability to adsorb moisture and has the capability to remove approximately 20% to 30% more of the humidity compared to silica gel [50].

A study ascertaining the hygroscopic effect of the composite material using silica gel (SG) and Calcium Chloride ($CaCl_2$) applied onto a corrugated paper (CP) shows the composite material CP-SG-$CaCl_2$ has a higher hygroscopic effect and is able to achieve an equilibrium when compared to CP-SG. [60].

A comparison between silica gel and composite desiccant material was made based on the combination of silica gel and Lithium Chloride (LiCl). The experiment

revealed that the composite desiccant material has the capacity to remove up to 50% moisture in the air. It has been observed that both desiccant materials showed weakening capability to remove moisture when the inlet temperature was increased [55].

Solid desiccant cooling systems using four types of desiccant materials were tested [58]. The materials used were 13 X molecular sieves, silica gel, DH-5 and DH-7. The results showed that DH-5 and DH-7 performed better when compared to silica gel and 13 X molecular sieves. It was also found that DH-7 has double the cooling capacity compared to silica gel. The outcome of the experiment revealed that DH-5 and DH-7 are suitable to operate in desiccant cooling system.

Desiccant materials are continuously exposed to cyclical hydrothermal adsorption and desorption processes; their performance deteriorates more rapidly in the beginning of the process and stabilises thereafter. Further deterioration would be more noticeable before the desiccant reaches the end of its life cycle. Alumina and silica gel are found to be ageing quicker after being exposed to a large number of adsorption/desorption cycles under desorbing temperature of 200 °C [53].

Due to the fact that desiccant systems are quite efficient in dealing with the latent load, but considerably less efficient in dealing with sensible load, two design solutions have been adopted to overcome this inefficiency. One design solution consists of using the desiccant cooling system to deal with the latent heat while a vapour-compression heat pump deals with the remaining sensible heat. The other solution consists of improving the performance of the desiccant wheel and making the process air sufficient dry so that the sensible heat can be removed entirely by means of evaporative cooling [50].

It has been experimentally tested that combining desiccant wheel technology with other systems, such as vapour-compression and chilled-ceiling systems, can increase the COP to 20-30% and create an operating savings of around 35% [64]. A feasibility study of a hybrid system combining a vapour-compression cycle and desiccant cooling technology increasing the efficiency of the latter found that hybrid desiccant wheels could save electricity energy of up to 37.5% when compared to conventional vapour compressors at a controlled air temperature of 30 °C and humidity of 55% [65]. The electricity savings were possible due to a high evaporation temperature of the hybrid desiccant wheel that allowed the evaporators to work in “dry conditions” (without condensation on the evaporator). Experimental tests investigating a hybrid desiccant cooling system and air conditioning system using lithium chloride as desiccant

material found that the performance of the system depends largely on the regeneration temperature and the rate of the processed air flow [57].

Various configurations of HVAC system with desiccant wheels, one step or more steps, have been employed for the conditioning of buildings. Energy comparisons between some of them are proposed in the technical literature. Energy savings with respect to traditional HVAC systems have been reported, the required thermal cooling power is reduced (up to 52%) with respect to the traditional system [66].

2.2.5.3 Shaw method of air conditioning (SMAC)

In the current typical design of an air conditioning system, air is treated in an AHU [67]. The treated air consists of a mix of air returning from the ambient air (return air) and fresh air (outside air) coming from the outside. The condition of the air stream that needs to be treated depends on the condition of the outside and return air.

The heat transfer through the coil in the AHU has the purpose of removing the sensible and latent heat from the air stream. This design of the air conditioning system cannot separate the sensible and latent heat loads which is a concern in any typical conventional system especially when it is needed to treat air with high relative humidity and low sensible loads.

In a typical AHU unit, the air is treated by passing across a cooling coil in which the chilled water passes inside the tubes while the air passes over the tubes and fins of the coil. The condition of the treated air depends on the psychometric performance of the cooling coil.

In the current design, air is cooled below the dew point temperature to remove the humidity and then reheated before being supplied to the areas that need to be air conditioned. The reheating of the air is an inefficiency of the current design. Nowadays it is good practice to reduce this inefficiency by reusing heat rejected by the condenser of the chiller for the reheating of the air.

Research performed in the past aimed at achieving energy efficient dehumidifying performances by addressing the air velocity across the coil, the chilled water velocity through the tubes of the coil, and by various configurations of the physical geometry of the coil [68].

A new developed twin cooling coil energy efficient method of air conditioning involves the independent control of temperature and humidity of two different air streams. The main difference is in dehumidifying the incoming air by a separate outside

coil before mixing it with the return air as shown in Figure 10. A separate dry cooling coil through which return air passes controls the temperature within the air conditioned air.

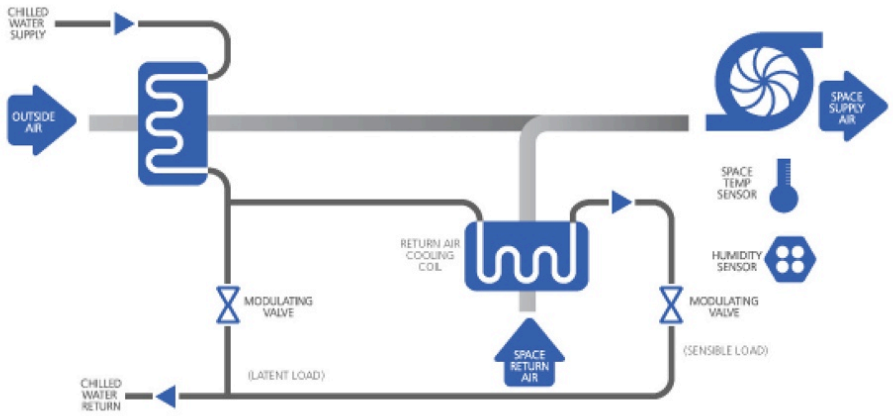

Figure 10 Diagram of the new design for the air conditioning (courtesy of www.smactec.com)

The key features of the new design are:

- Dual coils separate the process of treating latent loads (typically to remove moisture from outside air) and sensible loads (typically internal air which is dry).
- Series pipe circuiting maximises the system's efficiency.
- Controls provide integrated control of humidity, temperature and chiller operation to ensure that air treatment processes optimise energy performance at all times.

The Shaw method or process for air conditioning increases cooling energy efficiency by 30-50% compared to traditional systems through [69]:

- the ability to prevent "over cooling" in humid climates
- increase the temperature of chilled water up to 15 °C (current system use approximately 7 °C) so that the COP of the chiller increases
- reduced or eliminated reheat requirement.

2.3 SOLAR AIR CONDITIONING SYSTEMS

The sun's energy radiated on the Earth, properly collected and concentrated, can easily be used not only to produce a hot fluid or superheated steam at different

temperatures for domestic or industrial use, but also to produce a chilled fluid for refrigeration by providing hot water to the generator of an absorption chiller thereby creating a "solar cooling system". Most of the thermally driven cooling systems these days, including solar air conditioning systems, are based on absorption chillers [13, 70].

2.3.1 Introduction

Due to the increasing energy consumption of air conditioning in building and the need to reduce CO_2 emissions to the environment, the interest of using renewable energy sources to supply air conditioning in buildings is increasing [71]. Solar energy, often correlated to the cooling demand of a building [17, 72], is probably the best energy resource to be associated with an air conditioning system [70].

Studies of the different technologies for solar energy applications have been undertaken in the past [73] and it has been found that coupling solar thermal panels with a single effect absorption system is the best choice for a solar cooling system. Specifically, the major part of a solar cooling system uses a thermally driven single effect ammonia-water absorption chiller [74] because of its limited cost and maintenance required, or a lithium bromide water absorption chiller [70].

2.3.2 Solar collectors

Because the absorption chiller requires hot water at temperatures in the range of 125°C to 170°C with air cooled absorber and condenser in the range of 80°C to 120°C when water cooling is used [13, 17, 75], evacuated tube collectors are used in the system because of their high efficiencies at those temperatures [76] which are comparable to the efficiency of the compound parabolic collectors (CPC) but at lower cost [17].

An all-glass evacuated solar tube consists of two concentric tubes made by borosilicate material, sealed at one end with an annular vacuum space and a selective surface absorber on the out surface (vacuum side) of the inner tube. In practical applications, solar tubes can be horizontally arranged or tilt arranged to form a solar collector or module [77].

Maintenance costs for the evacuated tube collectors are reduced as their cylindrical shape allows them to shed dust and dirt that would otherwise accumulate on a flat surface. Evacuated tube collectors can be divided into two types: direct flow through collectors, and heat pipes inside the vacuum tubes. In the direct flow, the heat transfer fluid that needs to be heated flows through the tubes in the collectors. The second type consists of heat pipes inside vacuum sealed glass tubes which offers the advantage of a

simpler hydraulic interconnection of the solar circuit with a lower pressure drop while reducing the system load during stagnation. A reflector can be present to optimise the absorption of the solar radiation [76].

An advantage of using the heat pipes type collectors is the "dry" connection between the absorber and the header, which makes installation easier and also means that individual tubes can be exchanged without emptying the entire system of fluid. Also, tubes can easily and inexpensively be added, removed or replaced.

When evacuated tubes are made, air is evacuated from the space between the two tubes, forming a vacuum. Conductive and convective heat losses are eliminated because there is no air to conduct heat or to circulate and cause convective losses. The collectors perform well in both direct and diffuse solar radiation. Evacuated-tube collectors achieve high temperatures and do radiate some of the heat gained, but these losses are small compared to the amount collected.

The heat is transferred to a heat pipe. In turn, the pipe transfers heat to the water flowing through the header of the collectors.

When sunlight passes through the clear glass tube, it strikes the absorber plate, which is coated with a selective coating making it very efficient in absorbing and retaining heat. A round black copper absorber plate inside the tube's double glass wall wraps around a heat pipe. The heat pipe is hollow and the space inside, like that of the solar tube, is evacuated. As liquid inside of the heat pipe vaporises, it conducts heat to the collector's manifold and heats the water.

Unlike the flat-plate collectors, all-glass evacuated tube solar collectors should be generally mounted with a tilt-angle less than the site latitude in order to maximise the annual energy collection. For most areas with a site latitude larger than 30°, T-type collectors (collectors with solar tubes tilt-arranged) should be installed with a tilt angle about 10° less than the site latitude [77].

Efficiency of the solar panels is measured following the standard EN 12975-2 [76].

2.3.3 Cooling sources –Absorption chiller

Absorption systems are similar to vapour-compression air conditioning systems but differ in the pressurisation stages. They are heat-operated devices that produce chilled water without the use of a compressor via an absorption cycle allowing a significant reduction in the electricity consumption. The heat source usually consists of

gas fuel combustion, steam, high temperature exhaust gas or hot water. Very little electricity power is required to operate the pump, which is used to circulate the solution of refrigerant and transport medium in the chiller. This makes them also suitable for remote locations where electricity is not available.

In absorption chillers an absorbent fluid on the low-pressure side absorbs an evaporating refrigerant. The most usual combinations of fluids include lithium bromide–water ($LiBr–H_2O$) where water is the refrigerant and lithium bromide is the transport medium, and ammonia–water ($NH_3–H_2O$) systems where ammonia serves as the refrigerant and water as the transport medium [78]. As in the vapour compression, in the absorption refrigeration cycles the removal of heat is achieved through the evaporation of a refrigerant at a low pressure and the rejection of heat through the condensation of the refrigerant at a higher pressure. The pressurisation stage in the absorption cycle is achieved by dissolving the refrigerant in the absorbent in the absorber section. Subsequently, the solution is pumped to a high pressure with an ordinary liquid pump. The addition of heat in the generator is used to separate the low-boiling refrigerant from the solution. In this way the refrigerant vapour is compressed with little amount of mechanical energy.

Utilising a water/ammonia solution with the ammonia as refrigerant and the water as absorbent, it is possible to achieve temperatures as low as -30 °C [78], so this system is better suited for industrial fridge cycles. An absorption fridge cycle using water as refrigerant and lithium bromide as absorbents can attain a temperature between 3 °C and 5 °C which makes the system useful for air conditioning applications. Using the water as refrigerant means there is a limitation of the minimum temperature achievable which is above 0 °C.

Absorption chillers can be half-effect, single-effect or double-effect, where one or two vapour generators are used. Double-effect chillers use two generators where the second generator uses the heat rejected by the condenser of the first generator to increase the amount of refrigerant available through the cycle, thereby increasing the refrigeration effect and the efficiency.

The remainder of the system consists of an absorber, condenser, expansion valve and an evaporator, which function in a similar way as those in a vapour-compression refrigeration cycle. A typical schematic diagram of a single effect absorption chiller is shown in Figure 11 [79].

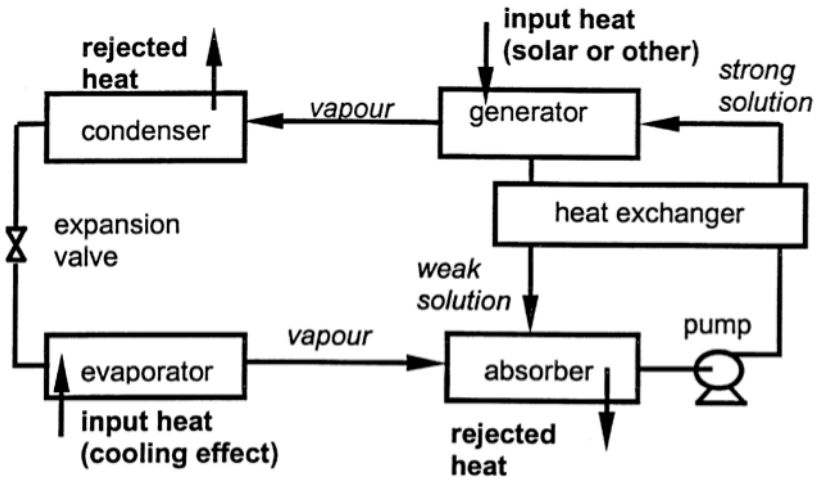

Figure 11 Flow diagram for absorption cycle system [17]

2.3.3.1 Single stage absorption chiller components

Several models of absorption chiller are available and are reported in literature [6, 80-84]. The following paragraphs describe the typical design of a water ammonia absorption chiller from Robur[2] that is one of the major absorption chiller manufacturer. The system includes several heat exchangers used as evaporator, condenser, solution absorber generator, rectifier, refrigerant heat exchanger and a solution heat exchanger. Two expansion devices are used as well.

Figure 12 below shows a conceptual diagram of the described system.

[2] www.robur.it Verdello (BG) Italy

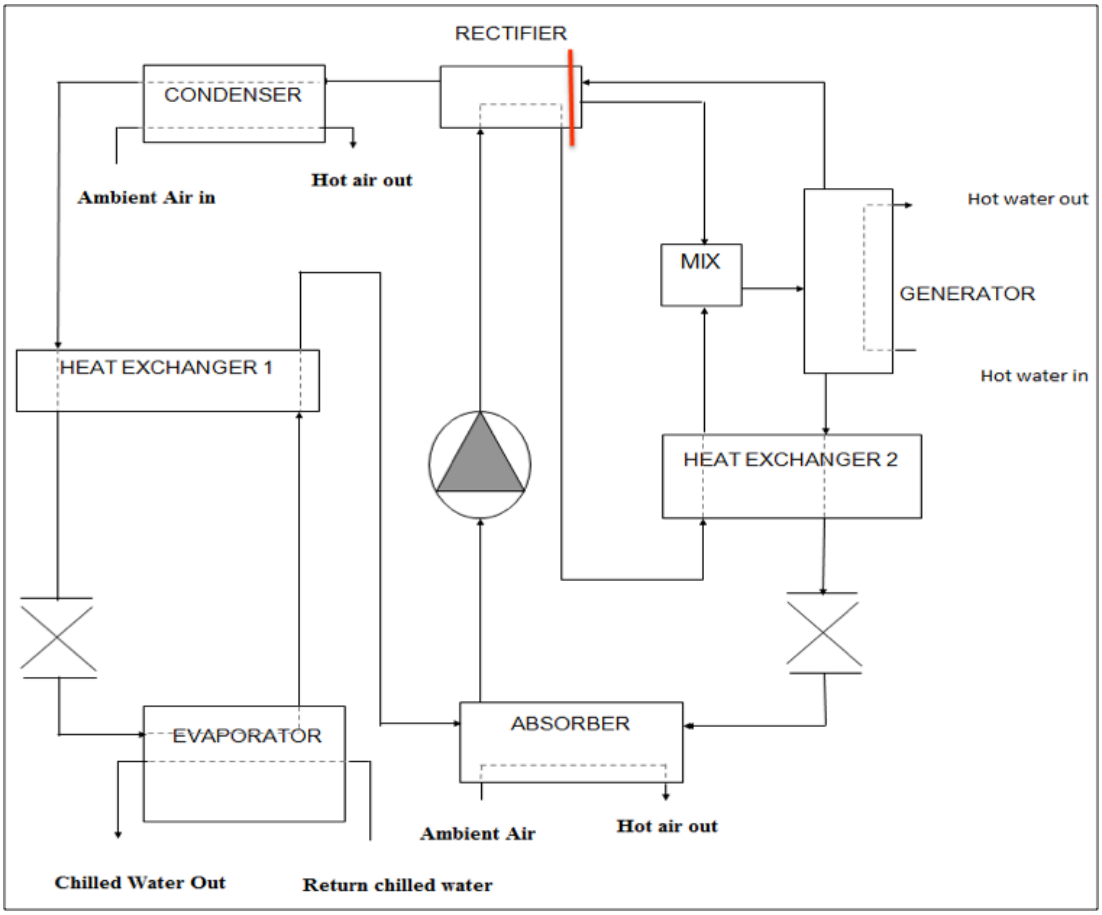

Figure 12 Diagram of the single stage absorption chiller described

The system has been numbered as shown in Figure 13 to identify the different sections and to help in understanding the states of the refrigerant/solution during the process as indicated in Table 1.

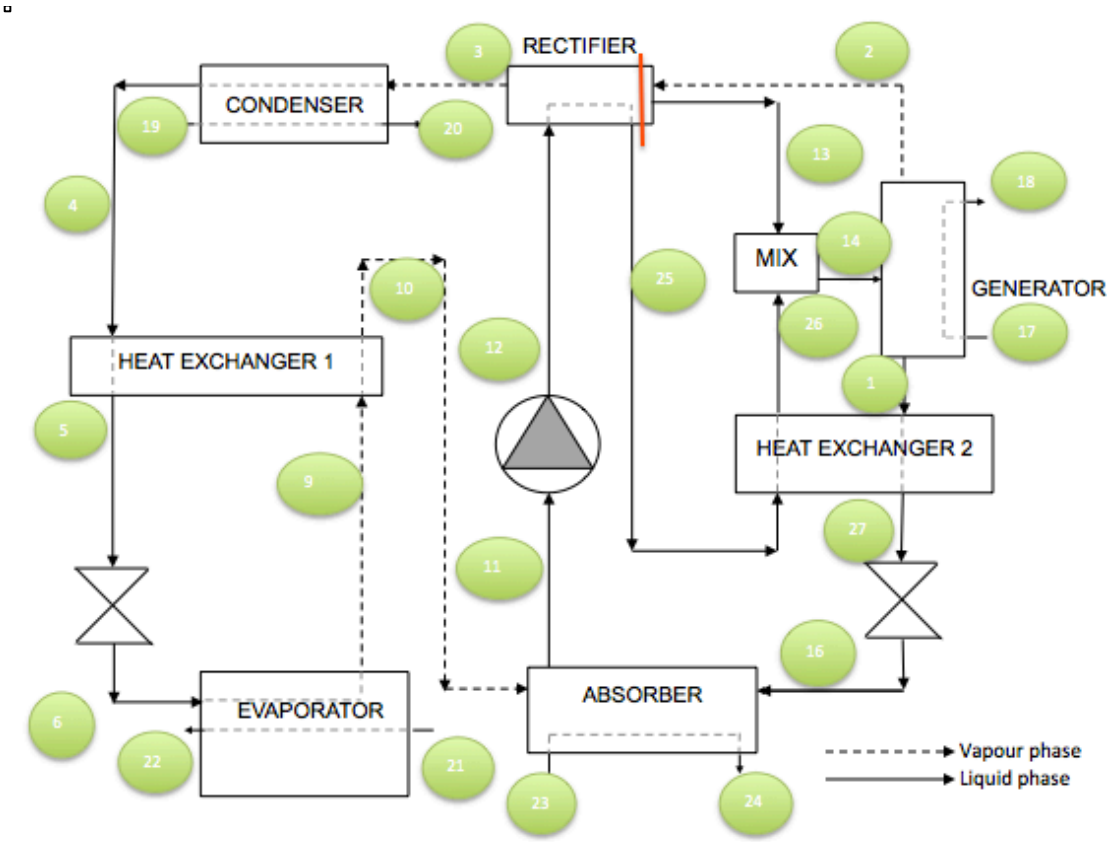

Figure 13 System states numbered

Dashed lines indicate the vapour phase in the cycle whereas solid lines indicate the liquid phase in the cycle. The direction of the cycle is indicated by the arrows in the diagram.

Number of each state and its state description is given in Table 1.

Table 1 State of the refrigerant /absorber in the system

States	Description
1	Weak solution from generator
2	Refrigerant vapour from generator
3	Refrigerant vapour from rectifier
4	Liquid refrigerant from condenser
5	Liquid refrigerant from heat exchanger 1
6	Liquid/vapour refrigerant from expansion valve 1
9	Strong vapour from evaporator
10	Strong vapour from heat exchanger 1

11	Strong solution from absorber
12	Strong solution from pump
13	Strong solution from rectifier
14	Strong solution from mix
16	Weak solution from expansion valve 2
25	Strong solution from rectifier, used for condensing the water in
26	Strong solution from heat exchanger 2
27	Weak solution from heat exchanger 2
17	Hot water from heat source
18	Warm water leaving from generator
19	Air for cooling condenser
20	Warm Air leaving condenser
21	Chilled air input
22	Chilled air output
23	Air for cooling absorber
24	Warm Air leaving absorber

In the following paragraphs each part of the chiller is described in detail, using the same numbering scheme as in Figure 13.

2.3.3.1.1 GENERATOR

The generator consists of a heat exchanger between the solution and the heat source of the system. The heat is transferred into the generator to boil the solution and to turn the refrigerant into vapour. The ammonia vapour moves then into the rectifier. The vaporisation of ammonia from the solution leads to the formation of a weak water-ammonia solution (low concentration of ammonia), which moves to the adsorber after flowing into the heat exchanger 2. Figure 14 shows the diagram of the generator in the system.

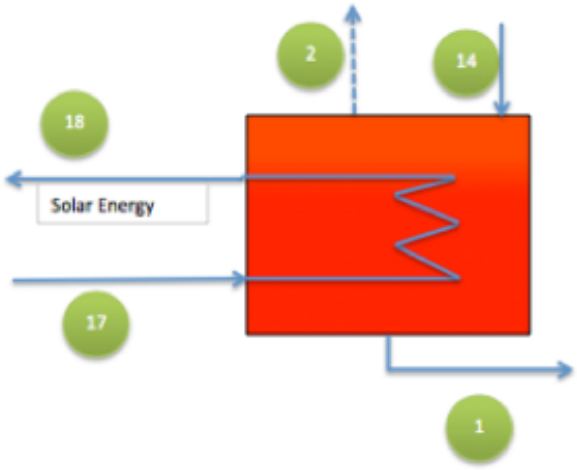

Figure 14 Scheme of the generator

The vapour leaving the generator at point 2 is rich in ammonia and the weak solution at point 1 is rich in water.

2.3.3.1.2 RECTIFIER

The vapour from the generator is a mixture of water and ammonia, but water vapour is undesirable in the refrigerant as it could get accumulated in the evaporator thereby reducing the refrigeration efficiency. The function of the rectifier is to remove water from the water-ammonia vapour by cooling and redirecting the condensate, called also reflux, rich in water into the generator to be treated again.

To condense the water in the vapour it is used the low temperature strong solution from the absorber which is pumped into the rectifier at high pressure.

The strong solution reduces the temperature of the vapour absorbing heat causing the water in the vapour to condense.

Figure 15 shows the diagram of the rectifier.

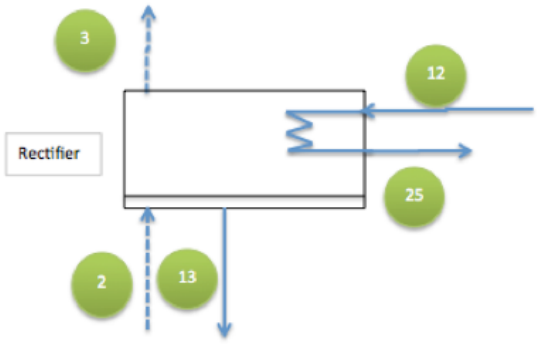

Figure 15 Scheme of the rectifier

The vapour leaving the rectifier (point 3) has higher ammonia concentration and it is directed to the condenser. It is to be noted that the pressure in the rectifier is the same as in the generator. The function of the rectifier is not only to condensate and to reduce the water vapour from the mixture but also to increase the temperature of the strong solution from the absorber. The medium temperature strong solution (point 13) flows into the heat exchanger 2 from the rectifier pipes.

2.3.3.1.3 CONDENSER

The condenser is where the saturated vapour condenses rejecting heat. During the condensation the heat rejected consists of latent heat so in this heat exchanger the temperature profile on the solution side is linear as shown in Figure 16.

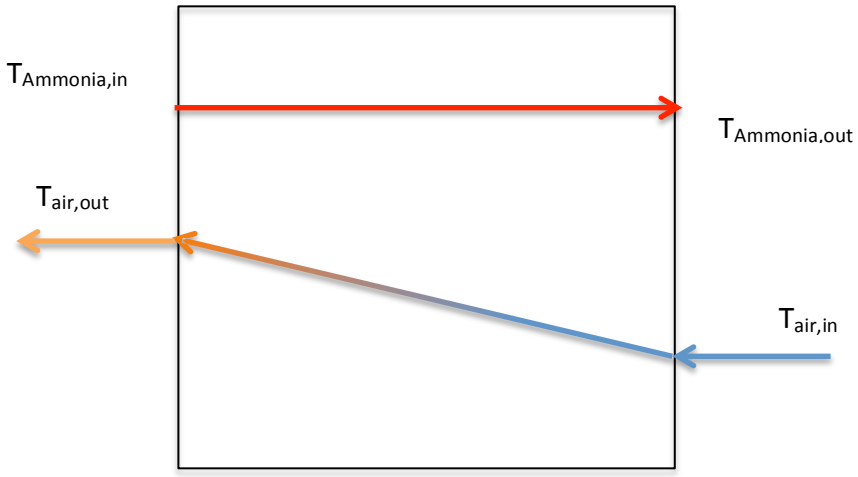

Figure 16 Variation of temperature across the heat exchanger

According to the laws of thermodynamics, it is easier to liquefy vapours at higher pressure. Figure 17 shows the diagram of the condenser in the system.

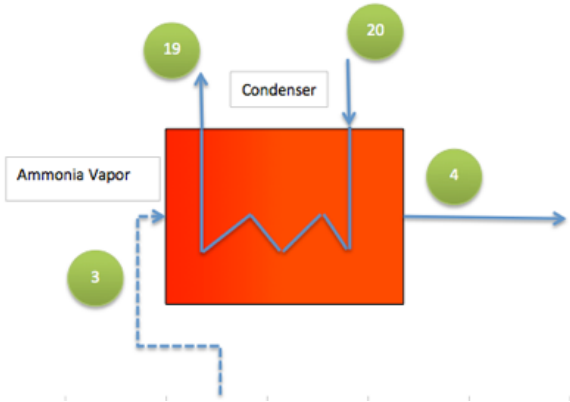

Figure 17 Scheme of the condenser

Pure ammonia is in vapour state at standard conditions (point 3). So reducing its t below the condensation temperature will turn ammonia into a liquid state. The nearly pure ammonia from the rectifier is condensed into liquid state by rejecting heat to the surrounding. The liquid ammonia from condenser (point 4) is passed through the heat exchanger 1 to recover some heat. The pressure in the condenser and in the rectifier is constant, only the temperature is reduced.

2.3.3.1.4 HEAT EXCHANGER 1

The liquid ammonia coming from the condenser is at high temperature and tends to convert back into gaseous state. In heat exchanger 1, the temperature of this liquid is further reduced by using cold vapour coming from the evaporator. This temperature reduction further enhances the efficiency of the system by improving its cooling capacity due to sub cooling of ammonia liquid. It is to be noted that the heat exchanger 1 transfers heat from high-pressure liquid ammonia to low-pressure ammonia vapour.

Figure 18 shows the diagram of the Heat exchanger 1 in the system.

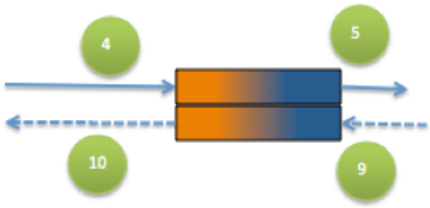

Figure 18 Scheme of heat exchanger 1

2.3.3.1.5 THROTTLE VALVE OR EXPANSION VALVE

The expansion valves in the circuit are used to create a pressure drop in the solution, producing an adiabatic expansion that leads to the refrigeration. During the expansion the solution increases its specific volume. Figure 19 shows the diagram of the expansion devices used in the system.

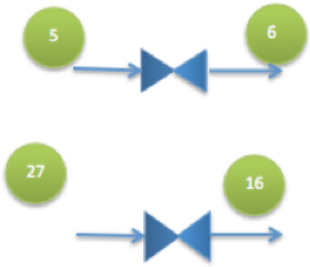

Figure 19 Expansion devices scheme

2.3.3.1.6 EVAPORATOR

The evaporator is the component where the heat exchange between air and refrigerant occurs. So the cooling effect of the machine is actually delivered at the evaporator. As the refrigerant is not pure ammonia but a solution of ammonia and water, a temperature glide occurs during the evaporation[3].

The liquid solution is allowed to flow from the condenser to the evaporator through an expansion valve. The pressure reduction of the liquid from high (in the condenser) to low (in the evaporator) reduces the boiling point of ammonia. Thus liquid ammonia absorbs heat from the air to evaporate and form vapours, which pass into heat exchanger 1. Figure 20 shows the diagram of the evaporator.

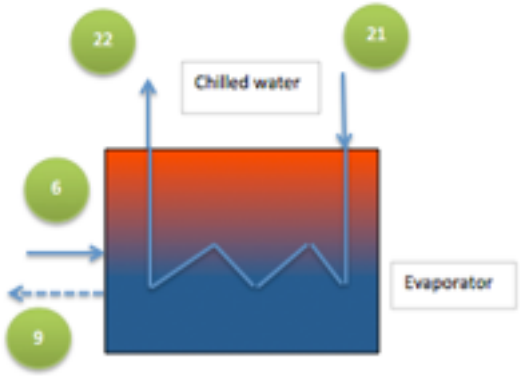

Figure 20 Scheme of the evaporator

2.3.3.1.7 ABSORBER

The vapour ammonia from heat exchanger 1 flows into the absorber Figure 21. Here, the low temperature gaseous ammonia is allowed to mix with weak solution of water-ammonia solution. The mix of weak solution and refrigerant is a saturated liquid and its concentration increases during cooling from the inlet to the outlet.

[3] glide is the temperature range within which the different components of the refrigerant/water evaporate at the same pressure

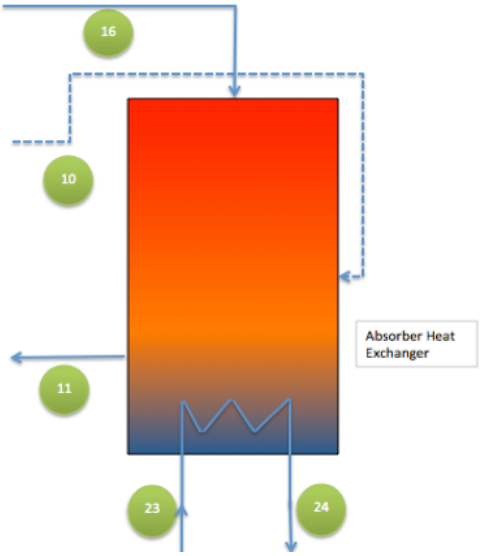

Figure 21 Scheme of the absorber

As the absorption of ammonia is an exothermic reaction, the heat has to be rejected to the surroundings. Also, by cooling the absorber the dissolution of ammonia speed up. Due to the absorption of ammonia, the pressure in the evaporator is reduced continuously. The weak solution is supplied from the heat exchanger 2.

The pressure in the absorber is equal to the pressure in the evaporator.

2.3.3.1.8 PUMP

The strong solution formed in the absorber has to be delivered back into the generator. A pump is required to push the strong solution from the absorber into the generator, thereby reducing the pressure in absorber and increasing the pressure in generator. Pump and throttle valves are responsible to generate the pressure difference in the system. As the pressure reduces the throttle valve 1 and 2 senses the pressure difference and allows the flow of fluid from the high pressure to the low-pressure section of the system. The low temperature strong solution from the absorber is pumped into the rectifier and heat exchanger 2 (point 12 and 25 of the diagram) before reaching the generator. The amount of energy used by the pump is usually very small.

Figure 22 shows the diagram of the pump used in the system.

Figure 22 Scheme of the pump

2.3.3.1.9 HEAT EXCHANGER 2

The high-pressure strong solution of ammonia water flowing from the rectifier (point 13) is passed through heat exchanger 2 (point 25) to absorb the heat from the hot weak solution flowing from the generator. This second heat exchanger reduces the heat required to increase the temperature of the new solution introduced into the generator. Also, the temperature reduction of the weak solution introduced into the absorber reduces the need of heat rejection considerably. So the coupling of heat exchanger 1 and 2 improves the efficiency of the whole system. Figure 23 shows the diagram of the heat exchanger 2.

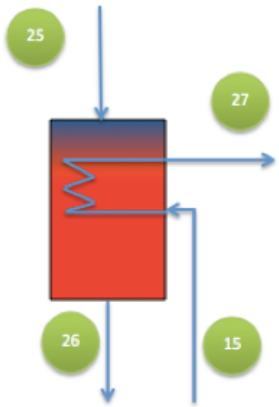

Figure 23 Scheme of heat exchanger 2

2.3.3.1.10 MIXER

In the mixer, two separate flows of strong solution from the absorber and condensate from the rectifier are mixed together through an adiabatic process before going to the generator. Figure 24 shows the diagram of the mixer.

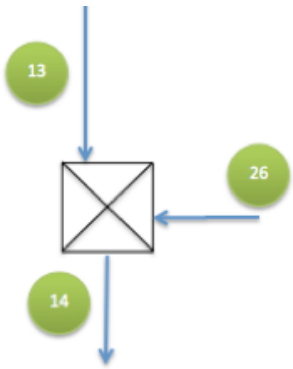

Figure 24 Scheme of the mixer

2.3.4 NH_3-H_2O absorption chillers in solar cooling

The NH_3–H_2O system is more complicated than the LiBr–H_2O system, since it needs a rectifying column to insure that no water vapour enters the evaporator where it could freeze. The NH_3–H_2O system requires temperatures in the range of 125 °C to 170 °C with air cooled absorber and condenser, and 80 °C to 120 °C when water cooling is used [17, 75].

Figure 25 shows the diagram of a typical solar cooling system.

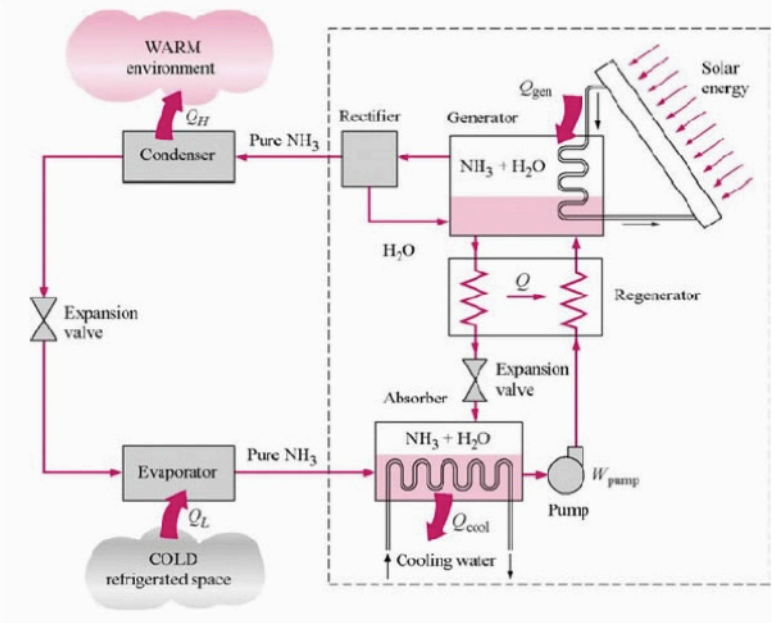

Figure 25 Solar cooling system schematic (courtesy of http://www.saylor.org)

The following paragraph describes the process of the absorption chiller applied to a solar cooling system [85] as indicated in Figure 25.

2.3.4.1 Description of the refrigeration process

The process starts with the water-ammonia solution heated using the solar energy Q_{gen} in the generator; the solution loses ammonia due to evaporation, creating a weak solution. The vapour stream is then passed through a rectifier to reduce its content of water before to be condensed in the condenser rejecting heat Q_H to the environment.

The flow is passed through an expansion valve to reduce its pressure and moves into the evaporator where the ammonia liquid absorbs heat Q_L from the surrounding to evaporate. The evaporation of ammonia requires latent heat of evaporation, which is responsible of the cooling effect of the system.

The vapour ammonia moves into the absorber where it meets with weak solution of ammonia water solution from the generator. Due to great affinity of ammonia towards

water, the vapour ammonia tends to form a strong solution of water-ammonia. The absorption of ammonia water by the weak solution is an exothermic reaction which liberates heat Q_{cool} which is removed using cooling water [86] resulting in the formation of a strong water-ammonia solution.

The strong ammonia water solution in the absorber at low pressure is pumped into the generator increasing the concentration of the liquid phase. The pump maintains the mass flow and pressure difference in the system. Two heat exchangers, not indicated in Figure 25, are usually added to the system. These heat exchangers have bee described in paragraph 2.3.3.1.4 and paragraph 2.3.3.1.9. The two heat exchangers improve the efficiency of the system, reducing the requirement of heat from solar panels significantly [87, 88].

Figure 26 shows the absorption cycle on a Dühring diagram, which relates the pressure and the temperature of the solution. In this representation the plots of saturation temperature versus saturation pressure are almost straight lines for most fluids and fluids mixture when the mass fraction is constant. The Dühring chart (Figure 26) is a useful tool to calculate the heat rejection temperatures, solution concentrations and equilibrium pressures [89].

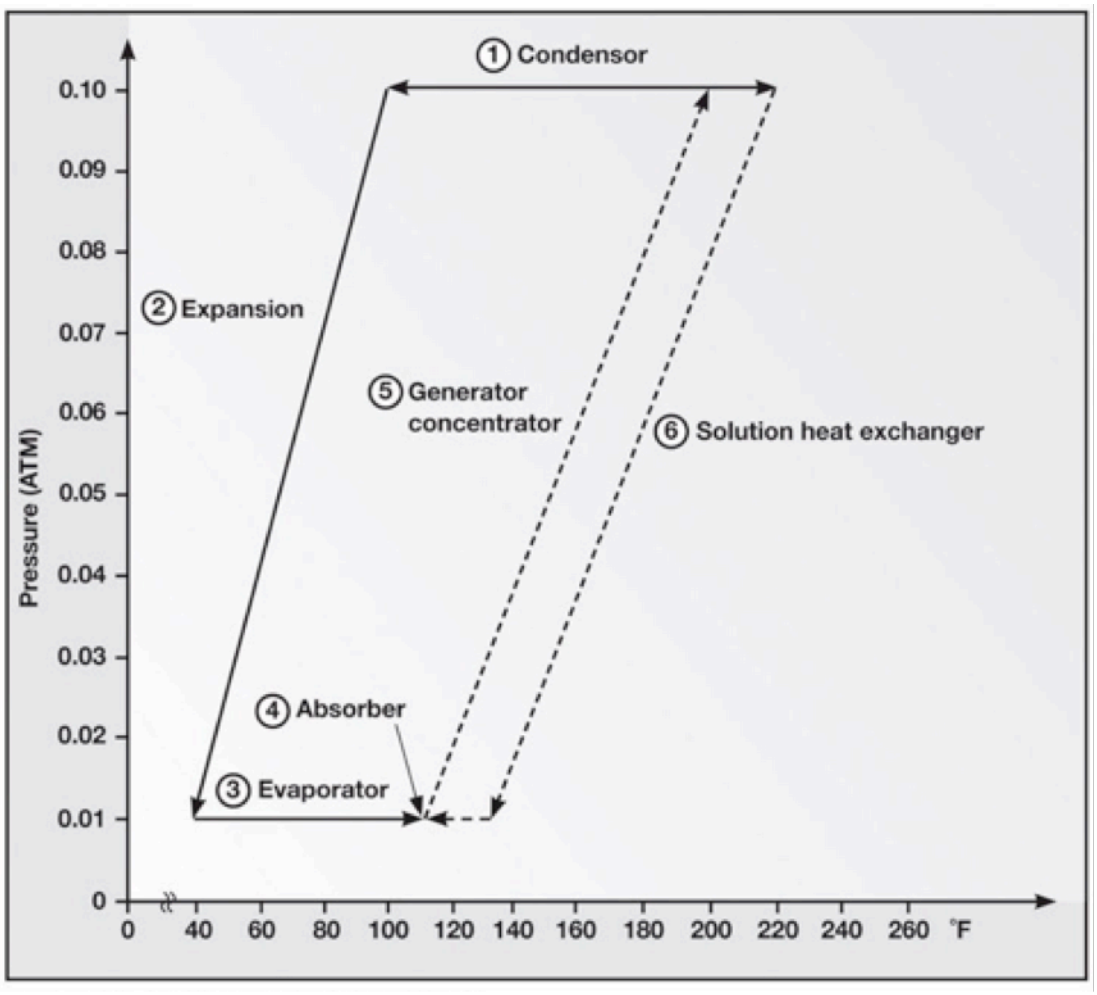

Figure 26 Dühring diagram

In the above diagram, the dashed lines are the NH_3-water sorbent solution and the solid lines represent the refrigerant. The lines are connected to form two complete cycles: the sorbent solution cycle and the refrigerant cycle [90]. The single-effect absorption chiller has five main steps: condensing (condenser), expansion (expansion pipe), evaporation (evaporator), absorption (absorber), and generator/concentrator. The major chiller components are indicated on the diagram. Like the vapour compression chillers, absorption chillers have a high-pressure side (generator/concentrator, condenser) and a low-pressure side (expansion pipe, evaporator, absorber).

Condenser: In the condenser, the heat of condensation from the vaporised refrigerant is rejected, changing the refrigerant into a liquid.

Expansion: The liquid refrigerant (ammonia) travels from the condenser through expansion piping to the evaporator during which the liquid refrigerant experiences a drop in pressure and temperature. The liquid refrigerant is discharged into a pan within the evaporator.

Evaporator: The liquid refrigerant (ammonia) is pumped to the chilled water tube bundle top and sprayed on the tube bundle. At a low evaporator pressure the liquid refrigerant vaporises removing energy from the chilled water. Liquid refrigerant that is not vaporised drops down to the pan and is recirculated. Liquid refrigerant that is vaporised travels from the evaporator to the absorber.

Absorber: The vaporised refrigerant enters a liquid ammonia-water weak solution (low concentration of ammonia) spray within the absorber. The weak solution absorbs the vaporised refrigerant and the heat of vapour absorption is rejected. After the absorption, the strong solution (high concentration of ammonia) is pumped to the generator/concentrator [82, 91, 92].

Generator/concentrator: The solution enters the generator/concentrator and is heated raising the solution to a temperature where the liquid refrigerant (ammonia) vaporises and travels to the condenser, completing the refrigerant cycle. The weak water-ammonia solution flows down to the absorber, completing the absorber cycle [93].

The work input to the pump is usually very small, and the COP of absorption refrigeration, which is defined as the ratio of the cooling capacity to the energy input into the system, is defined as:

$$COP = \frac{\text{Cooling } Capacity}{\text{Energy input}} = \frac{Q_L}{Q_{gen} + W_{Pump}} \tag{2-11}$$

The COP of the system can be modelled following Bosnjakovic [8].

First law of thermodynamics

$$\dot{q}_{abs} + \dot{q}_{con} = \dot{q}_{evap} + \dot{q}_{gen} + \dot{W}_p \tag{2-12}$$

Where $\dot{q}_{abs}$ is the heat rejected by the absorber, $\dot{q}_{con}$ is the heat rejected by the condenser, $\dot{q}_{evap}$ is the heat exchanged by the evaporator, $\dot{q}_{gen}$ is the heat exchanged in the generator and $\dot{W}_p$ is the external work supplied to the pump

$$\dot{q}_{amb} = \dot{q}_{abs} + \dot{q}_{con} \tag{2-13}$$

Second law of thermodynamics requires the net change in entropy for the system to be greater than zero.

$$\Delta S_{total} = \Delta S_{gen} + \Delta S_{evap} + \Delta S_{amb} \geq 0 \tag{2-14}$$

Rearrange the equation yields;

$$\Delta S_{gen} = \frac{\dot{q}_{gen}}{T_{gen}} \quad , \Delta S_{evap} = \frac{\dot{q}_{evap}}{T_{evap}} \quad , \Delta S_{amb} = \frac{\dot{q}_{amb}}{T_{amb}} \tag{2-15}$$

and

$$\Delta S_{total} = -\frac{\dot{q}_{gen}}{T_{gen}} - \frac{\dot{q}_{evap}}{T_{evap}} - \frac{\dot{q}_{amb}}{T_{amb}} \quad (2\text{-}16)$$

by combining equations (2-15)) and (2-16).

$$\dot{q}_{gen} \frac{T_{gen} - T_{amb}}{T_{gen}} \geq \dot{q}_{evap} \frac{T_{amb} - T_{evap}}{T_{evap}} - \dot{W}_p \quad (2\text{-}17)$$

Neglected pump power

$$COP = \frac{\dot{q}_{evap}}{\dot{q}_{gen}} \leq \frac{T_{evap}(T_{gen} - T_{amb})}{T_{gen}(T_{amb} - T_{evap})} \quad (2\text{-}18)$$

If all process are reversible, maximum COP

$$COP = \frac{T_{evap}(T_{gen} - T_{amb})}{T_{gen}(T_{amb} - T_{evap})} \quad (2\text{-}19)$$

Where T_{amb} = Ambient temperature, T_{gen} = generator temperature, T_{evap} = evaporator temperature. These temperatures need to be constant and absolute.

From this it can be seen that the maximal COP, theoretically, is the same as a Carnot cycle, however, in real life the COP is much smaller than equation (2-19). The COP is controlled by the temperatures of the generator, evaporator and ambient [94]where the latter relates to the cooling temperature of the medium (water or air) used to remove the rejected heat.

As suggested by [88, 94, 95], if the temperatures in the generator and ambient are kept constant, the COP of a chiller is directly proportional to the temperature in the evaporator. The performance of the absorption chiller decreases significantly when the required temperature in the evaporator decrease.

Keeping the generator and evaporator constant, the COP of the chiller is function of the cooling temperature in the condenser and absorber; by raising the temperature of the cooling medium, the COP of the absorption chiller decrease proportionally [88, 95].

The variation of COP related also to the variation of temperature of the heat source; an increase of the generator temperature increases proportionally the COP of the chiller if the cooling and evaporator temperatures are kept constant [88].

Studies found in literature state that a single stage absorption chiller can only work with generator temperatures in the range of 125 °C to 170 °C with air cooled absorber and condenser and 80 °C to 120 °C when water cooling is used [17, 75]. This limitation has been demonstrate by works done by recording experimental data from prototypes and are reported in literature [96, 97]. For generator temperatures below the

limit of 125 °C a half effect air-cooled absorption chiller can be used instead. The data available for a half effect air cooled have been published by Guerra [98] where experimental data have been recorded using a prototype of a half effect air cooled absorption chiller installed in the laboratory of the Politecnico di Milano.

2.3.4.2 Half-effect absorption chiller

When the temperature of the heat source at the generator is not high enough to fire a single stage absorption chiller, the half-effect chiller is usually used instead [98]. The configuration includes one generator and two absorbers. It is called half-effect chiller as not all the vapour generated in the generator is used to produce a cooling effect, but it is divided into two stream as indicated in Figure 27**Error! Reference source not found.** [98].

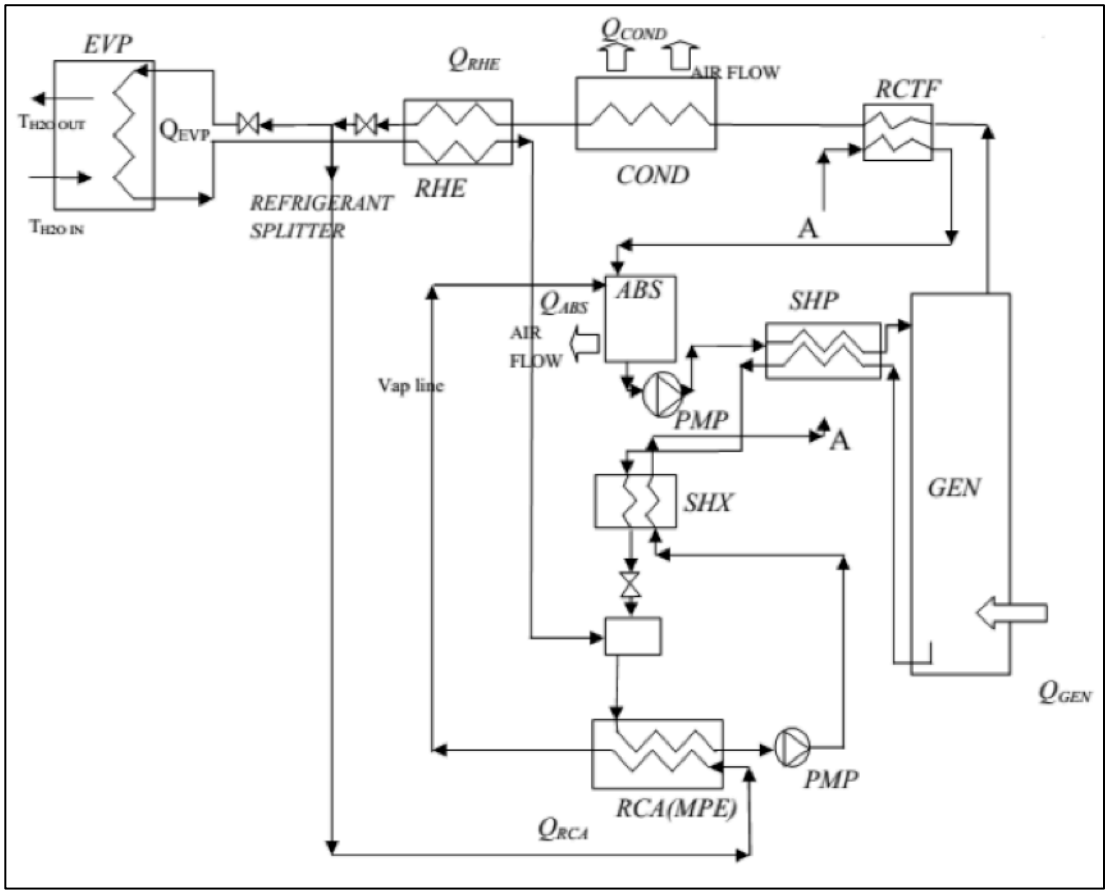

Figure 27 Schematic of the half-effect absorption chiller[98]

In a half-effect absorption chiller the refrigerant is divided into two flows, one goes in the evaporator generating the cooling effect, and the other flow is directed to the absorber in order to reduce its temperature. In this machine it is essential to control the amount of refrigerant going into the absorber as the efficiency drops if the amount of the

refrigerant has not the optimum value. In a dynamic situation the split of the refrigerant is a critical parameter as it continuously changes; typical values of the designed amount of refrigerant for an optimum performance are 42% refrigerant to the evaporator loop and 58% to the refrigerant cooled absorber, with a typical variation of 20% in most working conditions [98]. The variation of the working condition is related to variation of power supplied to the generator, variation of pressure and variation of cooling power required.

In conditions different to the design, it might happen that the split is done wrong causing problems to the machine operation. In an event where the flow rate of the refrigerant is not enough to remove the heat from the absorber, the absorber is not sufficiently cooled and the absorber cannot absorb the refrigerant from the evaporator. In an event where the refrigerant flow to the absorber is too high, the absorber will be sub-cooled with no usefulness and the reduced flow to the evaporator will reduce the cooling effect.

The main reason why these machines are used is because they can be fired with low temperature like, for example, water from the jacket of an engine or solar cooling using flat panels. At the end, the efficiency of these machines is half than that of a single stage machine.

2.4 APPLICATION OF MATHEMATIC MODELLING FOR SYSTEM IMPROVEMENT

Several mathematical models of the components of a solar cooling system have been presented over the past years.

Solar collectors have been simulated with the scope of estimating the best tilt angle at various latitudes [77, 99-105].

Desiccant wheels have been simulated and optimisations have been investigated using a one-dimensional gas side resistance model, which considers developing temperature and velocity profiles along the channels. Simulation results show a good agreement with experimental data available in the literature in a wide range of operating conditions. The model was used to analyse the influence of working conditions on desiccant wheel performance and on the optimal revolution speed [106].

Another mathematical model for predicting the performance of novel silica gel haloid compound desiccant wheel was developed, the model was then adopted to

investigate the influences of the main parameters on system performance and optimal rotation speed [107].

A numerical analysis and solar performance prediction of a solid adsorption solar system using an activated carbon/methanol adsorbent/adsorbate pair was developed taking into account all thermodynamics of the adsorption process, and heat and mass transfers within the adsorbent/adsorbate pair [108].

A single-stage, water–lithium bromide absorption chiller has been modelled to assess the influence of both the geometry parameters and operation parameters on thermal performance of the absorption chiller [82].

A simulation of two-stage air-cooled ammonia-water absorption refrigeration was undertaken investigating cycle and absorption performances. Both cycle analysis and absorption performances show that a two-stage air cooled ammonia-water absorption chiller is technically feasible in practical solar cooling applications but both the investment costs and electrical COP could be improved, especially for small capacity systems [109].

A solar cooling system using an absorption cycle combined with solar collectors has been modelled with the aim of satisfying a given cooling demand at minimum cost and environmental impact. The design of these systems has been formulated in mathematical terms as a multi-objective non-linear programming (NLP) problem that seeks to optimise simultaneously the economic and environmental performances of the cooling application. The results obtained show that with the current energy price and without considering government subsidies on solar technologies, the use of solar energy in cooling applications is not economically appealing [110].

A solar desiccant cooling system with heat recovery for the regeneration of the adsorption material was simulated. A hybrid configuration was chosen that uses two auxiliary cooling coils fed by a conventional compression chiller. One coil is used for pre-dehumidification whereas the other coil controls the air temperature if the desired supply temperature cannot be reached through indirect evaporative cooling alone. A specific feature of the system is the use of the heat rejected by the chiller to preheat regeneration airflow [51].

2.5 IMPLICATION

The total efficiency of an air conditioning system is calculated as the ratio between the useful output to the total input. In a cooling system, which only useful effect

is the delivery of cooling power, the heat rejected is considered a "waste" reducing the COP of the system. The COP of this system is measured as:

$$COP = \frac{Useful\ effect\ (kW)}{Energy\ Input\ (kW)} \tag{2-20}$$

To improve the COP of the system one needs to either reduce the energy input or increase the useful output. A way to increase the useful output is to reuse the total or part of the rejected heat for another process.

A few companies already provide an additional heat exchanger to recover some heat from the condenser of a vapour-compressor chiller, producing low-grade hot water.

An absorption chiller system rejects heat from the absorber and from the condenser. The amount of heat rejected by an absorption chiller is higher than the heat rejected by a vapour compressor chiller of the same cooling capacity. This heat is usually rejected to the ambient using a water cooled system or air cooled heat exchanger. At this stage, no study of the possibility to implement a heat recovery system in a solar cooling system or even in an absorption chiller has been found in the literature.

This research is aimed at exploring following options in order to maximise the efficiency of a solar cooling system:

1) to investigate the possibility of recovering heat from an absorption chiller
2) to maximise the total efficiency of the system by using this recovered heat
3) to reduce the energy input reducing the number of solar panels needed and then the installation costs.

In order to investigate the options outlined above, this research will design a solar cooling system using an ammonia absorption chiller and a desiccant wheel with the following key features:

1) production of conditioned air during summer time
2) use of the recovered heat to regenerate a desiccant wheel.

Chapter 3: Research design and methodology

This chapter describes the design that I adopted to achieve the aims and objectives stated in paragraph 1.3 of Chapter 1, i.e. to develop a solar cooling system based on absorption and adsorption technologies. The key innovations in this project are the implementation of a desiccant wheel in a common solar cooling system which is regenerated by using the heat rejected from the absorption chiller. Section 3.1 discusses the methodology used in the study and the stages in which this methodology will be implemented. Section 3.2 details the validation of the models used in the study, while section 3.3 describes the case studies used in this work.

3.1 OVERVIEW AND METHODOLOGY

The design of the system is based on a pure theoretical model. The model includes several parts, which are then integrated to develop the final model. An important part of the analysis undertaken is the assessment of how each item interacts with the other components. Thermodynamical modelling of the single components starts from basics assumptions and provides as output the properties of each component. In particular I developed the following mathematical models with the Matlab™ software for:

1) the estimation of energy output from a solar field
2) the absorption chiller
3) the desiccant wheel
4) an AHU.

Then I combined these four models to generate a solar cooling system implementing absorption and adsorption technologies and compare its efficiency with the efficiency of a traditional solar cooling system implementing only absorption technology.

A specific methodology has been conceived in order to separate and clearly accomplish the various tasks.

A flow chart of the main parameters for inputs and outputs, as well as the interconnection between the sub-models is shown in Figure 28.

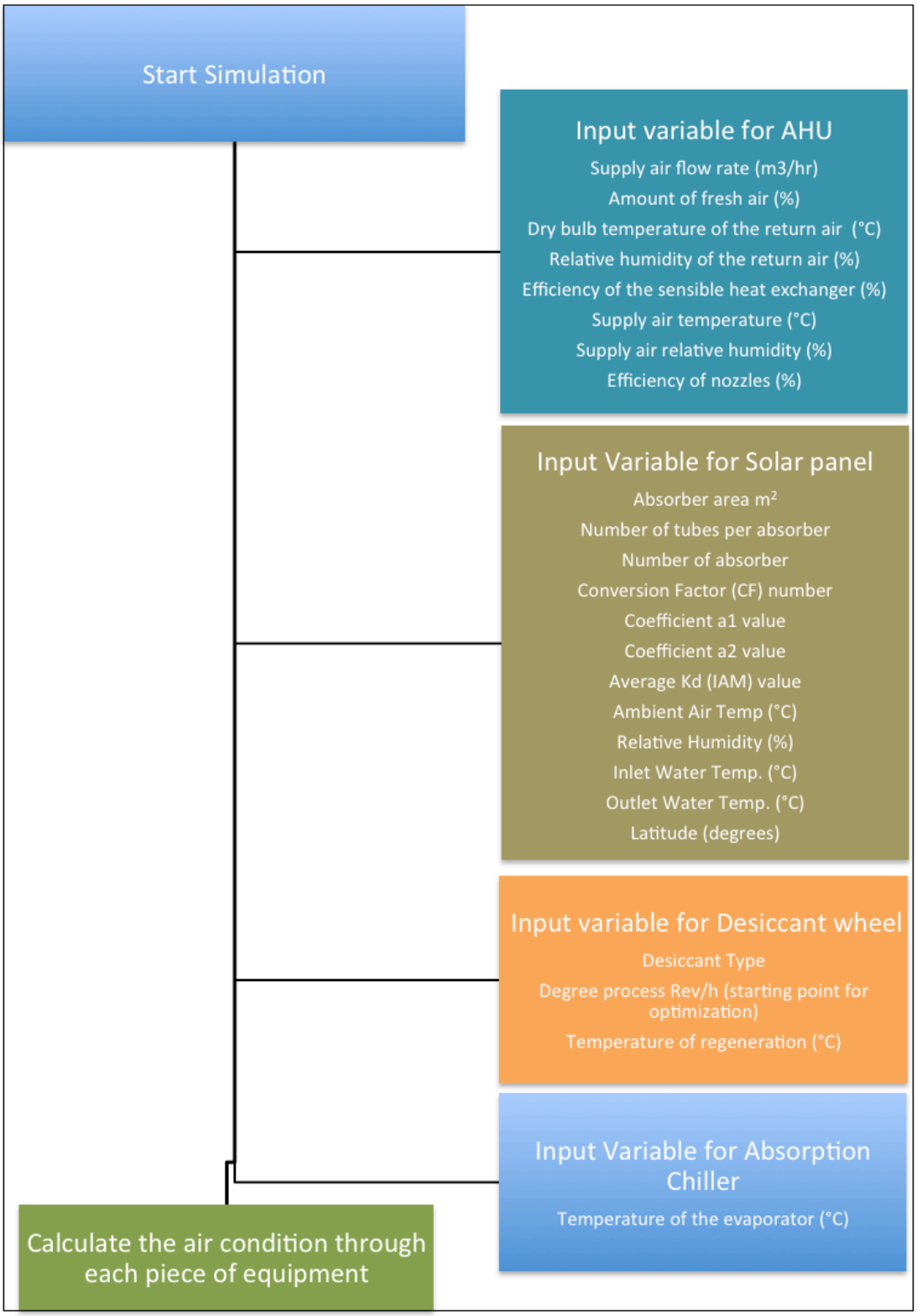

Figure 28 Flow chart diagram of the variable inputs for the mathematical model

3.2 VALIDATION OF MATHEMATICAL MODELS

The developed models will be validated by using data available in literature. The solar model will be validated by using a test report [111] of solar thermal panels performed using the EN 12975-2:2006 which is available in the literature [112]. To answer the two research questions, several models for the absorption chiller are needed. One model is used to answer the first question and one model is used to answer the second questions. The two models for the absorption chiller do not need to be validated as they only use data available from laboratory measurements on real absorption water-ammonia chillers [96, 98, 113]. The mathematical model of the desiccant wheel has been validated during previous works at the Milan university Politecnico di Milano [106]. The AHU model does not need to be validated as it only calculates the air conditions in several points of the AHU. The equation governing the AHU model are only mass and temperature balances.

3.3 CASE STUDIES

Two case studies have been performed, one includes the application of the proposed system to general case and one includes the application of the proposed system to a residential house. In the first case, various input parameters are changed; doing that it will be determinate where the new system will perform at its best achieving the higher saving when compared to a traditional solar cooling system.

3.3.1 General case - Study Scenarios

The first case study includes the application of the proposed system to a general case. Several scenarios will be assessed by varying the input values. Each model will provide an estimate of the variation of performance of the equipment.

3.3.1.1 Solar panels scenarios

A variation of the input and output water temperatures varies the efficiency of the solar panels. The model will be used to calculate the variation of efficiency related to the variation of input/output water temperatures required related to the ambient temperature. Also, by using a consistent set number of solar panels in the case study, the output variation has been calculated by varying the input/output water temperatures and the ambient air temperature.

3.3.1.2 Absorption chiller scenarios

Two models using real data from existing absorption chillers [96, 98, 113] are used in this thesis. The two models are used to calculate the saving achievable by implementing a desiccant wheel in a common solar cooling system (research question 1) and to asses the possibility of recovery some heat from their cooling system (research question 2).

One model simulates a water cooled single stage absorption chiller and another model simulate an air cooled half effect absorption chiller. The choose of using these two absorption chiller is motivated by the fact that they are the only two configuration of absorption chiller that can work at low temperature below 100 °C. The two models will be used to calculate the output variation (chilling power) by varying some variables. One simulation will assess the variation of the chiller performance by varying the temperature of the evaporator and keeping the temperatures of the generator and the ambient constant. Keeping the evaporator and generator temperatures constant the model will calculate the performance variation by varying the ambient temperature. The last simulation will assess the performance of the chiller by varying the temperatures of the generator, the ambient and evaporator.

The first step is to calculate the best operation temperature in coupling the solar panels and the absorption chiller. This is done by calculate the efficiency of the system solar panels-absorption chiller using the equation (4-38). The operating condition of the more efficient system will be used as reference and the desiccant wheel will be implemented in this system.

Using the same operation condition of the more efficient system the absorption chiller model is used to calculate the temperature of the reject heat to answer the research question 2.

3.3.1.3 Desiccant wheel scenarios

The desiccant wheel model has implemented several isotherms; each isotherm is characteristic of a hygroscopic material. The hygroscopic materials used in this calculation are Regular Density Silica Gel, Selective Water Sorbent Silica Gel+ Calcium Chloride (33%), Activated Carbon Fibre, Super Absorbent PolyAcrilic Polymer, Macroporoso silica gel and silica gel lithium chloride

For each material used the desiccant wheel model will calculate the humidity ratio reduction by varying the process air temperature. Another simulation will assess the

variation of the process air temperature output by varying the process air temperature input. The variation of the humidity ratio reduction by varying the humidity ratio of the process air inlet will be calculated in another simulation. Also, the model will assess the relation between the humidity ratio reduction and the regeneration temperature. Characteristic parameters of the desiccant wheels are the regeneration angle and the rotation speed; the model will calculate the optimum values for these parameters for each hygroscopic material.

3.3.2 Sample Residential House

For the second case study, the mathematical model will be used to calculate the savings achievable by implementing the new design of the solar cooling system in a residential house. The house, located in South East Queensland, has a ground floor area of approximately 150 m^2.

3.3.2.1 Study Location

The study has been undertaken in the South East Queensland region, the typical ambient air condition for the area has a high relative humidity, which is a good condition for implementing a desiccant wheel. The implementation of a desiccant wheel unit in a location where the relative humidity is low would not be beneficial for an air conditioning system.

Chapter 4: Mathematical model of major components

Several mathematical models for each piece of equipment included in the proposed system have been developed.

Paragraph 4.1 describe the mathematical model used to assess the performance of the solar system used in the solar cooling system suggested and the methodology adopted to develop the model.

The performance of the absorption chiller have been modelled by mathematical models described in paragraph 4.2. Two models, based on performance data of real commercial absorption chillers, have been used to estimate the temperature of the heat rejected and the COP of the absorption chiller in the integrated system.

Paragraph 4.3 describe the mathematical model of the desiccant wheel and the methodology adopted in developing the model.

The AHU implementing the proposed system is modelled and the mathematical model is described in paragraph 4.4.

Paragraph 4.5 describe the case studies adopted to calculate the saving achievable by the implementation of the proposed system, Paragraph 4.6 describe the procedure and the timeline of this thesis and paragraph 4.7 analyses the performances of the models.

4.1 MATHEMATICAL MODEL OF THE SOLAR FIELD

The first part of this research focuses on the development of a mathematical model for the simulation of the solar field. Because of the water temperature required by the absorption chiller, I chose to use evacuated tubes that produce higher water temperature. The evacuated tubes collector consists of heat pipes inside vacuum-sealed glass tubes. A reflector can be added to optimize the absorption of the solar radiation [76].

4.1.1 Methodology

The mathematical model is developed following the standard EN 12975-2 and includes the input/output data for the whole year. The European Standard EN 12975-2 is a unique standard used throughout Europe for solar thermal collector testing. This

standard specifies a reproducible procedure and thus guarantees comparable results. It includes two alternative test methods for the thermal performance characterization of solar collectors: steady-state and quasi-dynamic tests [76].

During steady-state operating conditions, the useful output power of a solar collector for near normal incidence angle of the solar radiation can be written as [14]:

$$Q = F' * A_a * [(\tau\alpha)_{en} * G - U * (t_m - t_a)] \quad (4\text{-}1)$$

Where:

- Q indicates the output power provided to the liquid circulating through the solar panels (in our case water)
- F' indicates the collector efficiency factor
- A_a is the area of the solar collector
- $(\tau\alpha)_{en}$ indicates the effective transmittance–absorbance product at normal incidence
- G is the global solar irradiance
- U is the overall heat loss coefficient and
- (t_m-t_a) indicates the difference between the average fluid temperature in the collector t_m and the ambient air t_a.
- t_m is the average temperature of the water through the solar field (t_{out}+t_{in})/2

The efficiency is then calculated as the ratio of the output energy from the collector and the incident radiation on the area occupied by the collector:

$$\eta_{collector} = \frac{Q_{collector}}{G * A_a} \quad (4\text{-}2)$$

$$\frac{Q}{G * A_a} = F' * [(\tau\ \alpha)_{en} - U * \frac{(t_m - t_a)}{G}] \quad (4\text{-}3)$$

If the variable $T_m^* = \frac{t_m - t_a}{G}$ indicating the reduced temperature difference is introduced, thus:

$$\eta = F' * [(\tau\alpha)_{en} - U * T_m^*] \quad (4\text{-}4)$$

Considering the heat losses as function of two terms, the first as a constant and the second dependent on the temperature difference between fluid and ambient (t_m-t_a) the efficiency can be rewritten as follows:

$$\eta = \eta_o - a_1 T_m^* - a_2 G (T_m^*)^2 \quad (4\text{-}5)$$

This formula is in agreement with the one provided by the standard EN 12975 for steady-state tests.

The values of η_o, a_1 and a_2 are usually provided by the manufacturer of the solar collectors. The model will be tested on the following collectors:

- Company: Thermomax Ltd
- Type DF 100 30
- Serial number 08631

Result from the model will be compared with the results of a report of performance test undertaken accordingly to the EN 12975-2 for a glazed solar collector [111] and the result will be described in paragraph 5.3.

Figure 29 Thermomax DF 100 30 Solar Thermal Evacuated Tube

4.2 MATHEMATICAL MODEL OF THE ABSORPTION CHILLER

Heat is rejected by an absorption chiller from the absorber and from the condenser [114].

Rejected heat could be recovered [115] at a temperature which could be useful for several applications.

One option could be the recovery of the heat available to regenerate a desiccant wheel, other options include the recovery of the heat to generate low temperature hot water or low temperature hot air.

The first option is the aim of the second research question of this thesis. To answer the question two simulators of a single stage absorption chiller and of a half effect absorption chiller have been developed to calculate the temperature of the heat rejected that could be recovered.

The simulators have been developed by using experimental data available in literature [98, 113]. Also, a simulator using the performance data of a real single stage absorption chiller has been developed to be included in the integrated system.

4.2.1 Mathematical model of a half effect absorption chiller

When the temperatures input in the model for the generator, the condenser and evaporator are not adequate to generate a concentration difference between the generator and absorber for the single effect absorption chiller to work, a half effect chiller model is used instead. A simple model has been developed by using the data recorded by previous work at Politecnico di Milano [98].

Measurements available for the air cooled half effect absorption chiller are listed in Appendix A .

The important feature of the half-effect chiller is that it can be fired by a heat source at a lower temperature compared to a single effect chiller. The drawback is that the COP of the half effect chiller is approximately half of the COP of a single effect machine.

4.2.2 Mathematical model of a single stage absorption chiller using recorded performance data

A model for a single effect absorption chiller has been generated using the data available from literature review for an absorption chiller produced on large scale by Solar Next AG. Chiller model chillii PSC12 [116] having the following technical specification indicate in Table 3.

Table 2 Technical specification of the chiller used for the simulator (rated power)

Cold water cycle	
Chiller capacity	12 kW
Chilled water temperature in/out	12/6 °C
Hot water cycle	
Capacity	18.5 kW
Hot water temperature in/out	85/78 °C
Cooling cycle	
Cooling capacity	31.4 kW
Cooling water temperature in/out	24/29°C

Measurements available for the water-cooled single stage absorption chiller are listed in Appendix B

4.3 MATHEMATICAL MODEL OF THE DESICCANT WHEEL

A rotary regenerative desiccant wheel is characterized by its diameter D_{wheel} and its length L. It is divided into two sections: adsorption section (angle fraction α_0) and regeneration section (fraction 1- α_0) [117]. One section is crossed by the stream of process air to be treated, and the other section is crossed by the air stream used to regenerate the wheel. Process and regeneration air streams are flowing in opposite directions. The wheel generally consists of a matrix of numerous flow channels having sinusoidal shape. The wheel rotates at constant velocity N and each channel of the wheel is periodically exposed to the two streams.

The mathematical model for the desiccant wheel is based on the following assumptions [106, 118]:

1) There are no chemical reactions
2) There are no energy sources within the system
3) The effect of gravity on the fluid is negligible
4) Viscous dissipations are negligible
5) The channels are equal and uniformly distributed throughout the wheel
6) Temperature, humidity and velocity of each inlet flow are uniform at the inlet face of the wheel
7) Heat and mass transfer between adjacent channels is negligible
8) Heat and mass transfer from the desiccant wheel to the surroundings is negligible
9) Axial heat conduction and water vapour diffusion in the air stream is negligible
10) Axial heat conduction and water vapour diffusion within the desiccant is negligible
11) The gaseous components of the fluid mixture are treated as ideal gases
12) The specific heat and thermal conductivity of dry air, water vapour and liquid water are assumed constant

13) The hygroscopic capacity of the matrix material is negligible

14) The rotary wheel is assumed as an inertial system

15) The adsorbed water is in thermal equilibrium with the desiccant material and the matrix material

16) Hysteresis effects during water desorption are negligible

17) Air leakages between the two streams are negligible

18) Radiation effects are negligible

The governing equations used in the model are developed on the above assumptions and include [106]:

1) conservation of water mass and of energy in the system consisting of the desiccant material, the support material and the adsorbed water

2) conservation of water mass, of dry air mass and of energy in the wet air stream

Mass balance of dry air in the stream [119]:

$$\frac{\partial \rho_{DA}}{\partial t} = \frac{\partial (\rho_{DA} u)}{\partial z} \tag{4-6}$$

where ρ_{DA} is the dry air density, u the air velocity through the channel, t the time and z the spatial direction along the channel. The term on the left-hand side is the dry air moisture storage term and the term on the right-hand side is the rate of dry air variation due to the axial flow in the channel.

Mass balance of water in the air stream [119]:

$$\frac{\partial X}{\partial t} = -\frac{\partial X}{\partial z} u - \frac{P h_m}{\rho_{DA} A} (X - X_W) \tag{4-7}$$

where X is the absolute humidity of the air stream, X_W is the absolute humidity of air on the desiccant wall, P the perimeter and A the cross sectional area of the channel, h_m the convective mass transfer coefficient. The term on the left-hand side is the water moisture storage term, the first and second term on the right side are respectively the rate of variation of water vapour due to air flow along the channel and the convective mass transfer between the desiccant and the air flow.

Mass balance of water in the desiccant material, support material and adsorbed water [119]:

$$\frac{\partial W}{\partial t} = \frac{h_m(X - X_W)P}{f_D} \tag{4-8}$$

where W is the amount of water adsorbed in the desiccant substrate and f_D is desiccant mass per unit of length in the channel. The term on the left-hand side is the moisture storage term in the desiccant material, the term on the right side is the water flux due to convective mass transfer with the airflow.

Energy balance for the desiccant material, support material and adsorbed water [119]:

$$(f_M c_M + f_D c_D)\frac{\partial T_D}{\partial t} + f_D W \frac{\partial T h_{ad,w}}{\partial t} + f_D h_{ad,w}\frac{\partial W}{\partial t} = h_m cp_v \mathrm{T}(\mathrm{X} - X_w)\mathrm{P} + h_T(\mathrm{T} - T_D)\mathrm{P} \tag{4-9}$$

$$\left(f_M cp_M + f_D cp_D + f_D c_{ad,w} W\right)\frac{\partial T_D}{\partial t} = (cp_v(\mathrm{T} - T_D) + Q_{ADS})h_m(\mathrm{X} - X_w)\mathrm{M} + h_T(\mathrm{T} - T_D)\mathrm{M} \tag{4-10}$$

where t and T_D are respectively the air and desiccant temperature, Q_{ADS} is the heat of adsorption, cp_D, cp_l and cp_M are respectively the specific heat of the desiccant, the liquid water and the supporting material, f_M is the matrix material mass per unit of length and h_T the heat transfer coefficient.

The term on the left-hand side is the energy storage term in the desiccant material including the energy stored in the desiccant and the support material, the first term on the right side is the energy flux due to convective mass transfer and the second term is the energy flux due to convective heat transfer.

The adsorbed water has been assumed to be in liquid phase and all the adsorption heat is assumed to be delivered to the desiccant.

Energy balance in the air stream [119]:

$$\frac{\partial(T\rho_{DA}cp_{WA})}{\partial t} = -\frac{\partial(T\rho_{DA}cp_{WA}u)}{\partial z} - \frac{h_T(T - T_D)P}{A} - \frac{h_m(X - X_W)Pcp_V T}{A} \tag{4-11}$$

where cp_{WA} is the specific heat of wet air defined as follow:

$$cp_{WA} = cp_{DA} + X_{cp_v} \tag{4-12}$$

with cp_{DA} and cp_v respectively the specific heat of dry air and water vapour. The term on the left-hand side is the energy storage term in the air, the first term on the right-hand side is the energy variation of air due to the axial flow, the second term is the energy flux due to convective mass transfer and the third term is the energy flux due to convective heat transfer.

Neglecting the space and time derivative of cp_{WA} and considering the equation of mass conservation of dry air in the air stream (4-6), the energy balance can be rearranged in this form:

$$\frac{\partial T}{\partial t} = -u\frac{\partial T}{\partial z} - \frac{h_T(T-T_D)M}{cp_{WA}\rho_{DA}A} - \frac{h_m(X-X_W)Mcp_VT}{cp_{WA}\rho_{DA}A} \tag{4-13}$$

Others equation are necessary to solve the system, one is the equation used is the ideal gas law for the wet air:

$$p_{tot} = \rho_{DA}(1/MM_{DA} + X/MM_V)RT \tag{4-14}$$

Where p_{tot} is the total pressure of the system which, is assumed constant and equal to 101325 Pa. The adsorption isotherm of desiccant material can be expressed in the following form [52]:

$$\varphi = \sum_{i=0}^{4} a_i W^i \tag{4-15}$$

or

$$W = a\varphi^n \tag{4-16}$$

Where W is the desiccant water content, a and n are respectively are respectively a coefficient and an exponent which depend on the adsorbent material and φ is the relative humidity value.

The relation between relative humidity and humidity ratio is [107]:

$$X = 0{,}622\frac{\varphi}{p_{tot}/p_{sat,w} - \varphi} \tag{4-17}$$

where $p_{sat,w}$ is the saturation pressure of the water which is calculated through the following relation proposed by Antoine [4, 120]:

$$p_{sat,w} = 133.32\, e^{\left(18.3-\frac{3816.44}{T-46.13}\right)} \tag{4-18}$$

The heat transfer coefficient is calculated from the local Nusselt number as follows [118]:

$$Nu_L = \frac{h_T D_{eq}}{k} \tag{4-19}$$

where k is the thermal conductivity of the dry air, and the mass transfer coefficient is calculated from the Sherwood number [107]:

$$Sh_L = \frac{h_M D_{eq}}{\rho_{DA} D} \tag{4-20}$$

where D is the mass diffusivity of vapour in air.

The local Nusselt number is evaluated along the channel through the following correlation [17]:

$$Nu_L = Nu_{FD} + \frac{0.0841}{0.002907 + Gz^{-0.6504}} \quad (4\text{-}21)$$

where Nu_{FD} is the Nusselt number for the fully developed flow and Gz the Great number [10]. The Lewis number is assumed constant and equal to 1 [118], so the local Sherwood number is assumed equal to the local Nusselt number.

The actual air velocity in the channel is:

$$u = \frac{v}{\varepsilon} \quad (4\text{-}22)$$

Where ε is the wheel porosity defined as the ratio of the void volume to the total volume of the desiccant wheel and v the face velocity. The isosteric heat of adsorption is defined as the standard enthalpy of adsorption and is calculated as:

$$Q_{ads} = h_v - h_{ad,w} - cp_v(T - T_D) \quad (4\text{-}23)$$

The model determines the optimum rotary speed for maximum efficiency. When a desiccant wheel rotates much faster than the optimum speed, the adsorption and regeneration times are too short resulting in poor performance. On the other hand, when the rotary speed is lower than the optimum, the adsorption phase becomes too long: the desiccant material reaches its maximum water vapour content and it is not able to dry process air anymore [117].

Also, the model determines the condition of the process air at the outlet of the desiccant wheel.

The inputs required by the model are the following:

1) Regeneration and process air temperatures

2) Humidity ratio and velocity of both air streams

The model assesses the output variation based on the variation of the input values. This assessment is useful to determine any change to the final design of the system. (i.e. a reduction of the temperature of the inlet process air increase the dehumidification capacity of the wheel [106] so it will be useful to asses the consequence of a pre-cooling of process air to increase dehumidification capacity of a desiccant wheel).

The model has been validated through experimental data available in literature of a sorption wheel used for air dehumidification [52, 121-123]. The device used in the comparison is a commercial unit built by the Japanese company Seibu-Giken.

The wheel is made of a ceramic porous fibre paper impregnated with 70-80% of type A silica gel. The main desiccant wheel data are reported in Table 3 and Table 4.

Table 3 Steady state validation – Desiccant wheel characteristics [122, 124]

Materials Data	*(Data in italic has been assumed)*		
Specific heat of silica gel	cp_D	*921*	*J/kgK*
Specific heat of matrix material	cp_M	*500*	*J/kgK*
Specific desiccant mass	f_D	*0.0003*	*kg/m*
Specific matrix mass	f_M	*0.000075*	*kg/m*
Geometrical Data			
Duct height	a	0.0018	m
Duct width	b	0.0032	m
Channel wall thickness	s	0.0002	m
Thickness of desiccant wheel	L	0.2	m
Desiccant wheel diameter	D	0.32	m
Wheel porosity	ε	0.55	-
Other data			
Adsorption isotherm	$W=0.24\ \varphi^{1/1.5}$		

Table 4 Desiccant wheel data used in the validation

Sim/Exp	$T_{reg,in}$ (°C)	A_{pro}/A_{reg}	v (m/s)
a	100	1	1
b	140	3.3	1
c	60	1	1
d	140	3.3	1

In literature, the moisture removal capacity (MRC) is commonly used as parameter indicating the performance of the desiccant wheel. The same parameter is used for the optimization of the wheel. MRC is defined as:

$$MRC = m_{pro}\left(X_{pro,in} - X_{pro,out}\right) \tag{4-24}$$

Another parameter used for the optimization of the wheel is the effectiveness, which is defined as [119]:

$$\varepsilon_D = \frac{X_{pro,in} - X_{pro,out}}{X_{pro,in}} \tag{4-25}$$

In this study, the reduction of the humidity ratio is used as the optimization parameter. Its definition is:

$$\Delta X_{pro} = X_{pro,in} - X_{pro,out} \tag{4-26}$$

Different performance criteria lead to different desiccant wheel optimal configurations in the case of unbalanced regeneration and process air flows [48, 125].

The assessment of the system uses several types of hygroscopic materials as following:

- SDA Regular Density Silica Gel
- SWSL Selective Water Sorbent Silica Gel+ Calcium Chloride (33%)
- ACF25 Activated Carbon Fibre
- Polym Super Absorbent PolyAcrilic Polymer
- rdtoth1 Macroporous silica gel
- SG_LiCl silica gel lithium chloride

The φ values used for each material are indicated in Table 5.

Table 5 φ values used in the model of the desiccant wheel

Material	φ values
SDA	(-1/23.3)*log(0.788/w_dec-1)+0.65
SWSL	((xn*w_dec/k/Ps)^t1*1/(xn^t1-w_dec^t1))^(1/t1)
ACF25	(-1/23.3)*log(0.788/w_dec-1)+0.65

Polym	exp(-1/k*(wm/w_dec)^s)
Rdtoth1	((xn*w_dec/k/Ps)^t1*1/(xn^t1-w_dec^t1))^(1/t1)
SG_LiCl	exp(-(1/0.342*log(0.489/w_dec))^(1/1.604))

4.4 MODELLING OF THE COMPONENTS INCLUDED IN THE AHU UNIT

4.4.1 Sensible heat wheel

The sensible and the latent efficiency of the wheel are calculated assuming that the exhaust airflow is equal or lower than the process one. With this assumption any contamination of the process air is avoided. Sensible efficiency is defined as:

$$\varepsilon_{DW\ sbl} = \frac{(mc_p)_{pro}\ (T_{pro,out} - T_{pro,in})}{(mc_p)_{exh}\ (T_{exh,out} - T_{pro,in})} \tag{4-27}$$

Latent efficiency is defined as:

$$\varepsilon_{DW\ ltn} = \frac{m_{pro}\ (X_{pro,out} - X_{pro,in})}{m_{exh}\ (X_{exh,out} - X_{pro,in})} \tag{4-28}$$

From the equations above, the temperature and absolute humidity of air which has passed the heat exchanger process can be calculated by the following equations:

$$T_{pro,out} = T_{pro,in} + \varepsilon_{DW\ sbl} \frac{(mc_p)_{exh}}{(mc_p)_{pro}} (T_{exh,out} - T_{pro,in}) \tag{4-29}$$

$$X_{pro,out} = X_{pro,in} + \varepsilon_{DW\ ltn} \frac{m_{exh}}{m_{pro}} (X_{exh,out} - X_{pro,in}) \tag{4-30}$$

4.4.2 Cooling and heating coil

Air to water exchangers coils used in the HVAC systems are well known pieces of equipment. Several coil models are available in literature. These models require the knowledge of the geometry of the cooling coil (such as the dimensions of the fins, the tube thickness, diameter and spacing), which is not always available from the manufacturer.

One of the reasons why air to water systems are used is due to the usually limited space available within the building; air to water exchangers need less room due to the distribution of pipes being a lot less. Another advantage of this type of exchanger is the energy requirement to circulate the water throughout the system is less compared to the

energy that is required to rotate the fans in a normal air to air exchanger. For these reasons (lower energy costs and reduced usage of space) air to water systems are very popular among commercial buildings.

4.4.2.1 Cooling coil

When a coil is used in a cooling and dehumidification process, the humid air is cooled below its dew-point by bringing it in contact with a cold surface at temperature T_s as shown in Figure 30, some of the water vapour in the air condenses and leaves the air stream as liquid, as a result both the temperature and humidity ratio of air decreases as shown. Air undergoes this process in a typical air conditioning system.

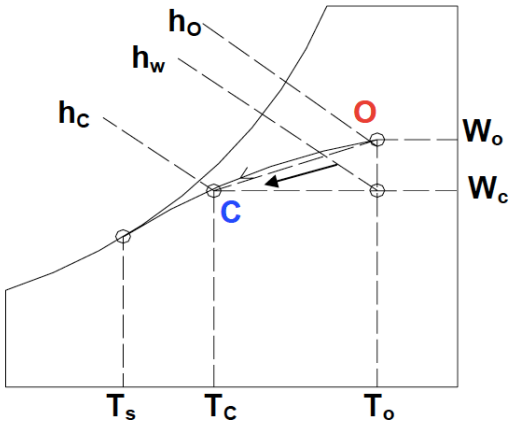

Figure 30 Cooling and dehumidification process (O-C)

The temperature T_s is the effective surface temperature of the cooling coil, and it is known as apparatus dew-point (ADP) temperature. In an ideal situation, with an infinite surface heat exchanger, when all the air comes in perfect contact with the cooling coil surface, the exit temperature of the air will be the same as the ADP of the coil. However, in this study, it is assumed that the exit temperature of the air will always be greater than the apparatus dew-point temperature due to development of a boundary layer, as air flows over the cooling coil surface and also due to temperature variation along the fins.

The parameter used to express a cooling coils efficiency is the by pass factor (BPF) which is calculated in this way:

- first we select:
    - the number of coil rows
    - the distance between fins
    - the frontal air velocity

- We estimate BPF from manufacturer diagram:

$$BPF = \frac{(X_{air,out} - X_{ADP})}{(X_{air,in} - X_{ADP})} \cong \frac{(T_{air,out} - T_{ADP})}{(T_{air,in} - T_{ADP})} \quad (4\text{-}31)$$

The following further assumptions have been done:

- $T_{ADP} = T_{eva} + \Delta T_{res}$,

  where T_{eva} is the working fluid evaporation temperature in the coil and ΔT_{res} is a conductive resistance.

The higher the by-pass factor, the larger will be the difference between air outlet temperature and the cooling coil temperature.

In the case of BPF = 1.0, the equation (4-31) becomes:

$$(T_{air,out} - T_{ADP}) = (T_{air,in} - T_{ADP}) \quad (4\text{-}32)$$

And as $T_{air,out} = T_{air,in}$, all the air by-passes the coil resulting in no cooling or de-humidification effect. In practice, the by-pass factor can be increased by increasing the number of rows in a cooling coil or by decreasing the air velocity or by reducing the fin pitch.

In the case of BPF equal to zero, the equation (4-31) becomes:

$$(T_{air,out} - T_{ADP}) = 0 \quad (4\text{-}33)$$

And as $T_{air,out} = T_{ADP}$, the coil ADP is equal to the temperature of the supply air .Alternatively, a contact factor (CF) can be defined by:

$$CF = 1 - BPF \quad (4\text{-}34)$$

When the BPF of the cooling coil is known, the supply air temperature $T_{air,out}$ is obtained from equation (4-31) by using the room conditions and coil ADP:

$$T_{air,out} = T_{ADP} + BPF(T_{air,in} - T_{ADP}) \quad (4\text{-}35)$$

Once the supply air temperature $T_{air,out}$ is known, the cooling coil energy consumption can be calculated as

$$\dot{Q}_{coil} = \dot{M}_{r,coil}(h_{r,in,ev} - h_{r,out,ev}) \quad (4\text{-}36)$$

The enthalpy ($h_{r,in,ev}$) at the coil (or evaporator) inlet is the same as the enthalpy at the outlet of the expansion device of the refrigeration cycle. If the expansion can be considered as isoenthalpic, this enthalpy is also the same at the condenser outlet. It can then be calculated as a function of the condensing pressure and of the condenser exit sub

cooling. This sub cooling essentially depends on the amount of refrigerant introduced in the refrigeration system.

The enthalpy at the outlet of the evaporator is calculated on the basis of the refrigerant pressure and the temperature at the outlet of the evaporator. The exiting temperature is computed by imposing a refrigerant superheating at the outlet of the cooling coil. The expansion device imposes this superheating.

4.4.2.2 Heating coil

The typical heating process of the air in the HVAC is described in Figure 31 that represents the sensible heating process on the psychometric diagram.

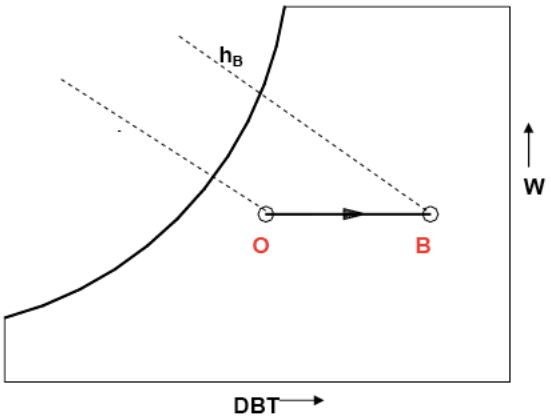

Figure 31 Sensible heating process on psychometric chart

The coil is fed by a constant water flow at a fixed water temperature.

The higher is the supply water temperature, the higher is the air temperature at the heating coil outlet. During this process, the moisture content of air remains constant and its temperature increases as it flows over a heating coil. The variation of the temperature of the air and water across the coil is shown in Figure 32.

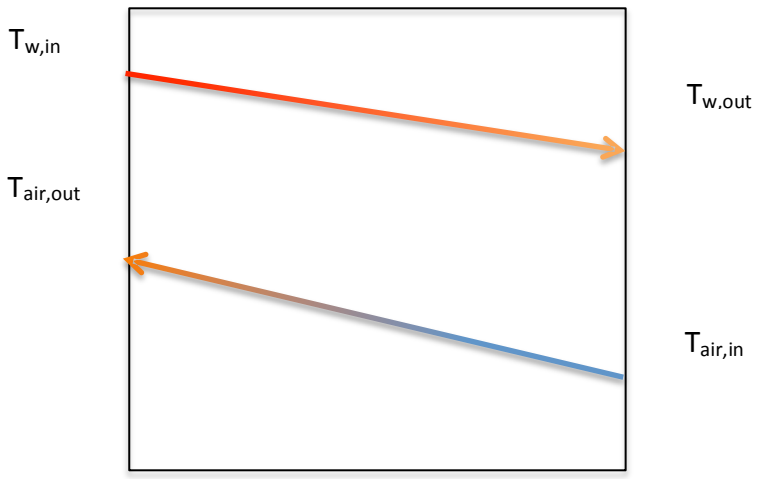

Figure 32 Air and water temperatures variation across a heating coil

The heating coil is therefore characterized by:

- choosing a geometric configuration.
- assuming that the control system is able to reach the desired air temperature at the coil outlet through the variation of the temperature of the supply water.

Therefore through this approach an increased number of rows and a reduced distance between fins should be considered. The heat transfer rate during this process is given by:

$$\dot{Q}_h = \dot{m}_{air}\left(h_{air,in} - h_{air,out}\right) = \dot{m}_{air}\, cp_{air}\left(T_{air,in} - T_{air,out}\right) \quad (4\text{-}37)$$

Where $T_{air,in}$ and $T_{air,out}$ represent the temperatures before and after air entered the heating coil, cp_{air} is the humid specific heat (≈1.0216 kJ/kg dry air) and m_{air} is the mass flow rate of dry air (kg/s).

4.4.3 Alternative configuration of solar cooling system used in this thesis

In a HVAC system, dehumidification of the air is usually achieved in the AHU where air flows through a cooling coil; air is cooled until its dew point and water vapour is condensed.

Dry air is then heated through a second coil until to the desired supply temperature is reached. This design of the AHU integrated in a solar cooling system is the most diffused and it is the reference one [126, 127].

Figure 33 shows the conventional design that is the main used in industrial and commercial air dehumidification processes.

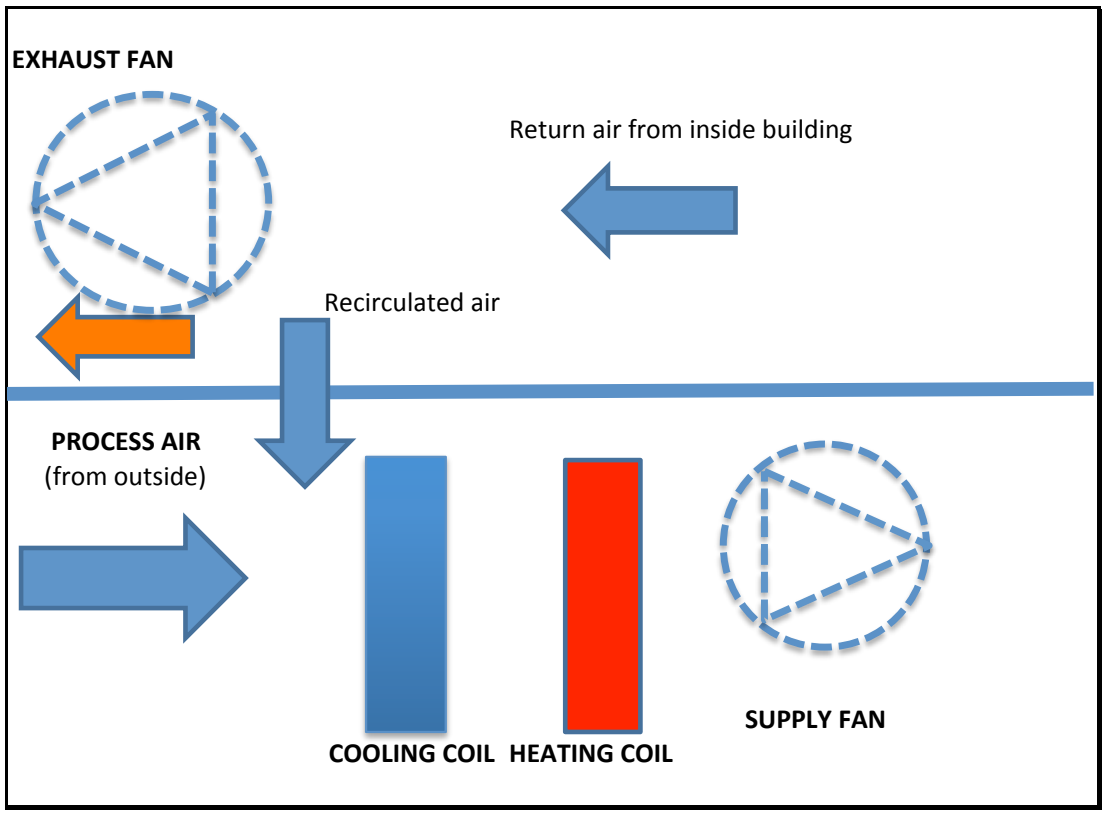

Figure 33 Schematic diagram of a conventional system

Referring to Figure 33, the AHU consists of the following components:

- cooling coil
- heating coil
- fans.

Air passing through the cooling coil is dehumidified and cooled while in the heating coil, air is heated in order to balance the ambient sensible load.

Figure 34 shows the air treatment processes in a typical AHU on the psychometric chart which indicates the properties of air and water vapour through the following parameters:

- dry bulb temperature
- wet bulb temperature (saturation temperature)
- dew point temperature
- relative humidity
- moisture content (humidity ratio)
- enthalpy

- specific volume

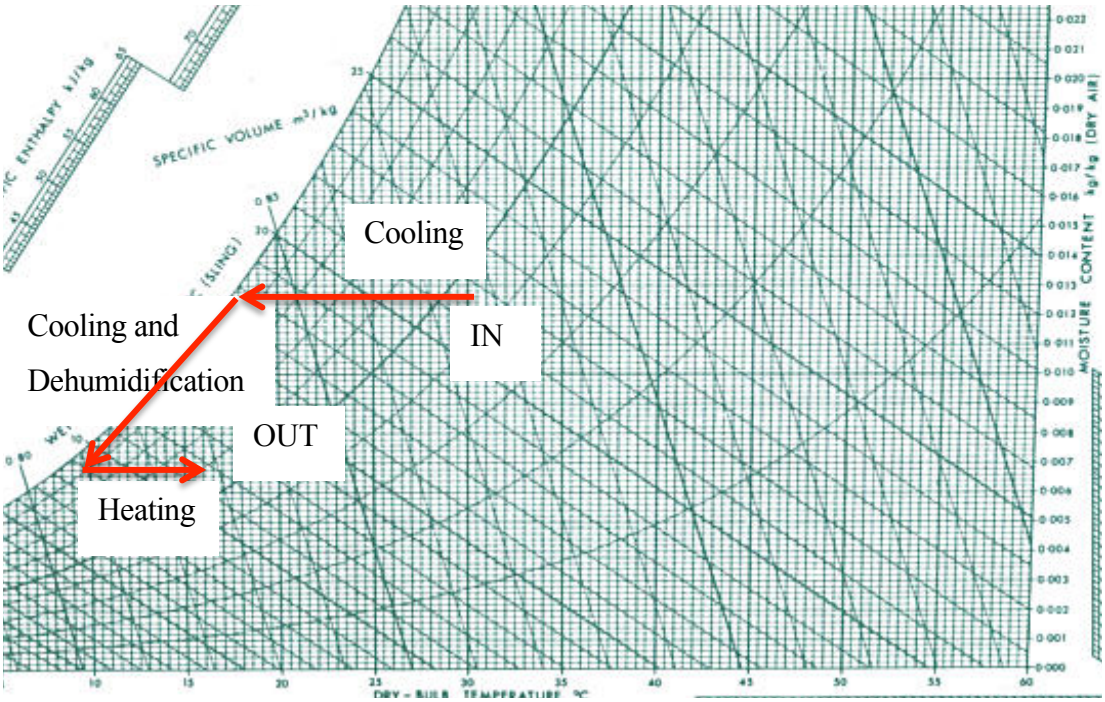

Figure 34 Air treatments on the psychometric chart for a typical design

Figure 35 shows the schematic of the AHU used in the proposed solar air-conditioning system.

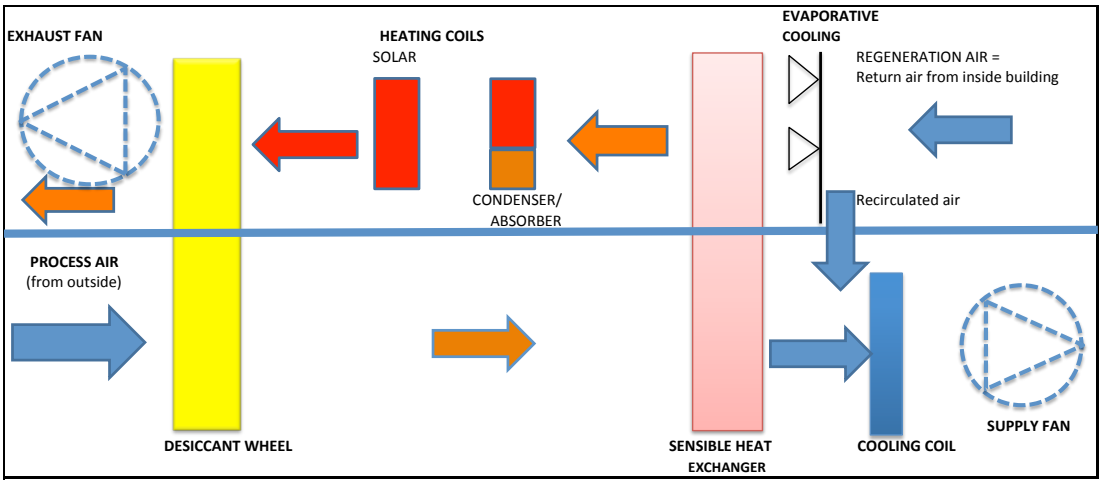

Figure 35 Schematic diagram of the proposed system

The main difference in the proposed system is the integration of a desiccant wheel and of a sensible heat exchanger in an AHU. Also the heating coil before the supply fan has been removed, as for the way humidity is removed, the treated air in this system does not need to be re-heated.

Two air streams are necessary in this configuration: the process air flow, which is the air flow treated in order to balance the ambient latent and sensible loads and the regeneration one which is necessary to remove water vapour from the desiccant wheel matrix.

Cooling coil, heating coil and fans are the same of the reference design and the other equipment are added to the typical design.

The proposed system consists of the following major components in order to condition the process air to the desired values of temperatures and humidity.

- A desiccant wheel is impregnated with desiccant material and is rotating continuously between the process and regeneration side.
- Sensible heat exchanger rotating between the process out of desiccant wheel and the evaporator.
- Cooling coil is located between the sensible heat exchanger and before the end user.
- Two heating coils are installed before the desiccant wheel at the regeneration side to heat up the air after the sensible heat exchanger. One heating coil is fed directly by dedicated solar thermal panels. The other heating coil is fed by the absorption chiller cooling system which remove heat from the absorber and condenser. In case the air cooled half effect absorption chiller is used, the absorber and condenser could be installed directly in the AHU minimising the heat loss as a cooling circuit is not required.

The outside air (process air), which is warm and humid, passes through a desiccant wheel and becomes warmer and drier. The air then flows through a sensible heat exchanger and the temperature is reduced. The dry, cooled air is then mixed with the return air from the conditioned areas before it passes through an evaporator where the air is further cooled to the required temperature before being supplied to the user. By removing the humidity of the outside air using a desiccant wheel the cooling load on the chiller is reduced and accordingly the size of the chiller can be reduced as well as its consumption. This cooled air provides the comfort condition of the space where is supplied.

On the regeneration side, the regeneration air from inside the conditioned areas is cooled by an evaporating cooler unit (spray water is used to saturate the air) before it enters the sensible heat exchanger where is heated by the heat absorbed by the process air. The regeneration air passes then through two (2) water to air heating coils to heat the regeneration air to the required regeneration temperature to regenerate the desiccant. The hot air then passes through the desiccant wheel at the regeneration side and exhausted to the surrounding.

The function of the desiccant wheel and sensible heat exchanger is to reduce the humidity (latent load) and the temperature (sensible load) of the air before it enters the cooling coil so that the cooling coil can be used only to remove the sensible heat reducing the energy consumption.

The amount of the return air varies from 0 to 100% according to the application of the system.

Figure 36 shows the air treatment processes in the proposed system on the psychometric chart.

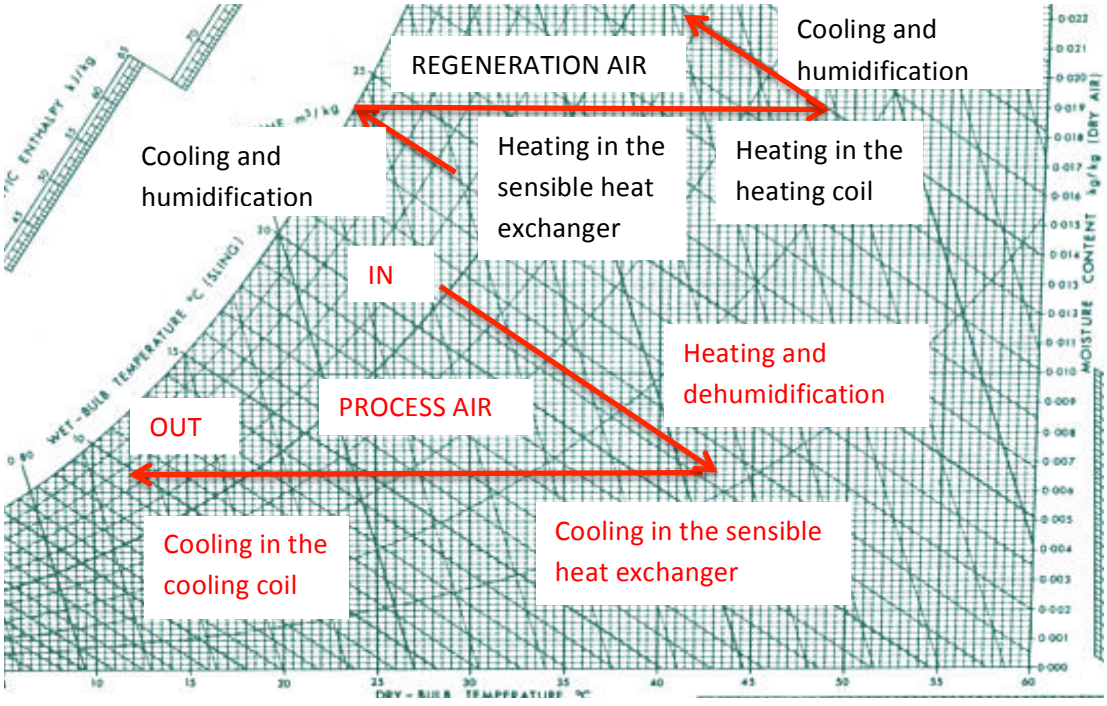

Figure 36 Air treatments on the psychometric chart for the suggest system

The suggested system includes the benefit of removing the sensible heat and the latent heat in two separate cooling coils in the AHU as proposed by Shaw [68] but the

new idea is to overcome this benefit by removing the latent heat using a desiccant wheel instead of using a secondary cooling coil.

As the desiccant wheel is generally regenerated through a high temperature air stream, it is also considered the possibility to use part of the heat rejected by the absorption chiller to pre-heat the regeneration air stream.

4.5 CASE STUDY SAMPLE RESIDENTIAL HOUSE

A case study has been assessed using the proposed solar cooling system applied to a residential application. To establish the cooling load applied to the chiller, it has been necessary to perform a simulation of the heat load of a typical dwelling. The scope of the simulation is the determination of the peak heat gain divided by sensible and latent heat. Sensible heat is added to the conditioned space by conduction, convection and radiation. Latent heat is added when moisture (water vapour) is added to the air in the space. (i.e. vapour emitted from occupants and equipment as bath, shower or kitchen processes).

Due to the thermal inertia of the wall of the dwelling, there is a time lag between the temperature rise in the outside environment and in the dwelling. The latent heat does not have this time lag effect.

Heat loads included in the simulation are the following:

- Direct solar radiation through transparent surface
- Heat conduction through wall and roof due to
    - o temperature difference
    - o incident solar radiation on outside surface
- Heat generated within the space by
    - o Occupants (sensible and latent)
    - o Lights (sensible only)
    - o Receptacles (sensible only and Equipment (sensible and latent)
- Energy transfer due to the outdoor air
    - o Infiltration (sensible and latent)
    - o Ventilation (sensible and latent)

The software used for this simulation is the TRACE® 700 v6.2.6.5 [128]

The software includes a database with all the weather data for several cities around the world so the input necessary for this simulation will be only the parameter of

the building as areas, exposition, insulation value for the perimeter walls and roof, internal lighting load and occupants in the dwelling.

The output includes total sensible heat gain and latent heat gain for each hour of the day for all year round. The peak maximum sensible heat gain and the corresponding latent heat gain will be used as cooling loads.

The inputs used in the software, suggested by the Building Code of Australia (BCA), corresponding to a residential house located in Brisbane are the following:

- Ambient DB/WB temperatures: 32°C / 25°C
- Gross area of the building: 150 m^2
- Height: 2.4 m
- Wall area: 113 m^2
- Glass area: 22 m^2
- Number of people: 4
- The following assumption have been used:
- U Value for walls: 0.7485 W/m^2 °C
- U Value for roof: 0.3323 W/m^2 °C
- Ceiling R value: 0.315 m2 °C/W
- U Value for windows: 5.84 W/m^2 °C
- U Value for door: 1.14 W/m^2 °C
- Ventilation value: 10.00 L/s/person
- Infiltration value: 0.5 air changes/hr
- Lighting type: Recessed fluorescent, not vented, 80% load to space lighting amount 15 W/m^2
- People sensible: 0.1 kW
- People latent: 0.1 kW

The performance of the entire system depends on both characteristics of the refrigeration and solar systems. As stated in Chapter 2: the performance of a refrigeration system is presented by its COP while the performance of the solar collector is defined as the ratio of the useful heat output to the total global radiation incident on the collector.

Combining the equation (2-20) and the equation (4-2) it is possible to define the efficiency of the total system as:

$$\eta_{system} = \mathrm{COP}_{chiller}\, \eta_{collector} \tag{4-38}$$

This value has been calculated for the case study and indicated in Table 9.

4.6 PROCEDURE AND TIMELINE

The following activities are included in the frame for my research thesis:

1) Development of mathematical model for the estimation of energy output from a solar field
2) Development of mathematical models for the absorption chiller
3) Development of a mathematical model for the desiccant wheel
4) Estimating of the cooling load of a typical dwelling using appropriate software
5) Combine the previous three models generating a solar cooling system that match the cooling load required
6) Optimization of the system

Accordingly, a specific methodology has been conceived in order to separate and clearly accomplish the various tasks. Mathematical models will be developed by Matlab™ software.

4.7 ANALYSIS

By using the mathematical model and appropriate set of input values we obtained a number of interesting results.

By varying the inputs we tried to estimate the maximum saving achievable by this new solar cooling system.

One inputs used is the output temperature of the water from the panels; the variation of this input, from 80 to 100 °C, affects the variation of the efficiency of the panels. It is expected that the increases of the temperature of the hot water required will reduce the efficiency of the panels. The variation of efficiency of the panels will be assessed in paragraph 5.4 whereas the variation of the efficiency of the absorption chiller due to the variation of the hot water temperature will be assessed in paragraph 5.5.3

Other parameter that will vary is the cooling water temperature that will simulate the implementation of the system at various locations. The cooling water temperature ranges from 27 to 33 °C. The expected effect on the absorption chiller performance by varying the cooling water temperature will be assessed in paragraph 5.5.2.

Other parameter that will vary is the chilled water temperature that will simulate the implementation of the system in different designs. The chilled water temperature

ranges from 5 to 12 °C. The expected effect of the variation of the cooling water temperature on the performance of the absorption chiller will be assessed in paragraph 5.5.1.

The variation of the humidity of the process air from 0.010 to 0.018 grwater/gr dry air, the variation of the temperature of the process air from 23 to 40 °C and the variation of the temperature of the regeneration air from 70 to 90 °C have effect on the performance of the desiccant wheel, the assessment of this effect will be assessed in paragraph 5.7

Also the quantity of fresh air will vary, this will simulate the implementation of the system in different application going from residential to industrial to hospital where 100% of fresh air is required. By varying the amount of fresh air supplied to the system the load on the chiller will vary and so the energy used by the system. The expected effect of the variation of the quantity of fresh air supplied on the performance of the full system will be assessed in paragraph 5.8.

Each simulation will be performed for each desiccant material assessed. The data obtained by the simulation will be analysed estimating for each application the best efficiency which can be obtained and estimate the saving achievable with this new design when compared to the current common design.

Chapter 5: Results and Analysis

The design of the system is controlled by many operating conditions: supply air temperature and humidity, regeneration air temperature, desiccant type, supply and return air flow rates and efficiency of the sensible heat exchangers.

Outside air conditions have been obtained from the weather data and design condition for Brisbane. The outside conditions based on the Brisbane dry bulb and wet bulb conditions are t = 32 °C and t = 25.5 °C respectively [129]. In this work the condition for the supply air to the user is fixed at t = 13℃ (Dry bulb) and 95% RH as commonly used in practical design.

The following paragraphs details all the results obtained by the mathematical models by varying the input parameters. Performances of each equipment have been optimized by varying the inputs and the working condition. The results for each section of the equipment are presented in separated paragraphs first and then collected in the overall result of the integrated system where each equipment is used at its optimized working condition.

5.1 SOLAR SYSTEM SIMULATION OUTPUT

The first calculation is performed to determine which kind of solar panel is better suited to work with an absorption chiller. Three typologies of panels have been considered:

- Flat panels
- Evacuated tube collectors
- Compound Parabolic Concentrating (CPC)

5.2 SOLAR PANEL CHOSEN

The efficiency of each panels has been calculated using equation (4-5) as a function of T^*_m.

Table 6 shows examples of parameters η_0, a_1 and a_2 for different kind of soalr collectors.

Table 6 Parameters η_0, a_1 and a_2 for different kind of solar collectors [130].

Parameter	Unit	Flat panel	Evacuated tube	CPC
Optical Efficiency η_0		0.8	0.832	0.622
Linear heat loss coefficient a_1	W/m^2K	4	1.140	0.74
Quadratic heat loss coefficient a_2	W/m^2K	0.01	0.0144	0.003

Using the above parameters the efficiency of the panels has been calculated and the results are shown in Figure 37.

In the calculation the values of the ambient temperature T_a has been kept fixed at 25 °C and the global solar irradiance G used is 1000 W/m^2.

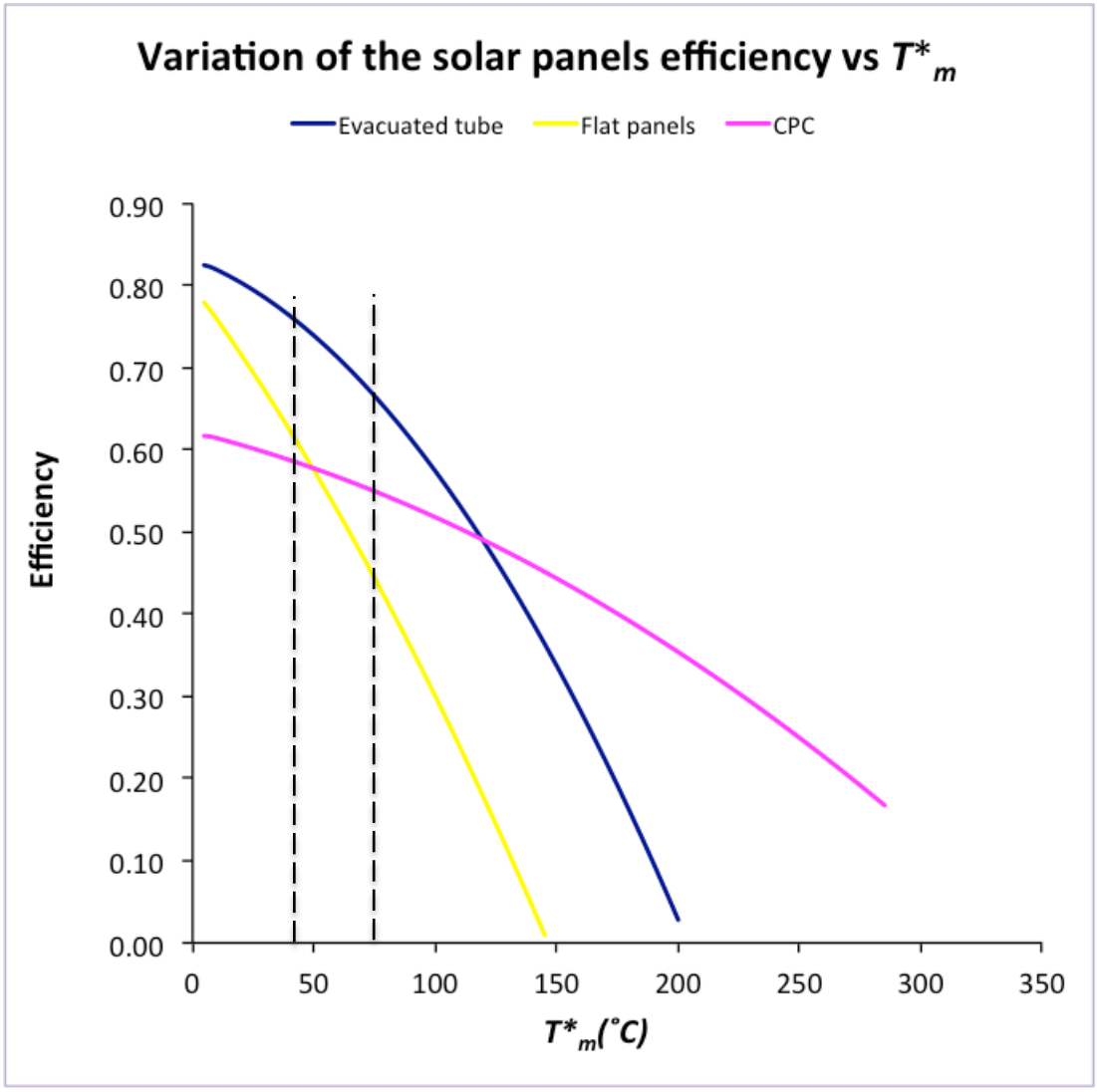

Figure 37 Variation of solar panel efficiency

Considering that in this study the range of temperatures required from the panels varies from approximately 80 °C to 100 °C and the ambient temperature T_a used varies from 25 °C to 40 °C the value of T^*_m varies from 40 °C to 75 °C (dashed black lines).

As shown in Figure 37, in the range of temperature used in this study, it has been found that the most suitable panels to generate water at the desired temperature are the evacuated tube. The same result has been found in literature from previous work performed at Politecnico di Milano [97].

5.3 VALIDATION OF THE SOLAR SYSTEM MODEL

The model results have been compared with data available from a report of performance test undertaken accordingly to the EN 12975-2 for a glazed solar collector [111]. From the measured data available in the report and listed in Appendix C the efficiency of the solar panels has been calculated with the mathematical model and the results have been compared with the panels efficiency data available in the report. The result is shown in Figure 38.

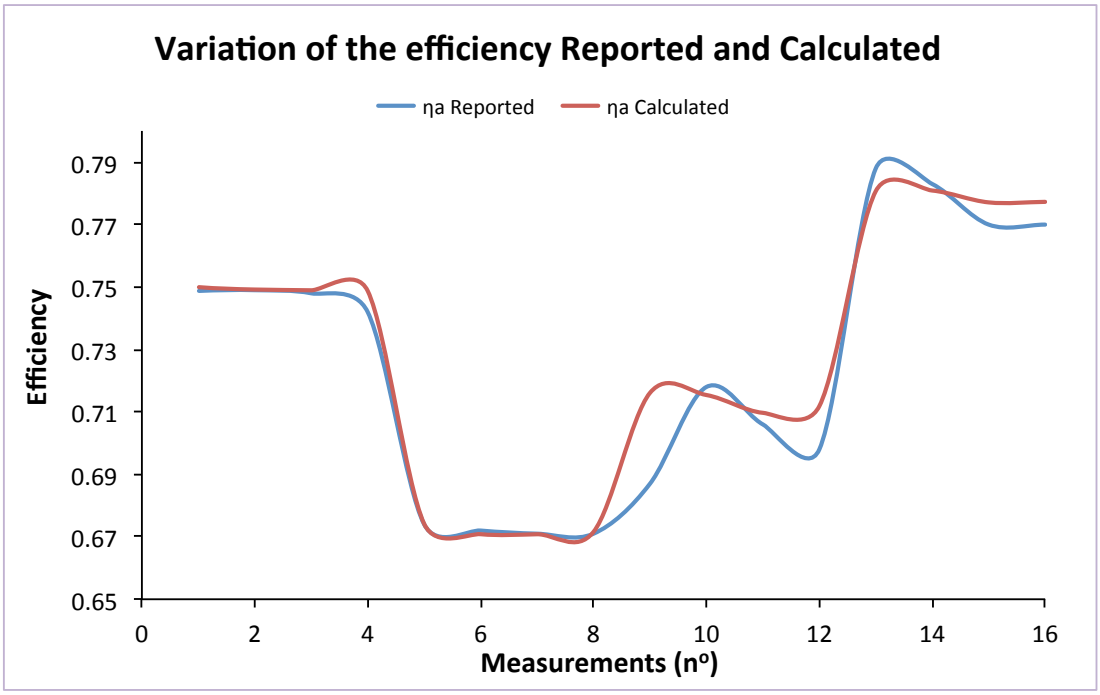

Figure 38 Comparison between calculated and measured solar panels efficiency

From the above graph it is evident that the delta between calculated and measured efficiency values is very considerate to be acceptable for the purpose of the model. The delta between the two values of the efficiency is between +0.73% and -2.91%.

5.4 EFFICIENCY OF THE EVACUATED TUBE SOLAR PANELS

Solar panels based on evacuated tubes are used, as explained above, as they show the highest efficiency in the range of temperatures used in the proposed solar cooling system. Their efficiency depends from the global solar irradiance G, ambient temperature T_a and the mean temperature of the water T_m, which is calculated by simply using the inlet and outlet temperatures T_{in}, T_{out} of the water from the panels.

Keeping the value of the global irradiance constant at 1000 W/m^2 and varying the three temperatures inputs the efficiency has been calculated and the results are shown in Figure 39.

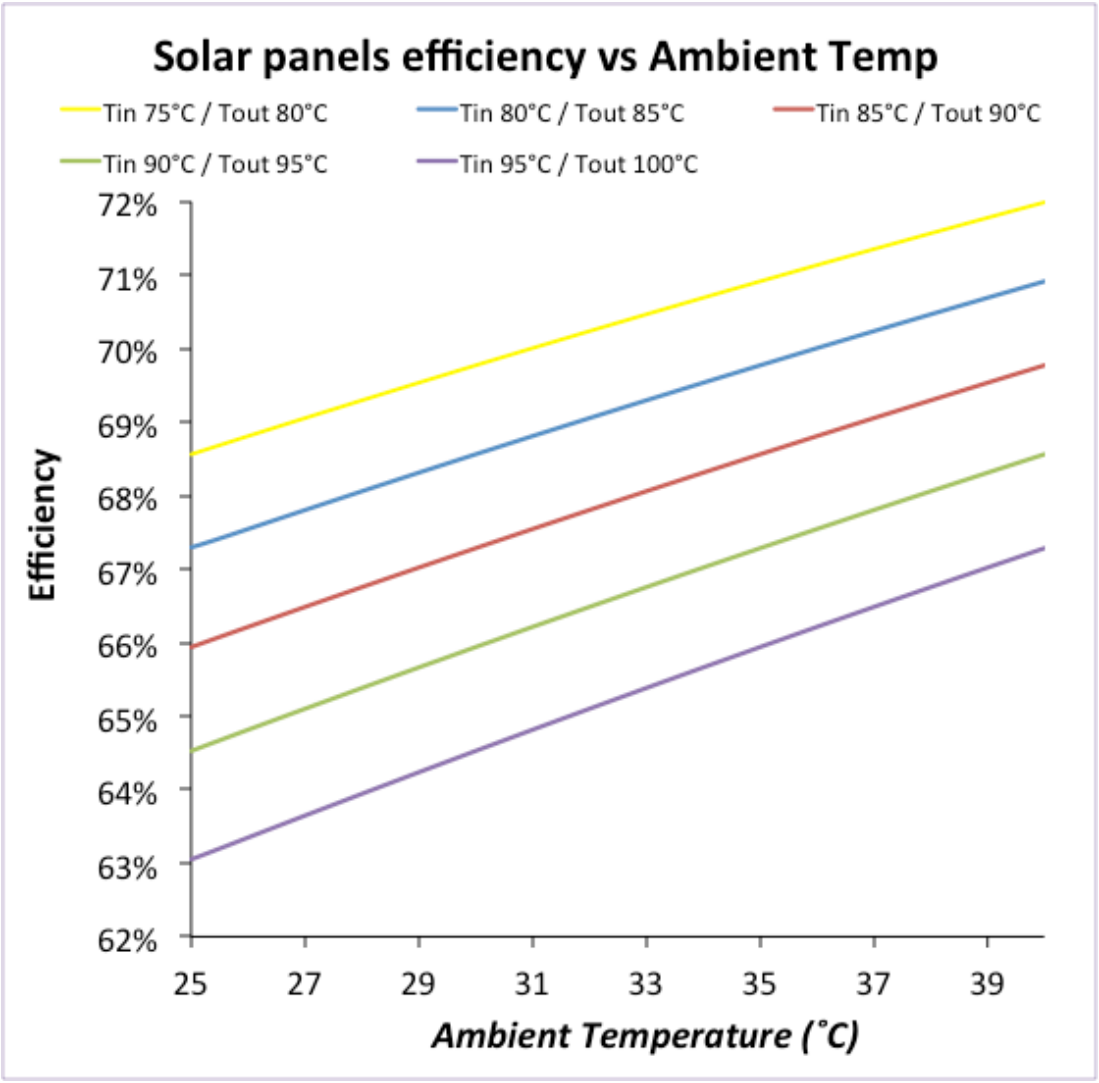

Figure 39 Variation of the solar panels efficiency vs ambient and water temperatures

The solar system simulation shows the direct impact of the ambient and hot water temperatures on the efficiency of the solar panels. From the simulation it is evident that an increase of the efficiency of the panels is obtained by lowering the hot water

temperature required. It is then desirable to use the panels at the as lower temperature as possible to achieve their highest efficiency.

5.5 SIMULATION OF THE SINGLE STAGE ABSORPTION CHILLER

The efficiency and the energy consumption of our air conditioning system are strongly dependent from the input conditions, so it is important to establish the trend of the COP of the chiller when the working condition inputs vary. A single effect absorption chiller data available in literature have been used to show the relation between the cooling water, the generator and the evaporator temperatures, leading to strong variations in the efficiency of the chiller. Variations of COP of the absorption chiller by varying the input parameters are described in the following paragraphs.

5.5.1 Variation of efficiency with variation in chilled water temperature

By keeping the temperature of the generator and the temperature of the cooling water constant, it has been generated a graph showing the variation of the COP of the absorption chiller when the temperature of the chilled water (evaporator) varies.

Figure 44 shows the results obtained with the following inputs:

- Temperature of generator = Varies from 80 °C to 100°C (as indicated in the legend)
- Cooling water temperature = 27 °C
- Chilled water temperature = Variable

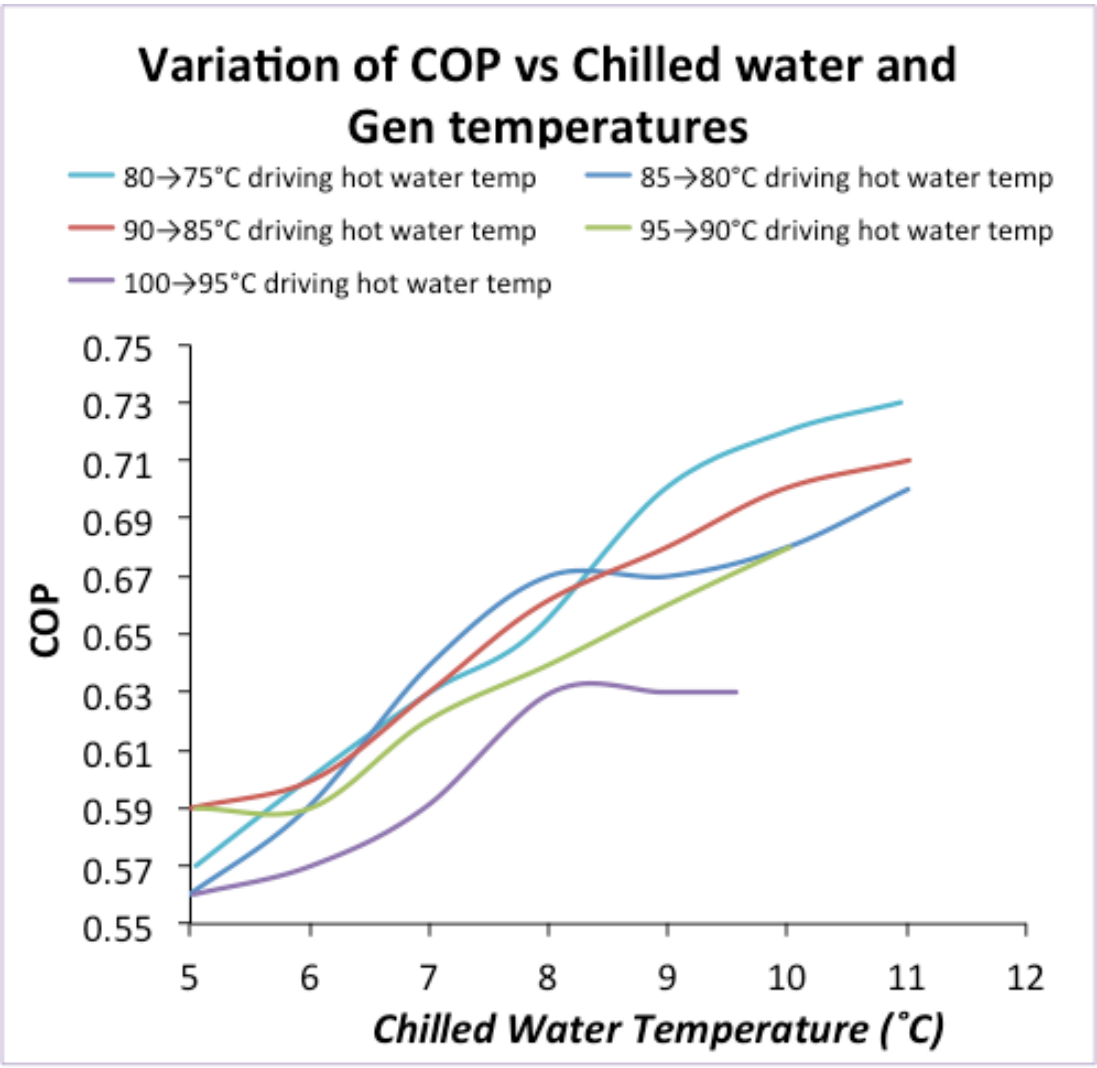

Figure 40 Variation of COP due to variation of chilled water and generator temperatures

As expected from the literature review, the COP of the absorption chiller increases when the temperature of the evaporator (chilled water) increases and the cooling and generator temperatures are kept constant. From the literature review it was expected that the COP of the chiller would increases with the increases of the temperature of the generator keeping the chilled water and cooling water temperature constant; from the above graph it is evident that the COP of the chiller do not follow always the expected path. Causes of this variation from the expected path are related to the variation of the other parameters involved in the calculation of the COP and the limited number of simulations.

5.5.2 Variation of efficiency with variation in cooling water temperature

By keeping the temperature of the generator constant, a graph showing the variation of the COP of the absorption chiller when the temperatures of the chilled water (evaporator) and cooling water vary.

Figure 41 shows the results obtained with the following inputs:

- Temperature of generator = 80 °C
- Cooling water temperature = 27 °C to 35°C (as indicated in the legend)
- Chilled water temperature = variable

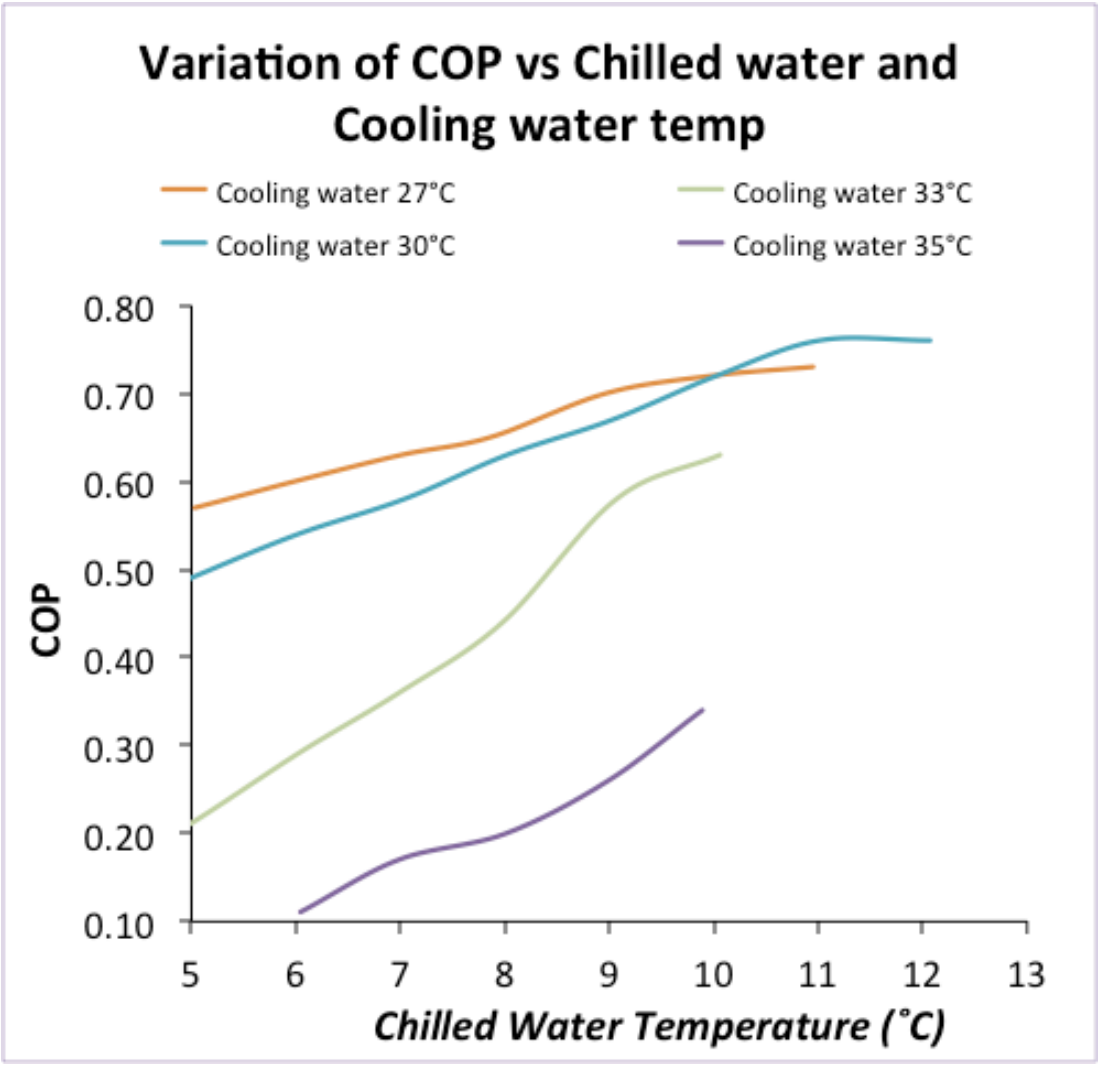

Figure 41 Variation of COP due to variation of chilled water and cooling water temperatures

The variation of the COP as indicated in the above graph follow the path expected from the literature review. By varying the temperature of the cooling water, the COP varies proportionally. Also, from the above graph, it is evident that the temperature

of the chilled water required impact on the COP of the chiller. By increasing the chilled water temperature the COP increases accordingly and vice versa.

From the above graph it is clear that by increasing the temperature of the cooling water from 30 °C to 35 °C the COP of the chiller approximately half its value. By using a pitch of 5°C between a stream of cooling air and cooling coil of the cooling circuit, the maximum temperature of the heat recovered could be only 30°C.

5.5.3 Variation of efficiency with generator temperature

A variation of the generator temperature affects the COP of the absorption chiller as stated in the literature review. The graph using the data available in literature review showing the variation of the COP when the generator temperature varies is shown in Figure 42. Inputs used are the following:

- Temperature of generator = variable
- Cooling water temperature = 27 °C to 35°C (as indicated in the legend)
- Chilled water temperature = 27 °C (most used temperature in industry for air conditioning system)

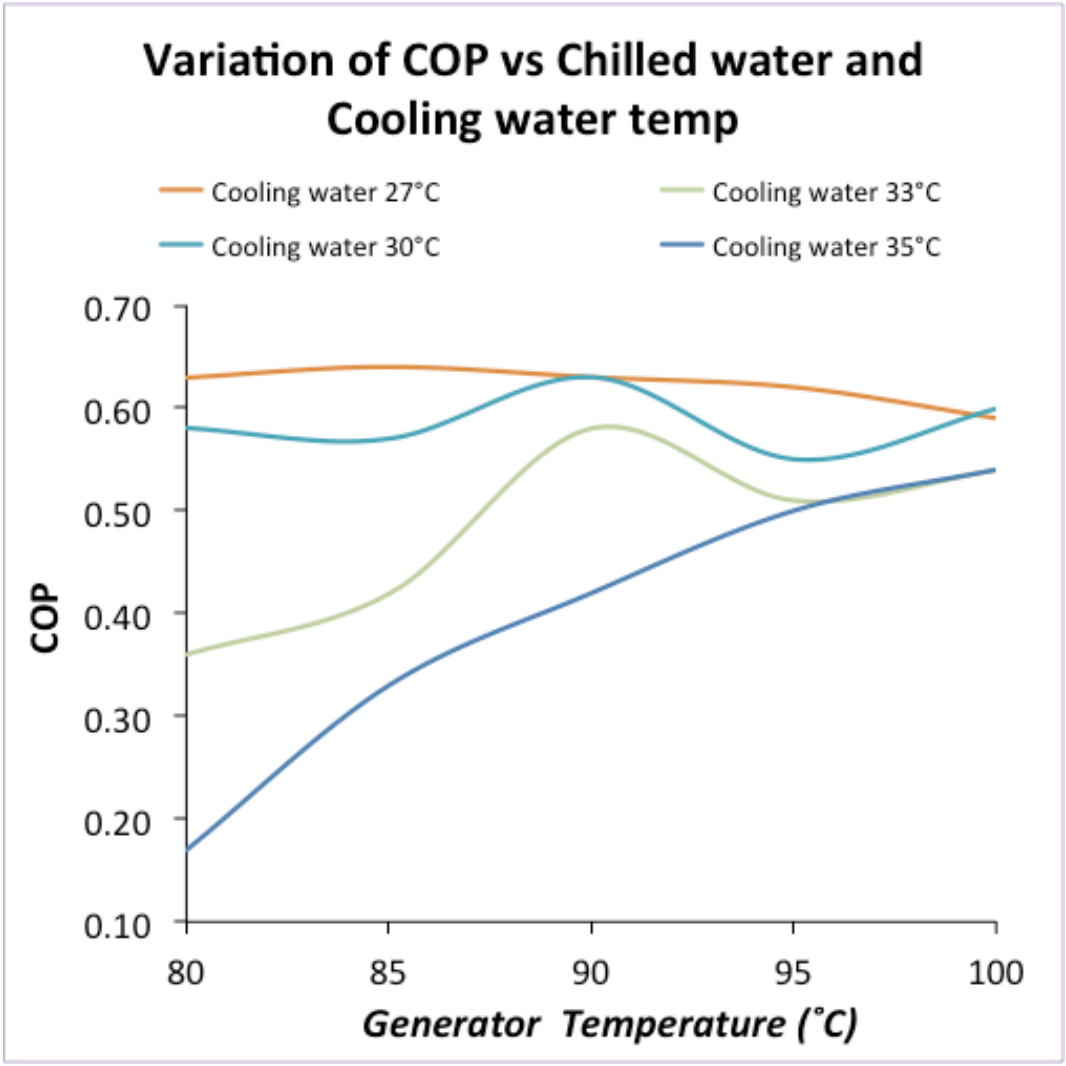

Figure 42 Variation of COP due to variation of generator and cooling temperatures

The expected path as in literature review was that the increase of the temperature in the generator increases the COP of the chiller. From the above graph, it is noticed that the expected path is only achieved when water cooling temperature is 35 °C. there is also a peak in the COP of the chiller when the generator temperature is 90 °C. one of the possible cause of this peak could be the higher ΔT in the cooling water in and out from the condenser and absorber.

5.6 SIMULATION OF THE HALF EFFECT ABSORPTION CHILLER

As shown in paragraph 5.5 the COP of the single stage absorption chiller is strongly related to the cooling temperature of the medium used to remove the rejected heat from the condenser and absorber. It is shown that with low temperature at the generator and high temperature of the cooling water the efficiency is very low and as

stated in literature review there is a limitation of working temperature for a single stage absorption chiller.

This limitation is then overcome by the use of a half effect chiller, which allows the use of air as medium to remove the rejected heat from the absorber and the condenser. Measurements from a prototype of a half effect chiller available at the Politecnico di Milano [98], have been used in the range of temperature where the single effect absorption chiller simulation could not be performed. The results are shown in Figure 43 and Figure 44.

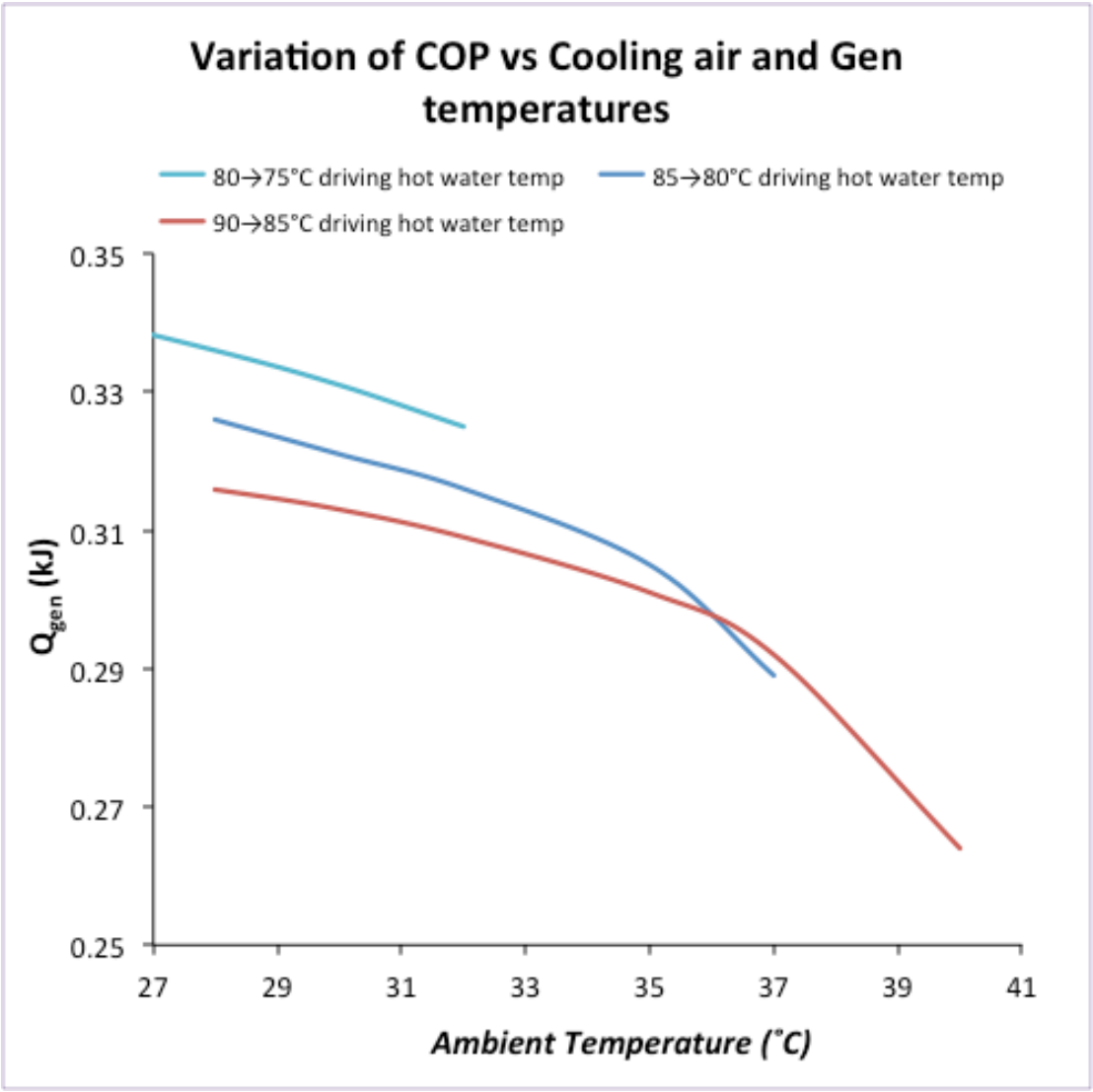

Figure 43 Variation of the COP of the half effect chiller as a function of the ambient temperature

Compared to the single effect chiller, the half effect chiller can work with lower temperatures, and the measurements available start at T_{gen} = 80°C.

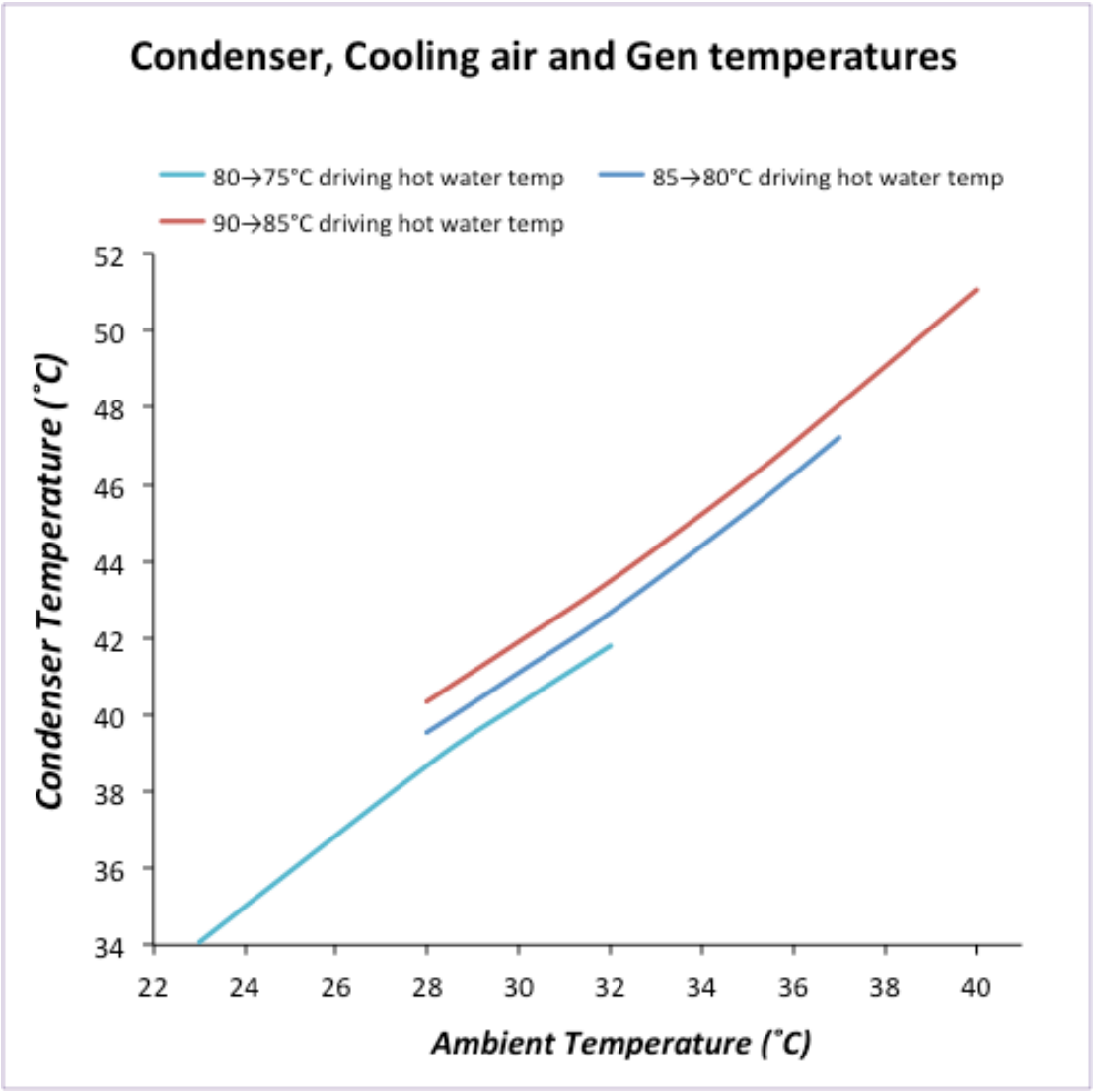

Figure 44 Variation of the Condenser of the half effect chiller as a function of the ambient temperature and hot water in the generator

The highest temperature in the condenser is achieved when T_{gen} = 90°C; in this case the temperature of the ammonia entering the condenser is of 51°C [98]. By using a pitch of 5°C between a stream of cooling air and the condenser, the maximum temperature of the heat recovered could be only 46°C.

5.7 DESICCANT WHEEL SIMULATION

A mathematical model has been used to assess the humidity ratio reduction of the desiccant wheel with different absorption materials as described in paragraph 4.3 of the methodology section. Flow rates in the process side and the regeneration side of the desiccant wheel are assumed to be equal to avoid any differential pressure between the channels which could end up to cause leakages between the stream. Figure 45 shows the

humidity reduction (X_{proIN}-X_{proOUT}) obtained through a desiccant wheel by varying the temperature of the process air in the range 23 – 40 ˚C. Main assumptions used in the simulation are:

- Regeneration speed = 1 m/s
- Process air speed = 1 m/s
- Process degrees = 180°
- Regeneration degrees = 180°
- Rotation speed = 10 Rev/h
- Regeneration temperature = 80°C
- $X_{reg,IN}$ = 0.01194 kg/kg
- $X_{pro,IN}$ = 0.01803 kg/kg

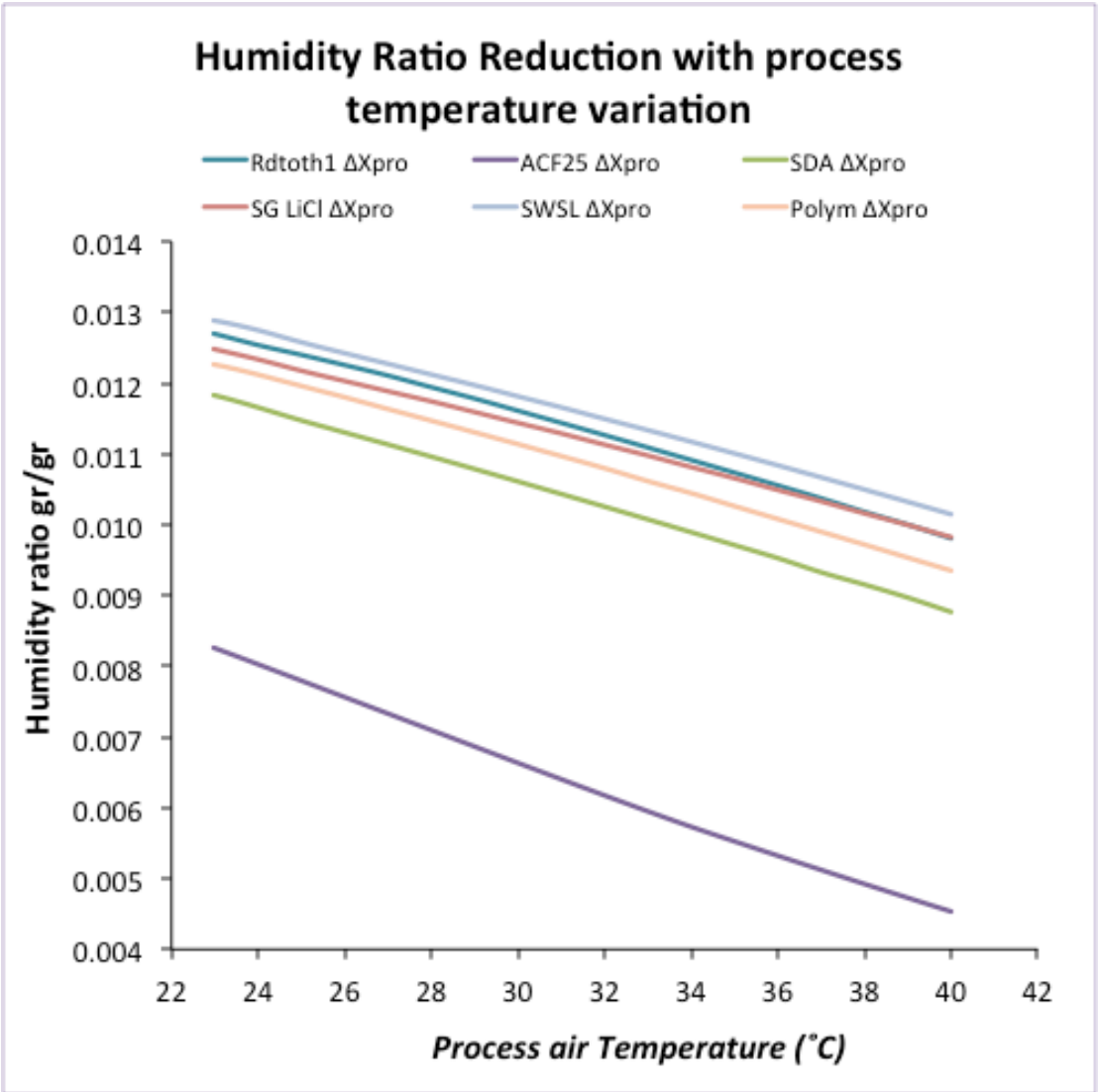

Figure 45 Humidity ratio reduction with variation of process air temperature

The performance of the wheel has been measured by the variation of the humidity ratio, which is linearly decreasing with the increase of the process air temperature. In this simulation the material that shows better performance is the SWSL and the material showing the lower performance is the ACF25.

Figure 46 shows the humidity reduction of desiccant wheel varying the humidity ratio of the process air input and keeping constant the following inputs:

Regeneration speed = 1 m/s

Process air speed = 1 m/s

Process degrees = 180°

Regeneration degrees = 180°

Rotation speed = 10 Rev/h

Regeneration temperature = 80°C

$X_{reg,IN}$ = 0.01194 g/kg

$T_{pro,IN}$ = 32°C

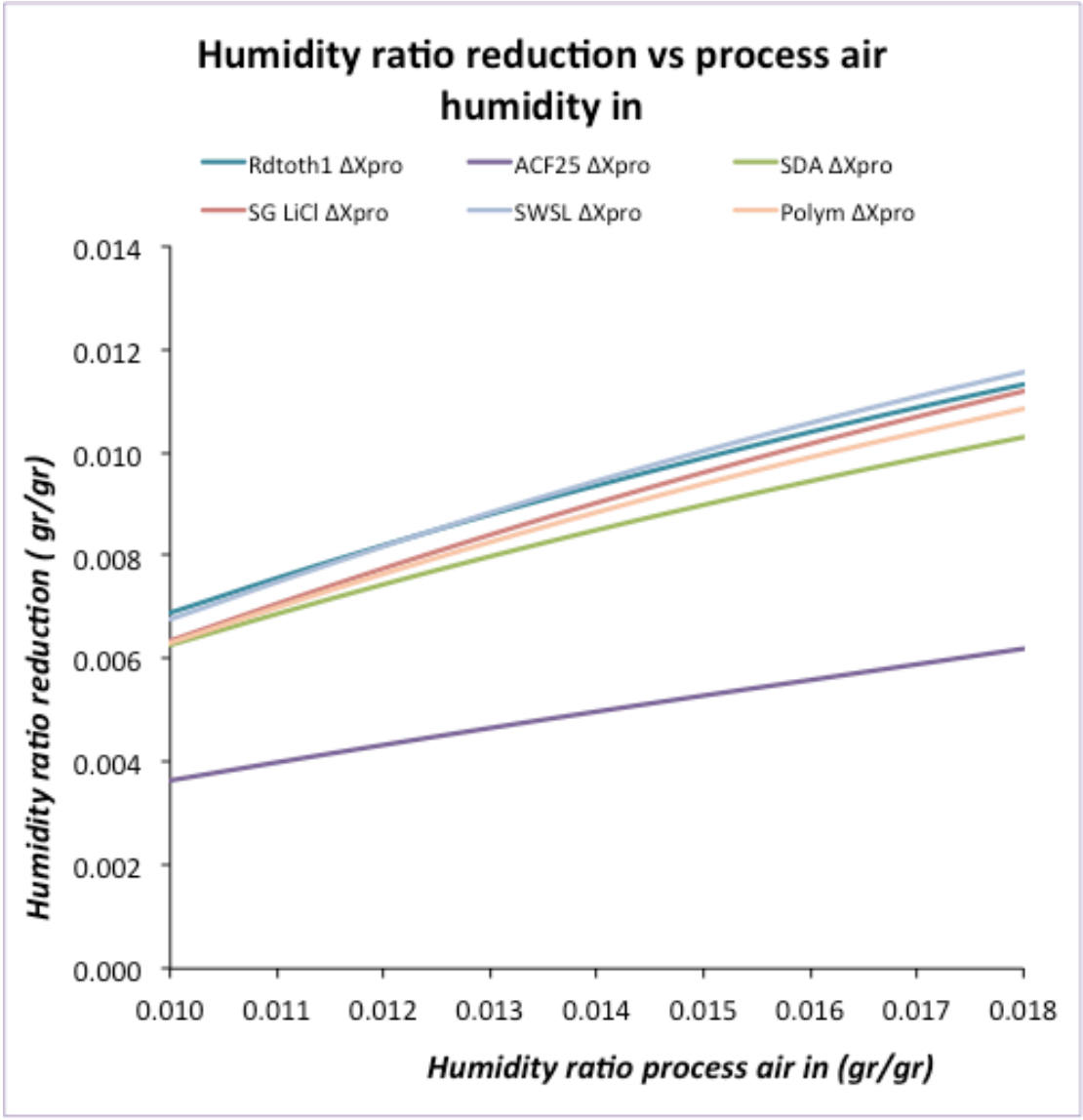

Figure 46 Humidity ratio reduction vs process air humidity ratio variation

With the above simulation, the humidity ratio reduction versus the process humidity variation has been assessed and the result is shown in Figure 47.

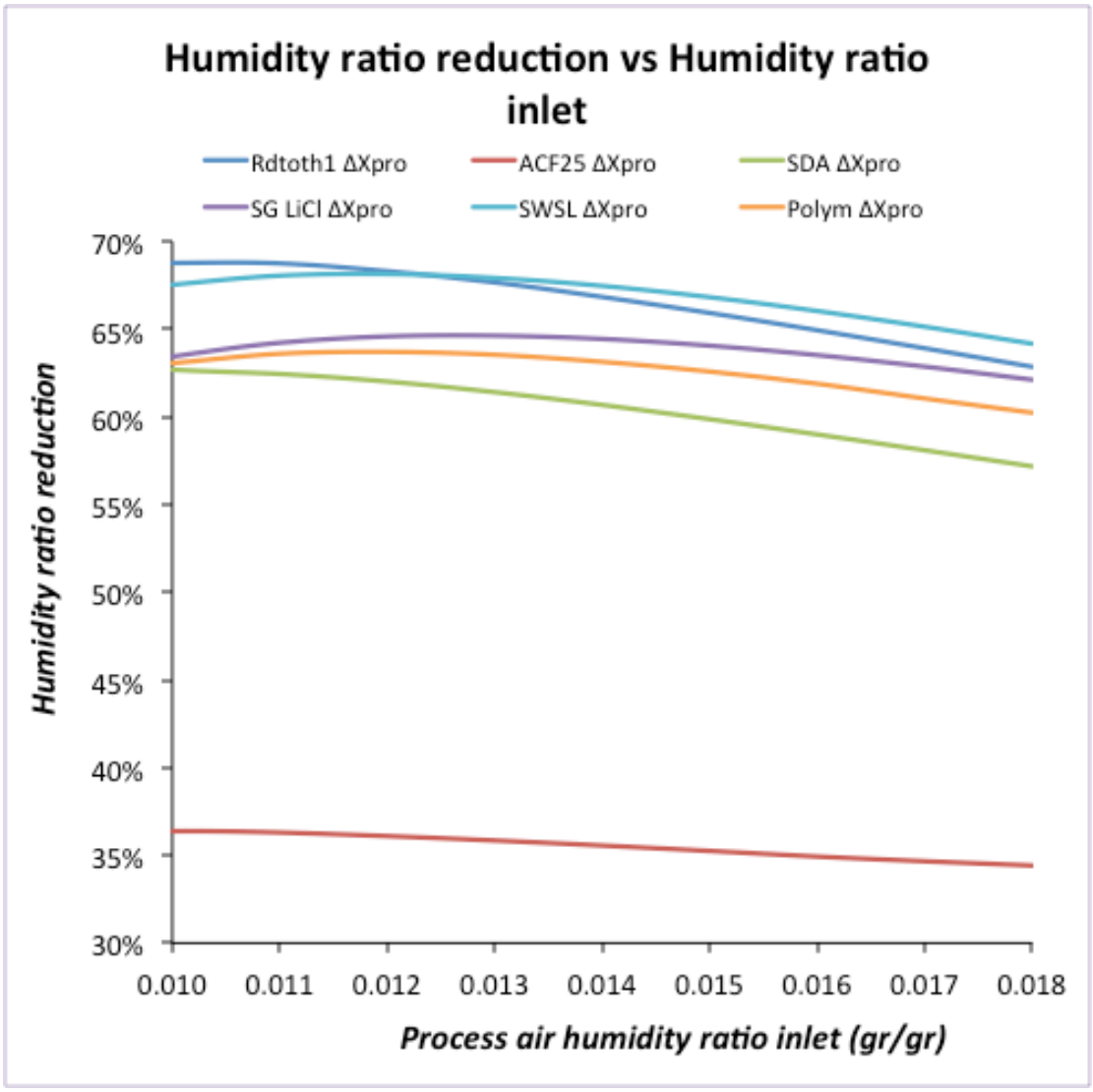

Figure 47 Humidity ratio reduction vs Humidity ratio inlet

The assessment has been performed varying the humidity ratio of the process air varies from 0.010 gr/gr_{dry_air} to 0.018 gr/gr_{dry_air}.

The results show that the desiccant material which performs better when the humidity ratio is below 0.013 gr/gr_{dry_air} is the Rdtoth which show to reduce the humidity ratio by 66.8%. When the humidity ratio is grater than 0.013 gr/gr_{dry_air} the SWSL perform better than the others desiccant materials. The behaviour of the SWSL shows a better response to the variation of the humidity ratio input and it is then more suited in real condition when the humidity ratio of the ambient air varies between the seasons and the day and night.

Another simulation conducted shows the humidity reduction of desiccant wheel varying the regeneration temperature process air input and keeping constant the following inputs:

Regeneration speed = 1 m/s

Process air speed = 1 m/s

Process degrees = 180°

Regeneration degrees = 180°

Rotation speed = 10 Rev/h

$X_{reg,IN}$ = 0.01194 gr/gr

$X_{pro,IN}$ = 0.01803 gr/gr

The results are shown in Figure 48.

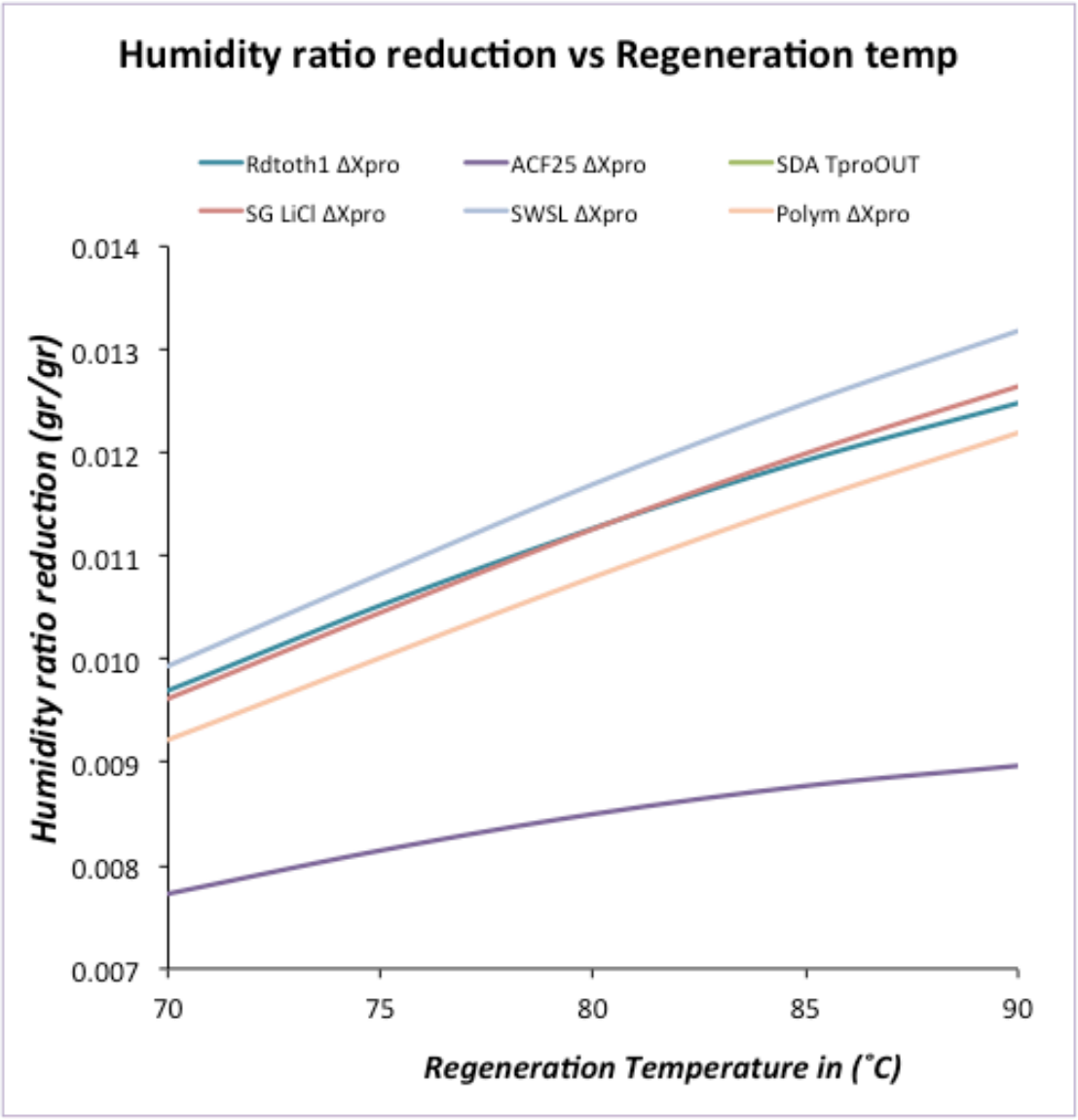

Figure 48 Humidity ratio reduction vs regeneration temperature

The material with the higher humidity ratio reduction using regeneration temperature between 70°C to 90°C has result of a simulation is the SWSL. This

simulation shows that the SWSL is the more appropriate material to be used in the range of temperature used in the proposed system.

The optimization of the performance of the desiccant wheel has had as target the reduction of humidity ratio using the minimum regeneration air temperature which accordingly leads to reduce the energy used for the regeneration.

For this purpose an assessment of the process air humidity ratio versus the angular position of the regeneration side and the revolution speed has been performed. The following inputs have been kept constant:

Regeneration speed = 1 m/s

Process air speed = 1 m/s

Process degrees = 180°

Regeneration degrees = 180°

$X_{reg,IN}$ = 0.01194 gr/gr

$X_{pro,IN}$ = 0.01803 gr/gr

T_{reg} = 90˚C

$T_{pro,IN}$ = 32 °C

The results show that an optimal revolution speed and optimum angular position of the regeneration side exist for each regeneration temperature.

As example, Figure 49 shows the trend of the humidity ratio reduction vs the revolution speed with T_{reg} = 90˚C. Other simulations with different temperatures are shown in Appendix E

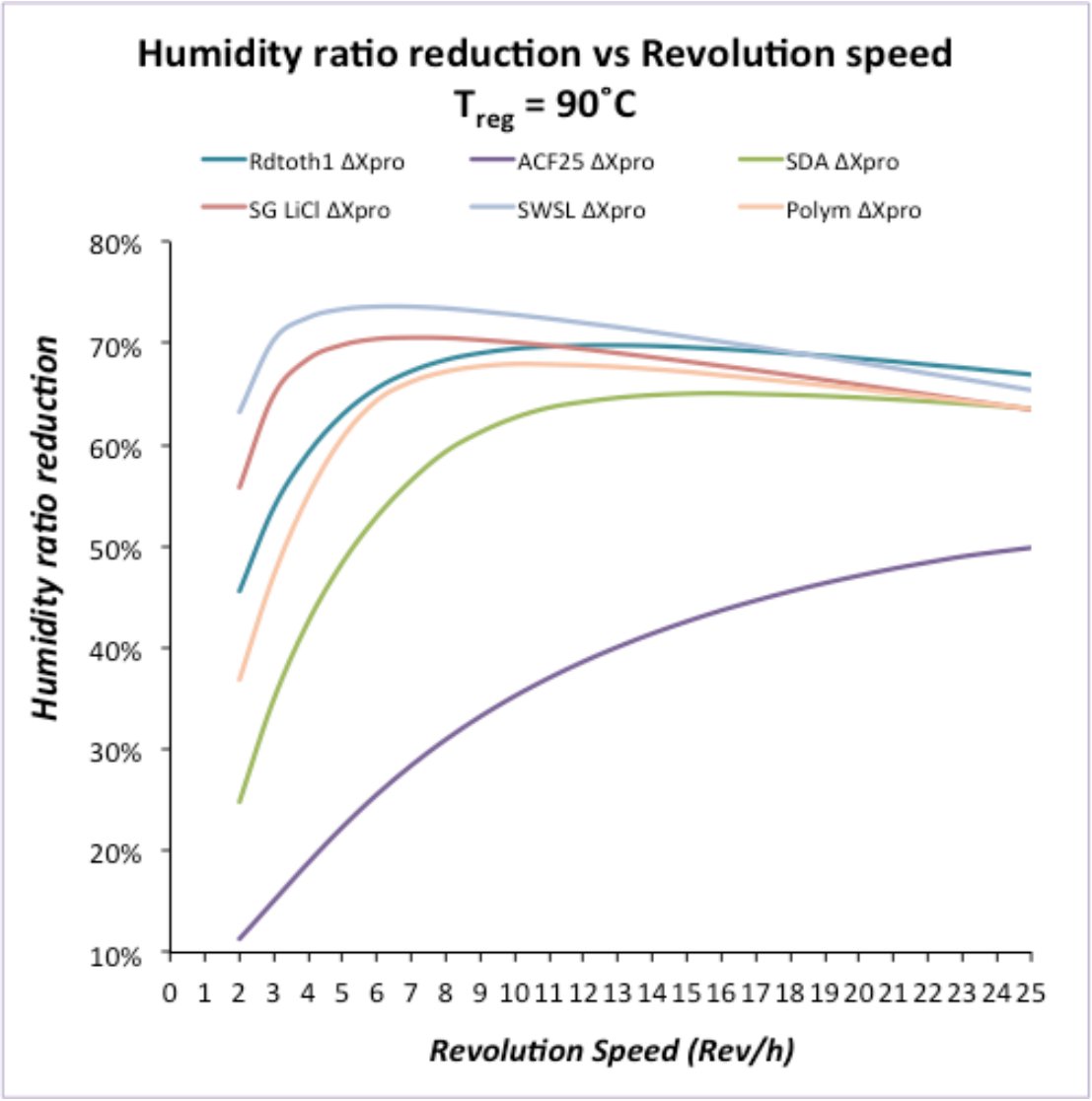

Figure 49 Humidity ratio reduction vs revolution speed at $T_{reg,IN}$ = 90 °C

For each regeneration temperature and each desiccant material, an optimum revolution speed has been estimated.

These estimated values have been used together with the values kept constant and the optimum angular position of the regeneration side has been calculated for each type of desiccant material at different regeneration temperatures. As example, the results for the case T_{reg} = 90˚C is shown in Figure 50.

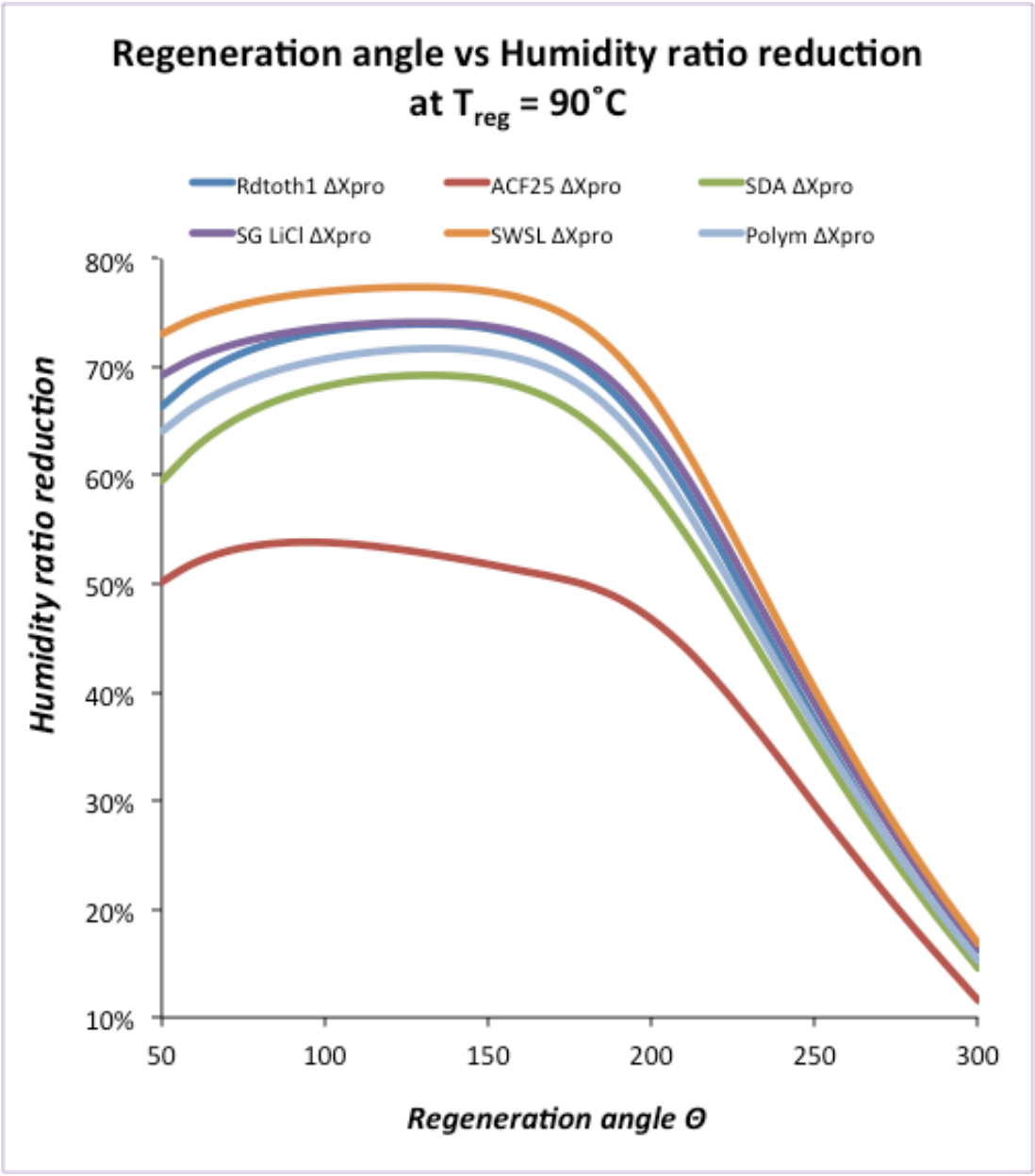

Figure 50 Regeneration angle vs Humidity ratio reduction using a $T_{reg,IN}$ = 90°C

Other simulation using different regeneration temperatures are shown in Appendix F

All the simulations performed with the mathematical models have shown results in line with the results expected after the assessment of books and articles found during the literature review.

5.8 INTEGRATED SYSTEM RESULTS

In this section are presented the calculation of the efficiency of the solar cooling system including the solar panels and the absorption chiller using the equation (4-38). The results are indicated in Table 7.

Table 7 Efficiency of the system including solar panels and absorption chiller

Solar panel Efficiency	
Efficiency Solar panels 80→75°C driving hot water temp	68.88%
Efficiency Solar panels 85→80°C driving hot water temp	67.49%
Efficiency Solar panels 90→85°C driving hot water temp	66.02%
Efficiency Solar panels 95→90°C driving hot water temp	64.47%
Efficiency Solar panels 100→95°C driving hot water temp	62.84%
Air cooled absorption chiller COP	
Efficiency Chiller 80→75°C driving hot water temp	0.325
Efficiency Chiller 85→80°C driving hot water temp	0.316
Efficiency Chiller 90→85°C driving hot water temp	0.309
Water cooled Single Stage absorption chiller COP	
Efficiency Chiller 80→75°C driving hot water temp	0.58
Efficiency Chiller 85→80°C driving hot water temp	0.57
Efficiency Chiller 90→85°C driving hot water temp	0.63
Efficiency Chiller 95→90°C driving hot water temp	0.55
Efficiency Chiller 100→95°C driving hot water temp	0.60

Solar cooling system efficiency with air cooled half effect absorption chiller	
Total Efficiency 80→75°C driving hot water temp	22.39%
Total Efficiency 85→80°C driving hot water temp	21.33%
Total Efficiency 90→85°C driving hot water temp	20.40%
Solar cooling system efficiency with water cooled absorption chiller	
Total Efficiency 80→75°C driving hot water temp	39.95%
Total Efficiency 85→80°C driving hot water temp	38.47%
Total Efficiency 90→85°C driving hot water temp	41.59%
Total Efficiency 95→90°C driving hot water temp	35.46%
Total Efficiency 100→95°C driving hot water temp	37.70%

In the above calculation the following assumption have been taken:

- Solar insolation: 850 W/m^2
- Cooling temperature: 30˚C
- Chilled water temperature: 7˚C

The maximum value of the efficiency achievable for the combination of solar panels and absorption chiller has been highlighted in Table 7. This combination of solar panel – absorption chiller has been used in the simulation of the integrated solar cooling system which includes includes solar thermal panels, absorption chiller, desiccant wheel and the AHU which includes sensible heat wheel and heat exchanger coils. The effectiveness of the sensible heat wheel is assumed to be at 75% [131, 132]. The performance of the system is measured in terms of the energy saving at solar field side when the proposed solar cooling system is compared to a conventional solar cooling system.

For each simulation different desiccant material are used; the rotation speed and the regeneration angle Θ used for each desiccant materials are the optimum values calculated in the above paragraph 5.7

The supply air, return air and ambient air conditions of the simulation are indicated in Table 8.

Table 8 Working condition assumed for the case study

	Supply air condition	Return air condition	Ambient air condition
Dry bulb *t* (˚C)	13	24	32
Humidity ratio (gr/kg)	8.89	9.34	18.03
RH (%)	95	50	60
Enthalpy (kJ/kg)	35.53	47.78	78.31

Figure 51 shows the saving of the proposed system versus a conventional solar cooling system by varying the dry bulb temperature of the process air (ambient air).

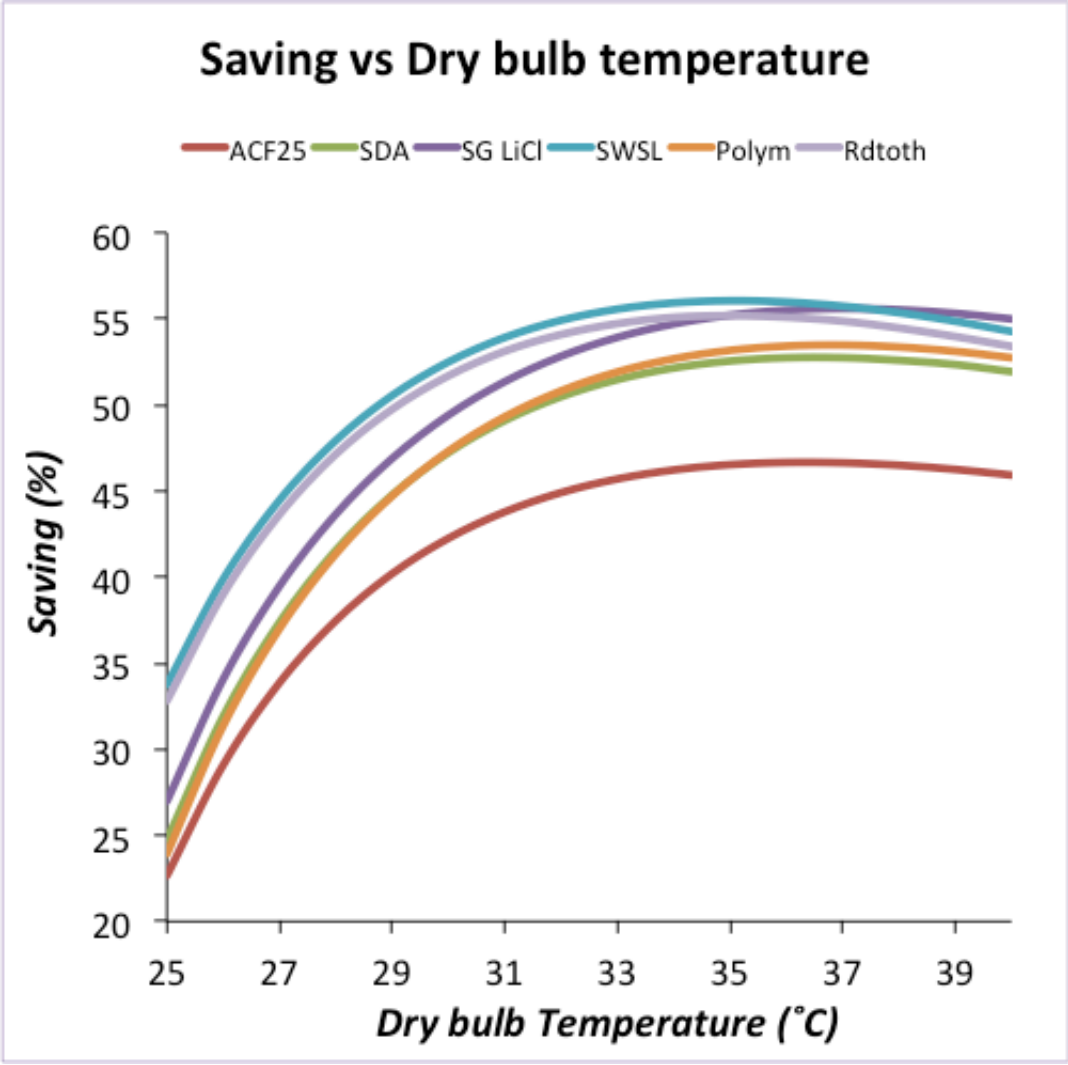

Figure 51 Saving achieved by varying the ambient temperature

In this simulation the following variables are kept constant:

- RH 60%
- Fresh air 100%
- Generator temperature 80°C
- Hot water temperature from the panels 80°C
- Cooling water temperature 30°C
- Desiccant wheel regeneration temperature 65°C

It is shown that using the SWSL material as desiccant in the proposed system the saving that can be achieved is up to maximum almost 56% when compared to the conventional system. The system using SWSL desiccant has higher saving when the dry bulb temperature of the process air is below or equal to 37°C whereas a system using SG

LiCl as desiccant is to be preferred when the dry bulb temperature of the process air is above 38°C.

Figure 52**Error! Reference source not found.** shows the saving of the proposed system versus a conventional solar cooling system by varying the amount of fresh air intake and the desiccant material. The fresh air ratio that goes into the system starts from 0% and increases every 10% until the air ratio reached 100%.

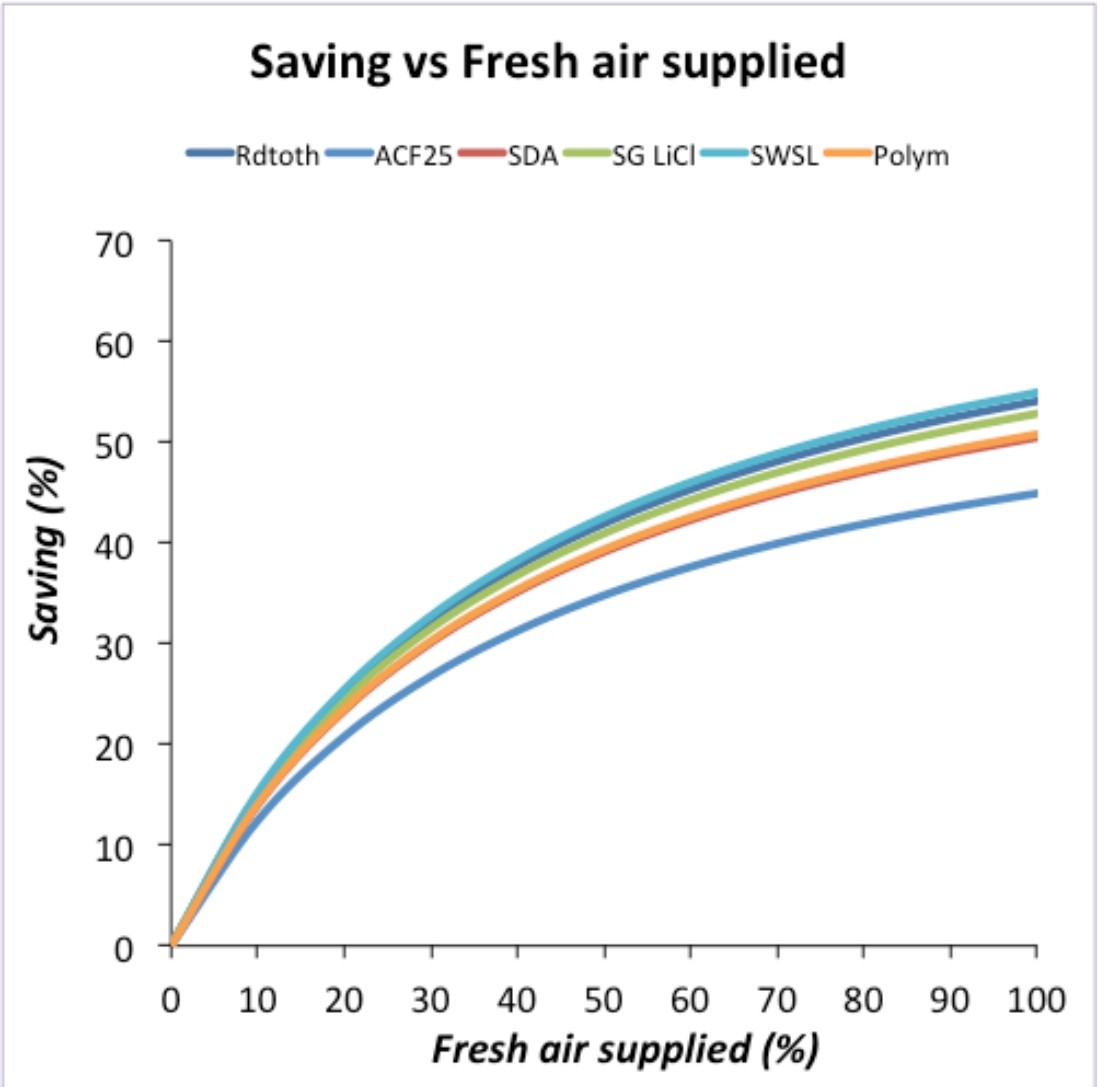

Figure 52 Saving achieved by varying the amount of the fresh air intake

In this simulation the following variables are kept constant:

- RH 60%
- Dry Bulb Temperature 32°C
- Generator temperature 80°C
- Hot water temperature from the panels 80°C
- Cooling water temperature 30°C

- Desiccant wheel regeneration temperature 65°C

This simulation shows that the maximum saving is achieved when the amount of the fresh air is 100%. When the fresh air input is limited the saving is limited; this is an expected result as the suggested system only achieve saving in removing the humidity from the fresh air supplied to the system.

Figure 53 shows the saving of the proposed machine versus a conventional solar cooling system by varying the RH of ambient air.

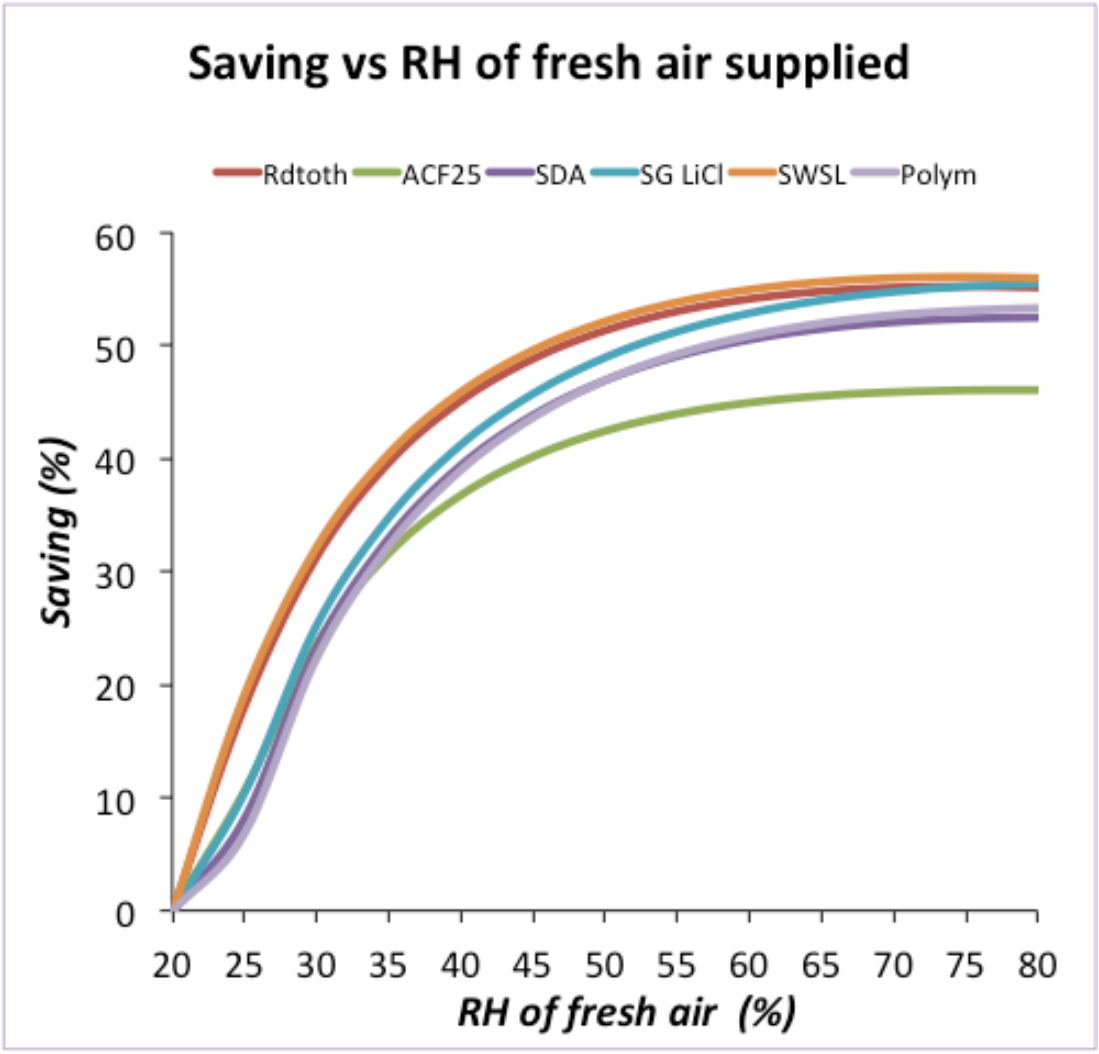

Figure 53 Saving achieved by varying the RH of the ambient air

In this simulation the following variables are kept constant:

- Fresh air 100%
- Dry Bulb Temperature 32°C

This simulation shows that the system using the SWSL as desiccant perform always better than the other materials.

Table 9 shows the results of the comparison between a traditional solar cooling system and the proposed system delivering the same amount of cooling needed by a building (57 kW). The variable inputs used in the simulation includes:

- Solar insolation 850 W/m^2
- Cooling water temp 30°C
- Chilled water temp 7°C
- RH_{amb} 60%
- Fresh air 100%
- Tamb 32°C
- RH 60%
- Treg 65°C
- Desiccant material Selective Water Sorbent Silica Gel+ Calcium Chloride (33%)

Table 9 Simulation results comparing a traditional and the suggested solar cooling system

	Traditional system	**Suggested system**
EnSolHX (kW)	N/A	21.30
Cool power evaporator (kW)	57.33	13.63
Cooling capacity (kW)	57.33	57.33
Solar energy for absorption chiller (kW)	137.83	32.76
Solar energy for desiccant wheel regeneration (kW)	N/A	30.93
Maximum solar power required (kW)	137.83	63.69
Saving in power required		53.8%
COP of Solar cooling system	0.416	0.900
Solar collectors area required (m^2)	238.58	108.72
Saving in area required		54.4%
Total insolation (kW)	203	92

5.9 SUMMARY OF THE RESULTS

The performance of the total system is connected to the performance of all the equipment used in the system.

From the above simulations it is evident that:

- The performance of the solar panels increase with the reduction of the temperature required at the outlet
- Selective Water Sorbent Silica Gel+ Calcium Chloride (33%) is the desiccant material that can remove the amount of humidity needed and be regenerated at the lower temperature of 65°C
- The efficiency of the half effect absorption chiller used as reference is at its maximum when the generator hot water is at 80˚C as shown in Table 7
- The efficiency of the single stage absorption chiller used as reference is at its maximum when the generator hot water is at 90˚C as shown in Table 7
- The higher efficiency of 41.6% for the system solar panels-absorption chiller is achieved by the water cooled single effect absorption chiller when the generator hot water is at 90˚C
- Higher saving is achieved by integrating a solar field of evacuated tube with a water cooled absorption chiller working with hot water at 90˚C and a desiccant wheel using Selective Water Sorbent Silica Gel+ Calcium Chloride (33%) as the desiccant material and regenerated at 65°C
- The maximum temperature of the heat reject available for recovering is of approximately 46˚C when air cooled half effect is used or 30˚C when water cooled single stage absorption chiller is used. Both temperatures do not allow any heat recovery at higher temperature than the already available heat after the sensible heat exchange indicated in Figure 35 which is approximately 49.5˚C
- From the result shown in Table 9 it is evident that the implementation of the suggested system can achieve a saving up to 54% in thermal energy required. Accordingly this saving can be translate in financial saving due to the reduced number of solar thermal panels required
- Other saving in installation cost is due to the reduced size of the absorption chiller needed. The conventional solar cooling system required a chiller of 57.33 kW whereas the proposed system only needs a chiller of 13.62 kW.

However, the proposed system required additional piece of equipment which are not included in the conventional system as desiccant wheel, sensible heat exchanger wheel and an additional coil.

The total financial saving needs to be calculated case by case as cost of each equipment varying based on the size of the equipment.

As example a case study simulation has been undertaken and it is described in the following paragraph.

5.10 CASE STUDY SAMPLE RESIDENTIAL HOUSE

The above results have been used to perform the assessment of a case study using a house of 150 m^2 as described in paragraph **Error! Reference source not found.**. The working conditions of the case study simulation are indicated in Table 10 and the heat loads estimated for the building are indicated in Table 11. Relevant calculation and assumption for the heat loads for the residential case study are listed in **Error! Reference source not found.**, Appendix J and Appendix K . As the case study is a residential application, it is assumed that the fresh air supplied to the building is only 10% of the total supplied air as there is no standard applicable to the residential sector for HVAC.

Table 10 Working condition assumed for the case study

	Supply air condition	Return air condition	Ambient air condition
Dry bulb t (˚C)	15.8	24	32
Humidity ratio (gr/kg)	8.86	9.34	18.03
RH (%)	78.96	50	60
Enthalpy (kJ/kg)	38.19	47.78	78.31

Table 11 Design cooling load summary

Load Component	Sensible (kW)	Latent (kW)	Total (kW)
Solar Gain	3.02		3.02
Glass Transmission	1.19		1.19
Wall Transmission	1.36		1.36
Roof Transmission	0.63		0.63
Lighting	1.27		1.27

People	0.03	0.02	0.05
Misc. Equipment Loads	1.46		1.46
Cooling Infiltration	0.44	1.01	1.45
Ventilation load	0.44	1.01	1.45
Exhaust Heat	-0.02		-0.02
Lighting Load to Plenum	0.32		0.32
Total cooling load	10.14	2.04	12.18

As example, in Figure 54 it is shown the solar energy used to provide the cooling demand required for January for 24 hr for the conventional system and for the proposed system.

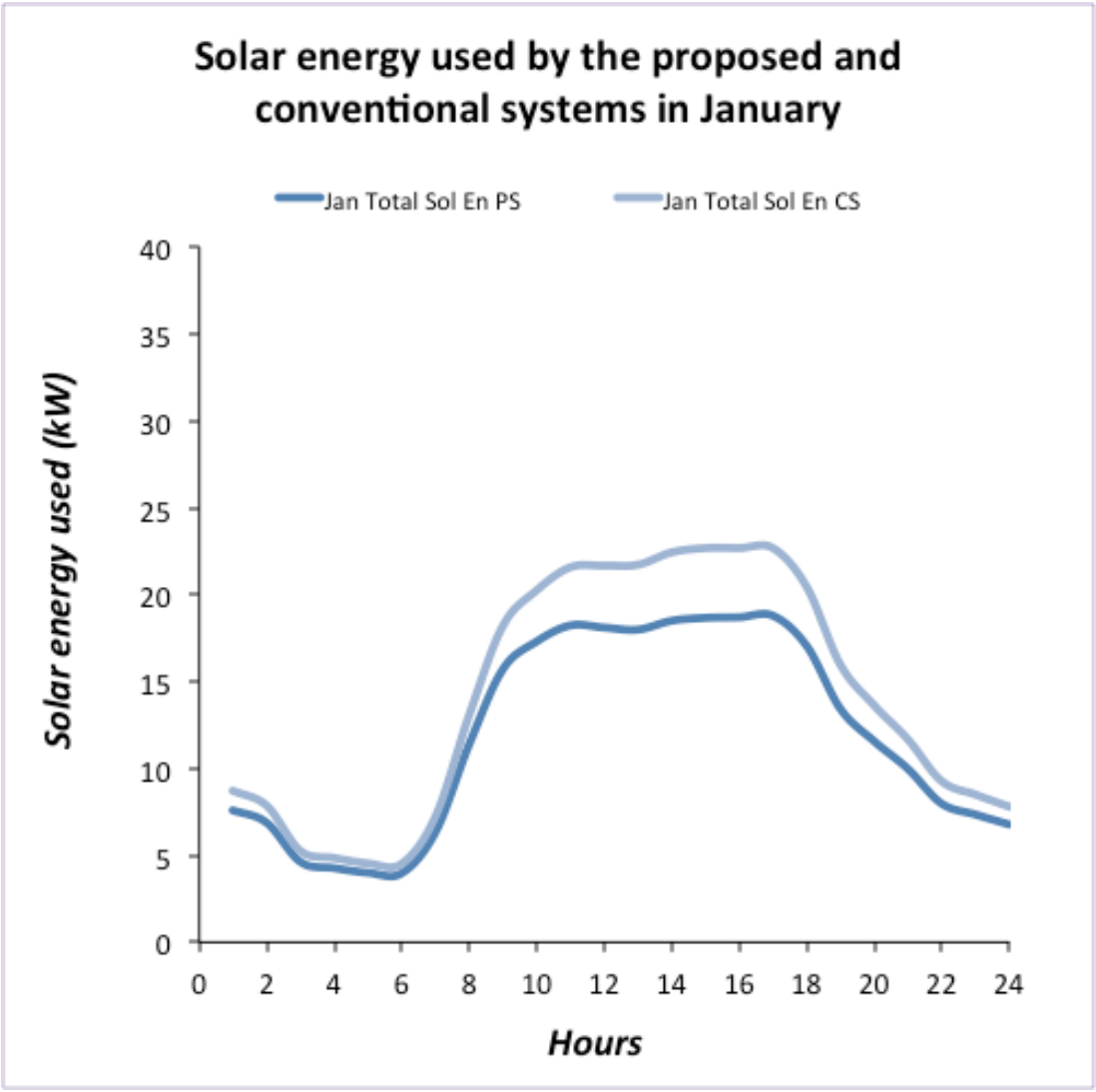

Figure 54 Solar energy used by the conventional system and the proposed system for January

The difference between the two lines is the saving achievable by implementing the proposed system. Similar graphs for the remaining months are included in Appendix G .

Figure 55 shows the saving in term of solar irradiation needed for each month and for each hour between a conventional system and the proposed system.

The performance of the system has been assessed for the 12 months of the year and shows that also during the winter season some cooling demand exists but the proposed system is slightly less efficient than the conventional system.

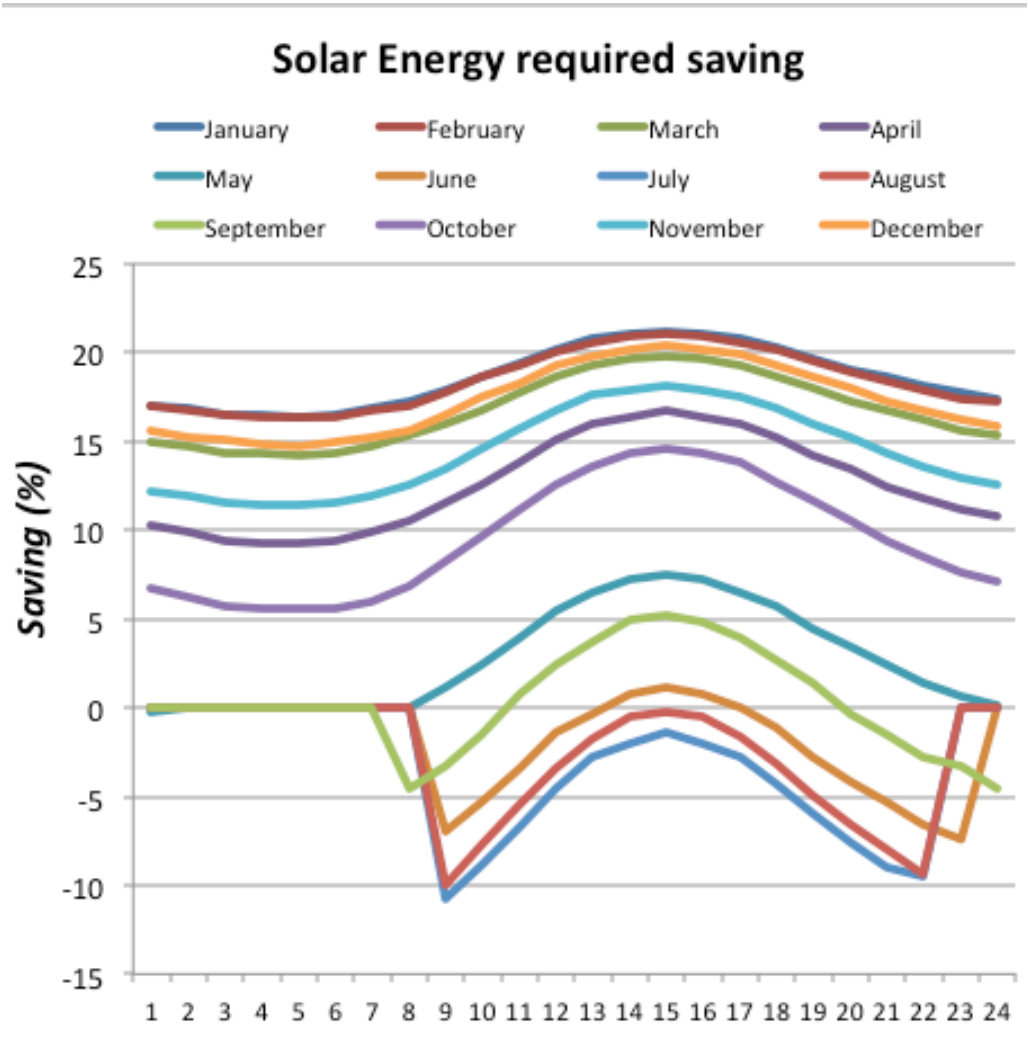

Figure 55 Solar energy required saving between conventional system and proposed system

This is due to the use of the desiccant wheel, which reduces the humidity ratio and increases the temperature of the process air before going to the sensible heat exchanger and then to the evaporator.

In these case the use of the desiccant wheel is not suggested and can be bypassed using the proposed system as a conventional system.

5.10.1 Summary of the results

Table 12 summarize the result of the simulation for one year of data.

Table 12 Summary of the result for the simulation for the case study

	Solar radiation	Solar energy	Cooling supplied	Solar panels (unit)	Roof area	COP
Conventional system	199,475 kWh	104,205 kWh	59,730 kWh	30	91 m^2	0.26
Proposed system	173,170 kWh	90,846 kWh	59,730 kWh	26	79 m^2	0.29

The case study has shown that the proposed system can supply the amount of cooling required by the building and it has a higher COP than the conventional system. due to the requirement for cooling of the building during periods when the solar energy is not available, both system require the installation of chilled water storage tanks. The saving achievable is of 13% in solar radiation needed. This value translates as saving in the roof area needed for the solar panels that is reduced from 91 m^2 to 79m^2. The COP of the full system calculated as:

$$COP_{Solar\ cooling\ system} = \frac{Cooling\ capacity}{Solar\ radiation} \quad (5\text{-}1)$$

The COP varies from 0.256 to 0.295 with an increase of 15%.

5.10.2 Estimation of the cost of the conventional and proposed systems

As shown in paragraph 5.10.1, by implementing the proposed system some energy saving is achieved. This saving can be translated in installation cost saving during the implementation of the system by the following:

- Reduced number of solar panels needed
- Reduced size of the chiller used

In the other end some cost of the proposed system are higher because of the following added cost:

- Desiccant wheel
- Heating coil

The total cost saving is the different between the reduced cost and the added cost. For this calculation some quotes have been obtained for the solar thermal panels (GreenLand System) and the AHU. Other cost have been obtained from the Rawlinson's book which is a reference book for small builder and consultant.

The prices used are:

Solar panel: $2,500 each

Water-cooled Water/Ammonia absorption chiller: $1,000 per $kW_{cooling}$ capacity

Heating coil: $500

Desiccant wheel: $3,000

AHU: 6,000

A summary of the financial assessment of saving achievable by implementing the proposed system instead of the conventional system are listed in Table 13.

Table 13 Cost saving achievable by implanting the proposed system vs conventional system

	Solar panels	AHU	Heating coil	Absorption chiller	Total Cost
Conventional system	$75,000	$6,000	N/A	$13,000	$94,000
Proposed system	$65,000	$9,000	$500	$9,700	$84,200

As shown in Table 13 the installation cost saving achievable by the proposed system are of approximately 10%.

Using the capital costs for the proposed system and the conventional system it has been calculated the payback period as measure of "how long the solar cooling systems take to pay for itself." The payback period has been calculated comparing the solar cooling system to an equivalent classical system using vapour compression cycle as indicated in Table 19.

The assumptions adopted in the calculation are:

Conventional system cooling capacity	14.8 kW
Power input	5.6 kW
Electricity tariff for residential	22.238 c$/kWh [133]
Cost of the unit	$8,000

The results of the calculation are shown in Table 14 and Appendix M

Table 14 Payback period of the solar cooling systems vs conventional system

	Initial investment	Payback (years)
Solar cooling conventional system	$94,000	14.98
Solar cooling proposed system	$84,203	13.98
Electric vapour compression cycle unit	$8,000	N/A

Chapter 6: Conclusions

This thesis has fully answered the original research questions laid out in paragraph 1.2, which can be summarised as an assessment of the possibility of reducing the installation costs of a typical solar cooling system by implementing a desiccant wheel which can be regenerated by hot air produced by solar thermal panels.

The methodology developed in this thesis has covered all the aspects of the simulation of a solar cooling system, looking at each part of the system the solar panel, desiccant wheel and the absorption chiller individually to find their most optimised working points, and assessing them subsequently as a complete system. Optimal working conditions for each part of the system have been estimated and adopted in the final system.

From the literature review I gained an understanding that energy recovery has already been implemented in electric chillers at a production level. Nowadays major chiller manufacturers produce electric chillers with an already implemented heat recovery system. Other research showed the possibility of recovering some of the heat rejected by an absorption chiller used in a solar cooling system [115].

The possibility of recovering part of the rejected heat from the absorption chiller has been assessed in this thesis by using an absorption chiller simulator. The simulator results show that the temperature of the heat rejected is too low to regenerate a desiccant wheel. However, it has been found that the implementation of a desiccant wheel in a typical solar cooling system used in conjunction with an absorption chiller results in significant energy and implementation cost savings.

The simulations have produced results in line with my expectations formed as a result of the literature review. As expected, the solar panels have shown that their efficiency is related to the ambient, inlet water and outlet water temperatures. The desiccant wheel performances showed that the Selective Water Sorbent Silica Gel and Calcium Chloride at a 33% concentration are the most suitable desiccant materials of the six assessed materials when used in the operational temperature ranges outlined in Chapter 1.

The complete system has been assessed and the results, as expected, show that energy savings increase when the amount of fresh air introduced in a building increases.

The total energy savings achievable by implementing the proposed system vary depending on the application and the working conditions of the system:

- In residential applications, where the amount of fresh air supplied is assumed to be 10% of the total supplied air, savings of 13% were achieved.
- In other applications, where 100% of fresh air is supplied to the conditioned space, savings of up to 56% were achieved.

A financial assessment of the proposed system for a residential application has been performed and the results show that a saving of approximately 10% of the total costs of installation can be achieved when compared to a typical design.

Also, as the cost savings of the proposed system increase with an increase of the humidity ratio inlet (ambient air), the system is most suited to climate zones with higher relative humidity stretching from latitude 30 degrees North to 30 degrees South. This would, for example, include the entire East coast of Australia and South East Asia.

This study also found that the physical size of the AHU unit could limit the implementation of the proposed system in the real world as it is larger than a typical AHU unit of the same cooling capacity used in a conventional solar cooling system. For larger dwellings the AHU unit would only be suited for centralised air conditioning were space can be set aside for the unit in the planning of the dwelling.

Based on research findings of this study, the most attractive markets for an application of the proposed system are the following:

- nursing homes
- hospitals (patient areas and operating rooms)
- hotels
- dormitories
- school and university classrooms.

The reason for that is that all of the above settings require a high proportion of fresh air which means that a high amount of latent heat load needs to be removed by the desiccant wheel instead of it being removed by the chiller.

6.1 FUTURE WORK

The research looked only at combining solar panels, desiccant wheel and an AHU unit. Future work on this system could potentially focus on the development of a controls strategy. Further savings are most likely achieved when a controls system is

implemented that would consist of pressure sensors, temperature gauges and flow meters which control the flow of the cooling and heating fluids. The control system would also need to control the humidity ratio varying the regeneration temperature, so that only the latent heat is removed leaving the sensible heat to be removed by the chiller

Other components, including a storage tank for cooling water, [134] need to be researched further. The tilt angle for the solar thermal panels could also be optimised using the research undertaken in my previous works [135, 136].

Since the design is a prototype, the components would need to be tested as one complete system, to see if they work in practice as described in theory.

Also, further investigations need to be undertaken for the dynamic assessment of the performance of the system in areal-world applications by varying the ambient temperature, the generator temperature and the cooling load required during the day.

As new and refined technologies become available on the market, this provides new opportunities for improving the proposed system into the future. A high efficiency direct solar air heater from Greenland System, for example, has now become available and could be implemented in the proposed system to generate hot air used for regenerating the desiccant wheel. The implementation of an air heater in the system will further reduce the cost of the system as the current water to air heat exchanger used to generate the hot air will then be redundant.

These technical options could be part of future research and development efforts to further increase the efficiency of the proposed solar cooling system and reduce the installation costs at the same time.

Bibliography

[1] W. R. Institue. (2010, 14 October 2012). Power Surge: Energy use and emissions continue to rise. Available: http://www.wri.org/publication/content/8601

[2] P. H. J.Pierce, "Future Possible Retail Electricity Price Movements: 1 July 2010 to 30 June 2013," Australian Energy Market Commission, Sydney Final Report Final Report, 30 November 2010 2010.

[3] E. R. a. A. W. LEHREN, "Relief in Every Window, but Global Worry Too," in *The New York Times*, ed. ONLINE, June 20, 2012.

[4] W. S. Loh, I. I. El-Sharkawy, K. C. Ng, and B. B. Saha, "Adsorption cooling cycles for alternative adsorbent/adsorbate pairs working at partial vacuum and pressurized conditions," *Applied Thermal Engineering,* vol. 29, pp. 793-798, 2009.

[5] C. Keil, S. Plura, M. Radspieler, and C. Schweigler, "Application of customized absorption heat pumps for utilization of low-grade heat sources," *Applied Thermal Engineering,* vol. 28, pp. 2070-2076, 2008.

[6] K. Byongjoo and P. Jongil, "Dynamic simulation of a single-effect ammonia-water absorption chiller," *International Journal of Refrigeration,* vol. 30, pp. 535-45, 2007.

[7] R. M. Lazzarin, A. Gasparella, and G. A. Longo, "Ammonia-water absorption machines for refrigeration: theoretical and real performances," *International Journal of Refrigeration,* vol. 19, pp. 239-246, 1996.

[8] Y. Fan, L. Luo, and B. Souyri, "Review of solar sorption refrigeration technologies: Development and applications," *Renewable and Sustainable Energy Reviews,* vol. 11, pp. 1758-1775, 10// 2007.

[9] D. Appleyard. (2010). *Chilling Out in the Sun: Solar Cooling*. Available: http://www.renewableenergyworld.com/rea/news/article/2010/06/chilling-out-in-the-sun-solar-cooling

[10] T. Otanicar, R. A. Taylor, and P. E. Phelan, "Prospects for solar cooling – An economic and environmental assessment," *Solar Energy,* vol. 86, pp. 1287-1299, 5// 2012.

[11] K. Sumathy, Z. C. Huang, and Z. F. Li, "Solar absorption cooling with low grade heat source — a strategy of development in South China," *Solar Energy,* vol. 72, pp. 155-165, 2// 2002.

[12] S. Lee, "Development of techniques for in-situ measurement of heat and mass transfer in ammonia-water absorption systems," S. Garimella, Ed., ed. United States -- Georgia: Georgia Institute of Technology, 2007.

[13] R. Z. Wang, T. S. Ge, C. J. Chen, Q. Ma, and Z. Q. Xiong, "Solar sorption cooling systems for residential applications: Options and guidelines," *International Journal of Refrigeration,* vol. 32, pp. 638-660, 2009.

[14] J. A. Duffie, William A. Beckman., *Solar engineering of thermal processes.*, 3rd ed. ed., 2006.

[15] A. Al-Alili, M. D. Islam, I. Kubo, Y. Hwang, and R. Radermacher, "Modeling of a solar powered absorption cycle for Abu Dhabi," 2011.

[16] P. Bermejo, F. J. Pino, and F. Rosa, "Solar absorption cooling plant in Seville," *Solar Energy,* vol. 84, p. 1503, 2010.

[17] G. A. Florides, S. A. Kalogirou, S. A. Tassou, and L. C. Wrobel, "Modelling and simulation of an absorption solar cooling system for Cyprus," *Solar Energy,* vol. 72, pp. 43-51, 2002.

[18] K. F. Fong, T. T. Chow, C. K. Lee, Z. Lin, and L. S. Chan, "Comparative study of different solar cooling systems for buildings in subtropical city," *Solar Energy,* vol. 84, pp. 227-244, 2010.
[19] K. Ghali, "Energy savings potential of a hybrid desiccant dehumidification air conditioning system in Beirut," *Energy Conversion and Management,* vol. 49, pp. 3387-3390, 2008.
[20] Y. Hang, M. Qu, and F. Zhao, "Economical and environmental assessment of an optimized solar cooling system for a medium-sized benchmark office building in Los Angeles, California," *Renewable Energy,* vol. 36, pp. 648-658, 2011.
[21] C. Monne, S. Alonso, F. Palacin, and L. Serra, "Monitoring and simulation of an existing solar powered absorption cooling system in Zaragoza (Spain)," *Applied Thermal Engineering,* vol. 31, pp. 28-35, 2011.
[22] J. P. Praene, O. Marc, F. Lucas, and F. Miranville, "Simulation and experimental investigation of solar absorption cooling system in Reunion Island," *Applied Energy,* vol. 88, pp. 831-839, 2011.
[23] M. Qu, H. Yin, and D. H. Archer, "A solar thermal cooling and heating system for a building: Experimental and model based performance analysis and design," *Solar Energy,* vol. 84, pp. 166-182, 2010.
[24] X. Q. Zhai and R. Z. Wang, "A review for absorbtion and adsorbtion solar cooling systems in China," *Renewable and Sustainable Energy Reviews,* vol. 13, pp. 1523-1531, 2009.
[25] Y. Gupta, L. Metchop, A. Frantzis, and P. E. Phelan, "Comparative analysis of thermally activated, environmentally friendly cooling systems," *Energy Conversion and Management,* vol. 49, pp. 1091-1097, 2008.
[26] D. S. C. Stanfield, *Fundamentals of HVACR*, 2nd ed ed.: Prentice Hall, 2013.
[27] C. W. H., "Air Conditioning System," 12 August 1939, 1939.
[28] S. Broadbent C., S., *Indoor air quality*: Melbourne : Australian Institute of Refrigeration Air-Conditioning and Heating Inc., 2004., 2004.
[29] R. R. C., *HVAC maintenance and operations handbook*. New York: McGraw-Hill, 1998.
[30] R. a. A.-C. E. American Society of Heating, *2006 Ashrae Handbook: Refrigeration*. Georgia, 2006.
[31] Trane, "Type A Energy wheels for Modular and T-Series Climate Chnager Air Handlers," ed, 2001.
[32] SEMCO, "Energy Recovery Wheel," in *Technical Guide*, ed. US: SEMCO Incorporated, 2006.
[33] C. Taylor, "Measurement of Finned-Tube heat exchanger performance," Master, Mechanical Engineering, Georgia Institute of Technology, http://www.smartech.gatech.edu, 2004.
[34] L. Perez-Lombard, J. Ortiz, J. F. Coronel, and I. R. Maestre, "A review of HVAC systems requirements in building energy regulations," *Energy and Buildings,* vol. 43, pp. 255-268, 2011.
[35] G. Gong, F. Chen, H. Su, and J. Zhou, "Thermodynamic simulation of condensation heat recovery characteristics of a single stage centrifugal chiller in a hotel," *Applied Energy,* vol. 91, pp. 326-333, 2012.
[36] C. E. L. Nobrega and N. C. L. Brum, "Modeling and simulation of heat and enthalpy recovery wheels," *Energy,* vol. 34, pp. 2063-2068, 2009.
[37] S. Deng, Z. Song, and K. Tan, "Air-cooled heat pump with desuperheater: Retrofit for year-round service hot water supply," *Building Services Engineering Research and Technology,* vol. 19, pp. 129-133, August 1, 1998 1998.
[38] K. Tan and S. Deng, "A simulation study on a water chiller complete with a desuperheater and a reversibly used water cooling tower (RUWCT) for service hot water generation," *Building and Environment,* vol. 37, pp. 741-751, 2002.

[39] Y. Asiedu, R. W. Besant, and C. J. Simonson, "Wheel Selection for Heat and Energy Recovery in Simple HVAC Ventilation Design Problems," *ASHRAE Transactions,* vol. 110, pp. 381-398, 2004.
[40] N. Subramanyam, M. P. Maiya, and S. S. Murthy, "Application of desiccant wheel to control humidity in air-conditioning systems," *Applied Thermal Engineering,* vol. 24, pp. 2777-2788, 12// 2004.
[41] Y. M. Harshe, R. P. Utikar, V. V. Ranade, and D. Pahwa, "Modeling of Rotary Desiccant Wheels," *Chemical Engineering & Technology,* vol. 28, pp. 1473-1479, 2005.
[42] F. E. Nia, D. van Paassen, and M. H. Saidi, "Modeling and simulation of desiccant wheel for air conditioning," *Energy and Buildings,* vol. 38, pp. 1230-1239, 2006.
[43] B. S. Davanagere, S. A. Sherif, and D. Y. Goswami, " A Feasibility Study Of A Solar Desiccant Air-Conditioning Systems part I: Psychrometrics and Analysis Of The Conditioned Zone," *International Journal Of Energy Research,* vol. Int. J. Energy Res., 23, 7Ð 21 (1999), 1999.
[44] T. S. Ge, Y. Li, R. Z. Wang, and Y. J. Dai, "A review of the mathematical models for predicting rotary desiccant wheel," *Renewable and Sustainable Energy Reviews,* vol. 12, pp. 1485-1528, 2008.
[45] R. Narayanan, W. Y. Saman, S. D. White, and M. Goldsworthy, "Comparative study of different desiccant wheel designs," *Applied Thermal Engineering,* vol. 31, pp. 1613-1620, 7// 2011.
[46] K. Daou, R. Z. Wang, and Z. Z. Xia, "Desiccant cooling air conditioning: a review," *Renewable and Sustainable Energy Reviews,* vol. 10, pp. 55-77, 4// 2006.
[47] G. Heidarinejad and H. Pasdarshahri, "The effects of operational conditions of the desiccant wheel on the performance of desiccant cooling cycles," *Energy and Buildings,* vol. 42, pp. 2416-2423, 12// 2010.
[48] J. D. Chung, D.-Y. Lee, and S. M. Yoon, "Optimization of desiccant wheel speed and area ratio of regeneration to dehumidification as a function of regeneration temperature," *Solar Energy,* vol. 83, pp. 625-635, 2009.
[49] Z. Hatami, M. H. Saidi, M. Mohammadian, and C. Aghanajafi, "Optimization of solar collector surface in solar desiccant wheel cycle," *Energy and Buildings,* vol. 45, pp. 197-201, 2012.
[50] C. X. Jia, Y. J. Dai, J. Y. Wu, and R. Z. Wang, "Use of compound desiccant to develop high performance desiccant cooling system," *International Journal of Refrigeration,* vol. 30, pp. 345-353, 2007.
[51] M. Beccali, P. Finocchiaro, and B. Nocke, "Energy performance evaluation of a demo solar desiccant cooling system with heat recovery for the regeneration of the adsorption material," *Renewable Energy,* vol. 44, pp. 40-52, 2012.
[52] A. Kodama, T. Hirayama, M. Goto, T. Hirose, and R. E. Critoph, "The use of psychrometric charts for the optimisation of a thermal swing desiccant wheel," *Applied Thermal Engineering,* vol. 21, pp. 1657-1674, 2001.
[53] W. A. Belding, M. P. F. Delmas, and W. D. Holeman, "Desiccant aging and its effects on desiccant cooling system performance," *Applied Thermal Engineering,* vol. 16, pp. 447-459, 5// 1996.
[54] J.-W. Jeong and S. A. Mumma, "Practical thermal performance correlations for molecular sieve and silica gel loaded enthalpy wheels," *Applied Thermal Engineering,* vol. 25, pp. 719-740, 4// 2005.
[55] C. X. Jia, Y. J. Dai, J. Y. Wu, and R. Z. Wang, "Experimental comparison of two honeycombed desiccant wheels fabricated with silica gel and composite desiccant material," *Energy Conversion and Management,* vol. 47, pp. 2523-2534, 2006.
[56] C. K. Qin, and G. Schmitz. , "Performance Prediction of LiCl Rotor," *International Journal of Architecture Science* vol. no. 3, pp. 20-29, 2002.
[57] L. Yong, K. Sumathy, Y. J. Dai, J. H. Zhong, and R. Z. Wang, "Experimental Study on a Hybrid Desiccant Dehumidification and Air Conditioning System," *Journal of Solar Energy Engineering,* vol. 128, p. 77, 2006.

[58] Q. Cui, H. Chen, G. Tao, and H. Yao, "Performance study of new adsorbent for solid desiccant cooling," *Energy,* vol. 30, pp. 273-279, 2// 2005.
[59] S. D. White, M. Goldsworthy, R. Reece, T. Spillmann, A. Gorur, and D.-Y. Lee, "Characterization of desiccant wheels with alternative materials at low regeneration temperatures," *International Journal of Refrigeration,* vol. 34, pp. 1786-1791, 12// 2011.
[60] X. J. Zhang, K. Sumathy, Y. J. Dai, and R. Z. Wang, "Dynamic hygroscopic effect of the composite material used in desiccant rotary wheel," *Solar Energy,* vol. 80, pp. 1058-1061, 8// 2006.
[61] D. La, Y. J. Dai, Y. Li, R. Z. Wang, and T. S. Ge, "Technical development of rotary desiccant dehumidification and air conditioning: A review," *Renewable and Sustainable Energy Reviews,* vol. 14, pp. 130-147, 1// 2010.
[62] X. J. S. Zhang, K. Dai, Y.J. Wang, R.Z., "Parametric study on the silica gel–calcium chloride composite desiccant rotary wheel employing fractal BET adsorption isotherm," *International Journal of Energy Research,* p. 29:37, 2005.
[63] L. X. W. Gong, R. Z. Xia, Z. Z. Chen, C. J., "Adsorption Equilibrium of Water on a Composite Adsorbent Employing Lithium Chloride in Silica Gel," *Journal of Chemical & Engineering Data,,* vol. 55, pp. 2920-2923, 2010.
[64] Y. J. Dai, R. Z. Wang, H. F. Zhang, and J. D. Yu, "Use of liquid desiccant cooling to improve the performance of vapor compression air conditioning," *Applied Thermal Engineering,* vol. 21, pp. 1185-1202, 8// 2001.
[65] C. X. Jia, Y. J. Dai, J. Y. Wu, and R. Z. Wang, "Analysis on a hybrid desiccant air-conditioning system," *Applied Thermal Engineering,* vol. 26, pp. 2393-2400, 12// 2006.
[66] P. Mazzei, F. Minichiello, and D. Palma, "Desiccant HVAC systems for commercial buildings," *Applied Thermal Engineering,* vol. 22, pp. 545-560, 2002.
[67] C. Guangnan and G. Lisa, "Air Conditioning Systems: Design and Energy Efficiency," in *Encyclopedia of Energy Engineering and Technology*. vol. null, ed: Taylor & Francis, 2008, pp. 1-8.
[68] A. Shaw, "Energy Conservation in a New Method of Air Conditioning through Dehumidifier Selection," presented at the Engineering Conference 1980: Engineering in the 80s, Engineering Conference (1980 : Adelaide, S.A.), 1980.
[69] W. L. Lee, H. Chen, Y. C. Leung, and Y. Zhang, "Decoupling dehumidification and cooling for energy saving and desirable space air conditions in hot and humid Hong Kong," *Energy Conversion and Management,* vol. 53, pp. 230-239, 2012.
[70] X. Q. Zhai, M. Qu, Y. Li, and R. Z. Wang, "A review for research and new design options of solar absorption cooling systems," *Renewable and Sustainable Energy Reviews,* vol. 15, pp. 4416-4423, 12// 2011.
[71] F. ß. Boud√©henn, H. l. n. Demasles, J. l. Wyttenbach, X. Jobard, D. Ch√®ze, and P. Papillon, "Development of a 5 kW Cooling Capacity Ammonia-water Absorption Chiller for Solar Cooling Applications," *Energy Procedia,* vol. 30, pp. 35-43, 2012.
[72] A. Lecuona, R. Ventas, M. Venegas, A. ZacarÌas, and R. Salgado, "Optimum hot water temperature for absorption solar cooling," *Solar Energy,* vol. 83, pp. 1806-1814, 2009.
[73] D. S. Kim and C. A. Infante Ferreira, "Solar refrigeration options ‚Äì a state-of-the-art review," *International Journal of Refrigeration,* vol. 31, pp. 3-15, 2008.
[74] G. Grossman, "Solar-powered systems for cooling, dehumidification and air-conditioning," *Solar Energy,* vol. 72, pp. 53-62, 2002.
[75] S. A. Kalogirou, "Recent Patents in Absorption Cooling Systems," Cyprus Patent, 2007.
[76] E. Zambolin and D. Del Col, "Experimental analysis of thermal performance of flat plate and evacuated tube solar collectors in stationary standard and daily conditions," *Solar Energy,* vol. 84, pp. 1382-1396, 2010.
[77] R. Tang, W. Gao, Y. Yu, and H. Chen, "Optimal tilt-angles of all-glass evacuated tube solar collectors," *Energy,* vol. 34, pp. 1387-1395, 2009.

[78] H. Z. Hassan and A. A. Mohamad, "A review on solar cold production through absorption technology," *Renewable and Sustainable Energy Reviews,* vol. 16, pp. 5331-5348, 9// 2012.
[79] Y. T. Kang, A. Akisawa, and T. Kashiwagi, "Experimental correlation of combined heat and mass transfer for NH3-H2O falling film absorptionCorrÈlation expÈrimentale entre le transfert de chaleur et de masse pour de l'absorption au NH3-H2O ‡ film tombant," *International Journal of Refrigeration,* vol. 22, pp. 250-262, 1999.
[80] K. Aghabararpourtabakhi, "Absorption heat pump: Simulation and model validation," ed. Canada: Ecole Polytechnique, Montreal (Canada), 2008.
[81] F. Assilzadeh, S. A. Kalogirou, Y. Ali, and K. Sopian, "Simulation and optimization of a LiBr solar absorption cooling system with evacuated tube collectors," *Renewable Energy,* vol. 30, pp. 1143-1159, 2005.
[82] K. Banasiak and J. Kozio, "Mathematical modelling of a LiBr-H2O absorption chiller including two-dimensional distributions of temperature and concentration fields for heat and mass exchangers," *International Journal of Thermal Sciences,* vol. 48, pp. 1755-1764, 2009.
[83] H. T. Chua, H. K. Toh, and K. C. Ng, "Thermodynamic modeling of an ammonia-water absorption chiller," *International Journal of Refrigeration,* vol. 25, pp. 896-906, 2002.
[84] D. Kong, J. Liu, L. Zhang, H. He, and Z. Fang, "Thermodynamic and Experimental Analysis of an Ammonia-Water Absorption Chiller," *Energy and Power Engineering,* vol. 2, pp. 298-305, 2010.
[85] R. Tozer, A. Syed, and G. Maidment, "Extended temperature-entropy (T-s) diagrams for aqueous lithium bromide absorption refrigeration cycles," *International Journal of Refrigeration,* vol. 28, pp. 689-697, 2005.
[86] N. Velazquez, D. Sauceda, M. Quintero-Nunez, and R. Best, "Design and Construction of an Air Cooled Ammonia Absorber," *Journal of Solar Energy Engineering,* vol. 131, pp. 021006-7, 2009.
[87] J. Scharfe, F. Ziegler, and R. Radermacher, "Analysis of advantages and limitations of absorber-generator heat exchange," *International Journal of Refrigeration,* vol. 9, pp. 326-333, 11// 1986.
[88] D. W. Sun, "Comparison of the performances of NH3-H2O, NH3-LiNO3 and NH3-NaSCN absorption refrigeration systems," *ENERGY CONVERSION AND MANAGEMENT,* vol. 39, pp. 357-368, 1998.
[89] X. Liao, "The development of an air-cooled absorption chiller concept and its integration in CHP systems," R. Radermacher, Ed., ed. United States -- Maryland: University of Maryland, College Park, 2005.
[90] D. P. Hildbrand C., Pons M., Buchter F., "A new solar powered adsorption refrigerator with high performance," 2004.
[91] J. Cerezo, M. Bourouis, M. Valles, A. Coronas, and R. Best, "Experimental study of an ammonia-water bubble absorber using a plate heat exchanger for absorption refrigeration machines," *Applied Thermal Engineering,* vol. 29, pp. 1005-1011, 2009.
[92] M. Venegas, D. Arzoz, P. Rodriguez, and M. Izquierdo, "Heat and mass transfer in LiNO3-NH3 spray absorption system," *International Communications in Heat and Mass Transfer,* vol. 30, pp. 805-815, 2003.
[93] Y. Wang, J. Yu, and F. Ma Chong, "Experimental research of a novel vortex generator for solar absorption chiller," *Science in China Series E: Technological Sciences,* vol. 52, pp. 1793-8, 2009.
[94] B. Le Lostec, N. Galanis, and J. Millette, "Experimental study of an ammonia-water absorption chiller," *International Journal of Refrigeration,* vol. 35, pp. 2275-2286, 12// 2012.

[95] D. G. Z. Crepinsek, J.Krope, "Comparison of the Performances of Absorption Refrigeration Cycles," *WSEAS TRANSACTIONS on HEAT and MASS TRANSFER,* vol. 4, 2009, 2009.
[96] G. Tanda, "Optimization of a Solar Ammonia Absorption Chiller," Master Thesis, Mechanical Engineering, DELF University of Technology, The Energy Thecnology Section, The Netherlands, 2004.
[97] S. De Antonellis, "Redesign of a direct fired ammonia water absorption chiller for adaptation to solar driven air conditioning mode," Engineering Degree, Energetic department, Politecnico di Milano, 2002.
[98] M.Guerra, "Self adaptive refrigerant flow low temperature driven dual lift absorption cycle," in *10th IIR Gustav Lorentzen Conference on Natural Refrigerants* Delft, The Netherlands, 2012.
[99] N. Nijegorodov, K. R. S. Devan, P. K. Jain, and S. Carlsson, "Atmospheric transmittance models and an analytical method to predict the optimum slope of an absorber plate, variously oriented at any latitude," *Renewable Energy,* vol. 4, pp. 529-543, 1994.
[100] G. R. Saraf and F. A. W. Hamad, "Optimum tilt angle for a flat plate solar collector," *Energy Conversion and Management,* vol. 28, pp. 185-191, 1988.
[101] V. H. Morcos, "Optimum tilt angle and orientation for solar collectors in Assiut, Egypt," *Renewable Energy,* vol. 4, pp. 291-298, 1994.
[102] H. Moghadam, F. F. Tabrizi, and A. Z. Sharak, "Optimization of solar flat collector inclination," *Desalination,* vol. 265, pp. 107-111, 2011.
[103] K. Skeiker, "Optimum tilt angle and orientation for solar collectors in Syria," *Energy Conversion and Management,* vol. 50, pp. 2439-2448, 2009.
[104] M. A. b. H. M. Yakup and A. Q. Malik, "Optimum tilt angle and orientation for solar collector in Brunei Darussalam," *Renewable Energy,* vol. 24, pp. 223-234, 2001.
[105] A. Shariah, M. A. Al-Akhras, and I. A. Al-Omari, "Optimizing the tilt angle of solar collectors," *Renewable Energy,* vol. 26, pp. 587-598, 2002.
[106] S. De Antonellis, C. M. Joppolo, and L. Molinaroli, "Simulation, performance analysis and optimization of desiccant wheels," *Energy and Buildings,* vol. 42, pp. 1386-1393, 2010.
[107] T. S. Ge, F. Ziegler, and R. Z. Wang, "A mathematical model for predicting the performance of a compound desiccant wheel (A model of compound desiccant wheel)," *Applied Thermal Engineering,* vol. 30, pp. 1005-1015, 2010.
[108] N. Allouache, "Numerical Modelling of an Adsorption Solar Cooling System," *Lecture Notes in Engineering and Computer Science,* vol. 2206, pp. 1959-1963, 2013.
[109] P. Lin, R. Z. Wang, and Z. Z. Xia, "Numerical investigation of a two-stage air-cooled absorption refrigeration system for solar cooling: Cycle analysis and absorption cooling performances," *Renewable Energy,* vol. 36, pp. 1401-1412, 2011.
[110] B. H. Gebreslassie, G. Guillén-Gosálbez, L. Jiménez, and D. Boer, "Solar assisted absorption cooling cycles for reduction of global warming: A multi-objective optimization approach," *Solar Energy,* vol. 86, pp. 2083-2094, 7// 2012.
[111] "report of performance," EN 12975-2 Institut für Solarenergieforschung GmbH Hameln / Emmenthal 107-06/D, 02/11/2006 2006.
[112] "BS EN 12975-2:2006: Thermal solar systems and components. Solar collectors. Test methods," ed: British Standards Institute, 2006.
[113] J. Labus, "Modelling of small capacity absorption chillers driven by solar thermal energy or waste heat," PhD, DEPARTAMENT D'ENGINYERIA MECÀNICA, UNIVERSITAT ROVIRA I VIRGILI, 2011.
[114] N. Velazquez and R. Best, "Methodology for the energy analysis of an air cooled GAX absorption heat pump operated by natural gas and solar energy," *Applied Thermal Engineering,* vol. 22, pp. 1089-1103, 2002.
[115] P. Corrada, J. M. Bell, L. Guan, and N. Motta, "Heat reject recovery in solar air conditioning."

[116] S. AG, "chillii PSC12 - Absorption Chiller," ed, 2008.
[117] L. Z. Zhang and J. L. Niu, "Performance comparisons of desiccant wheels for air dehumidification and enthalpy recovery," *Applied Thermal Engineering,* vol. 22, pp. 1347-1367, 2002.
[118] C. Zhai, "Performance modeling of desiccant wheel design and operation," 3309580 Ph.D., Carnegie Mellon University, Ann Arbor, 2008.
[119] S. De Antonellis, "Desiccant wheel dehumidification systems: componentes modelling and systems optimization," PhD degree PhD dissertation, Department of Energy, Politecnico di Milano, 2010.
[120] G. W. Thomson, "The Antoine equation for vapor-pressure data," *Chemical reviews,* vol. 38, pp. 1-39, 1946.
[121] A. Kodama, M. Goto, T. Hirose, and T. Kuma, "Experimental Study of Optimal Operation for a Honeycomb Adsorber Operated with Thermal Swing," *JOURNAL OF CHEMICAL ENGINEERING OF JAPAN,* vol. 26, pp. 530-535, 1993.
[122] A. Kodama, M. Goto, T. Hirose, and T. Kuma, "Temperature Profile and Optimal Rotation Speed of a Honeycomb Rotor Adsorber Operated with Thermal Swing," *JOURNAL OF CHEMICAL ENGINEERING OF JAPAN,* vol. 27, pp. 644-649, 1994.
[123] A. Kodama, M. Goto, T. Hirose, and T. Kuma, "Performance Evaluation for a Thermal Swing Honeycomb Rotor Adsorber Using a Humidity Chart," *JOURNAL OF CHEMICAL ENGINEERING OF JAPAN,* vol. 28, pp. 19-24, 1995.
[124] M. Beccali, F. Butera, R. Guanella, and R. S. Adhikari, "Simplified models for the performance evaluation of desiccant wheel dehumidification," *International Journal of Energy Research,* vol. 27, pp. 17-29, 2003.
[125] J. D. Chung and D.-Y. Lee, "Effect of desiccant isotherm on the performance of desiccant wheel," *International Journal of Refrigeration,* vol. 32, pp. 720-726, 2009.
[126] R. N., *Manuale del termotecnico. Fondamenti, riscaldamento, condizionamento, refrigerazione, risorse energetiche*, 6 ed., 2014.
[127] S. W.F., *Manuale della refrigerazione industriale*: Tecniche nuove, 2001.
[128] Trane. (2012). *TRACE® 700 v6.2.6.5*. Available: http://www.trane.com/content/trane-commercial/north-america/us/en/products-systems/design-and-analysis-tools/download-center/hvac-design-software-download-center.html?projectName=TRACE700&fileType=All Resources&projectNodePath=/content/trane-commercial/north-america/us/en/products-systems/design-and-analysis-tools/download-center/hvac-design-software-download-center
[129] R. a. A. C. E. ASHRAE (American Society of Heating, "Thermal Environmental Conditions for Human Occupancy," in *Standard 55-2013 -- Thermal Environmental Conditions for Human Occupancy (ANSI Approved)*, ed: ASHRAE, 2013, p. 54.
[130] H.-M. Henning, *Solar-assisted air-conditioning in buildings*. Wien, New York: Springer, 2004.
[131] C. M. J. S. De Antonellis, L. Molinaroli, A. Pasini, "Modelling and simulation of sensible heat wheels," presented at the 48th AiCARR International Conference - Energy refurbishment of existing buildings: which solutions for an integrated system, envelope, plant and control, Baveno, Italy, 2011.
[132] A. A. Rabah, A. Fekete, and S. Kabelac, "Experimental Investigation on a Rotary Regenerator Operating at Low Temperatures," *Journal of Thermal Science and Engineering Applications,* vol. 1, pp. 041004-041004, 2010.
[133] Q. C. Authority, "Retail Electricity Prices For Standard Contract Customers," vol. 369, ed. Queensland Government Gazette, 2015, p. 14.
[134] M. A. Karim, "Experimental investigation of a stratified chilled-water thermal storage system," *Applied Thermal Engineering,* vol. 31, pp. 1853-1860, 2011.

[135] P. Corrada, Bell, J., Guan, L., Motta, N., Piloto, C., "Determination of the optimum tilt angle for solar collectors in Australia using new correlations," *Solar energy,* in review.
[136] P. Corrada, J. Bell, L. Guan, and N. Motta, "Optimizing solar collector tilt angle to improve energy harvesting in a solar cooling system," *Energy Procedia,* vol. 48, pp. 806-812, 2014.

Chapter 7: Appendices

Appendix A Measurement available for the half effect absorption chiller

Table 15 Data available for the half effect absorption chiller

Tamb [°C]	PGEN [barabs]	Tcon [°C]	Pm [barabs]	PEVP [barabs]	QEVP [kW]	QRCA [kW]	QABS [kW]	QCOND [kW]	QGEN [kW]	Mlret kg h-1	COP	Sratio
Result of steady state simulations at *12→7°C* chilled water temp, *80→75°C* driving hot water temp												
23	13.24	34.079	8.39	4.92	3.5	4.31	5.26	8.33	10.09	53.75	0.347	0.457
28	15.08	38.680	8.97	4.92	3.5	4.45	5.51	8.39	10.41	73.1	0.336	0.441
30	15.76	40.272	9.16	4.92	3.5	4.56	5.62	8.44	10.56	85.21	0.331	0.434
32	16.43	41.790	9.34	4.92	3.17	4.22	5.22	7.72	9.77	93.84	0.325	0.425
Result of steady state simulations at 12→7°C chilled water temp, *85→80°C* driving hot water temp												
28	15.44	39.529	9.24	4.92	3.53	4.56	5.82	8.54	10.83	68.68	0.326	0.441
30	16.12	41.094	9.46	4.92	3.53	4.63	5.94	8.55	10.97	78.02	0.321	0.434
32	16.82	42.653	9.66	4.92	3.52	4.71	6.08	8.58	11.13	90.84	0.316	0.427
35	18.06	45.297	9.89	4.92	2.64	3.69	4.79	6.5	8.66	94.17	0.305	0.411
37	19	47.212	9.98	4.92	1.87	2.78	3.61	4.73	6.47	94.05	0.289	0.393
Result of steady state simulations at *12→7°C* chilled water temp, *90→85°C* driving hot water temp												
28	15.79	40.341	9.34	4.92	3.49	4.6	5.95	8.6	11.06	62.8	0.316	0.441
30	16.48	41.902	9.6	4.92	3.49	4.65	6.07	8.6	11.17	69.87	0.313	0.436
32	17.2	43.479	9.82	4.92	3.49	4.72	6.2	8.6	11.31	78.87	0.309	0.429
35	18.46	46.121	10.1	4.92	3.29	4.56	6.08	8.13	10.92	94.49	0.301	0.417
37	19.43	48.063	10.24	4.92	2.62	3.74	5.04	6.53	8.95	94.41	0.292	0.407
40	21	51.056	10.34	4.92	1.51	2.39	3.27	3.97	5.73	94.17	0.264	0.377

Appendix B Measurement available for the single stage absorption chiller

Table 16 Data available for the single stage absorption chiller

No	$T_{cwh,in}$	$T_{cwh,out}$	V_{cwh}	$T_{cw,in}$	$T_{cw,out}$	V_{cw}	$T_{hw,in}$	$T_{hw,out}$	V_{hw}	Q_{eva}	Q_{ac}	Q_{gen}	$COP_{chiller}$
1	8.66	5.04	1.72	27.00	30.84	4.75	80.01	75.00	2.24	7.24	21.21	13.05	0.55
2	9.94	5.99	1.72	27.00	31.06	4.76	79.97	74.77	2.24	7.90	22.48	13.55	0.58
3	11.26	7.01	1.72	27.02	31.18	4.78	79.99	74.68	2.24	8.50	23.13	13.83	0.61
4	12.50	7.86	1.72	27.00	31.48	4.78	80.00	74.38	2.24	9.28	24.91	14.64	0.63
5	14.12	8.97	1.72	27.02	31.75	4.78	79.98	74.19	2.24	10.30	26.30	15.08	0.68
6	15.41	9.99	1.72	27.03	31.93	4.77	79.97	74.05	2.24	10.84	27.18	15.42	0.70
7	16.59	10.95	1.72	27.02	32.11	4.77	79.98	73.89	2.24	11.28	28.24	15.87	0.71
8	7.01	4.98	1.72	30.00	32.46	4.75	79.99	76.73	2.24	4.06	13.59	8.49	0.48
9	8.36	6.02	1.72	29.99	32.65	4.76	80.00	76.59	2.24	4.68	14.73	8.88	0.53
10	9.66	7.04	1.72	29.99	32.79	4.76	80.00	76.44	2.24	5.24	15.50	9.27	0.57
11	10.95	8.02	1.72	30.00	32.95	4.76	80.00	76.33	2.24	5.86	16.33	9.56	0.61
12	12.25	9.03	1.72	30.00	33.10	4.76	79.99	76.18	2.24	6.44	17.16	9.93	0.65
13	13.88	10.03	1.72	30.00	33.52	4.76	80.01	75.82	2.24	7.70	19.49	10.92	0.71
14	15.16	11.01	1.72	30.01	33.67	4.76	80.00	75.70	2.24	8.30	20.26	11.20	0.74
15	16.37	12.07	1.72	29.99	33.80	4.77	80.00	75.58	2.24	8.60	21.14	11.52	0.75
16	5.52	5.00	1.72	33.00	34.23	4.8	80.00	77.99	2.24	1.04	6.87	5.24	0.20
17	6.82	6.01	1.72	32.98	34.48	4.8	80.02	77.80	2.24	1.62	8.37	5.78	0.28
18	8.09	6.99	1.72	33.00	34.66	4.8	79.99	77.59	2.24	2.20	9.27	6.25	0.35
19	9.27	7.98	1.72	33.00	34.70	4.79	79.90	77.59	2.24	2.58	9.47	6.02	0.43
20	10.92	9.07	1.72	33.02	34.97	4.78	79.94	77.41	2.24	3.70	10.84	6.59	0.56

21	12.20	10.06	1.72	33.01	35.09	4.79	80.00	77.35	2.24	4.28	11.59	6.90	0.62
22	6.29	6.04	1.72	35.00	36.08	4.79	80.00	78.17	2.24	0.50	6.02	4.77	0.10
23	7.39	6.98	1.72	35.00	36.17	4.79	80.01	78.10	2.24	0.82	6.52	4.98	0.16
24	8.50	8.01	1.72	34.99	36.20	4.79	80.02	78.07	2.24	0.98	6.74	5.08	0.19
25	9.65	8.99	1.72	35.00	36.31	4.79	80.00	77.95	2.24	1.32	7.30	5.34	0.25
26	10.8	9.89	1.72	34.99	36.49	4.79	79.94	77.82	2.24	1.82	8.36	5.52	0.33
27	9.15	5.00	1.71	27.00	31.38	4.78	84.99	79.09	2.23	8.25	24.35	15.30	0.54
28	10.45	5.98	1.72	27.00	31.55	4.78	85.00	79.01	2.23	8.94	25.30	15.54	0.58
29	12.03	7.02	1.72	27.00	31.82	4.78	84.99	78.84	2.24	10.02	26.80	16.02	0.63
30	13.23	8.00	1.72	26.98	31.91	4.78	84.98	78.81	2.24	10.46	27.41	16.07	0.65
31	14.44	9.01	1.72	27.04	32.24	4.78	84.99	78.62	2.24	10.86	28.91	16.60	0.65
32	15.75	10.00	1.72	27.07	32.29	4.78	85.03	78.39	2.24	11.50	29.02	17.30	0.66
33	17.04	11.01	1.72	27.05	32.45	4.77	85.02	78.27	2.24	12.06	29.96	17.59	0.69
34	8.00	5.04	1.73	30.00	33.38	4.76	85.01	80.38	2.24	5.96	18.71	12.06	0.49
35	9.22	6.04	1.71	30.00	33.5	4.77	84.99	80.29	2.23	6.32	19.42	12.19	0.52
36	10.65	6.99	1.72	30.00	33.79	4.77	84.98	79.94	2.24	7.32	21.03	13.13	0.56
37	11.97	7.98	1.73	30.00	34.05	4.77	85.01	79.65	2.24	8.03	22.47	13.96	0.57
38	13.10	8.99	1.74	30.00	34.1	4.77	84.98	79.62	2.24	8.32	22.75	13.96	0.60
39	14.39	10.01	1.74	30.00	34.22	4.77	85.03	79.67	2.24	8.86	23.41	13.96	0.63
40	15.71	10.98	1.72	29.99	34.41	4.77	85.00	79.41	2.24	9.46	24.52	14.56	0.65
41	17.00	12.00	1.72	29.98	34.59	4.77	84.97	79.23	2.23	10.00	25.58	14.89	0.67
42	6.47	5.03	1.72	33.00	35.04	4.79	85.01	81.88	2.24	2.88	11.36	8.15	0.35
43	7.68	6.01	1.71	33.00	35.18	4.8	85.01	81.7	2.23	3.32	12.17	8.58	0.39
44	8.87	6.99	1.71	33.01	35.37	4.81	85.04	81.51	2.23	3.74	13.20	9.16	0.41

45	10.51	7.99	1.71	33.01	35.85	4.78	85.01	81.06	2.24	5.01	15.79	10.29	0.49
46	11.83	8.98	1.71	33.00	36.07	4.78	85.00	80.76	2.24	5.67	17.07	11.05	0.51
47	13.10	10.02	1.71	33.00	36.24	4.79	85.01	80.57	2.24	6.13	18.05	11.57	0.53
48	14.45	11.10	1.72	32.99	36.42	4.78	85.00	80.36	2.24	6.70	19.07	12.09	0.55
49	15.62	12.05	1.72	33.00	36.56	4.78	85.00	80.22	2.24	7.14	19.79	12.45	0.57
50	5.52	5.01	1.73	35.00	36.36	4.79	85.01	82.62	2.25	1.03	7.58	6.25	0.16
51	6.83	5.99	1.73	34.99	36.59	4.79	85.01	82.43	2.24	1.69	8.91	6.72	0.25
52	8.18	7.01	1.73	35.00	36.81	4.77	85.00	82.18	2.24	2.35	10.04	7.35	0.32
53	9.50	8.01	1.73	35.00	37.03	4.77	85.00	81.94	2.23	3.00	11.26	7.94	0.38
54	10.77	9.02	1.73	35.00	37.23	4.77	85.00	81.73	2.23	3.52	12.37	8.48	0.42
55	12.12	10.02	1.73	35.00	37.43	4.77	85.00	81.53	2.23	4.23	13.48	9.00	0.47
56	13.40	11.04	1.73	35.00	37.61	4.76	84.99	81.36	2.23	4.75	14.45	9.41	0.50
57	14.60	12.03	1.73	35.00	37.8	4.75	85.00	81.16	2.23	5.17	15.47	9.96	0.52
58	9.96	5.01	1.72	27.02	32.04	4.76	90.04	83.39	2.24	9.90	27.79	17.32	0.57
59	11.17	6.04	1.72	26.99	32.2	4.75	90.04	83.23	2.24	10.26	28.78	17.74	0.58
60	12.58	7.00	1.72	27.00	32.42	4.75	90.04	83.05	2.24	11.16	29.94	18.21	0.61
61	13.89	7.93	1.72	27.05	32.61	4.75	90.04	82.92	2.24	11.92	30.72	18.55	0.64
62	15.28	8.99	1.72	27.00	32.88	4.75	89.99	82.68	2.24	12.58	32.48	19.04	0.66
63	16.51	9.96	1.72	26.95	32.98	4.75	90.04	82.67	2.24	13.10	33.31	19.20	0.68
64	17.78	11.02	1.72	27.02	33.1	4.75	90.07	82.54	2.24	13.52	33.59	19.62	0.69
65	8.73	5.00	1.72	30.00	33.92	4.76	90.01	84.81	2.24	7.46	21.70	13.55	0.55
66	10.08	6.02	1.72	30.00	34.13	4.76	90.00	84.60	2.24	8.12	22.86	14.07	0.58
67	11.41	7.01	1.72	30.01	14.31	4.76	90.01	84.46	2.24	8.80	-86.92	14.46	0.61
68	13.06	7.99	1.72	30.01	34.79	4.77	90.00	83.95	2.24	10.14	26.52	15.76	0.64

69	14.40	9.00	1.72	30.02	34.95	4.77	90.01	83.88	2.24	10.80	27.35	15.97	0.68
70	15.67	10.01	1.72	30.01	35.09	4.78	90.02	83.72	2.24	11.32	28.24	16.41	0.69
71	16.83	10.93	1.72	30.00	35.19	4.79	90.02	83.66	2.24	11.80	28.91	16.57	0.71
72	7.62	5.03	1.72	33.00	35.99	4.78	90.00	85.82	2.24	5.18	16.62	10.89	0.48
73	8.92	6.02	1.72	33.00	36.18	4.78	90.00	85.65	2.24	5.80	17.68	11.33	0.51
74	10.32	7.01	1.72	33.00	36.39	4.78	90.00	85.50	2.24	6.62	18.85	11.72	0.56
75	11.71	8.01	1.72	32.99	36.66	4.78	90.00	85.22	2.24	7.40	20.40	12.45	0.59
76	13.01	9.02	1.72	33.01	36.77	4.79	90.00	85.16	2.24	7.98	20.95	12.61	0.63
77	14.14	10.04	1.72	32.99	37.03	4.76	90.00	84.82	2.24	8.20	22.37	13.50	0.61
78	15.45	11.05	1.72	33.00	37.21	4.76	89.99	84.65	2.24	8.80	23.31	13.91	0.63
79	16.62	12.05	1.72	33.00	37.25	4.79	90.00	84.61	2.24	9.14	23.68	14.04	0.65
80	6.40	4.98	1.72	35.00	37.21	4.78	90.00	86.57	2.24	2.84	12.29	8.94	0.32
81	7.77	6.05	1.72	35.00	37.43	4.78	89.99	86.36	2.24	3.44	13.51	9.46	0.36
82	9.07	7.00	1.72	35.00	37.66	4.79	90.01	86.11	2.24	4.14	14.82	10.16	0.41
83	10.42	8.02	1.72	35.00	37.86	4.78	89.99	85.91	2.24	4.80	15.90	10.63	0.45
84	11.72	9.04	1.72	35.00	38.09	4.78	89.99	85.64	2.24	5.36	17.18	11.33	0.47
85	13.04	10.04	1.72	35.00	38.32	4.78	89.98	85.39	2.24	6.00	18.46	11.96	0.50
86	14.32	10.99	1.72	35.00	38.52	4.78	90.00	85.20	2.24	6.66	19.57	12.51	0.53
87	15.66	12.10	1.72	34.99	38.72	4.77	89.99	85.03	2.24	7.12	20.69	12.92	0.55
88	10.80	5.05	1.72	27.01	33.01	4.75	95.03	87.31	2.24	11.50	33.15	20.11	0.57
89	11.94	6.01	1.72	27.01	33.20	4.77	95.07	87.06	2.24	11.86	34.34	20.87	0.57
90	13.37	6.98	1.72	27.05	33.32	4.78	95.06	86.94	2.24	12.78	34.86	21.15	0.60
91	14.74	8.03	1.72	27.03	33.55	4.78	95.05	86.75	2.24	13.42	36.25	21.62	0.62
92	16.02	8.99	1.72	26.99	33.73	4.78	95.04	86.57	2.24	14.06	37.47	22.07	0.64

93	17.38	10.02	1.72	27.05	33.99	4.78	95.02	86.51	2.24	14.72	38.58	22.17	0.66
94	9.22	5.00	1.72	30.00	34.83	4.76	95.05	88.33	2.24	8.44	26.74	17.51	0.48
95	10.66	5.99	1.72	30.01	35.10	4.76	95.03	88.16	2.24	9.34	28.18	17.90	0.52
96	12.08	7.01	1.72	30.01	35.42	4.76	95.05	87.81	2.24	10.14	29.95	18.86	0.54
97	13.78	7.99	1.72	30.00	35.48	4.76	95.04	88.21	2.24	11.58	30.34	17.79	0.65
98	14.69	9.01	1.72	30.00	35.68	4.76	95.07	87.71	2.24	11.36	31.45	19.17	0.59
99	16.05	9.98	1.72	30.03	35.92	4.76	95.03	87.43	2.24	12.14	32.61	19.80	0.61
100	17.27	11.01	1.72	30.03	36.10	4.75	95.07	87.27	2.24	12.52	33.53	20.32	0.62
101	7.81	5.00	1.72	33.00	36.71	4.77	95.00	89.53	2.24	5.62	20.58	14.25	0.39
102	9.41	6.00	1.72	33.00	37.01	4.77	95.01	89.38	2.24	6.82	22.25	14.67	0.47
103	10.80	7.00	1.72	33.00	37.25	4.77	95.00	89.14	2.24	7.60	23.58	15.27	0.50
104	12.08	8.00	1.72	33.00	37.48	4.76	95.01	88.87	2.24	8.16	24.80	16.00	0.51
105	13.49	9.00	1.72	33.01	37.72	4.77	95.01	88.63	2.24	8.98	26.13	16.62	0.54
106	14.72	10.00	1.72	33.00	37.91	4.77	95.02	88.42	2.24	9.44	27.24	17.19	0.55
107	16.12	11.00	1.72	33.00	38.14	4.76	95.04	88.26	2.24	10.24	28.46	17.66	0.58
108	17.21	11.92	1.72	32.99	38.31	4.76	95.04	88.11	2.24	10.58	29.45	18.05	0.59
109	7.42	5.01	1.72	35.00	38.04	4.80	95.00	90.61	2.24	4.82	16.97	11.44	0.42
110	8.74	6.02	1.72	35.00	38.23	4.79	95.01	90.40	2.24	5.44	17.99	12.01	0.45
111	10.04	7.01	1.72	35.00	38.43	4.79	95.00	90.20	2.24	6.06	19.11	12.51	0.48
112	11.23	7.99	1.72	35.00	38.59	4.79	95.00	90.04	2.24	6.48	20.00	12.92	0.50
113	12.63	9.00	1.72	35.01	38.73	4.79	94.99	89.99	2.24	7.26	20.72	13.03	0.56
114	13.81	10.03	1.72	35.00	39.17	4.77	95.01	89.35	2.24	7.56	23.13	14.75	0.51
115	15.08	11.04	1.72	35.00	39.35	4.77	95.00	89.14	2.24	8.08	24.13	15.27	0.53
116	16.35	12.03	1.72	35.00	39.49	4.77	94.99	88.99	2.24	8.64	24.91	15.63	0.55

117	11.22	5.03	1.72	27.01	33.68	4.77	100.01	91.19	2.24	12.38	37.00	22.98	0.54
118	12.50	6.01	1.72	27.01	33.92	4.77	99.99	90.92	2.24	12.98	38.34	23.63	0.55
119	13.84	6.96	1.72	26.99	34.03	4.77	100.03	90.84	2.24	13.76	39.06	23.94	0.57
120	15.40	8.03	1.72	27.06	34.26	4.77	99.94	90.71	2.24	14.74	39.94	24.05	0.61
121	16.46	8.96	1.72	27.03	34.41	4.77	99.99	90.58	2.24	15.00	40.94	24.52	0.61
122	17.19	9.57	1.72	26.95	34.57	4.77	99.93	90.39	2.24	15.24	42.27	24.85	0.61
123	10.20	5.00	1.72	30.00	35.43	4.76	100.05	93.01	2.24	10.40	30.06	18.34	0.57
124	11.25	6.00	1.72	30.00	35.51	4.76	100.06	92.86	2.24	10.50	30.50	18.76	0.56
125	12.70	6.99	1.72	30.00	35.85	4.76	100.07	92.51	2.24	11.42	32.39	19.70	0.58
126	14.10	7.96	1.72	29.99	36.13	4.76	100.12	92.25	2.24	12.28	33.99	20.50	0.60
127	15.75	9.03	1.72	30.04	36.47	4.77	100.07	92.01	2.24	13.44	35.67	21.00	0.64
128	16.67	9.83	1.72	29.93	36.58	4.76	100.11	91.98	2.24	13.68	36.82	21.18	0.65
129	8.71	5.01	1.72	32.99	37.40	4.76	100.03	93.81	2.24	7.40	24.41	16.20	0.46
130	10.11	6.00	1.72	33.00	37.74	4.76	100.05	93.44	2.24	8.22	26.24	17.22	0.48
131	11.64	7.03	1.72	33.00	38.00	4.77	100.06	93.27	2.24	9.22	27.74	17.69	0.52
132	12.94	8.01	1.72	33.00	38.17	4.76	100.04	93.15	2.24	9.86	28.62	17.95	0.55
133	14.23	8.99	1.72	33.00	38.41	4.76	100.09	92.90	2.24	10.48	29.95	18.73	0.56
134	15.63	9.99	1.72	33.00	38.55	4.77	100.01	92.85	2.24	11.28	30.79	18.65	0.60
135	8.10	5.00	1.72	35.00	38.77	4.77	100.01	94.60	2.24	6.20	20.92	14.09	0.44
136	9.62	6.03	1.72	35.00	39.05	4.77	100.01	94.43	2.24	7.18	22.47	14.54	0.49
137	10.96	7.04	1.72	35.00	39.28	4.76	100.00	94.19	2.24	7.84	23.69	15.14	0.52
138	12.18	7.99	1.72	35.00	39.47	4.76	100.02	93.97	2.24	8.38	24.75	15.76	0.53

Appendix C Measurement from the Solar Panel

No	G (W/m^2)	m (kg/h)	t_{in} (°C)	t_e (°C)	t_e-t_{in} (K)	t_m (°C)	t_a (°C)	t_m-t_a (°C)	T_m (Km_2/W)	η_a Reported	η Calculated
1	949.4	221.5	39.6	48.5	8.9	44.00	23.4	20.6	0.0217	0.749	0.7497
2	940.1	221.9	39.5	48.4	8.8	44	23.2	20.7	0.022	0.749	0.7492
3	927.2	222.6	39.5	48.2	8.7	43.9	23.2	20.7	0.0223	0.748	0.7490
4	923.8	223.1	39.5	48.1	8.5	43.8	23.1	20.7	0.0224	0.742	0.7488
5	1016.3	221.1	76.5	85	8.6	80.7	23.1	57.6	0.0567	0.674	0.6742
6	1039.2	226.5	77.1	85.6	8.5	81.4	21.5	59.9	0.0576	0.672	0.6708
7	1041.5	226.2	77.2	85.7	8.6	81.5	21.5	59.9	0.0575	0.671	0.6708
8	1036.3	226.2	77.2	85.7	8.5	81.5	22	59.5	0.0574	0.671	0.6716
9	983.2	222.5	58.6	67	8.4	62.8	24	38.8	0.0395	0.687	0.7161
10	972.5	225.4	58.5	67.1	8.6	62.8	24	38.9	0.04	0.718	0.7154
11	891	228.1	58.5	66.2	7.7	62.4	23.6	38.8	0.0435	0.706	0.7097
12	917.8	228.1	58.5	66.3	7.8	62.4	23.7	38.7	0.0422	0.698	0.7119
13	1005.4	232.7	18.6	28.1	9.5	23.3	25	-1.7	-0.0017	0.788	0.7807
14	1010.8	232.7	18.6	28.1	9.5	23.3	25.2	-1.9	-0.0018	0.783	0.7809
15	1014.1	223.1	15.4	25.1	9.7	20.3	18.5	1.7	0.0017	0.77	0.7771
16	1019.3	223.1	15.4	25.2	9.8	20.3	18.7	1.6	0.0016	0.77	0.7773

Appendix D Solar panels efficiency varying the inlet and outlet water temperatures T_{amb}=32°C

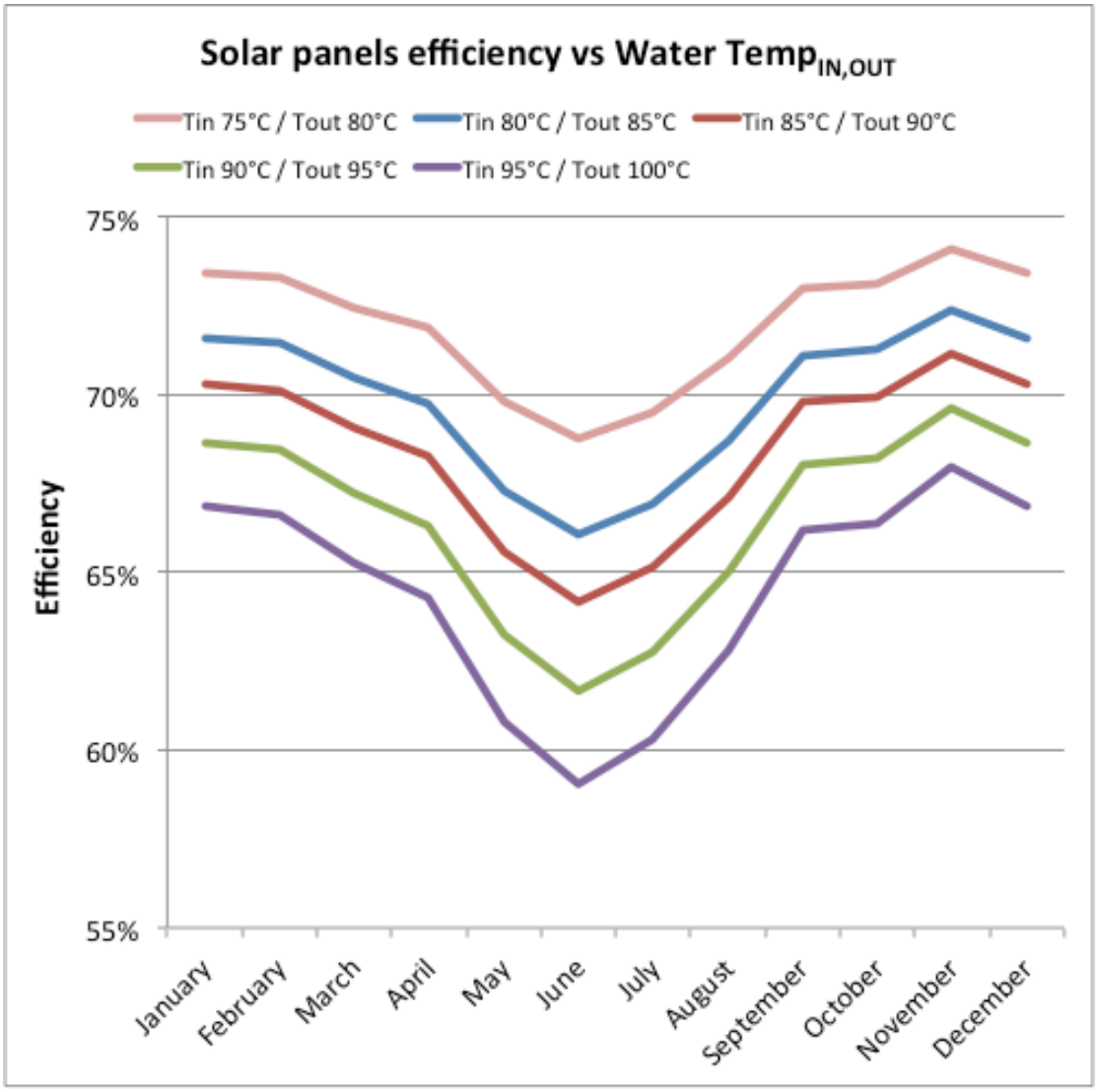

Figure 56 Solar panels efficiency vs water temperature in and out

Appendix E Desiccant wheel simulation: Humidity ratio reduction vs revolution speed

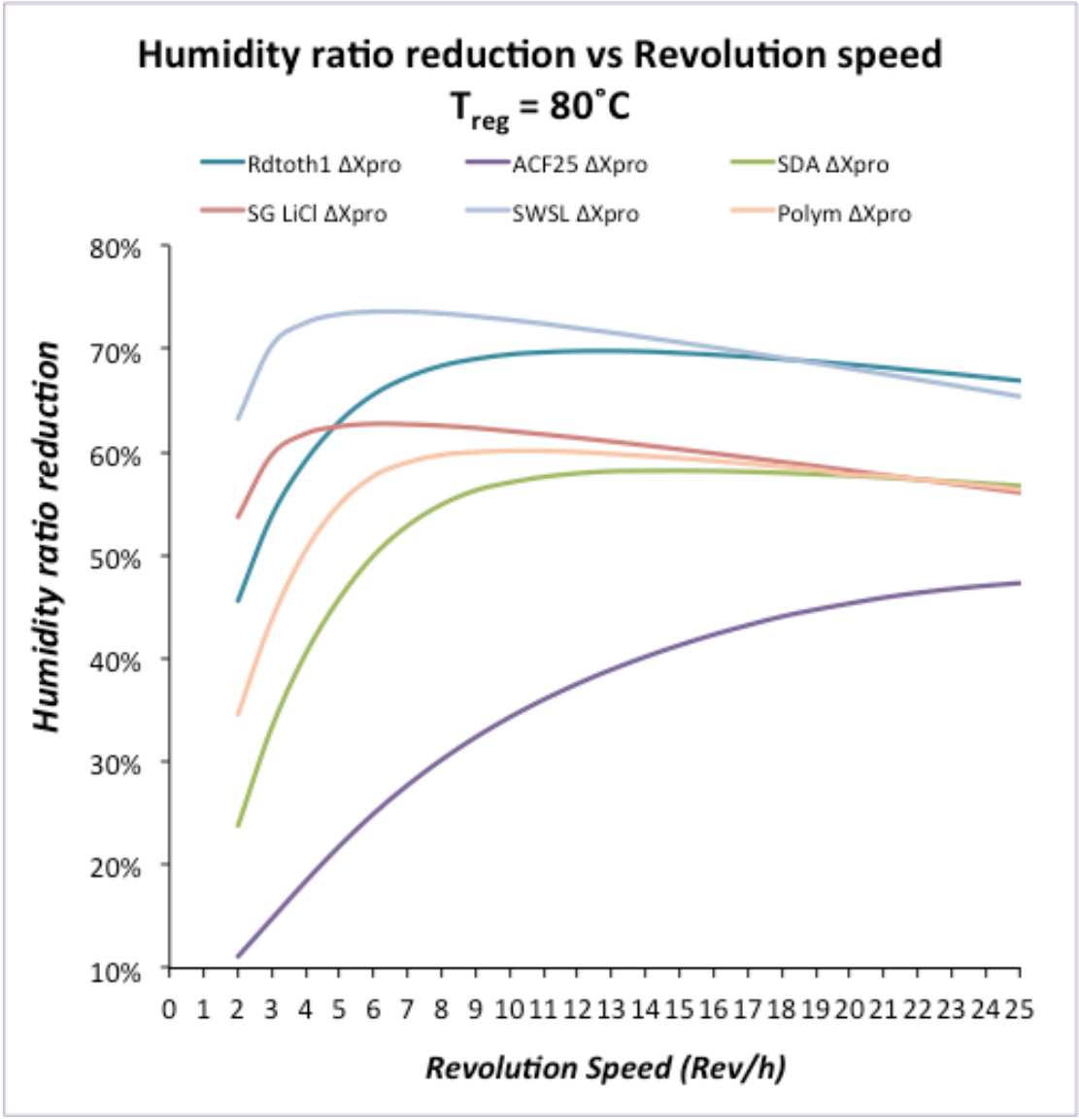

Figure 57 Humidity ratio reduction vs revolution speed at $T_{reg,IN}$ = 80 °C

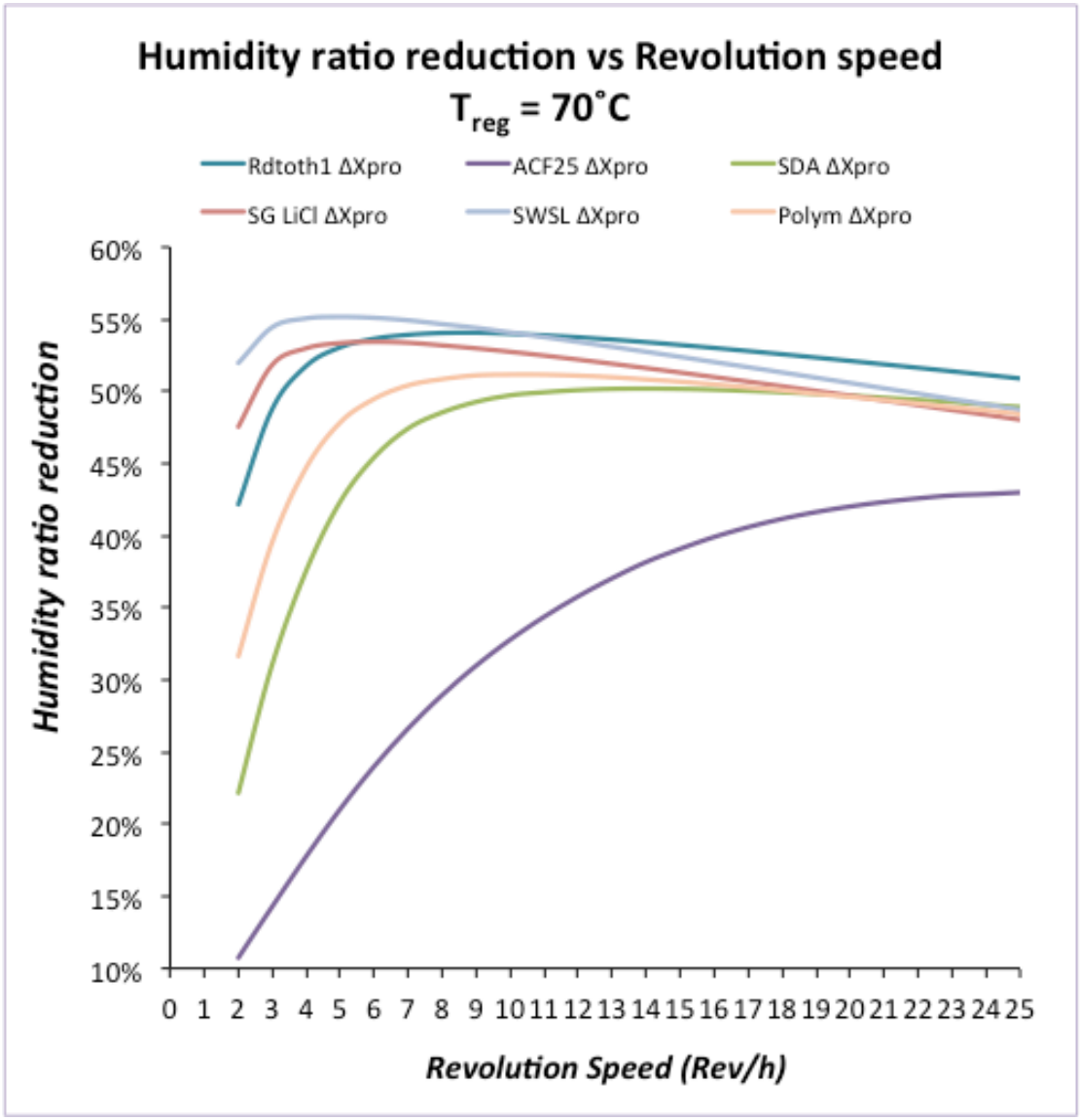

Figure 58 Humidity ratio reduction vs revolution speed at $T_{reg,IN}$ = 70 °C

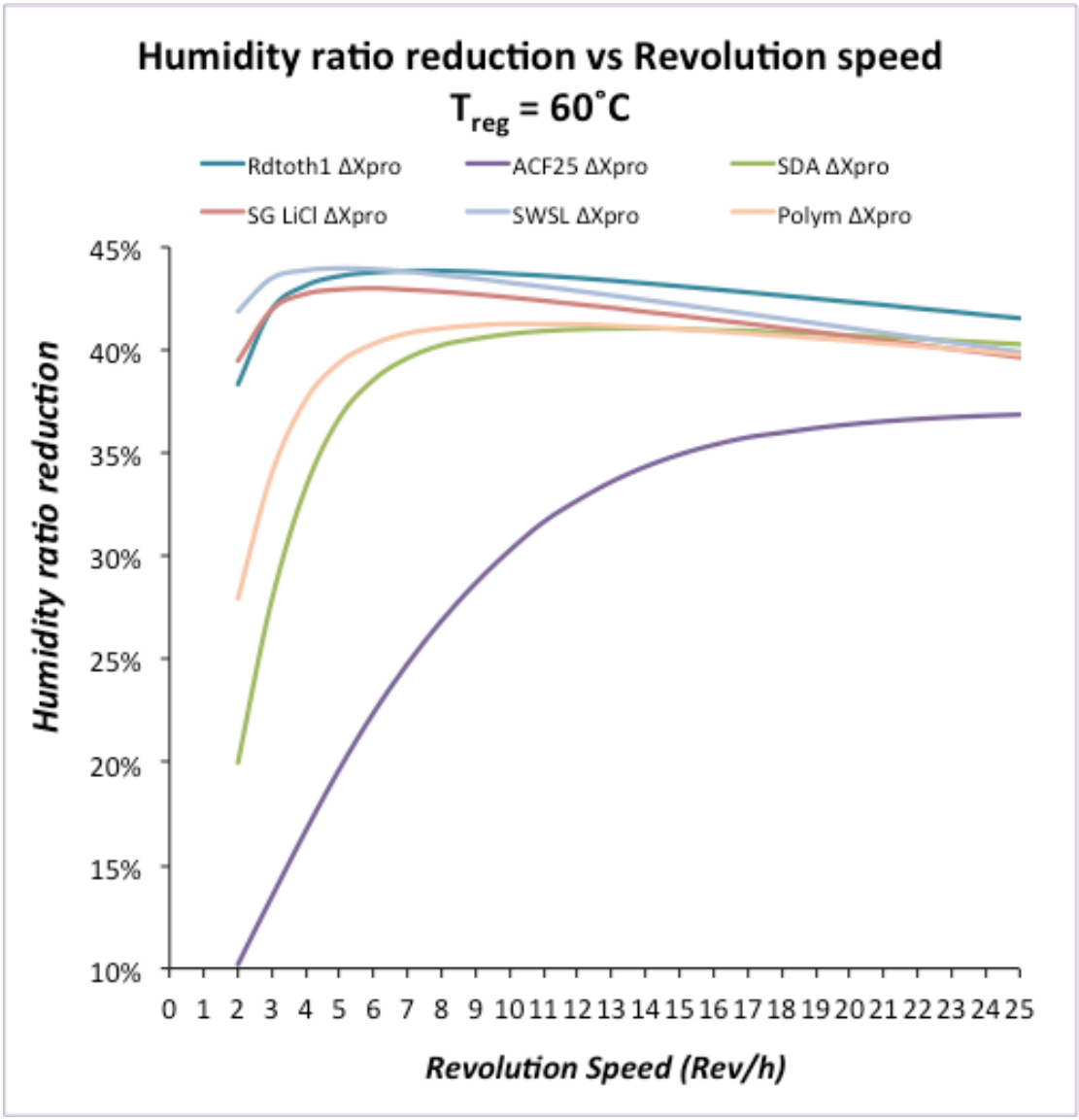

Figure 59 Humidity ratio reduction vs revolution speed at $T_{reg,IN}$ = 60 °C

Appendix F Desiccant wheel simulation: Humidity ratio reduction vs regeneration angle

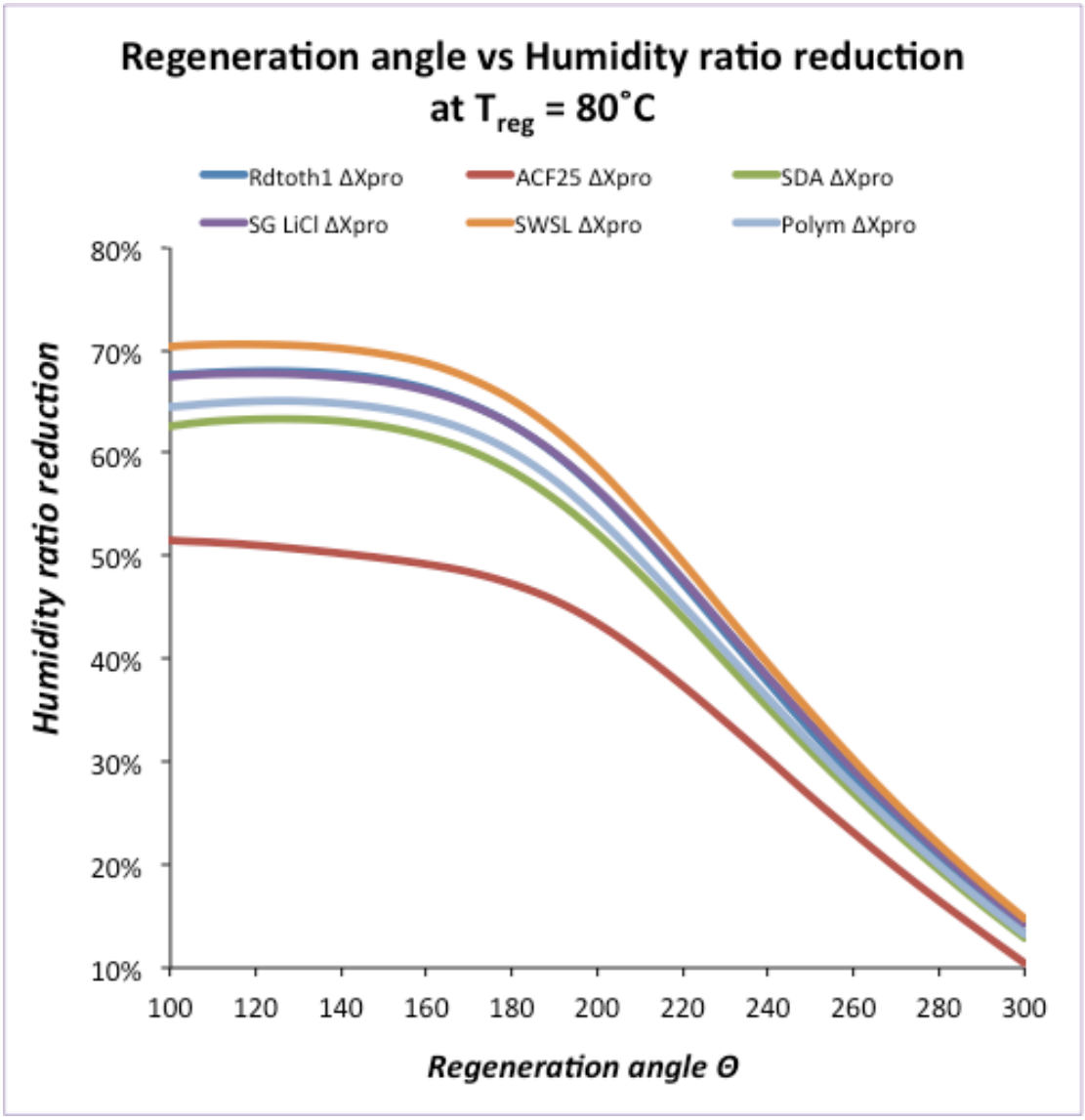

Figure 60 Regeneration angle vs Humidity ratio reduction using a $T_{reg,IN}$ = 80°C

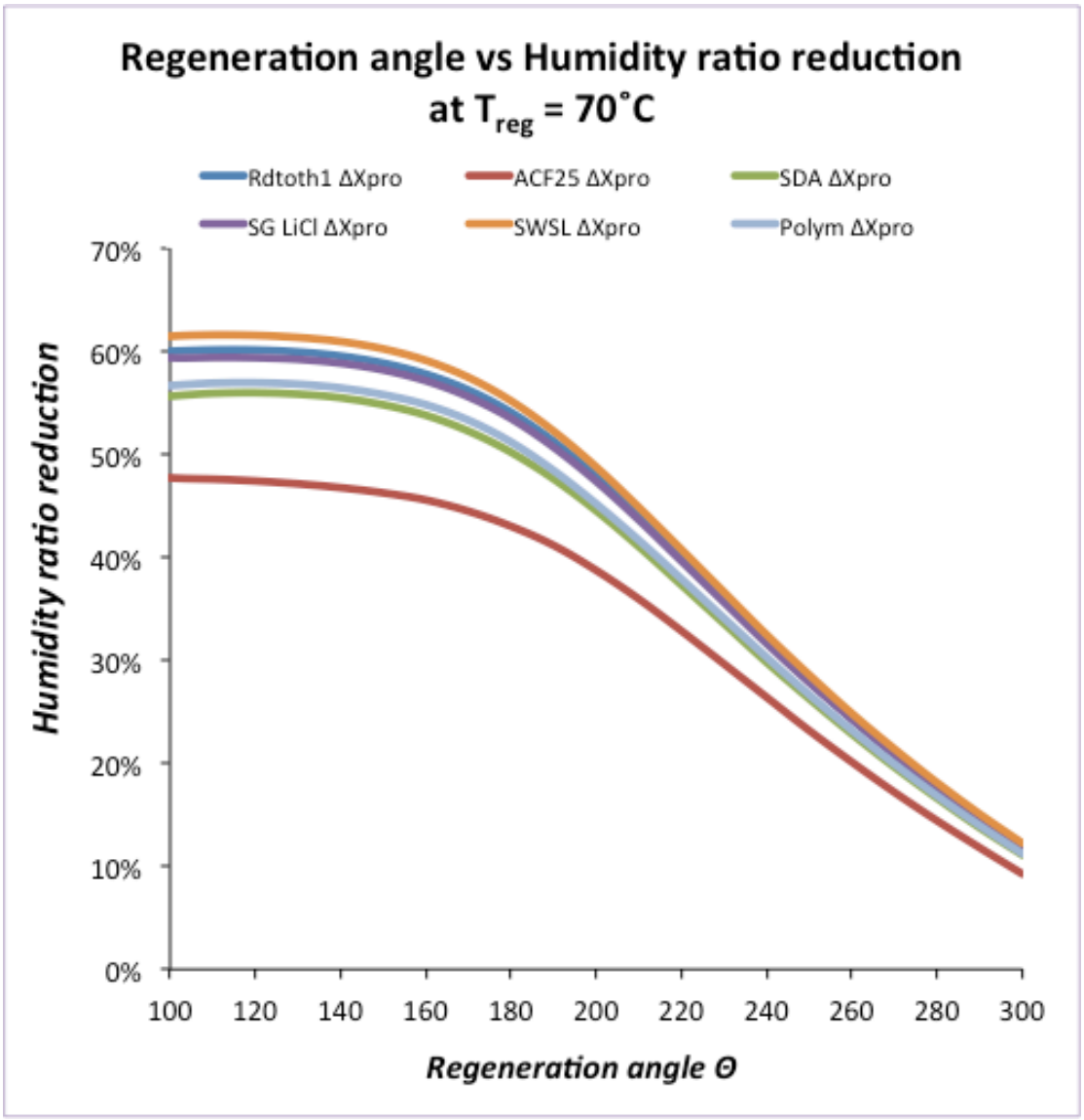

Figure 61 Regeneration angle vs Humidity ratio reduction using a $T_{reg,IN}$ = 70°C

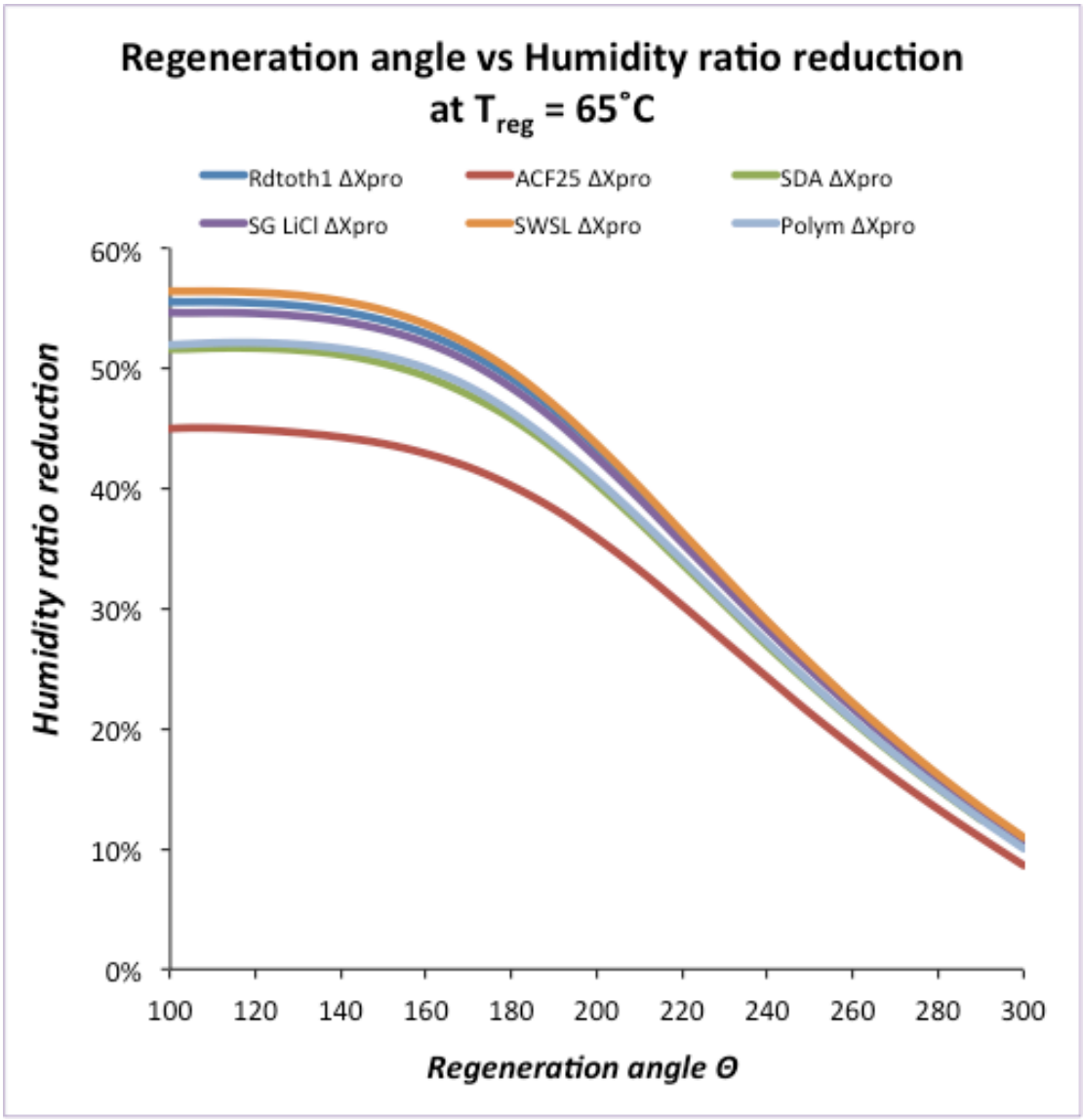

Figure 62 Regeneration angle vs Humidity ratio reduction using a $T_{reg,IN}$ = 65°C

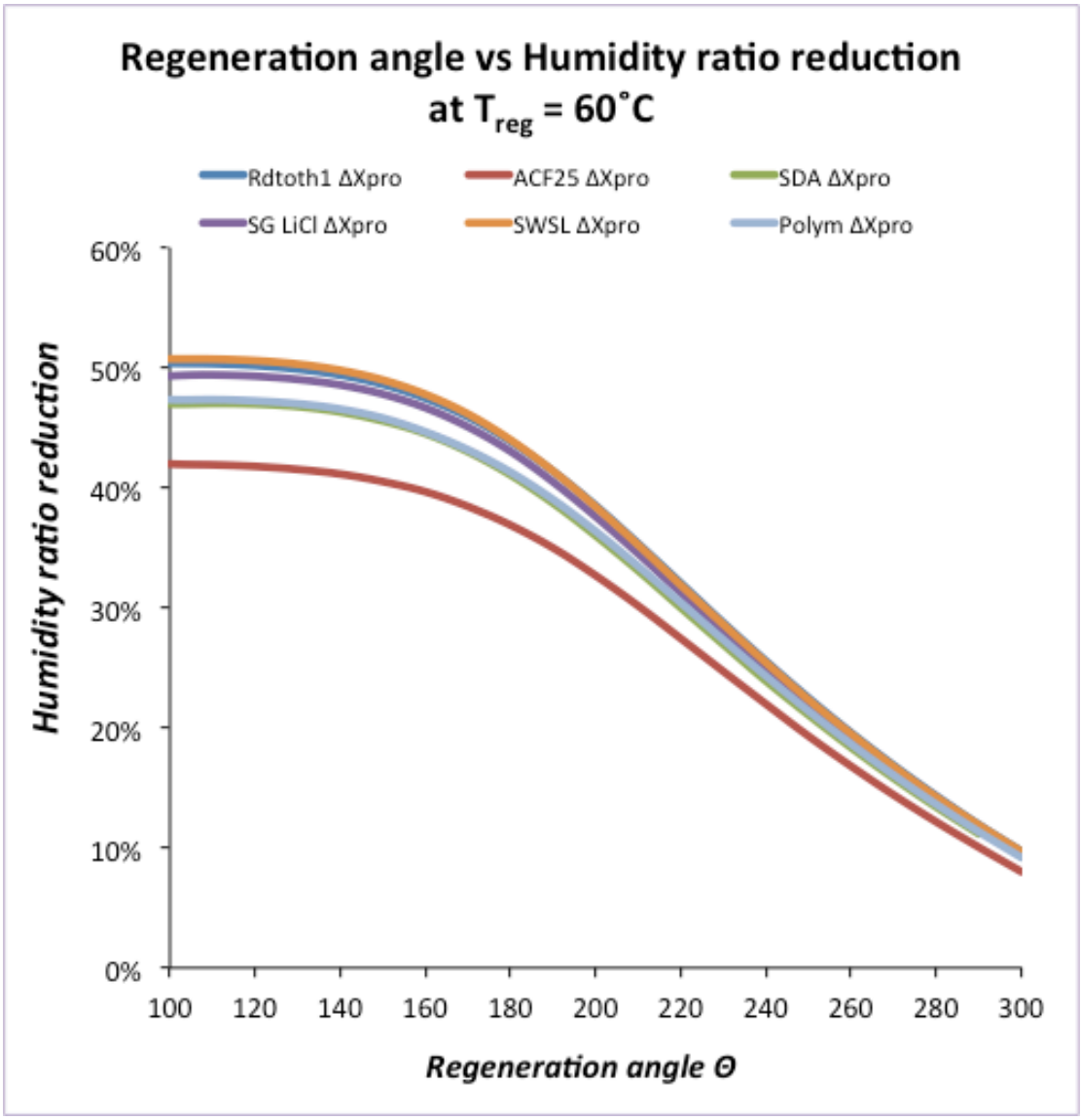

Figure 63 Regeneration angle vs Humidity ratio reduction using a $T_{reg,IN}$ = 60°C

Appendix G Solar energy used by the proposed and conventional systems

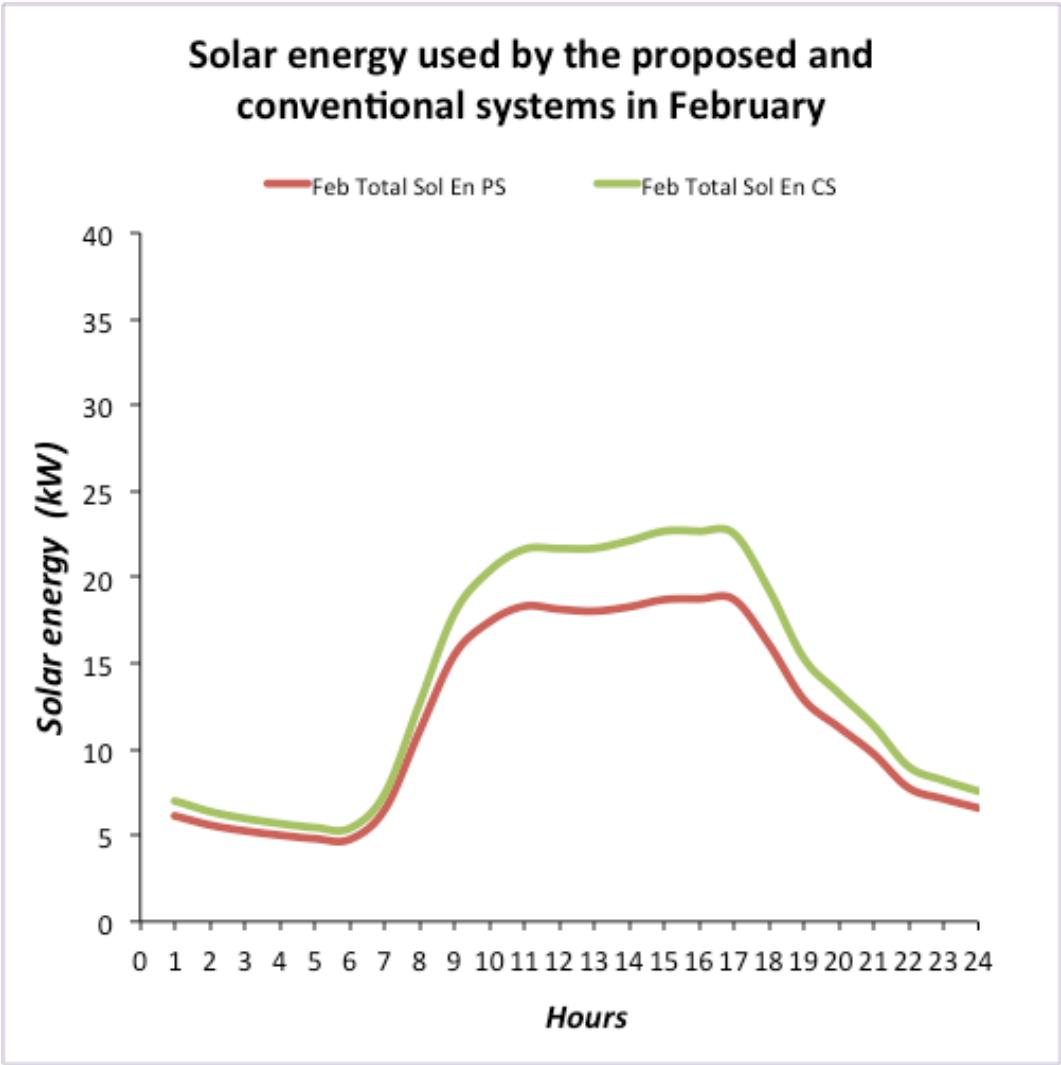

Figure 64 Solar energy used by the conventional system and the proposed system for February

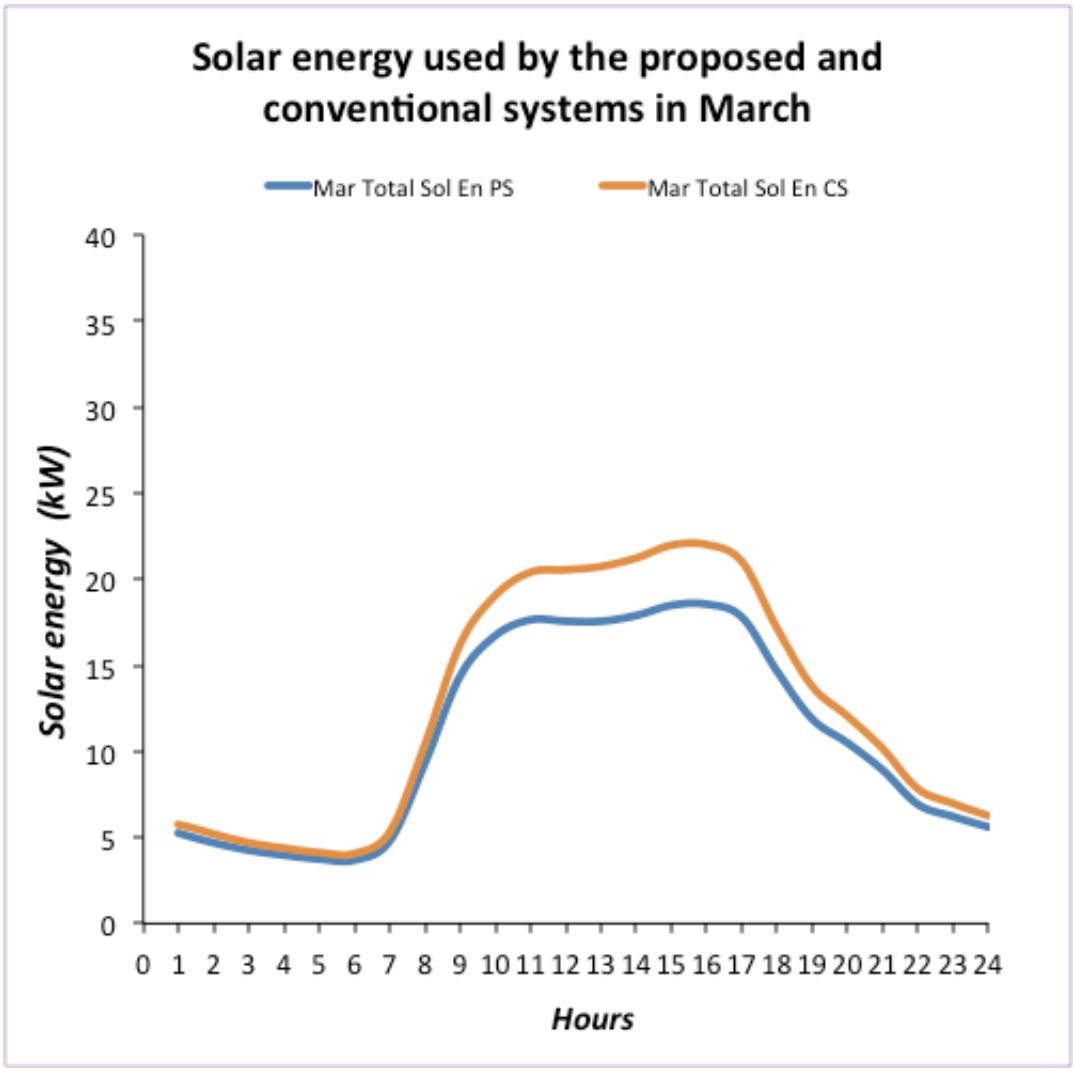

Figure 65 Solar energy used by the conventional system and the proposed system for March

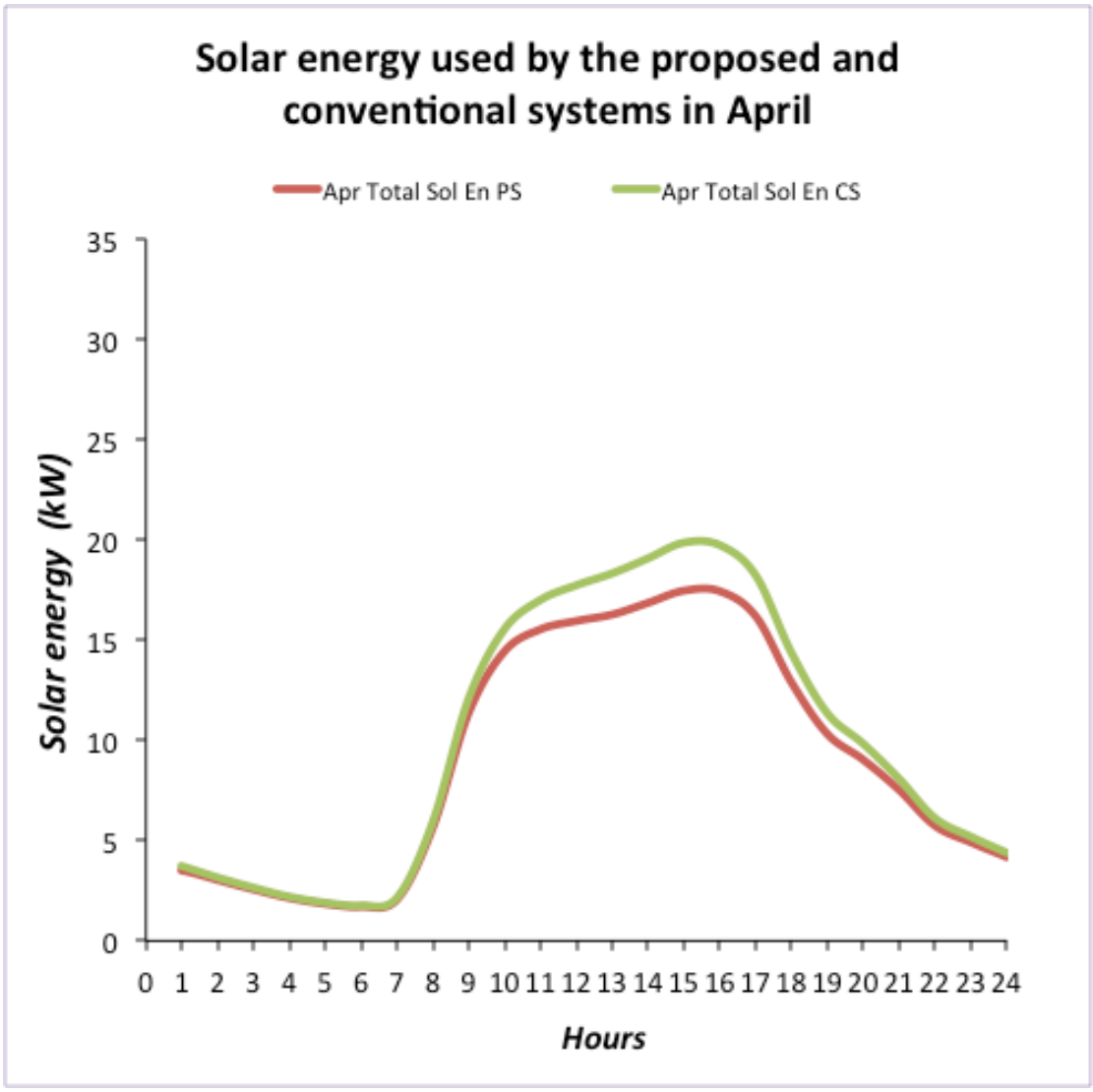

Figure 66 Solar energy used by the conventional system and the proposed system for April

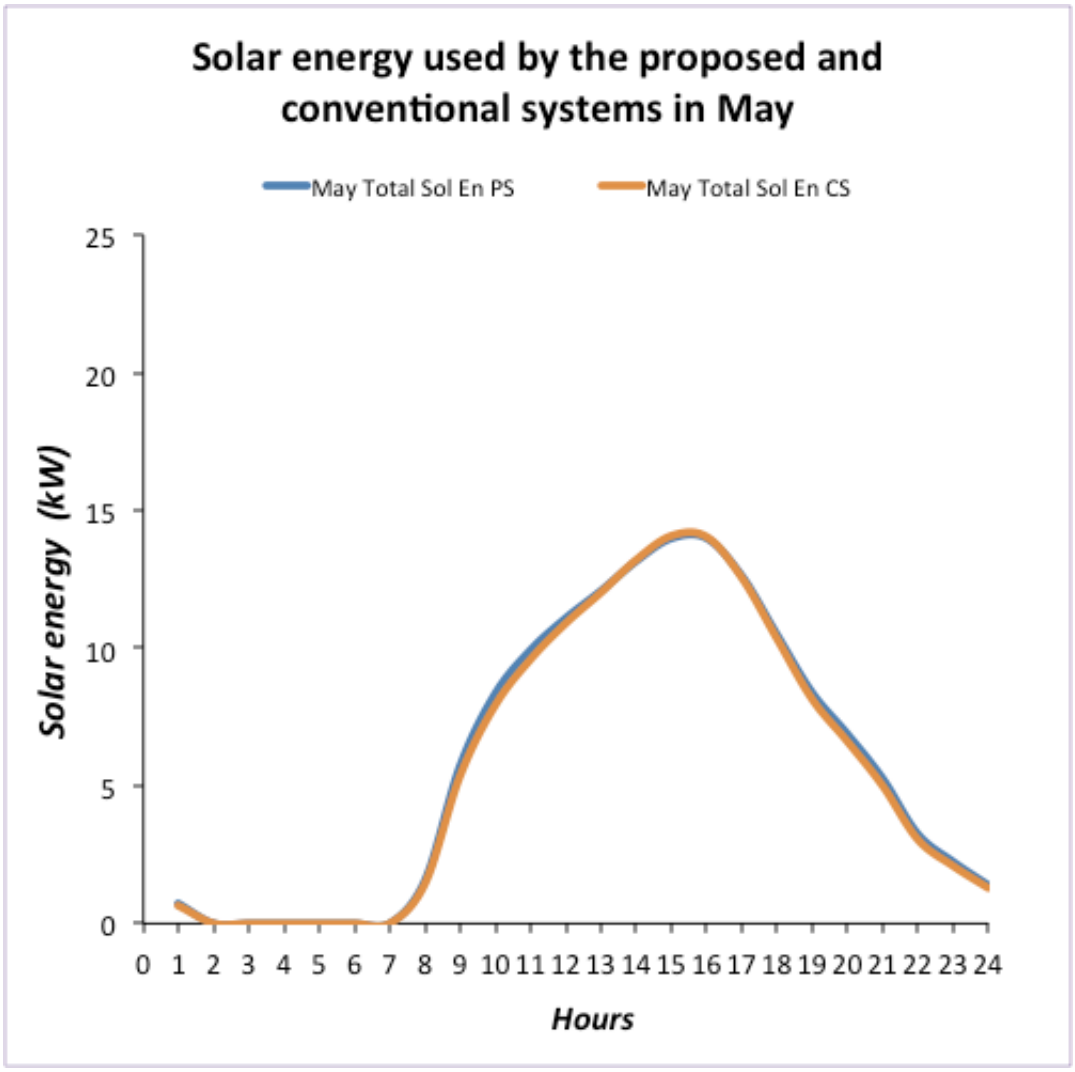

Figure 67 Solar energy used by the conventional system and the proposed system for May

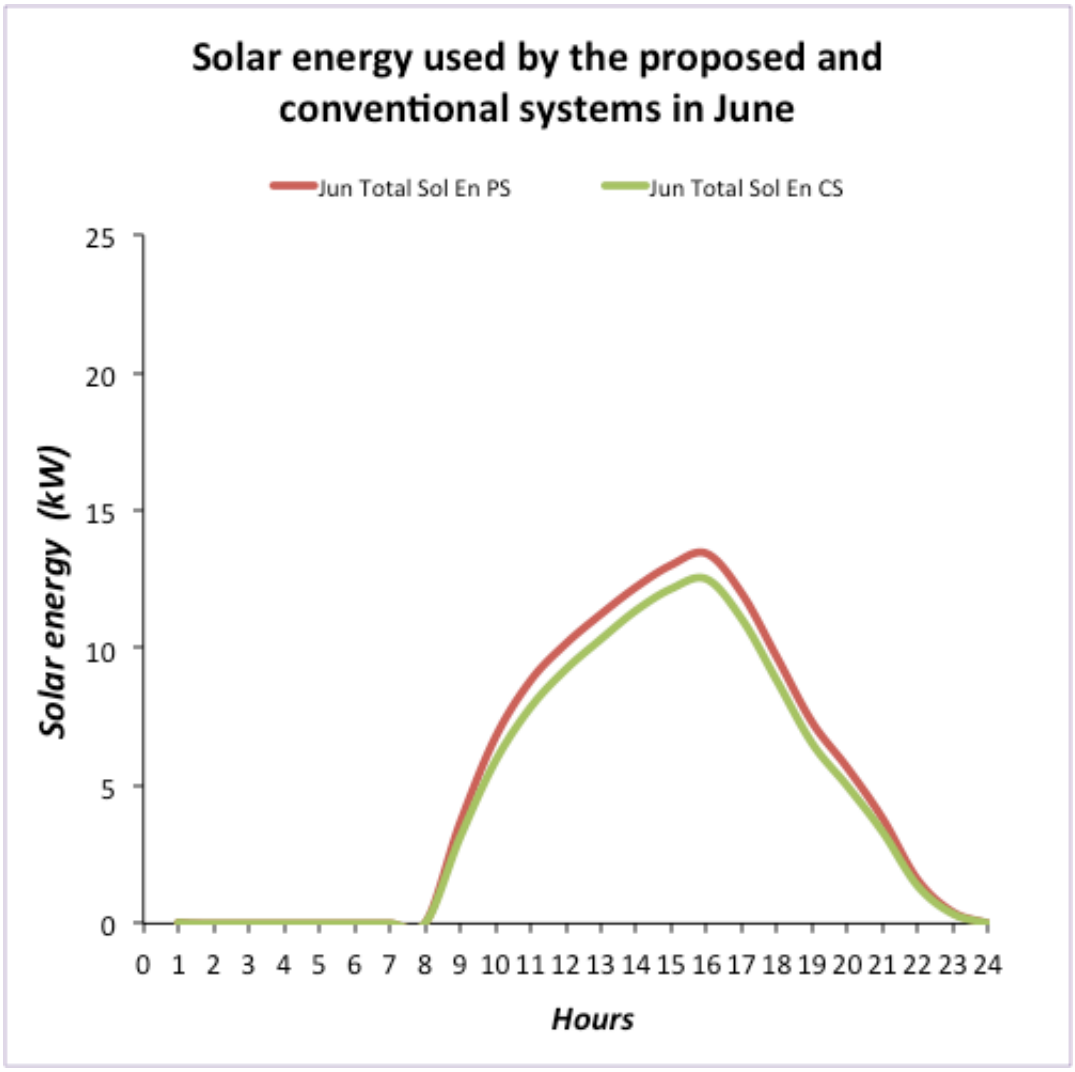

Figure 68 Solar energy used by the conventional system and the proposed system for June

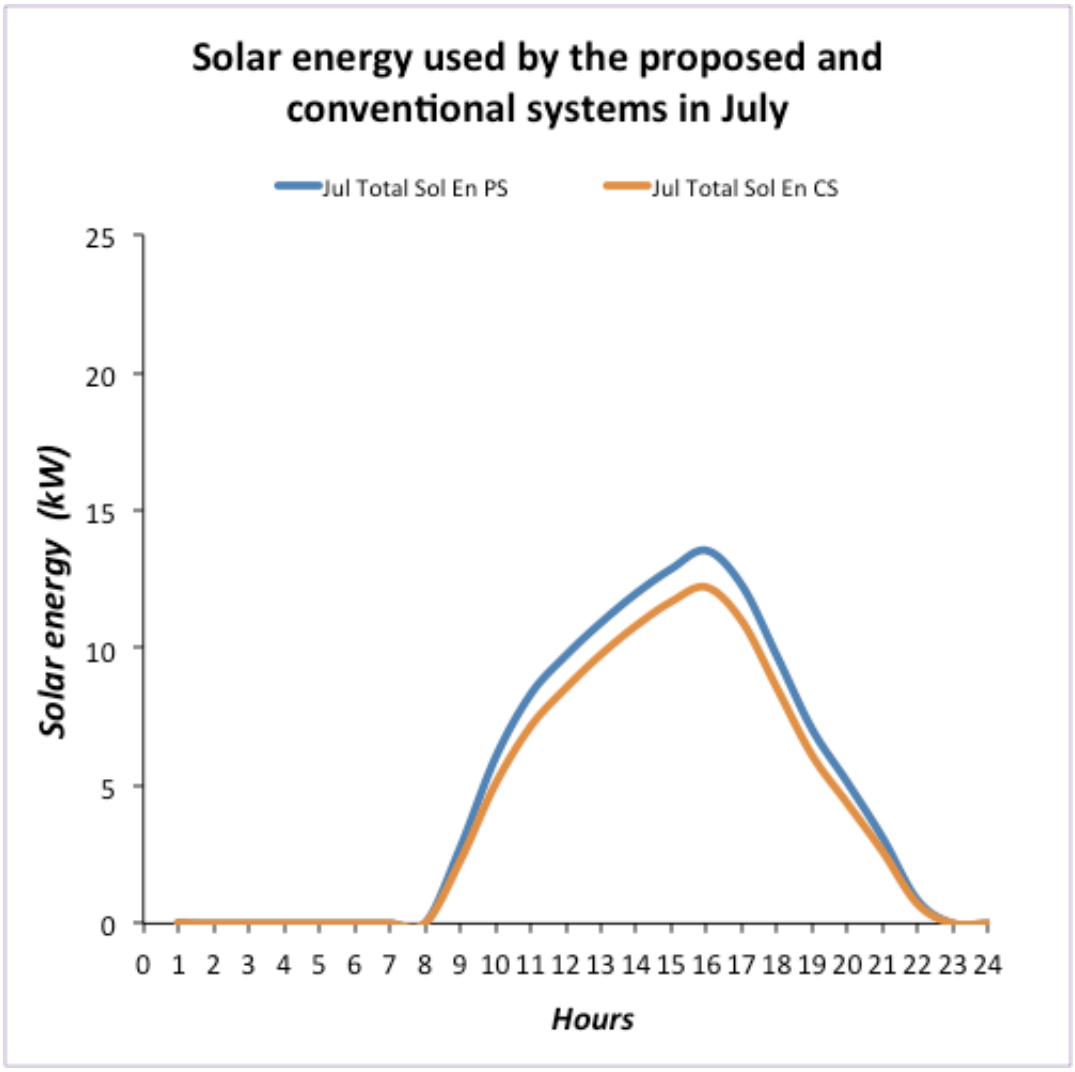

Figure 69 Solar energy used by the conventional system and the proposed system for July

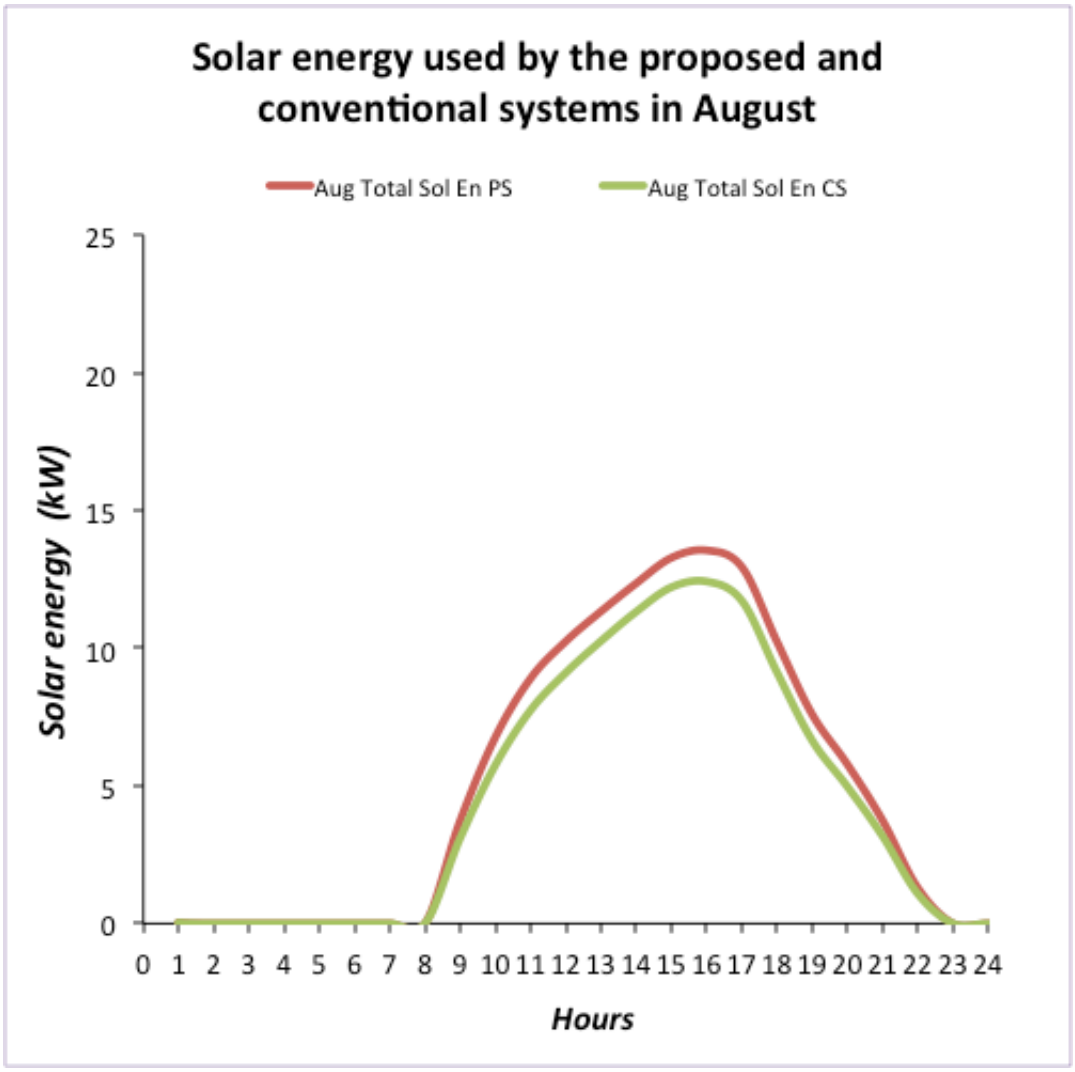

Figure 70 Solar energy used by the conventional system and the proposed system for August

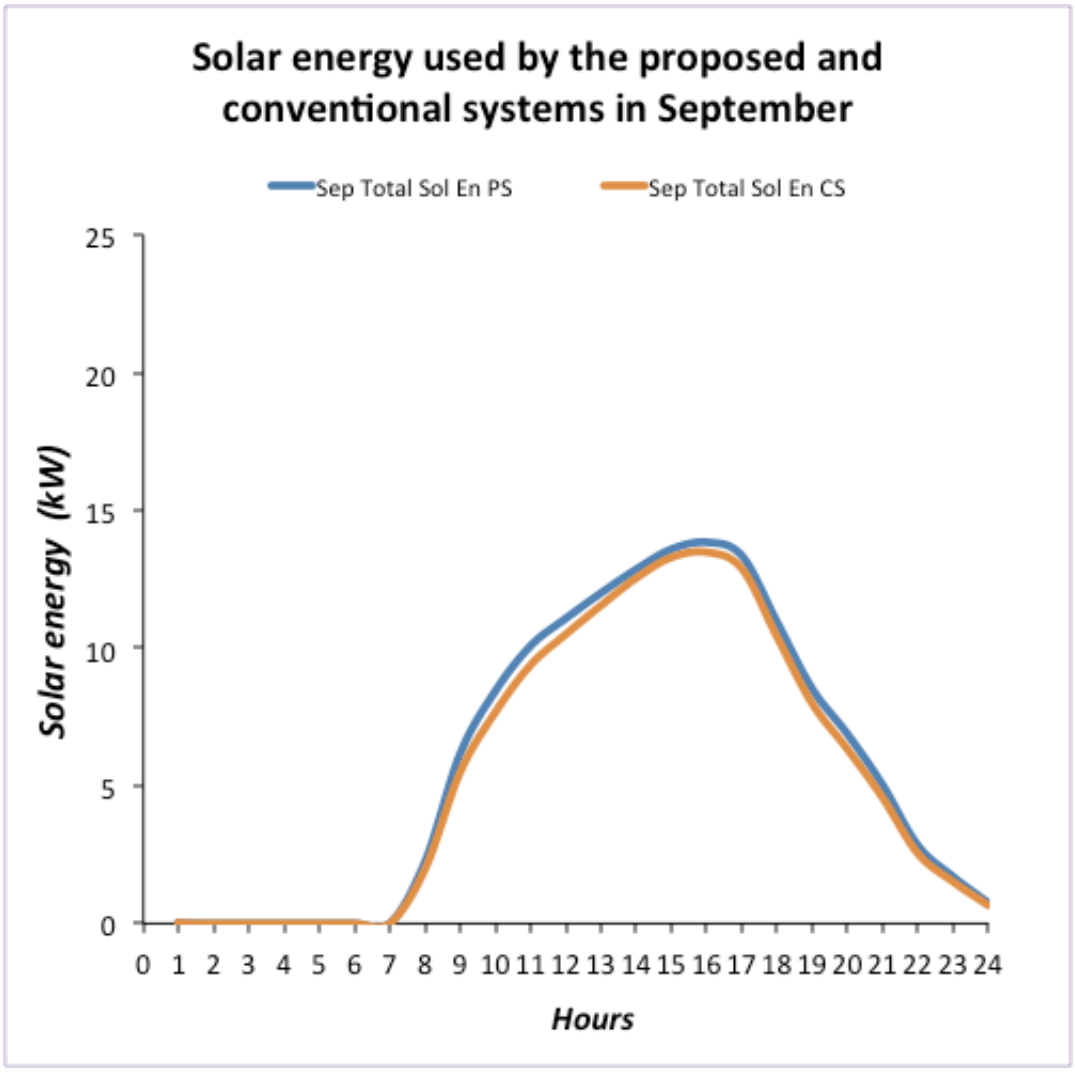

Figure 71 Solar energy used by the conventional system and the proposed system for September

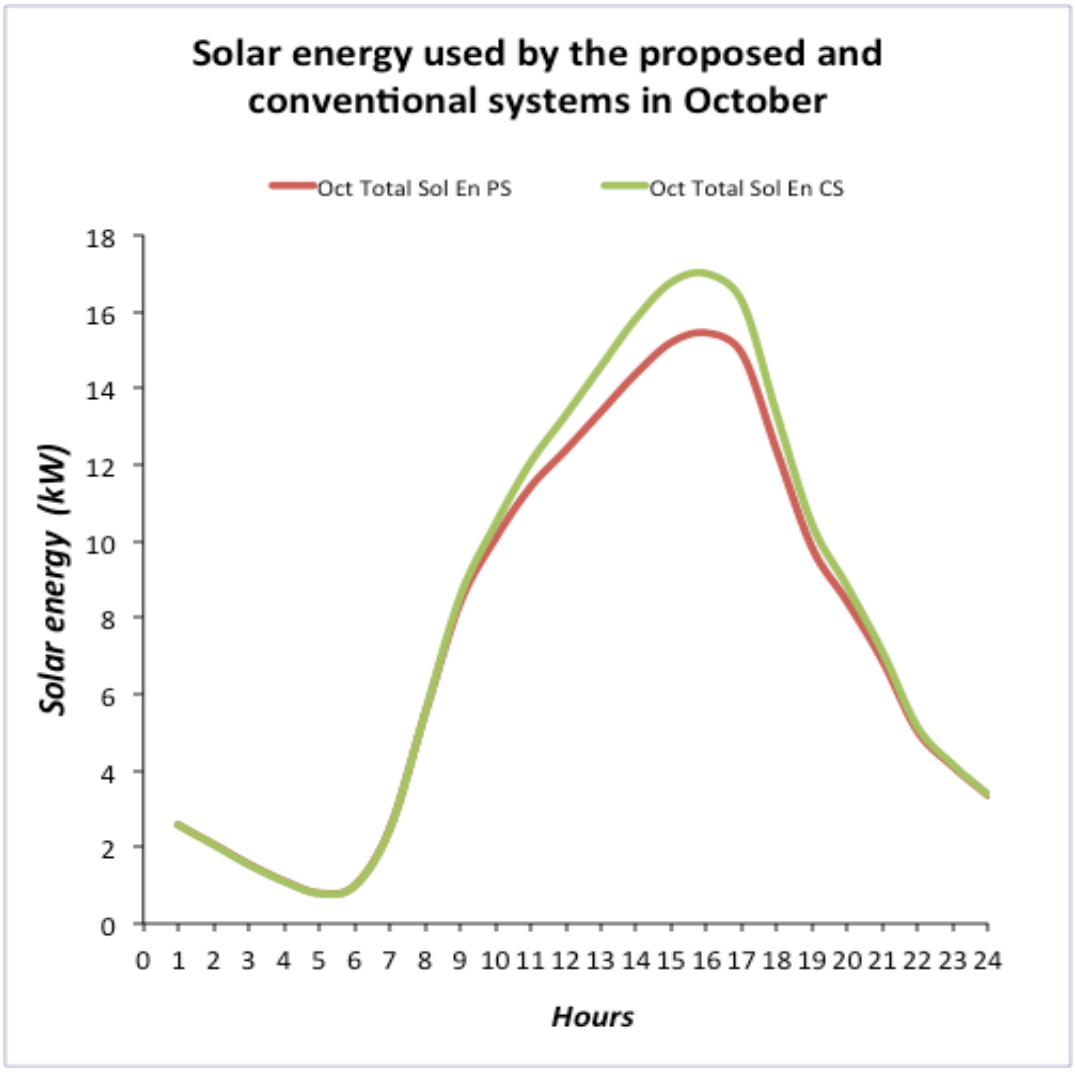

Figure 72 Solar energy used by the conventional system and the proposed system for October

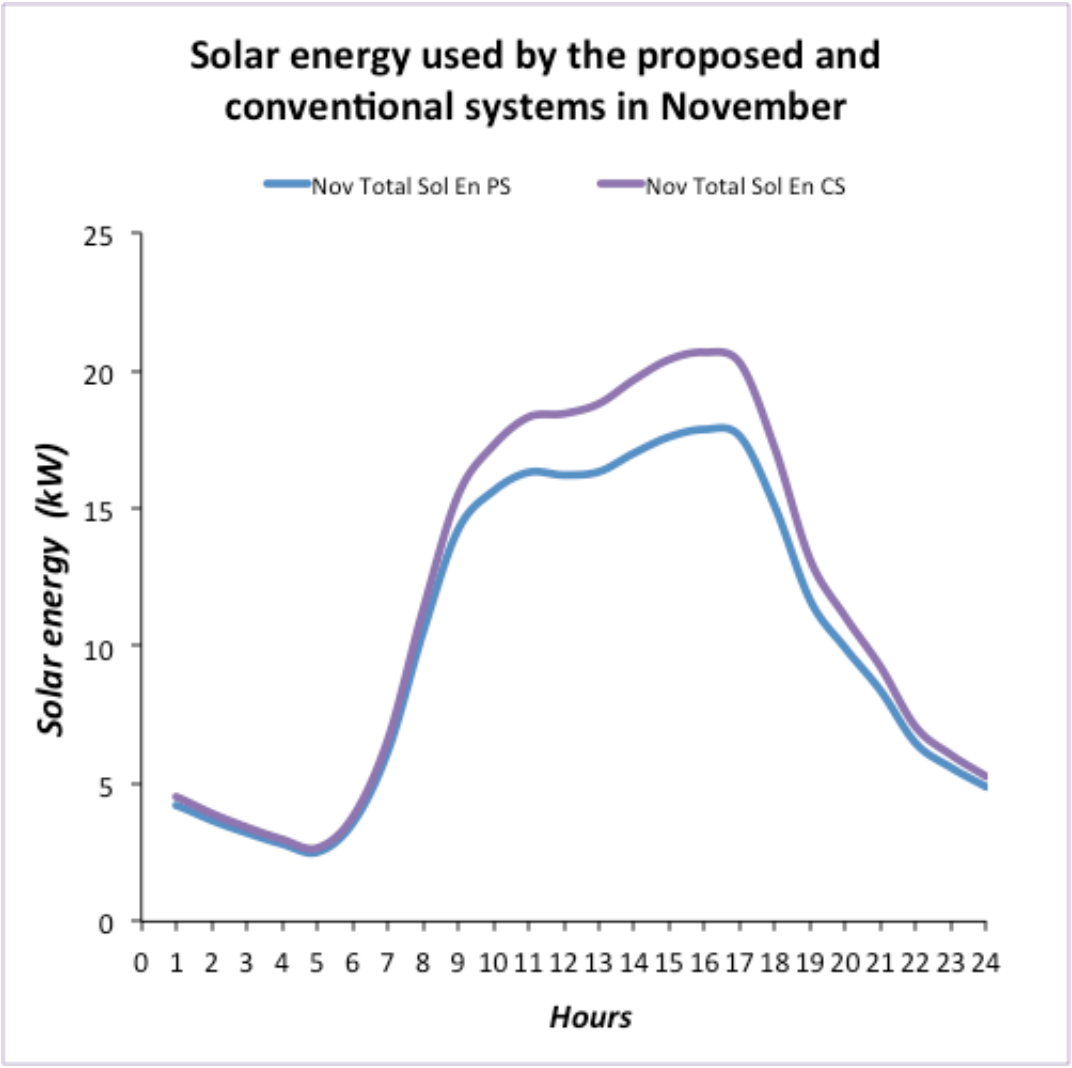

Figure 73 Solar energy used by the conventional system and the proposed system for November

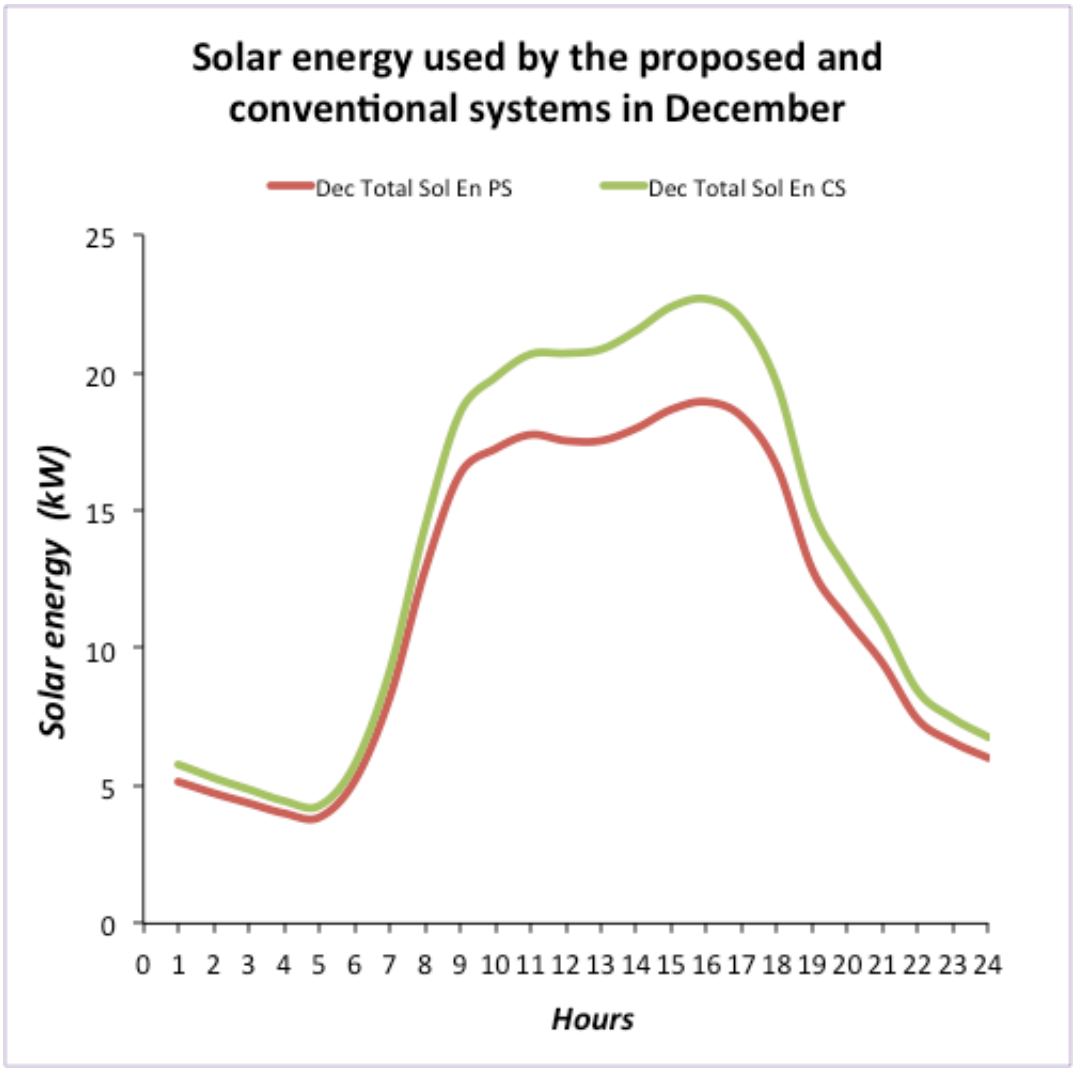

Figure 74 Solar energy used by the conventional system and the proposed system for December

Appendix H Program Code #1

```
% function [ COP ] = Single_Stage_COP_calculator(thw_in,thw_out,tc_in, tcw_out)
function          [          cop_out,thw_out1,thw_out2          ]          =
Single_Stage_COP_calculator(thw_in,tc_in,tcw_out)
% Calculator of the efficiency of the chiller
%   This function use as input the temperature of the hot water in and out,
%   the temperature of the cooling water in and the temperature of the
%   chilled water out and calculate the efficiency of the chiller based on
%   the data available from a real chiller Pink chilli 12
global tc_in
PERC1 = 0.05/100; %tollerance
PERC2 = 0.12/100;
load Single_effect_data;
mask1 = Single_effect_data(:,7) <= thw_in*(1+PERC1) & Single_effect_data(:,7)
>= thw_in*(1-PERC1);
% Tab1 = Single_effect_data(mask1,7);
mask2 = Single_effect_data(:,4) <= tc_in*(1+PERC2) & Single_effect_data(:,4) >=
tc_in*(1-PERC2);
tcwh_out = Single_effect_data(mask1&mask2,2);
cop = Single_effect_data(mask1&mask2,13);
thw_out = Single_effect_data(mask1&mask2,8);
sm =  Single_effect_data(:,7) == thw_in;
if any(sm)
    thw_out1 = Single_effect_data(sm,8);
end
p = polyfit(tcwh_out,cop,2);
cop_out = polyval(p,tcw_out);
 [~,mI] = min(abs(tcwh_out-tcw_out));
thw_out2 = thw_out(mI);

end


% Imposing a value for the latitude and the average monthly insolation data for
a wherever place the hourly insolation data are obtained


% Initialization
% clear all
% close all
% clc

global Aa Tn An Cf a1 a2 Kd Ta Twi Two Panel_efficiency Latitude tdb
global sa fa Cond_T hwt rat ra_rh eff_HX tev sat sa_rh eff_noozles

%tdb = Ta;

% Latitude = input ('Insert Latitude (?) (-ve in Southern Hemisphere):
');%latitude value for the place
load Solar_data.mat;
load Hour_Angle.mat;


Mean_Day = [17  47  75  105 135 162 198 228 258 288 318 344];% Day of Year

T   = 23.45*(sin(360.*((284+(Mean_Day))./365).*pi/180)); % Solar Declination
Angle (?)

Z = (2/15)*(Degrees(acos((-tan(Radians(Latitude))).*(tan(Radians(T)))))); % Day
Length(Hours)

H =(Degrees(acos((-tan(Radians(Latitude))).*(tan(Radians(T)))))));% Sunset Hour
Angle (?s)

G = 0.409+0.5106*(sin(Radians((H-60))));% Coefficient a

F =0.6609-0.4767*(sin(Radians((H-60))));% Coefficient b
```

```
Dati = [Solar_data; Mean_Day; T; Z; H; G; F];


m =length (Dati(1,:));
n =length (Hour_Angle);

for i=1:n
    for j=1:m

if(((pi/24)*(G(j)+F(j)*cos(Radians(Hour_Angle(i))))*(((cos(Radians(Hour_Angle(i
))))-(cos(Radians(H(j)))))/((sin(Radians(H(j))))-
(((pi*H(j))/180)*(cos(Radians(H(j)))))))<0)
R(i,j)=0;
else
R(i,j)                                                                    =
(((pi/24)*(G(j)+F(j)*cos(Radians(Hour_Angle(i))))*(((cos(Radians(Hour_Angle(i))
))-(cos(Radians(H(j)))))/((sin(Radians(H(j))))-
(((pi*H(j))/180)*(cos(Radians(H(j)))))));
end
    end
end

for i=1:n
    for j=1:m

K(i,j)= R(i,j)*Solar_data(j);
    end
end

% prompt={'Absorber area [m2]','Number of tubes per absorber:','Number of
absorber:','Conversion Factor (CF) number:','Coefficient a1 value:
','Coefficient a2 value: ','Average Kd (IAM) value: ','Ambient Air Temp (∞C):
','Inlet Water Temp. (∞C): ','Outlet Water Temp. (∞C): '};
% def={'3.02','30','8','0.832','1.14','0.0144','1','32','75','80'};
% title='Insert Solar panel data';
% dati1=inputdlg(prompt,title,1,def,'on');
% Solar_panel=str2double(dati1);
% Aa=Solar_panel(1);
% Tn=Solar_panel(2);
% An=Solar_panel(3);
% Cf=Solar_panel(4);
% a1=Solar_panel(5);
% a2=Solar_panel(6);
% Kd=Solar_panel(7);
% Ta=Solar_panel(8);
% Twi=Solar_panel(9);
% Two= Solar_panel(10);
At = Aa*An;
Tt = Tn*An;
DeltaT = (((Twi+Two)/2)-Ta);

%str = sprintf('Total Area %s m2, Total number of tubes %d, Delta t = %d ', At,
Tt, DeltaT);
%disp(str);


% Efficincy of the solar panels
%stupid = sprintf('Debug: tdb %d Ta %d deltaT %d', tdb, Ta, DeltaT);
%disp(stupid);

for i=1:n
    for j=1:m
        thingy               =               Kd*Cf-(a1*(DeltaT/(1000*K(i,j))))-
(a2*1000*K(i,j)*((DeltaT/(1000*K(i,j)))^2));
        debug = sprintf('(i,j) = ( %d , %d ) and value of thingy %d', i, j,
thingy);
        disp(debug);
        if K(i,j)==0
            Panel_efficiency(i,j)=0;
```

```
        elseif (thingy < 0)
            Panel_efficiency(i,j)=0;
        else
            Panel_efficiency(i,j)=thingy;
        end %endif
    end %endfor j
end %endfor i

% for i=1:n
%     for j=1:m
%  if K(i,j)==0
%      Panel_efficiency(i,j)=0;
%                                    elseif(Kd*Cf-(a1*(DeltaT/(1000*K(i,j))))-
(a2*1000*K(i,j)*((DeltaT/(1000*K(i,j)))^2)))<0
%  Panel_efficiency(i,j)=0;
%  else
%                      Panel_efficiency(i,j)=(Kd*Cf-(a1*(DeltaT/(1000*K(i,j))))-
(a2*1000*K(i,j)*((DeltaT/(1000*K(i,j)))^2)));
%  end
%     end
% end

E = Panel_efficiency.*K.*Aa*An;
Te= sum(E);

Max_efficiency = max(Panel_efficiency)

% load Hourly_tem_brisbane.mat %matrix of hourly temperature in Brisbane
%
% load DeltaT_monthly.mat
%
%
% DeltaTwaterT = DeltaT_monthly (1,:)-DeltaT_monthly(2,:);
%
% max(Panel_efficiency);
%*************************************************************************
*******
%                     AHU simulator                                *
%                                                               *
%                    Main files: AHU_model.m                *
%               Sub-files: psy.m, psydescription.m             *
%                                                               *
%                     by:   Paolo Corrada                       *
%            Science and Engineering faculty                          *
%            Queensland University of Technology                   *
%                                                                  *
%*************************************************************************
*******

%clear all;                     % clear all variables

global  Air_density  v2  pws  EnSolHX  SenHX  Cool_power_evap  Conventional_system
Saving;
global    indoor_return    indoor_exhaust_air    return_air    regeneration_inlet
process_inlet   process_outlet   regeneration_outlet   exhaust_air   supply_air
mixed_air supply_air_room Outside_air Cooling_air Reject_heat_air
global Aa Tn An Cf a1 a2 Kd Ta Twi Two Panel_efficiency tdb RH_ambient
global sa fa Cond_T hwt rat ra_rh eff_HX tev sat sa_rh eff_noozles tc_in
global COP
Air_density = 1.204;

option=1
%%%%%%%%%%%%%%%%%%%%%%%%%%%%%%%%%
   clc;                             % clear command window
   disp('Software name: Solar air conditioning unit simulator (Ver. 1.0)');
   disp('developed  by: Paolo Corrada');
   disp('               Ph.D. Candidate');
   disp('               Science and engineering faculty');
   disp('               Queensland university of technology');
```

```
   fprintf('\n');
   disp('Data available for the outside air:');
   disp('(1) Tdb, rh');
   disp('(2) Tdb, Twb');
   disp('(3) Tdb, Pw');
   disp('(4) Tdb, ah');
   disp('(5) Tdb, Tdp');
   fprintf('Select: 0 to quit, 1:5 to run. ');
%    option=input('');
   option=1; % change the value of option everytime yuo have different data
input
   fprintf('\n');
   if option ~=0

%       out=input(' Patm            (in kPa 101.325 kPa as default)= ');
%       if isempty(out)
        patm=101.325;
%          fprintf(' Patm            (in kPa)=%6.3f \n ', patm);
%
%       else
%          patm=out;
%       end

%      tdb=input('Dry bulb t (in degree C)= ');
       pws=psy(tdb,0,0,'pws');              % in kPa
       hfg=psy(tdb,0,0,'hfg');              % in kJ/kg
       ahoftdb=psy(patm,pws,100,'ah');      % in kg/kg


   end
   %%%%%%%%%%%%%%%%%%%%%%%%%%%%%%%

while option~=0


    switch option
   case 1
        fprintf(' Rel. humidity (within 0 to 100%%) = ' );
        rh=RH_ambient;
            pw=psy(pws,rh,0,'pw');              % in kPa
            ah=psy(patm,pws,rh,'ah');           % in kg/kg
            tdp=psy(tdb,pw,0,'tdp');            % in degree C
            h=psy(tdb,ah,0,'h');                % in kJ/kg
            sv=psy(patm,tdb,ah,'sv');           % in m3/kg
            dos=psy(patm,pws,rh,'dos');         % in kg/kg
            twb=psy(tdb,tdp,0,'twb');           % in degree C

    case 2
        fprintf(' Wet bulb t (C) = ');
        twb=input('');
            rh=psy(tdb,twb,0,'rh2');
            pw=psy(pws,rh,0,'pw');              % in kPa
            ah=psy(patm,pws,rh,'ah');           % in kg/kg
            tdp=psy(tdb,pw,0,'tdp');            % in degree C
            h=psy(tdb,ah,0,'h');                % in kJ/kg
            sv=psy(patm,tdb,ah,'sv');           % in m3/kg
            dos=psy(patm,pws,rh,'dos');         % in kg/kg

   case 3
        fprintf(' Vapor pressure');
        pw=input('');
            rh=pw/pws*100;
            ah=psy(patm,pws,rh,'ah');           % in kg/kg
            tdp=psy(tdb,pw,0,'tdp');            % in degree C
            h=psy(tdb,ah,0,'h');                % in kJ/kg
            sv=psy(patm,tdb,ah,'sv');           % in m3/kg
            dos=psy(patm,pws,rh,'dos');         % in kg/kg
            twb=psy(tdb,tdp,0,'twb');           % in degree C
```

```
    case 4
        fprintf(' Abs. humidity = ');
        ah=input('');
            pw=psy(patm,ah,0,'pw2');            % in kPa
            rh=pw/pws*100;                      % in %
            tdp=psy(tdb,pw,0,'tdp');            % in degree C
            h=psy(tdb,ah,0,'h');                % in kJ/kg
            sv=psy(patm,tdb,ah,'sv');           % in m3/kg
            dos=psy(patm,pws,rh,'dos');         % in kg/kg
            twb=psy(tdb,tdp,0,'twb');           % in degree C

   case 5
        fprintf(' Dew pt. t ');
        tdp=input('');
            pw=psy(tdp,0,0,'pws');              % in kPa
            rh=pw/pws*100;                      % in %
            ah=psy(patm,pws,rh,'ah');           % in kg/kg
            h=psy(tdb,ah,0,'h');                % in kJ/kg
            sv=psy(patm,tdb,ah,'sv');           % in m3/kg
            dos=psy(patm,pws,rh,'dos');         % in kg/kg
            twb=psy(tdb,tdp,0,'twb');           % in degree C

    end   % for switch(option)

        z=zeros(1,12);
    z(1)=patm; z(2)=tdb; z(3)=twb;z(4)=tdp; z(5)=rh;
    z(6)=dos;z(7)=pws; z(8)=pw;z(9)=ah; z(10)=h;
    z(11)=sv; z(12)=hfg;
    %z(13)=THI1;z(14)=THI2;z(15)=DI;

    %calAHU(z)

   clc;

   disp('Software name: Solar air conditioning unit simulator (Ver. 1.0)');
   disp('developed  by: Paolo Corrada');
   disp('               Ph.D. Candidate');
   disp('               Science and engineering faculty');
   disp('               Queensland university of technology');
   fprintf('\n');

  %-------------------------------------------------------------------------------
-----------
  if option ==0
      fprintf('\n\n');
      disp('Thank you for using this program.');
      fprintf('\n\n');
   else


%-------------------------------------------------------------------------------
---------
    textcont='';
    disp('External condition of the air:');
    fprintf('\n')
    for i=1:12
    [cont,unit]=psydescription(i);
       fprintf('%s =  %10.5f  %s \n', cont, z(i), unit);

    end

    fprintf('\n');
    fprintf('\n  Press Enter to continue.');
    %pause;
    clc;
%-------------------------------------------------------------------------------
---------
```

```
    end % if option ~=0
   calAHU3(z);

   % disp('Press any key to continue: ')
   % dummy = input('');


   %    clc;                              % clear command window
   %%%%%%%%%%%%%%%%%%%%%%%%%%%%%%%%%%%%%%%%
%    disp('Software name: Solar air conditioning unit simulator (Ver. 1.0)');
%    disp('developed  by: Paolo Corrada');
%    disp('               Ph.D. Candidate');
%    disp('               Science and engineering faculty');
%    disp('               Queensland university of technology');
   fprintf('\n');
   disp('Data available for the outside air:');
   disp('(1) Tdb, rh');
   disp('(2) Tdb, Twb');
   disp('(3) Tdb, Pw');
   disp('(4) Tdb, ah');
   disp('(5) Tdb, Tdp');
   fprintf('Select: 0 to quit, 1:5 to run. ');
  % option=input('');
  option=0;
   fprintf('\n');
   if option ~=0
      out=input(' Patm            (in kPa 101.325 kPa as default)= ');
      if isempty(out)
         patm=101.325;
         fprintf(' Patm            (in kPa)=%6.3f \n ', patm);

      else
         patm=out;
      end

       tdb=input('Dry bulb t (in degree C)= ');
       pws=psy(tdb,0,0,'pws');              % in kPa
       hfg=psy(tdb,0,0,'hfg');              % in kJ/kg
       ahoftdb=psy(patm,pws,100,'ah');      % in kg/kg


   end
   %%%%%%%%%%%%%%%%%%%%%%%%%%%%%%%%%%%%%%%%

end     % for while


function [ results ] = calAHU3(z)
%Result Calculate the air condition in the AHU unit
%   This function get the condition of the external air from the matrix Z
%   and calculate the condition of the air after each equipment in the AHU
% working_conds = [m x 1] matix of values

global Air_density v2 pws EnSolHX SenHX Cool_power_evap Conventional_system
Saving;
global   indoor_return   indoor_exhaust_air   return_air   regeneration_inlet
process_inlet   process_outlet   regeneration_outlet   exhaust_air   supply_air
mixed_air supply_air_room Outside_air Cooling_air Reject_heat_air
global Aa Tn An Cf a1 a2 Kd Ta Twi Two Panel_efficiency var10 var4 var6
global sa fa Cond_T hwt rat ra_rh eff_HX tev sat sa_rh eff_noozles Reg_T tc_in
global COP mixed_air_Conventional_system
%matrix of the working conditions
Air_density = 1.204;
Air_specific_heat_capacity = 1.005;
% prompt={'Supply air flow rate (m3/hr)','Amount of fresh air (%)','Temperature
of the condenser/absorber (degree C)','Dry bulb temperature of the return air
(degree C) ','Relative humidity of the return air (%)','Efficiency of the
sensible heat exchanger (%) ','Temperature of the evaporator (degree C)
','Supply air temperature (degree C) ','Supply air relative humidity (%)
```

```
','Efficiency of noozles (%) ','Heat exchanger pitch on solar hot water (degree
C)' };
% def={'3996','100','50','24','50','80','7','13','95','90','10'};
% title='Insert working condition';
% dati1=inputdlg(prompt,title,1,def,'on');
% working_condition=str2double(dati1);
%
%
% sa=working_condition(1);
% fa=working_condition(2);
% Cond_T=working_condition(3);
% hwt=Two;
% rat=working_condition(4);
% ra_rh=working_condition(5);
% eff_HX=working_condition(6);
% tev=working_condition(7);
% sat=working_condition(8);
% sa_rh=working_condition(9);
% eff_noozles=working_condition(10);
% hw_pitch=working_condition(11);

% prompt={'Supply air flow rate (m3/hr)','Amount of fresh air (%)','Temperature
of the condenser/absorber (degree C)','Temperature of the hot water from the
panels (degree C)','Dry bulb temperature of the return air   (degree C)
','Relative humidity of the return air (%)','Efficiency of the sensible heat
exchanger (%) ','Temperature of the evaporator (degree C) ','Supply air
temperature (degree C) ','Supply air relative humidity (%) ','Efficiency of
noozles (%) ','Precooling temperature of the air (degree C)'};
% def={'3996','100','50','80','24','50','80','7','13','95','90','23.5'};
% title='Insert working condition';
% dati1=inputdlg(prompt,title,1,def,'on');
% working_condition=str2double(dati1);
%
%
% sa=working_condition(1);
% fa=working_condition(2);
% Cond_T=working_condition(3);
% hwt=working_condition(4);
% rat=working_condition(5);
% ra_rh=working_condition(6);
% eff_HX=working_condition(7);
% tev=working_condition(8);
% sat=working_condition(9);
% sa_rh=working_condition(10);
% eff_noozles=working_condition(11);
% pre_cool_temp=working_condition(12);
v2=zeros(1,12);
% Condition of the return air
indoor_return = tdb_rh_gen(rat,ra_rh);
% Condition of the exhaust air (from indoor)
indoor_exhaust_air = tdb_rh_gen(rat,ra_rh);
% Condition of the regeneration air before the sensible heat exchanger
return_air          =          tdb_twb_gen(indoor_return(2)-((indoor_return(2)-
indoor_return(3))*eff_noozles/100),indoor_return(3));
% Condition of air after the solar heater, regeneration air for the wheel
regeneration_inlet = tdb_ah_gen((Reg_T),return_air(9));
% Process air conditions (to be dehumidified)
process_inlet=z;
var1=process_inlet(2);%Tpro [∞C]
var9=process_inlet(9);%Xpro [kg/kg]
var3=1;%VelPro [m/s]
% var4=180;%GradiProcesso [∞]

% Regeneration air conditions
var7=regeneration_inlet(2);%Trig [∞C]
var8=regeneration_inlet(9);%Xrig [kg/kg]
var2=1;%VelRig1 [m/s]

% Rotation
```

```
% var6=ENNE;%Velocit‡ rotazione [rev/h]
% var6=10;
var5=360-var4;%DgreeRig1 [∞]

% contatore=0;
% for ENNE=5:1:15
%     contatore=contatore+1;
%     var6=ENNE;

output=RuotaFast_corrada(var1,var2,var3,var4,var5,var6,var7,var8,var9,var10);
%     if contatore==1
%             Risutato_paolo(1)=output(2); %TproOUT;
%             Risutato_paolo(2)=output(1); %XproOUT; questo e' il parametro
%             da ottimizzare
%             Risutato_paolo(3)=output(8); %TrigOUT;
%             Risutato_paolo(4)=output(7); %XrigOUT;
%             giroruota=ENNE;
%     else
%         if output(1)<Risutato_paolo(2)
            Risutato_paolo(1)=output(2); %TproOUT;
            Risutato_paolo(2)=output(1); %XproOUT;
            Risutato_paolo(3)=output(8); %TrigOUT;
            Risutato_paolo(4)=output(7); %XrigOUT;
%             giroruota=ENNE;
%         end
%     end
% end


% Condition of the process outlet
process_outlet = tdb_ah_gen(output(2),output(1));
% Condition of the Regeneration Outlet
regeneration_outlet = tdb_ah_gen(output(8),output(7));
% Condition of the exhaust air
exhaust_air           =           tdb_ah_gen(return_air(2)+(process_outlet(2)-
return_air(2))*eff_HX/100,return_air(9));

% Condition of the supply air
supply_air          =          tdb_ah_gen(process_outlet(2)-(process_outlet(2)-
return_air(2))*eff_HX/100,process_outlet(9));
% Condition of mixed air
mixed_air             =             tdb_ah_gen((sa*fa/100*supply_air(2)+sa*(1-
fa/100)*indoor_return(2))/(sa*fa/100+sa*(1-
fa/100)),(sa*fa/100*supply_air(9)+sa*(1-
fa/100)*indoor_return(9))/(sa*fa/100+sa*(1-fa/100)));
% Condition of the supply air to the room
supply_air_room = tdb_rh_gen(sat,sa_rh);
% Outside air condition
Outside_air=z;
% Cooling air
Cooling_air           =           tdb_twb_gen(Outside_air(2)-((Outside_air(2)-
Outside_air(3))*eff_noozles/100),Outside_air(3));
% Calculating the COP of the chiller using the outside air sprayed
%COP = COP_calculator(Cooling_air(2),hwt);
%tc_in=(z(2)-(z(2)-z(3))*.65);
COP = Single_Stage_COP_calculator(Two,tc_in,tev);
% EnSolHX2= working_condition(1)*Air_density/3600*(f2(10)-A2(10));
EnSolHX = sa*fa/100*Air_density/3600*(regeneration_inlet(10)-exhaust_air(10));
% SenHX2 = working_condition(1)*Air_density/3600*(j2(10)-g2(10));
SenHX = sa*fa/100*Air_density/3600*(process_outlet(10)-supply_air(10));
% Cool_power_evap = working_condition(1)*Air_density/3600*(k2(10)-s2(10));
Cool_power_evap = sa*Air_density/3600*(mixed_air(10)-supply_air_room(10));
% Condition of air after the condenser/absorber
Reject_heat_air                                                              =
tdb_ah_gen((Cooling_air(2)+(Cool_power_evap/0.7)/(sa*Air_density/3600*Air_speci
fic_heat_capacity+sa*Air_density/3600*Cooling_air(9))),Cooling_air(9));
% Conventional_system = working_condition(1)*Air_density/3600*(z(10)-s2(10));
```

```
mixed_air_Conventional_system        =        tdb_ah_gen((sa*fa/100*z(2)+sa*(1-
fa/100)*indoor_return(2))/(sa*fa/100+sa*(1-fa/100)),(sa*fa/100*z(9)+sa*(1-
fa/100)*indoor_return(9))/(sa*fa/100+sa*(1-fa/100)));
Conventional_system  =  sa*Air_density/3600*(mixed_air_Conventional_system(10)-
supply_air_room(10));
% Saving compared to a conventional system
Saving                          =                      ((Conventional_system/COP)-
((Cool_power_evap)/COP+EnSolHX))/(Conventional_system/COP)*100;
clc
textcont='';
    disp('Condition of the return air from indoor:');
    fprintf('\n')
    for i=1:12
    [cont,unit]=psydescription(i);
       fprintf('%s =  %10.5f  %s \n', cont, indoor_return(i), unit);
    end
textcont='';
fprintf('\n')
disp('Condition of the exhaust air (from indoor):');
    fprintf('\n')
    for i=1:12
    [cont,unit]=psydescription(i);
       fprintf('%s =  %10.5f  %s \n', cont, indoor_exhaust_air(i), unit);
    end
fprintf('\n')
textcont='';
fprintf('\n')
disp('Condition of the return air ');
    fprintf('\n')
    for i=1:12
    [cont,unit]=psydescription(i);
       fprintf('%s =  %10.5f  %s \n', cont, return_air(i), unit);
    end
fprintf('\n')
textcont='';
fprintf('\n')
disp('Condition of the exhaust air from indoor');
    fprintf('\n')
    for i=1:12
    [cont,unit]=psydescription(i);
       fprintf('%s =  %10.5f  %s \n', cont, exhaust_air(i), unit);
    end

textcont='';
fprintf('\n')
disp('Condition of the exhaust air after the sensible heat exchanger:');
    fprintf('\n')
    for i=1:11
    [cont,unit]=psydescription(i);
       fprintf('%s =  %10.5f  %s \n', cont, exhaust_air(i), unit);
    end

textcont='';
fprintf('\n')
disp('Condition  of  the  air  after  the  solar  heater,  regeneration  of  the
wheel:');
    fprintf('\n')
    for i=1:12
    [cont,unit]=psydescription(i);
       fprintf('%s =  %10.5f  %s \n', cont, regeneration_inlet(i), unit);
    end
%Condition of the Regeneration Outlet
textcont='';
fprintf('\n')
disp('Condition of the Regeneration outlet:');
    fprintf('\n')
    for i=1:12
    [cont,unit]=psydescription(i);
       fprintf('%s =  %10.5f  %s \n', cont, regeneration_outlet(i), unit);
```

```
    end

 %Condition of the process air
fprintf('\n')
textcont='';
    disp('Condition of the process air inlet:');
    fprintf('\n')
    for i=1:12
    [cont,unit]=psydescription(i);
       fprintf('%s =  %10.5f  %s \n', cont, process_inlet(i), unit);
    end
fprintf('\n')
textcont='';
fprintf('\n')
disp('Condition of the process outlet air before the sensible heat exchanger');
    fprintf('\n')
    for i=1:12
    [cont,unit]=psydescription(i);
       fprintf('%s =  %10.5f  %s \n', cont, process_outlet(i), unit);
    end
fprintf('\n')
textcont='';
fprintf('\n')
disp('Condition of the supply air:');
    fprintf('\n')
    for i=1:12
    [cont,unit]=psydescription(i);
       fprintf('%s =  %10.5f  %s \n', cont, supply_air(i), unit);
    end

 textcont='';
fprintf('\n')
disp('Condition of the mixed air:');
    fprintf('\n')
    for i=1:11
    [cont,unit]=psydescription(i);
       fprintf('%s =  %10.5f  %s \n', cont, mixed_air(i), unit);
    end
fprintf('\n')
textcont='';
fprintf('\n')
disp('Condition of the supply air to the room:');
    fprintf('\n')
    for i=1:12
    [cont,unit]=psydescription(i);
       fprintf('%s =  %10.5f  %s \n', cont, supply_air_room(i), unit);
    end

 fprintf('\n')
textcont='';
fprintf('\n')
disp('Condition of the outside air for cooling');
    fprintf('\n')
    for i=1:12
    [cont,unit]=psydescription(i);
       fprintf('%s =  %10.5f  %s \n', cont, z(i), unit);
    end
fprintf('\n')
textcont='';
fprintf('\n')
disp('Condition of the cooling air');
    fprintf('\n')
    for i=1:12
    [cont,unit]=psydescription(i);
       fprintf('%s =  %10.5f  %s \n', cont, Cooling_air(i), unit);
    end
%  fprintf('\n')
% textcont='';
% fprintf('\n')
```

```
% disp('Condition of air after the condenser/absorber');
%     fprintf('\n')
%   for i=1:12
%       [cont,unit]=psydescription(i);
%      fprintf('%s =  %10.5f  %s \n', cont, Reject_heat_air(i), unit);
%     end
end
% This script is used to insert all the input required by the system
% simulator

%clear all

global Aa Tn An Cf a1 a2 Kd Ta Twi Two Latitude var10 RH_ambient tdb
global sa fa Cond_T hwt rat ra_rh eff_HX tev sat sa_rh eff_noozles Reg_T var4
var6
prompt={'Absorber area [m2]','Number of tubes per absorber:','Number of
absorber:','Conversion Factor (CF) number:','Coefficient a1 value:
','Coefficient a2 value: ','Average Kd (IAM) value: ','Ambient Air Temp (∞C):
','Relative Humidity: (%)','Inlet Water Temp. (∞C): ','Outlet Water Temp. (∞C):
','Latitude () (-ve in Southern Hemisphere)','Desiccant Type','Degree
process','Rev/h'};
def={'3.02','30','8','0.832','1.14','0.0144','1','32','60','75','80','-
27.46794','1','180','10'};
title='Insert Solar panel data';
dati1=inputdlg(prompt,title,1,def,'on');
Solar_panel=str2double(dati1);
% debug = sprintf('(Ta,tdb) = ( %d , %d ) and value of thingy %d', Ta, tdb);
% disp(debug);
Aa=Solar_panel(1);
Tn=Solar_panel(2);
An=Solar_panel(3);
Cf=Solar_panel(4);
a1=Solar_panel(5);
a2=Solar_panel(6);
Kd=Solar_panel(7);
Ta=Solar_panel(8);
RH_ambient=Solar_panel(9);
Twi=Solar_panel(10);
Two= Solar_panel(11);
Latitude= Solar_panel(12);
var10=Solar_panel(13);
var4=Solar_panel(14);
var6=Solar_panel(15);

prompt={'Supply air flow rate (m3/hr)','Amount of fresh air (%)','Temperature
of regeneration (degree C)','Dry bulb temperature of the return air (degree C)
','Relative humidity of the return air (%)','Efficiency of the sensible heat
exchanger (%) ','Temperature of the evaporator (degree C) ','Supply air
temperature (degree C) ','Supply air relative humidity (%) ','Efficiency of
noozles (%) ','Cooling water temperature (degree C)'};
def={'3996','100','65','24','50','80','7','13','95','90','30'};
title='Insert working condition';
dati1=inputdlg(prompt,title,1,def,'on');
working_condition=str2double(dati1);
sa=working_condition(1);
fa=working_condition(2);
Reg_T=working_condition(3);
hwt=Two;
rat=working_condition(4);
ra_rh=working_condition(5);
eff_HX=working_condition(6);
tev=working_condition(7); %chilled water
sat=working_condition(8);
sa_rh=working_condition(9);
eff_noozles=working_condition(10);
tc_in=working_condition(11);
tdb=Ta;
```

Appendix I Ambient air condition values used in the simulation for the case study

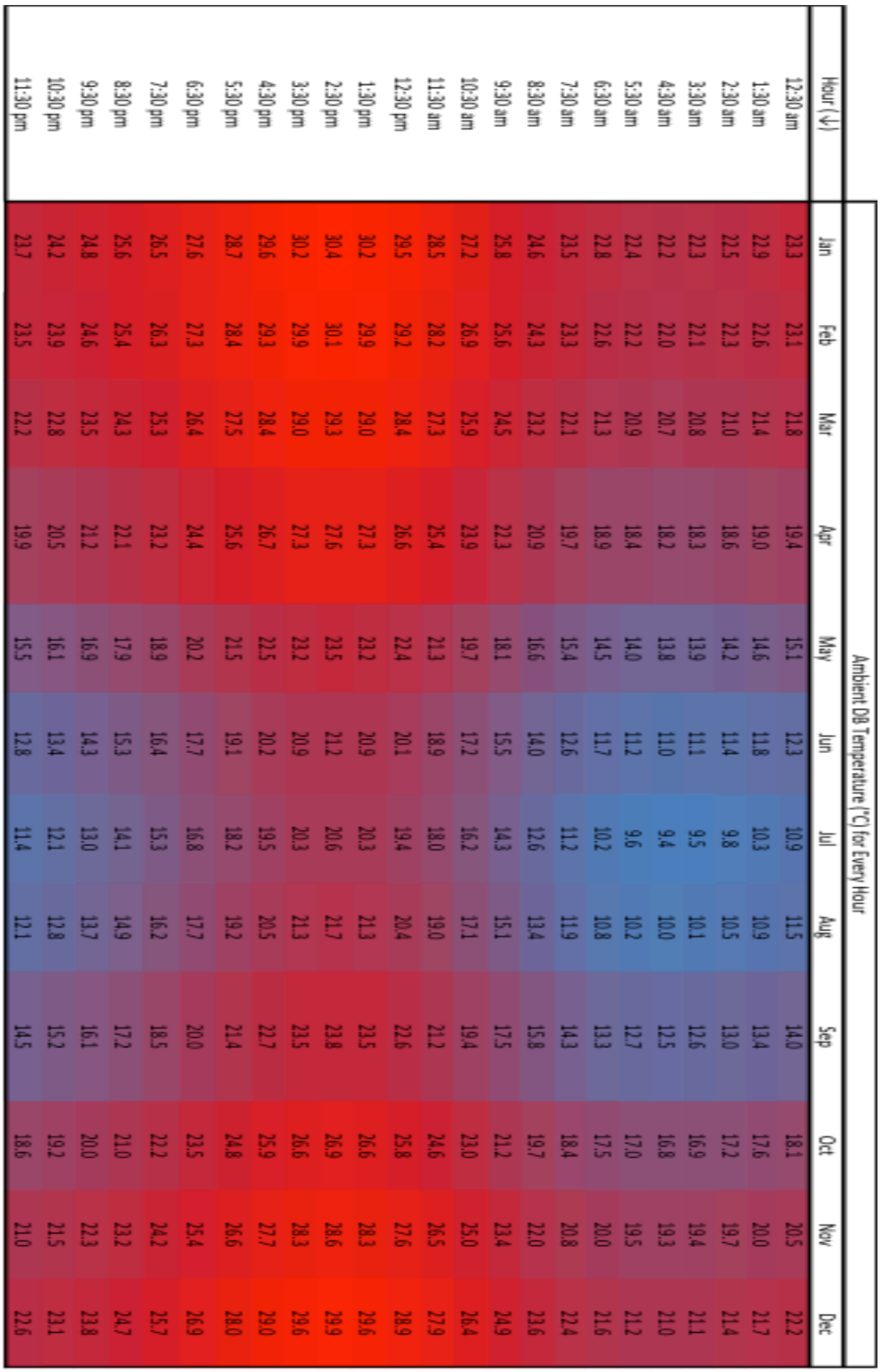

Ambient DB Temperature (°C) for Every Hour

Hour (↓)	Jan	Feb	Mar	Apr	May	Jun	Jul	Aug	Sep	Oct	Nov	Dec
12:30 am	23.3	23.1	21.8	19.4	15.1	12.3	10.9	11.5	14.0	18.1	20.5	22.2
1:30 am	22.9	22.6	21.4	19.0	14.6	11.8	10.3	10.9	13.4	17.6	20.0	21.7
2:30 am	22.5	22.3	21.0	18.6	14.2	11.4	9.8	10.5	13.0	17.2	19.7	21.4
3:30 am	22.3	22.1	20.8	18.3	13.9	11.1	9.5	10.1	12.6	16.9	19.4	21.1
4:30 am	22.2	22.0	20.7	18.2	13.8	11.0	9.4	10.0	12.5	16.8	19.3	21.0
5:30 am	22.4	22.2	20.9	18.4	14.0	11.2	9.6	10.2	12.7	17.0	19.5	21.2
6:30 am	22.8	22.6	21.3	18.9	14.5	11.7	10.2	10.8	13.3	17.5	20.0	21.6
7:30 am	23.5	23.3	22.1	19.7	15.4	12.6	11.2	11.9	14.3	18.4	20.8	22.4
8:30 am	24.6	24.3	23.2	20.9	16.6	14.0	12.6	13.4	15.8	19.7	22.0	23.6
9:30 am	25.8	25.6	24.5	22.3	18.1	15.5	14.3	15.1	17.5	21.2	23.4	24.9
10:30 am	27.2	26.9	25.9	23.9	19.7	17.2	16.2	17.1	19.4	23.0	25.0	26.4
11:30 am	28.5	28.2	27.3	25.4	21.3	18.9	18.0	19.0	21.2	24.6	26.5	27.9
12:30 pm	29.5	29.2	28.4	26.6	22.4	20.1	19.4	20.4	22.6	25.8	27.6	28.9
1:30 pm	30.2	29.9	29.0	27.3	23.2	20.9	20.3	21.3	23.5	26.6	28.3	29.6
2:30 pm	30.4	30.1	29.3	27.6	23.5	21.2	20.6	21.7	23.8	26.9	28.6	29.9
3:30 pm	30.2	29.9	29.0	27.3	23.2	20.9	20.3	21.3	23.5	26.6	28.3	29.6
4:30 pm	29.6	29.3	28.4	26.7	22.5	20.2	19.5	20.5	22.7	25.9	27.7	29.0
5:30 pm	28.7	28.4	27.5	25.6	21.5	19.1	18.2	19.2	21.4	24.8	26.6	28.0
6:30 pm	27.6	27.3	26.4	24.4	20.2	17.7	16.8	17.7	20.0	23.5	25.4	26.9
7:30 pm	26.5	26.3	25.3	23.2	18.9	16.4	15.3	16.2	18.5	22.2	24.2	25.7
8:30 pm	25.6	25.4	24.3	22.1	17.9	15.3	14.1	14.9	17.2	21.0	23.2	24.7
9:30 pm	24.8	24.6	23.5	21.2	16.9	14.3	13.0	13.7	16.1	20.0	22.3	23.8
10:30 pm	24.2	23.9	22.8	20.5	16.1	13.4	12.1	12.8	15.2	19.2	21.5	23.1
11:30 pm	23.7	23.5	22.2	19.9	15.5	12.8	11.4	12.1	14.5	18.6	21.0	22.6

Figure 75 Representative hourly average dry bulb temperature by hour for each month of the year in Brisbane

Ambient WB Temperature (°C) for Every Hour												
Jan	Feb	Mar	Apr	May	Jun	Jul	Aug	Sep	Oct	Nov	Dec
22.1	22.1	20.9	18.6	14.2	11.2	9.8	10.1	12.5	17.0	19.5	21.3
22.0	21.9	20.8	18.4	14.0	11.0	9.5	9.8	12.3	16.8	19.4	21.1
21.8	21.8	20.6	18.2	13.9	10.8	9.3	9.6	12.1	16.6	19.2	21.0
21.8	21.7	20.6	18.1	13.8	10.7	9.2	9.5	12.0	16.5	19.1	20.9
21.7	21.7	20.5	18.1	13.7	10.6	9.1	9.4	11.9	16.5	19.1	20.8
21.8	21.7	20.6	18.2	13.8	10.7	9.2	9.5	12.0	16.5	19.2	20.9
22.0	21.9	20.8	18.4	14.0	11.0	9.5	9.8	12.2	16.7	19.4	21.1
22.2	22.1	21.1	18.7	14.3	11.3	9.9	10.3	12.7	17.1	19.7	21.3
22.6	22.5	21.5	19.2	14.8	11.9	10.6	10.9	13.2	17.7	20.1	21.8
23.0	23.0	21.9	19.7	15.3	12.5	11.3	11.7	13.9	18.3	20.7	22.3
23.5	23.4	22.5	20.3	15.9	13.2	12.1	12.5	14.7	19.0	21.3	22.8
24.0	23.9	23.0	20.9	16.5	13.9	12.8	13.2	15.3	19.6	21.8	23.4
24.4	24.2	23.4	21.4	16.9	14.3	13.4	13.8	15.8	20.1	22.3	23.7
24.6	24.5	23.6	21.6	17.2	14.7	13.7	14.2	16.2	20.5	22.5	24.0
24.7	24.6	23.7	21.8	17.3	14.8	13.9	14.3	16.3	20.6	22.6	24.1
24.6	24.5	23.6	21.6	17.2	14.7	13.7	14.2	16.2	20.5	22.5	24.0
24.4	24.3	23.4	21.4	16.9	14.4	13.4	13.8	15.9	20.2	22.3	23.8
24.1	24.0	23.0	21.0	16.6	14.0	12.9	13.3	15.4	19.7	21.9	23.4
23.7	23.6	22.6	20.5	16.1	13.4	12.3	12.7	14.9	19.2	21.4	23.0
23.3	23.2	22.2	20.1	15.7	12.9	11.7	12.1	14.3	18.7	21.0	22.6
23.0	22.9	21.9	19.6	15.3	12.5	11.2	11.6	13.8	18.2	20.6	22.2
22.7	22.6	21.6	19.3	14.9	12.0	10.7	11.1	13.4	17.8	20.2	21.9
22.5	22.3	21.3	19.0	14.6	11.7	10.3	10.7	13.0	17.4	19.9	21.6
22.3	22.2	21.1	18.8	14.4	11.4	10.0	10.4	12.8	17.2	19.7	21.4

Figure 76 Representative hourly average wet bulb temperature by hour for each month of the year in Brisbane

Humidity Ratio for Every Hour

Jan	Feb	Mar	Apr	May	Jun	Jul	Aug	Sep	Oct	Nov	Dec
16.34	16.42	15.24	13.16	9.77	7.85	7.11	7.14	8.44	11.72	13.87	15.64
16.36	16.34	15.27	13.07	9.76	7.87	7.08	7.11	8.49	11.69	13.95	15.57
16.23	16.32	15.16	12.99	9.82	7.84	7.10	7.09	8.45	11.62	13.81	15.55
16.32	16.26	15.24	12.99	9.84	7.87	7.13	7.16	8.52	11.62	13.81	15.54
15.96	16.30	15.15	13.03	9.77	7.81	7.08	7.11	8.46	11.66	13.85	15.44
16.28	16.22	15.20	13.07	9.80	7.83	7.09	7.12	8.48	11.58	13.90	15.49
16.40	16.34	15.31	13.12	9.80	7.91	7.12	7.15	8.43	11.61	13.95	15.61
16.40	16.34	15.40	13.16	9.75	7.83	7.07	7.16	8.52	11.71	14.02	15.56
16.53	16.51	15.50	13.31	9.80	7.84	7.16	7.11	8.42	11.90	14.05	15.77
16.63	16.72	15.54	13.39	9.74	7.83	7.13	7.19	8.46	12.03	14.29	15.96
16.81	16.78	15.83	13.53	9.76	7.84	7.14	7.17	8.54	12.17	14.46	16.08
17.05	17.02	16.00	13.73	9.79	7.88	7.10	7.10	8.46	12.29	14.55	16.36
17.27	17.08	16.15	13.93	9.81	7.81	7.15	7.16	8.45	12.46	14.82	16.41
17.30	17.26	16.21	13.93	9.84	7.92	7.09	7.21	8.54	12.67	14.83	16.59
17.38	17.34	16.24	14.09	9.84	7.91	7.18	7.16	8.53	12.69	14.85	16.62
17.30	17.26	16.21	13.93	9.84	7.92	7.09	7.21	8.54	12.67	14.83	16.59
17.23	17.19	16.15	13.89	9.77	7.88	7.11	7.12	8.52	12.56	14.78	16.52
17.13	17.09	15.92	13.79	9.83	7.90	7.12	7.13	8.49	12.34	14.65	16.32
16.96	16.93	15.77	13.59	9.78	7.85	7.09	7.12	8.51	12.22	14.44	16.17
16.80	16.73	15.64	13.55	9.86	7.86	7.11	7.14	8.47	12.12	14.37	16.07
16.72	16.65	15.62	13.34	9.82	7.91	7.11	7.17	8.47	11.99	14.23	15.89
16.60	15.53	15.52	13.32	9.79	7.82	7.09	7.18	8.51	11.90	14.06	15.83
16.55	16.38	15.39	13.22	9.79	7.89	7.08	7.17	8.46	11.74	13.99	15.69
16.46	16.40	15.35	13.21	9.82	7.84	7.08	7.17	8.54	11.75	13.93	15.61

Figure 77 Representative hourly average humidity ratio by hour for each month of the year in Brisbane (g_{water}/kg_{air})

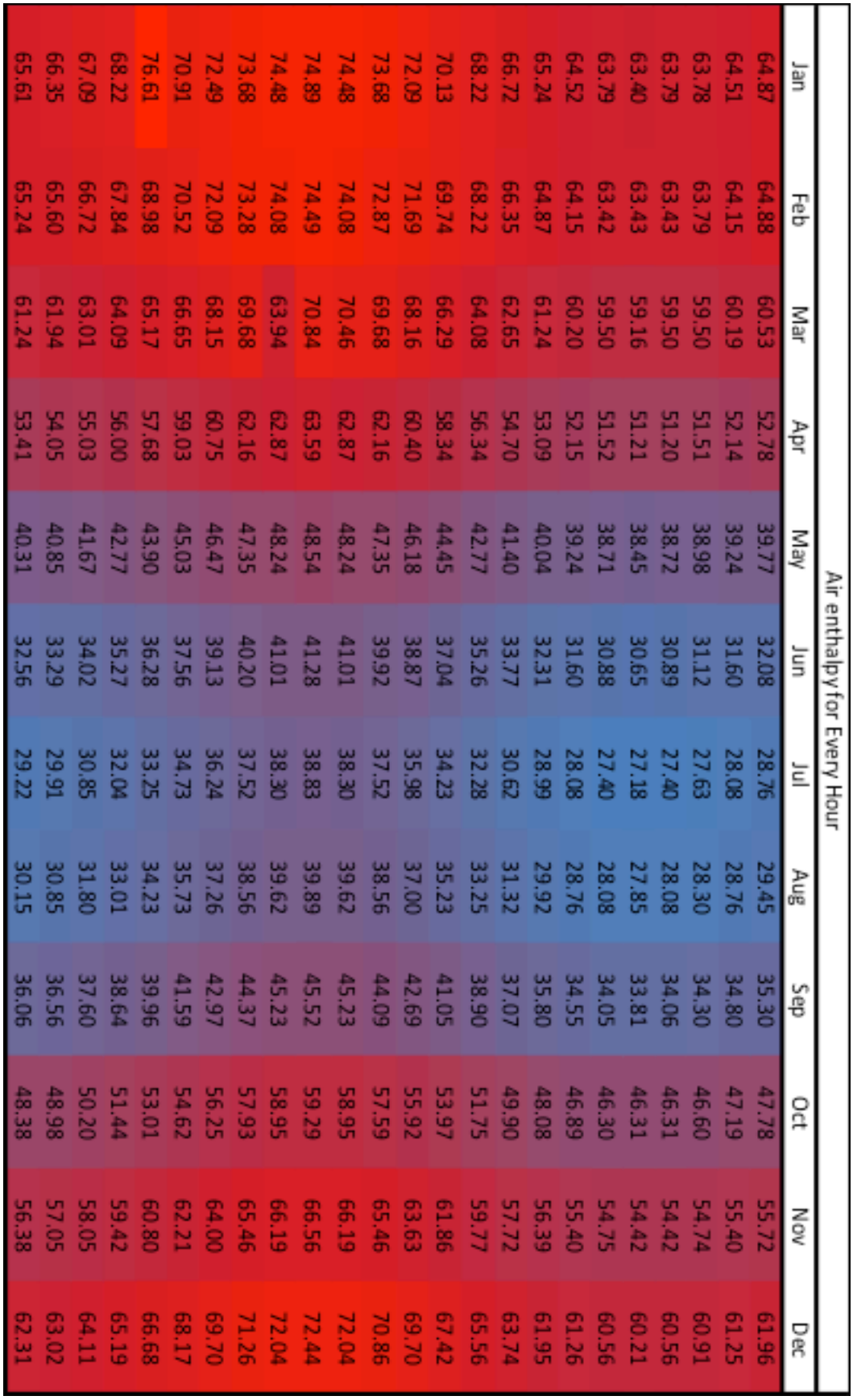

Air enthalpy for Every Hour											
Jan	Feb	Mar	Apr	May	Jun	Jul	Aug	Sep	Oct	Nov	Dec
64.87	64.88	60.53	52.78	39.77	32.08	28.76	29.45	35.30	47.78	55.72	61.96
64.51	64.15	60.19	52.14	39.24	31.60	28.08	28.76	34.80	47.19	55.40	61.25
63.78	63.79	59.50	51.51	38.98	31.12	27.63	28.30	34.30	46.60	54.74	60.91
63.79	63.43	59.50	51.20	38.72	30.89	27.40	28.08	34.06	46.31	54.42	60.56
63.40	63.43	59.16	51.21	38.45	30.65	27.18	27.85	33.81	46.31	54.42	60.21
63.79	63.42	59.50	51.52	38.71	30.88	27.40	28.08	34.05	46.30	54.75	60.56
64.52	64.15	60.20	52.15	39.24	31.60	28.08	28.76	34.55	46.89	55.40	61.26
65.24	64.87	61.24	53.09	40.04	32.31	28.99	29.92	35.80	48.08	56.39	61.95
66.72	66.35	62.65	54.70	41.40	33.77	30.62	31.32	37.07	49.90	57.72	63.74
68.22	68.22	64.08	56.34	42.77	35.26	32.28	33.25	38.90	51.75	59.77	65.56
70.13	69.74	66.29	58.34	44.45	37.04	34.23	35.23	41.05	53.97	61.86	67.42
72.09	71.69	68.16	60.40	46.18	38.87	35.98	37.00	42.69	55.92	63.63	69.70
73.68	72.87	69.68	62.16	47.35	39.92	37.52	38.56	44.09	57.59	65.46	70.86
74.48	74.08	70.46	62.87	48.24	41.01	38.30	39.62	45.23	58.95	66.19	72.04
74.89	74.49	70.84	63.59	48.54	41.28	38.83	39.89	45.52	59.29	66.56	72.44
74.48	74.08	63.94	62.87	48.24	41.01	38.30	39.62	45.23	58.95	66.19	72.04
73.68	73.28	69.68	62.16	47.35	40.20	37.52	38.56	44.37	57.93	65.46	71.26
72.49	72.09	68.15	60.75	46.47	39.13	36.24	37.26	42.97	56.25	64.00	69.70
70.91	70.52	66.65	59.03	45.03	37.56	34.73	35.73	41.59	54.62	62.21	68.17
76.61	68.98	65.17	57.68	43.90	36.28	33.25	34.23	39.96	53.01	60.80	66.68
68.22	67.84	64.09	56.00	42.77	35.27	32.04	33.01	38.64	51.44	59.42	65.19
67.09	66.72	63.01	55.03	41.67	34.02	30.85	31.80	37.60	50.20	58.05	64.11
66.35	65.60	61.94	54.05	40.85	33.29	29.91	30.85	36.56	48.98	57.05	63.02
65.61	65.24	61.24	53.41	40.31	32.56	29.22	30.15	36.06	48.38	56.38	62.31

Figure 78 Representative hourly average air enthalpy by hour for each month of the year in Brisbane

Appendix J Cooling load values used in the simulation for the case study

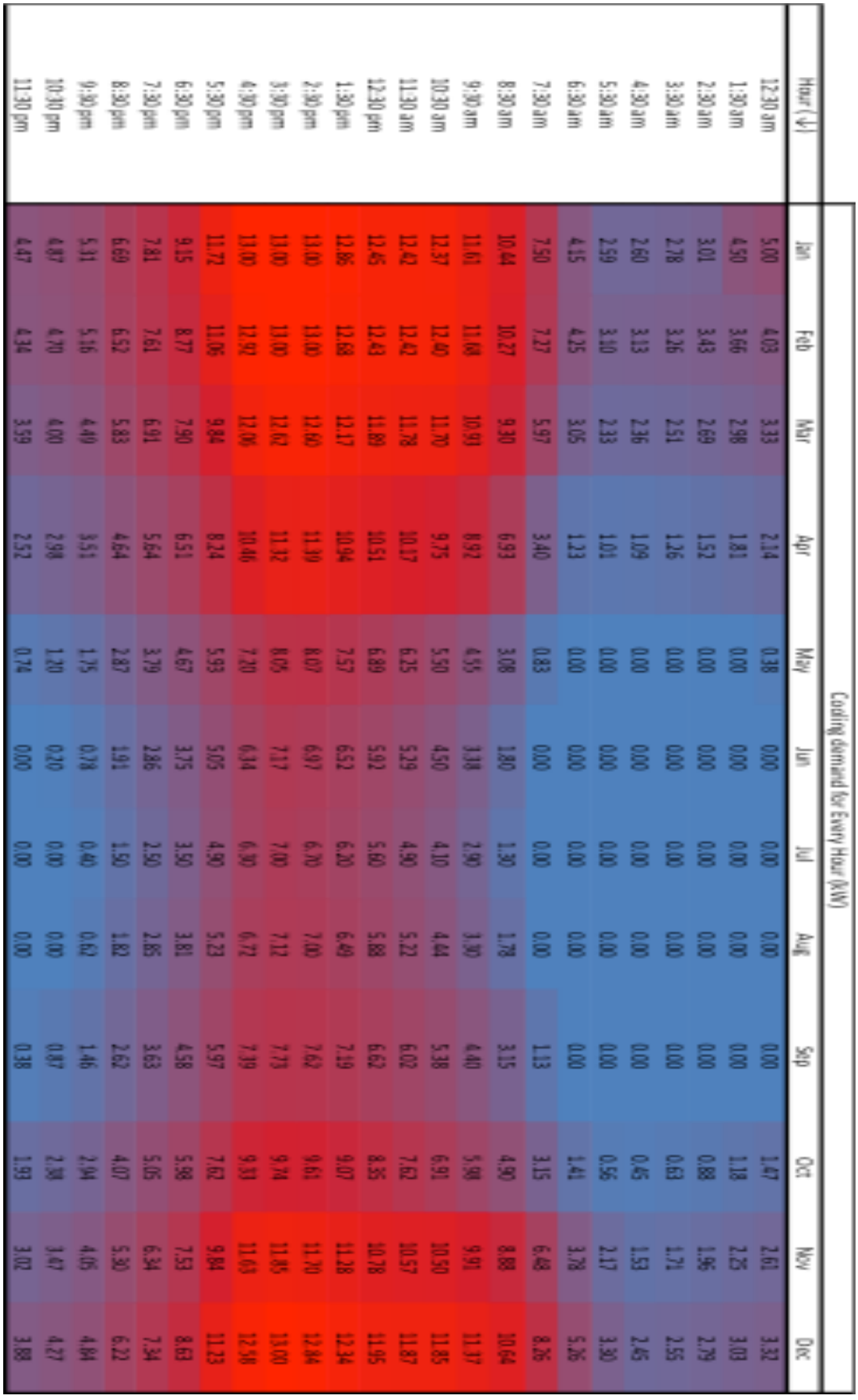

Hour (hr)	Cooling demand for Every Hour (kW)											
	Jan	Feb	Mar	Apr	May	Jun	Jul	Aug	Sep	Oct	Nov	Dec
12:30 am	5.00	4.03	3.33	2.14	0.38	0.00	0.00	0.00	0.00	1.47	2.61	3.32
1:30 am	4.50	3.66	2.98	1.81	0.00	0.00	0.00	0.00	0.00	1.18	2.25	3.03
2:30 am	3.01	3.43	2.69	1.52	0.00	0.00	0.00	0.00	0.00	0.88	1.96	2.79
3:30 am	2.78	3.26	2.51	1.26	0.00	0.00	0.00	0.00	0.00	0.63	1.71	2.55
4:30 am	2.60	3.13	2.36	1.09	0.00	0.00	0.00	0.00	0.00	0.45	1.53	2.45
5:30 am	2.59	3.10	2.33	1.01	0.00	0.00	0.00	0.00	0.00	0.56	2.17	3.30
6:30 am	4.15	4.25	3.05	1.23	0.00	0.00	0.00	0.00	0.00	1.41	3.78	5.26
7:30 am	7.50	7.27	5.97	3.40	0.83	0.00	0.00	0.00	1.13	3.15	6.48	8.26
8:30 am	10.44	10.27	9.30	6.93	3.08	1.80	1.30	1.78	3.15	4.90	8.88	10.64
9:30 am	11.61	11.68	10.93	8.92	4.55	3.38	2.90	3.30	4.40	5.98	9.91	11.37
10:30 am	12.37	12.40	11.70	9.75	5.50	4.50	4.10	4.44	5.38	6.91	10.50	11.85
11:30 am	12.42	12.42	11.78	10.17	6.25	5.29	4.90	5.22	6.02	7.62	10.57	11.87
12:30 pm	12.45	12.43	11.89	10.51	6.89	5.92	5.60	5.88	6.62	8.35	10.78	11.95
1:30 pm	12.86	12.68	12.17	10.94	7.57	6.52	6.20	6.49	7.19	9.07	11.28	12.34
2:30 pm	13.00	13.00	12.60	11.39	8.07	6.97	6.70	7.00	7.62	9.61	11.70	12.84
3:30 pm	13.00	13.00	12.62	11.92	8.05	7.17	7.00	7.12	7.73	9.74	11.85	13.00
4:30 pm	13.00	12.92	12.06	10.46	7.20	6.34	6.30	6.72	7.39	9.33	11.63	12.56
5:30 pm	11.72	11.06	9.84	8.24	5.93	5.05	4.90	5.23	5.97	7.62	9.84	11.23
6:30 pm	9.15	8.77	7.90	6.51	4.67	3.75	3.50	3.81	4.58	5.98	7.53	8.63
7:30 pm	7.81	7.61	6.91	5.64	3.79	2.86	2.50	2.85	3.63	5.05	6.34	7.34
8:30 pm	6.69	6.52	5.83	4.64	2.87	1.91	1.50	1.82	2.62	4.07	5.30	6.22
9:30 pm	5.31	5.16	4.49	3.51	1.75	0.78	0.40	0.62	1.46	2.94	4.05	4.84
10:30 pm	4.87	4.70	4.00	2.98	1.20	0.20	0.00	0.00	0.87	2.38	3.47	4.27
11:30 pm	4.47	4.34	3.59	2.52	0.74	0.00	0.00	0.00	0.38	1.93	3.02	3.88

Figure 79 Cooling load demand hourly variation

Chiller Thermal COP for Every Hour												
Jan	Feb	Mar	Apr	May	Jun	Jul	Aug	Sep	Oct	Nov	Dec	
0.3464	0.3468	0.3491	0.3528	0.3575	0.3593	0.3598	0.3596	0.3584	0.3545	0.3512	0.3484	
0.3472	0.3477	0.3498	0.3533	0.3579	0.3595	0.3600	0.3598	0.3587	0.3551	0.3519	0.3493	
0.3479	0.3482	0.3504	0.3539	0.3582	0.3597	0.3600	0.3599	0.3590	0.3555	0.3524	0.3498	
0.3482	0.3486	0.3507	0.3542	0.3584	0.3598	0.3601	0.3600	0.3592	0.3558	0.3528	0.3503	
0.3484	0.3488	0.3509	0.3544	0.3585	0.3598	0.3601	0.3600	0.3592	0.3559	0.3529	0.3504	
0.3481	0.3484	0.3506	0.3541	0.3584	0.3597	0.3601	0.3600	0.3591	0.3557	0.3527	0.3501	
0.3474	0.3477	0.3499	0.3535	0.3580	0.3596	0.3600	0.3599	0.3588	0.3552	0.3519	0.3494	
0.3460	0.3464	0.3486	0.3524	0.3573	0.3592	0.3597	0.3595	0.3581	0.3541	0.3507	0.3481	
0.3439	0.3445	0.3466	0.3506	0.3562	0.3584	0.3592	0.3587	0.3569	0.3524	0.3488	0.3459	
0.3413	0.3417	0.3441	0.3482	0.3545	0.3572	0.3581	0.3575	0.3552	0.3501	0.3462	0.3432	
0.3381	0.3388	0.3411	0.3453	0.3524	0.3555	0.3566	0.3556	0.3528	0.3470	0.3430	0.3399	
0.3348	0.3356	0.3378	0.3422	0.3499	0.3535	0.3546	0.3533	0.3501	0.3439	0.3397	0.3364	
0.3322	0.3330	0.3351	0.3395	0.3481	0.3518	0.3528	0.3514	0.3477	0.3413	0.3371	0.3338	
0.3303	0.3311	0.3335	0.3378	0.3466	0.3506	0.3515	0.3499	0.3460	0.3395	0.3354	0.3319	
0.3297	0.3306	0.3327	0.3371	0.3460	0.3501	0.3511	0.3493	0.3455	0.3388	0.3346	0.3311	
0.3303	0.3311	0.3335	0.3378	0.3466	0.3506	0.3515	0.3499	0.3460	0.3395	0.3354	0.3319	
0.3319	0.3327	0.3351	0.3393	0.3479	0.3517	0.3527	0.3512	0.3475	0.3411	0.3369	0.3335	
0.3343	0.3351	0.3373	0.3417	0.3496	0.3532	0.3544	0.3531	0.3498	0.3434	0.3395	0.3361	
0.3371	0.3378	0.3399	0.3443	0.3517	0.3550	0.3559	0.3550	0.3519	0.3460	0.3422	0.3388	
0.3397	0.3402	0.3424	0.3466	0.3535	0.3564	0.3574	0.3566	0.3540	0.3484	0.3447	0.3415	
0.3417	0.3422	0.3445	0.3486	0.3547	0.3574	0.3583	0.3577	0.3555	0.3504	0.3466	0.3437	
0.3434	0.3439	0.3460	0.3501	0.3558	0.3581	0.3590	0.3586	0.3566	0.3519	0.3482	0.3455	
0.3447	0.3453	0.3474	0.3512	0.3566	0.3587	0.3594	0.3591	0.3574	0.3531	0.3496	0.3468	
0.3457	0.3460	0.3484	0.3521	0.3572	0.3591	0.3597	0.3594	0.3580	0.3539	0.3504	0.3477	

Figure 80 Chiller COP hourly variation

Hour (↓)	Instantaneous Efficiency (%) for Every Hour																							
12:30 am	0.00%	0.00%	0.00%	0.00%	0.00%	0.00%	0.00%	0.00%	0.00%	0.00%	0.00%	0.00%	0.00%	0.00%	0.00%	0.00%	0.00%	0.00%	0.00%	0.00%	0.00%	0.00%	0.00%	0.00%
1:30 am	0.00%	0.00%	0.00%	0.00%	0.00%	0.00%	0.00%	0.00%	0.00%	0.00%	0.00%	0.00%	0.00%	0.00%	0.00%	0.00%	0.00%	0.00%	0.00%	0.00%	0.00%	0.00%	0.00%	0.00%
2:30 am	0.00%	0.00%	0.00%	0.00%	0.00%	0.00%	0.00%	0.00%	0.00%	0.00%	0.00%	0.00%	0.00%	0.00%	0.00%	0.00%	0.00%	0.00%	0.00%	0.00%	0.00%	0.00%	0.00%	0.00%
3:30 am	0.00%	0.00%	0.00%	0.00%	0.00%	0.00%	0.00%	0.00%	0.00%	0.00%	0.00%	0.00%	0.00%	0.00%	0.00%	0.00%	0.00%	0.00%	0.00%	0.00%	0.00%	0.00%	0.00%	0.00%
4:30 am	0.00%	0.00%	0.00%	0.00%	0.00%	0.00%	0.00%	0.00%	0.00%	0.00%	0.00%	0.00%	0.00%	0.00%	0.00%	0.00%	0.00%	0.00%	0.00%	0.00%	0.00%	0.00%	0.00%	0.00%
5:30 am	0.00%	0.00%	0.00%	0.00%	0.00%	0.00%	0.00%	0.00%	0.00%	0.00%	0.00%	0.00%	0.00%	0.00%	0.00%	0.00%	0.00%	0.00%	0.00%	0.00%	0.00%	0.00%	0.00%	0.00%
6:30 am	28.07%	11.77%	0.00%	0.00%	0.00%	0.00%	0.00%	0.00%	0.00%	0.00%	0.00%	0.00%	0.00%	0.00%	0.00%	0.00%	0.00%	0.00%	0.00%	0.00%	0.00%	0.00%	0.00%	0.00%
7:30 am	55.68%	52.22%	42.83%	25.95%	0.00%	0.00%	0.00%	0.00%	0.00%	0.00%	0.00%	0.00%	0.00%	0.00%	0.00%	0.00%	32.42%	45.62%	54.81%	55.49%	0.00%	0.00%	0.00%	0.00%
8:30 am	65.58%	64.31%	60.62%	55.33%	42.38%	33.23%	35.56%	45.35%	56.25%	60.97%	65.27%	65.26%	0.00%	0.00%	0.00%	0.00%	0.00%	0.00%	0.00%	0.00%	0.00%	0.00%	0.00%	0.00%
9:30 am	70.22%	69.68%	67.65%	65.07%	58.25%	53.76%	54.74%	59.25%	65.12%	67.52%	70.13%	69.93%	0.00%	0.00%	0.00%	0.00%	0.00%	0.00%	0.00%	0.00%	0.00%	0.00%	0.00%	0.00%
10:30 am	72.66%	72.35%	70.99%	69.40%	64.67%	61.72%	62.36%	65.26%	69.26%	70.82%	72.67%	72.41%	0.00%	0.00%	0.00%	0.00%	0.00%	0.00%	0.00%	0.00%	0.00%	0.00%	0.00%	0.00%
11:30 am	73.85%	73.63%	72.55%	71.32%	67.43%	65.05%	65.58%	67.92%	71.17%	72.38%	73.91%	73.67%	0.00%	0.00%	0.00%	0.00%	0.00%	0.00%	0.00%	0.00%	0.00%	0.00%	0.00%	0.00%
12:30 pm	74.14%	73.92%	72.90%	71.73%	67.90%	65.62%	66.21%	68.48%	71.63%	72.75%	74.22%	73.96%	0.00%	0.00%	0.00%	0.00%	0.00%	0.00%	0.00%	0.00%	0.00%	0.00%	0.00%	0.00%
1:30 pm	73.60%	73.30%	72.08%	70.70%	66.36%	63.71%	64.47%	67.14%	70.74%	72.04%	73.66%	73.42%	0.00%	0.00%	0.00%	0.00%	0.00%	0.00%	0.00%	0.00%	0.00%	0.00%	0.00%	0.00%
2:30 pm	71.92%	71.42%	69.73%	67.65%	61.63%	57.82%	58.99%	63.02%	67.94%	69.87%	71.99%	71.79%	0.00%	0.00%	0.00%	0.00%	0.00%	0.00%	0.00%	0.00%	0.00%	0.00%	0.00%	0.00%
3:30 pm	68.32%	67.24%	64.17%	59.98%	48.96%	41.33%	43.98%	52.28%	61.24%	64.88%	68.27%	68.20%	0.00%	0.00%	0.00%	0.00%	0.00%	0.00%	0.00%	0.00%	0.00%	0.00%	0.00%	0.00%
4:30 pm	60.25%	57.27%	49.59%	36.18%	0.00%	0.00%	0.00%	16.03%	42.41%	52.65%	59.89%	60.37%	0.00%	0.00%	0.00%	0.00%	0.00%	0.00%	0.00%	0.00%	0.00%	0.00%	0.00%	0.00%
5:30 pm	36.84%	22.91%	0.00%	0.00%	0.00%	0.00%	0.00%	0.00%	0.00%	6.30%	34.36%	38.37%	0.00%	0.00%	0.00%	0.00%	0.00%	0.00%	0.00%	0.00%	0.00%	0.00%	0.00%	0.00%
6:30 pm	0.00%	0.00%	0.00%	0.00%	0.00%	0.00%	0.00%	0.00%	0.00%	0.00%	0.00%	0.00%	0.00%	0.00%	0.00%	0.00%	0.00%	0.00%	0.00%	0.00%	0.00%	0.00%	0.00%	0.00%
7:30 pm	0.00%	0.00%	0.00%	0.00%	0.00%	0.00%	0.00%	0.00%	0.00%	0.00%	0.00%	0.00%	0.00%	0.00%	0.00%	0.00%	0.00%	0.00%	0.00%	0.00%	0.00%	0.00%	0.00%	0.00%
8:30 pm	0.00%	0.00%	0.00%	0.00%	0.00%	0.00%	0.00%	0.00%	0.00%	0.00%	0.00%	0.00%	0.00%	0.00%	0.00%	0.00%	0.00%	0.00%	0.00%	0.00%	0.00%	0.00%	0.00%	0.00%
9:30 pm	0.00%	0.00%	0.00%	0.00%	0.00%	0.00%	0.00%	0.00%	0.00%	0.00%	0.00%	0.00%	0.00%	0.00%	0.00%	0.00%	0.00%	0.00%	0.00%	0.00%	0.00%	0.00%	0.00%	0.00%
10:30 pm	0.00%	0.00%	0.00%	0.00%	0.00%	0.00%	0.00%	0.00%	0.00%	0.00%	0.00%	0.00%	0.00%	0.00%	0.00%	0.00%	0.00%	0.00%	0.00%	0.00%	0.00%	0.00%	0.00%	0.00%
11:30 pm	0.00%	0.00%	0.00%	0.00%	0.00%	0.00%	0.00%	0.00%	0.00%	0.00%	0.00%	0.00%	0.00%	0.00%	0.00%	0.00%	0.00%	0.00%	0.00%	0.00%	0.00%	0.00%	0.00%	0.00%

Figure 81 Solar panels instantaneous efficiency hourly variation

Appendix K Assumptions and results of the simulation with TRACE® 700 v6.2.6.5

PEAK COOLING LOADS
MAIN SYSTEM

System	Zone	Room	Floor Area m²	SPACE Peak Time Mo/Hr	OA Condition DB °C	OA Condition WB °C	Room Dry Bulb °C	Supply Dry Bulb °C	Space Air Flow L/s	Space Sensible Load kW	Space Latent Load kW	COIL Peak Time Mo/Hr	OA Condition DB °C	OA Condition WB °C	Supply Dry Bulb °C	Coil Airflow L/s	Coil Sensible Load kW	Coil Latent Load kW
Alternative 1																		
		Whole house																
	Zone - 001		150	Peak	1/16	32	26	23.0	15.8	1,097	9.90	1.29	1/16	32	26	15.8	1,097	10.70	2.30
		Peak	150		32	26	23.0	15.8	1,097	9.90	1.29		32	26	15.8	1,097	10.70	2.30
		Zone - 001																
		Block	150		1/16	32	25	23.0	15.8	1,097	9.90	1.29	1/16	32	25	15.8	1,097	10.70	2.30
		Peak Block	150		1/16	32	25	23.0	15.8	1,097	9.90	1.29	1/16	32	25	15.8	1,097	10.76	2.30
System - 001			150															
System - 001			150		1/16	32	25	23.0	15.8	1,097	9.90	1.29	1/16	32	25	15.8	1,097	10.76	2.30

Project Name: Simplified House AC
Dataset Name: Simplified House AC.trc

TRACE® 700 v6.2.6.5 calculated at 01:36 PM on 03/15/2012
Peak Clg Loads Main System Report Page 1 of 1

Figure 82 Peak cooling loads

SYSTEM SUMMARY

DESIGN AIRFLOW QUANTITIES

System Description	System Type	MAIN SYSTEM					Auxiliary System	Room
		Outside Airflow L/s	Cooling Airflow L/s	Heating Airflow L/s	Return Airflow L/s	Exhaust Airflow L/s	Supply Airflow L/s	Exhaust Airflow L/s
Alternative 1								
System - 001	Packaged Terminal Air Conditioner	40	1,097	1,097	1,147	90	0	0
Totals		40	1,097	1,097	1,147	90	0	0

Note: Airflows on this report are not additive because they are each taken at the time of their respective peaks. To view the balanced system design airflows, see the appropriate Checksums report (Airflows section).

Project Name: Simplified House AC
Dataset Name: Simplified House AC.trc

TRACE® 700 v6.2.6.5 calculated at 01:36 PM on 03/15/2012
Design Airflow Quantities Report Page 1 of 1

Figure 83 Design airflow quantities

ENTERED VALUES
Walls by Direction

Alternative 1

North (0 degrees)

Room Description	Wall Description	Area	Tilt	Const Type	U Value W/m²·°C	Alpha	Glass Type	Glass Area m²	Glass SHGC	Glass U Value W/m²·°C	External Shading	Internal Shading
Whole house	Wall - N	28.8	0	Discounted BCA wall R1.4	0.7485	0.90	6mm Sgl Clear	8.6	0.82	5.8427	Overhang - 1m	None
[illegible]	N windows			Window								
		28.8			**0.7485**			**8.6**	**0.82**	**5.8427**		

East (90 degrees)

Room Description	Wall Description	Area	Tilt	Const Type	U Value W/m²·°C	Alpha	Glass Type	Glass Area m²	Glass SHGC	Glass U Value W/m²·°C	External Shading	Internal Shading
Whole house	Wall E	28.8	0	Discounted BCA wall R1.4	0.7485	0.90	6mm Sgl Clear	4.3	0.82	5.8427	Overhang - 1m	None
[illegible]	E windows			Window								
		28.8			**0.7485**			**4.3**	**0.82**	**5.8427**		

South (180 degrees)

Room Description	Wall Description	Area	Tilt	Const Type	U Value W/m²·°C	Alpha	Glass Type	Glass Area m²	Glass SHGC	Glass U Value W/m²·°C	External Shading	Internal Shading
Whole house	Wall S	28.8	0	Discounted BCA wall R1.4	0.7485	0.90						
[illegible]	Door			Door			Standard Door	2.5	0.00	1.1358	Overhang - None	None
[illegible]	S windows			Window			6mm Sgl Clear	8.6	0.82	5.8427	Overhang - None	None
		28.8			**0.7485**			**11.2**	**0.41**	**3.4891**		

West (270 degrees)

Room Description	Wall Description	Area	Tilt	Const Type	U Value W/m²·°C	Alpha	Glass Type	Glass Area m²	Glass SHGC	Glass U Value W/m²·°C	External Shading	Internal Shading
Whole house	Wall W	28.8	0	Discounted BCA wall R1.4	0.7485	0.90	6mm Sgl Clear	2.9	0.82	5.8427	Overhang - 1.5m	None
[illegible]	W windows			Window								
		28.8			**0.7485**			**2.9**	**0.82**	**5.8427**		

Total Area **115.2** **27.0**

Project Name: Simplified House AC
Dataset Name: C:\Documents and Settings\ghabi\My Documents\Simplified House AC.trc

TRACE® 700 v6.2.6.5 calculated at 01:36 PM on 03/15/2012
Alternative - 1 Entered Values - Rooms Page 1 of 1

Figure 84 Wall areas and U value of the case study

ENTERED VALUES
ROOM BY ROOM

Room Description: Whole house | **Zone Description: Zone - 001** | **System Description: System - 001**

GENERAL INFORMATION

Floor Area: 150 m² Flr-Flr Height: 2.4 m
Plenum Height: 0.0 m Height Above Flr:
Slab Constr Type: 100mm Concrete Slab, Carpet & Underlay
Room Mass: Time delay based on actual mass
Ceiling R-Value: 0.315 m²·°C/W
Is There Carpet?: YES
Design Clg DB / Draft Point: 23.0 °C / 25.0 °C
Design Htg DB / Draft Point: 21.0 °C / 20.0 °C
Design Relative Humidity: 55 %
Moisture Capacitance: Medium
Clg Tstat: 24degC 24/7
Htg Tstat: 24degC 24/7
Thermostat Location: Room
Humidistat Location: Room
CO2 Sensor Location: None
Room Type: Conditioned
Floor Multiplier: 1
Room Multiplier: 1

PEOPLE

People Type: AS1668.2 - Office Area
# of People: 4 People
People Sensible: 0.1 kW
People Latent: 0.1 kW
People Schedule: ABGR - Infiltration - 365/24/7

Workstation: 0.0 workstations

LIGHTS

Lighting Type: Recessed fluorescent, not vented, 80% load to space
Fixture Type: RECFL-NV
% Load to RA: 20 %
Lighting Schedule: ABGR - Lights (Limited Ctrl)
Lighting Amount: 15.0 W/sq m
Ballast Factor: 1.0

AIRFLOW INFORMATION

Cooling
Vent Type: None
Vent Value: 10.00 L/s/person
Vent Schedule: Available (100%)
Infil Type: None
Infil Value: 0.50 air changes/hr
Infil Schedule: Available (100%)
Vav Min Airflow: 75.00 % Clg Airflow
Vav Min Sched: Available (100%)
Supply: To be calculated
Aux Supply: To be calculated
Room Exhaust:
Rm Exh Sched: Available (100%)

Heating
None
10.00 L/s/person

None
0.50 air changes/hr

To be calculated
To be calculated

Description	Area/ Amount	Dir	Tilt	Const Type / Schedule	U Value W/m²·°C	Alpha	Glass Type / Energy Type	Area m²	Shade Coef	U Value W/m²·°C	External Shading	Internal Shading	Adj Temp/ Grnd Refl	Pct Sen/ Rmv Cool Tmp	Pct Rmv/ Ret/ Heat Tmp	Pct Rad Frc/ Perm Loss Len Coef
Roof - 1	150 m²	90	10	BCA compliant roof	0.3323	0.90		0			Overhang - None	None				
Wall E	29 m²	90	0	Discounted BCA wall R1.4	0.7485	0.90										
E windows				Window			6mm Sgl Clear	4	0.95	5.84	Overhang - 1m	None	0.00			
Wall S	29 m²	180	0	Discounted BCA wall R1.4	0.7485	0.90										
S windows				Window			6mm Sgl Clear	9	0.95	5.84	Overhang - None	None	0.00			
Door				Door			Standard Door	3	0.00	1.14	Overhang - None	None	0.00			
Wall W	29 m²	270	0	Discounted BCA wall R1.4	0.7485	0.90										
W windows				Window			6mm Sgl Clear	3	0.95	5.84	Overhang - 1.5m	None	0.00			
Wall - N	29 m²	0	0	Discounted BCA wall R1.4	0.7485	0.90										
N windows				Window			6mm Sgl Clear	9	0.95	5.84	Overhang - 1m	None	0.00	100	100	0 60.00
equipment	1,500.0 W			ABGR - Misc Equip - None												

Project Name: Simplified House AC
Dataset Name: C:\Documents and Settings\phtb\My Documents\Simplified House AC.trc

TRACE® 700 v6.2.6.5 calculated at 01:38 PM on 03/15/2012
Alternative - 1 Entered Values - Rooms Page 1 of 1

Figure 85 U-values and areas of the case study

Appendix L Data Sheets for Solar panels, Absorption chiller and vapour compressor chiller used in the simulation of the case study

Table 17 Data sheet of the solar panels used in the simulations

Brand	Thermomax
Model	DF 100 30
Number of tubes	30
Dimensions	
Absorber Area (m^2)	3.020
Overall Dimensions (mm)	1996x2127x97
Width of Manifold (mm)	2127
Length (tube and manifold) (mm)	1996
Depth (mm)	97
Aperture Area (m^2)	3.23
Fluid Volume (ltr)	5.6
Inlet and Outlet Dimensions (mm)	22
Weight (empty) (kg)	81.4
Mounting	
Recommended Inclination (°)	0-90
Performance Data	
Efficiency	Based on Aperture
Eta 0	0.779
a1 (W/m^2K)	1.07
a2 (W/m^2K)	0.0135
Solar Keymark Licence Numbers	011-7S060R
Operating Data	

Flow rate (ltr/h)	
Rated	240
Minimum	180
Maximum	480
Maximum Operating Pressure	8 Bar
Stagnation Temperature (°C)	286
Heat Transfer Fluid	Water/Glycol
Materials	
Absorber	Copper
Coating	Selective coating
Absorbance (%)	95
Emissivity (5)	5
Mounting frame and Clips	Stainless Steel, Aluminium, EPDM
Glass	Low Iron – Transm. 0.92
Vacuum	$<10^{-6}$mbar
Quality Certification/Solar Keymark	Yes

Table 18 Data sheet of the water cooled absorption chiller used in the simulations

Brand	SolarNext AG
Model	chilli® PSC12
Working pair	Ammonia/Water
7.1.1.1 Dimensions (LxDxH) (m)	0.8x0.6x2.2
Operating weight (kg)	approx. 350
Electrical Input	
Voltage (V)	400
Power (W)	300
Cold Water Cycle (fan coils)	
Cooling capacity (kW)	12
Temperature in/out (°C)	12/6
Flow rate (m^3/h)	3.4
Connection	1’ internal thread
Hot water cycle	
Capacity (kW)	18.5
Temperature in/out (°C)	75/68
Flow rate (m^3/h)	2.3
Connection	1’ internal thread
Re-cooling cycle	Wet cooling tower
Capacity (kW)	30.5
Temperature in/out (°C)	24/29
Flow rate (m^3/h)	5.2
Connection	1’ internal thread

Table 19 Data sheet of the typical roof top unit for residential application used in the financial calculation

Brand	Dunnair
Model	PHS15 Rooftop package model
Total Cooling Capacity (kW)	14.8
Sensible Cooling Capacity (kW)	13
Heating Capacity (kW)	14.6
Refrigerant	R410a
Number of compressor	1
Power Input (kW)	5.6
Evaporator Coil	
Type	Copper tube/Aluminium Fins
Face Area (m^2)	0.38
Nominal Evaporator Air Flow (l/s)	850
Evaporator Fan	
Number of Fans	1
Type	Centrifugal
Drive	Direct
Motor Voltage/Phase/Frequency	415/3/50
Motor Power (kW)	0.48
Maximum Fan Speed (rpm)	1045
Electrical	
Power requirements (Volt/Phase)	415/3
Normal Max Current (Amps/Phase)	12.6
Condenser Coil	

Type	Copper tube/Aluminium Fins
Face Area (m^2)	0.55
Condenser Fan Motor	
Number of Fans	1
Type	Axial
Drive	Direct
Motor Watts/rpm	370/950
Motor Voltage/Phase/Frequency	415/3/50

Table 20 Data sheet of the typical roof top unit for commercial application used in the financial calculation

Brand	Temperzone
Model	OPA550
Nominal Cooling Capacity (kW)	56.1
Net Cooling Capacity (kW)	53.9
Heating Capacity (kW)	49.5
Refrigerant	R410a
E.E.R.	3.05
Air Flow (l/s)	2800
Power Source	3 phase 342-436 V a.c. 50 Hz
Indoor Fan motor size (kW)	3
Max fan speed (rpm)	950

Appendix M Payback period calculations

Conventional system	2015	2016	2017	2018	2019	2020	2021	2022	2023	2024	2025	2026	2027	2028	2029	2030
Initial investment	$86,000															
Cash flows	$86,000	$5,026	$5,147	$5,270	$5,397	$5,526	$5,659	$5,795	$5,934	$6,076	$6,222	$6,371	$6,524	$6,681	$6,841	$7,005
Cumulative cash flows	$86,000	$80,974	$75,828	$70,557	$65,161	$59,635	$53,976	$48,182	$42,248	$36,172	$29,950	$23,579	$17,055	$10,374	$3,533	$3,472
Fraction calculations		n/m	n/m	n/m	n/m	n/m	n/m	n/m	n/m	n/m	n/m	n/m	n/m	n/m	n/m	0.98
Payback period	14.98															
Conventional system	2015	2016	2017	2018	2019	2020	2021	2022	2023	2024	2025	2026	2027	2028	2029	2030
Initial investment	$76,203															
Cash flows	$76,203	$5,026	$5,147	$5,270	$5,397	$5,526	$5,659	$5,795	$5,934	$6,076	$6,222	$6,371	$6,524	$6,681	$6,841	$7,005
Cumulative	$76,203	$71,177	$66,030	$60,760	$55,364	$49,838	$44,179	$38,385	$32,451	$26,375	$20,153	$13,782	$7,258	$577	$6,264	$13,269

cash flows																
Fraction calculations		n/m	n/m	n/m	n/m	n/m	n/m	n/m	n/m	n/m	n/m	n/m	n/m	n/m	0.97656	0.97656
Payback period	13.98															